THEME SECTION

Innovative use of sclerochronology in marine resource management

Organizers: E. Hunter, V. V. Laptikhovsky, P. R. Hollyman
Editors: Y. Cherel, S. Somarakis, S. R. Wing

Marine Ecology Progress Series Vol. 598, pages 153–291

This Theme Section represents a selection of studies exploring the innovative use of sclerochronology in resource management. Topics covered showcase the potential for sclerochronology to provide a deeper understanding of the interaction between marine life and its environment.

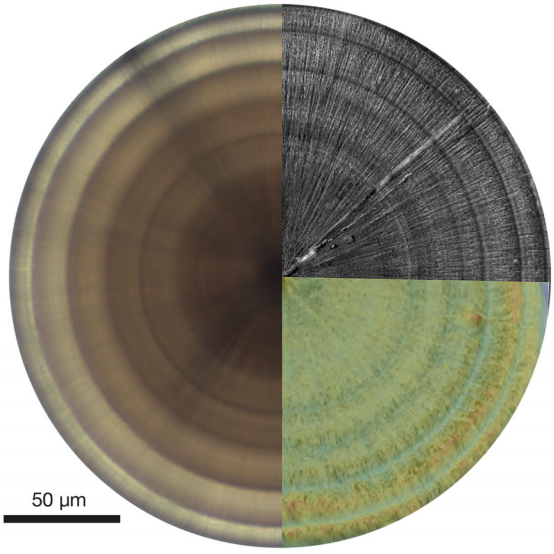

Composite image of 2 statoliths from the same *Buccinum undatum* specimen displaying different sclerochronological techniques.

Photo credit: Philip Hollyman

CONTENTS

Vol. 598: 155–158, 2018
https://doi.org/10.3354/meps12664

MARINE ECOLOGY PROGRESS SERIES
Mar Ecol Prog Ser

Published June 28

Contribution to the Theme Section 'Innovative use of sclerochronology in marine resource management'

INTRODUCTION

Innovative use of sclerochronology in marine resource management

Ewan Hunter[1,2,*], Vladimir V. Laptikhovsky[1], Philip R. Hollyman[3,4]

[1]Centre for Environment, Fisheries and Aquaculture Science, Lowestoft Laboratory, Lowestoft, Suffolk NR33 0HT, UK
[2]School of Environmental Sciences, University of East Anglia, Norwich Research Park, Norwich NR4 7TJ, UK
[3]School of Ocean Sciences, College of Natural Sciences, Bangor, Menai Bridge, Anglesey LL59 5AB, UK
[4]*Present address:* British Antarctic Survey, High Cross, Madingley Rd, Cambridge CB3 0ET, UK

ABSTRACT: In recent years, technical and analytical developments in sclerochronology, based on the analysis of accretionary hard tissues, have improved our ability to assess the life histories of a wide range of marine organisms. This Theme Section on the innovative use of sclerochronology was motivated by the cross-disciplinary session 'Looking backwards to move ahead — how the wider application of new technologies to interpret scale, otolith, statolith and other biomineralised age-registering structures could improve management of natural resources' convened at the 2016 ICES Annual Science Conference in Riga, Latvia. The contributions to this Theme Section provide examples of applications to improve the assessment and management of populations and habitats, or showcase the potential for sclerochronology to provide a deeper understanding of the interaction between marine life and its environment, including the effects of changing climate.

KEY WORDS: Sclerochronology · Otoliths · Statoliths · Scales · Beaks · Life-histories · Ageing · Fisheries management

INTRODUCTION

In recent years, insights gained from sclerochronology-based studies, primarily obtained through isotopic and trace element analyses of age-registering accretionary hard tissues, have contributed significantly to understanding the life-history biology of marine organisms, and the assessment and management of populations and habitats (Arkhipkin 2005, Geffen et al. 2016, Grønkjær 2016, Tanner et al. 2016, Tzadik et al. 2017). Beyond single species and niche analyses, sclerochronology has provided a deeper understanding of the interaction between marine life and its environment, including the effects of changing climate (Morrongiello et al. 2012, Ong et al. 2016, 2018). At a time of worldwide funding constraints in applied science (UNESCO 2017), sclerochronological analyses of existing time-series sample collections are a comparatively affordable way of data mining. The combined analysis of historical and new data allows insights into past marine environmental conditions that can inform future decision-making in fisheries management and environmental sciences.

At the 2016 ICES Annual Science Conference in Riga, Latvia, the session 'Looking backwards to move ahead — how the wider application of new technologies to interpret scale, otolith, statolith and other biomineralised age-registering structures could improve management of natural resources' (ICES 2016) was held to broaden understanding, expedite cross-fertilisation between different but related areas of sclerochronology, and facilitate the wider uptake of state-of-the-art approaches. The session attendees aimed to address assessment and management applications, from species-specific ageing methods and migration studies to analytical stock assessments, using data collected with novel techniques. The cross-disciplinary session was intended to include technical

*Corresponding author: ewan.hunter@cefas.co.uk

Publisher: Inter-Research · www.int-res.com

and ecological studies emphasising new methods and approaches to ageing and the use of aging data in a broad range of species and taxa. This resultant Theme Section presents a selection of papers either presented at, or representative of, the session at the 2016 ICES meeting. Held over 2 days, we attracted 43 contributions from 34 institutes (across 17 countries), over half of which were fish-centred, most focussing on aspects of otolith science.

INNOVATIVE USE OF SCLEROCHRONOLOGY

Otolith chemistry remains a driving force in fish population dynamics studies (e.g. Sturrock et al. 2012, Tanner et al. 2016, Izzo et al. 2018). The potential of sulphur isotopes ($\delta^{34}S$) as biogeochemical markers in fish was examined by Doubleday et al. (2018 in this Theme Section), who provided evidence suggesting that otolith $\delta^{34}S$ concentrations recorded by juvenile tank-grown barramundi were influenced by both ambient water and diet. Underlining the importance of validating chemical signatures observed in the otoliths of wild fishes, Darnaude & Hunter (2018 in this Theme Section) explored spatial and temporal variability in the acuity of otolith $\delta^{18}O$ for providing fishery-independent estimates of fish location, by comparing the ambient environmental experience of North Sea plaice *Pleuronectes platessa* achival tags with $\delta^{18}O$ recorded simultaneously in the otoliths from the same fish. Schilling et al. (2018 in this Theme Section) combined adult otolith elemental signatures with length frequency data of trawled fish to identify facultative estuary use by juvenile bluefish *Pomatomus saltatrix* in eastern Australia.

Otoliths are also instrumental in gauging the relative importance of, and interaction between, natural and anthropogenic drivers in shaping marine systems (e.g. Morrongiello et al. 2012, Black et al. 2016, Ong et al. 2016). Barrow et al. (2018 in this Theme Section) recreated a 32 yr growth history of rock flathead *Platycephalus laevigatus* and related growth variation to changes in freshwater flows, temperature, wind, and the Southern Oscillation Index. By disentangling the drivers of long-term growth variation in harvested fishes, future productivity under a range of environmental and management scenarios can be predicted. Fisher & Hunter (2018 in this Theme Section) reviewed digital imaging techniques in otolith data capture, analysis and interpretation, and considered why computer-assisted age and growth estimation systems have yet to be adopted more widely. Other otolith work presented in the session but not included in the Theme Section comprised examples of incremental analysis and morphometrics, pollution monitoring, and chemical marking to assess the effectiveness of artificial restocking.

Otoliths remain the focus for most fish ageing research; however, fish chemical archives beyond otoliths are also important (Tzadik et al. 2017), notably non-lethal sampling strategies for rare, endangered, and long-lived fishes. Seeley & Walther (2018 in this Theme Section) successfully applied inorganic and organic proxies to reconstruct migration and dietary histories from scales of the Atlantic tarpon *Megalops atlanticus*, demonstrating transhaline migrations associated with ontogenetic trophic shifts. With scale architecture facilitating sequential sub-sampling, this approach is an encouraging example of a non-lethal natural tag with clear fisheries management applications and citizen-science engagement opportunities.

The non-fish contributions to our meeting were almost exclusively molluscan (cephalopod, gastropod and bivalve ageing, and biochronology studies), reflecting the increasing scale and commercial importance of cephalopod and shellfish fisheries (Anderson et al. 2011, Doubleday et al. 2016). Until recently, squid have been aged primarily from statolith growth increments. Daily periodicity in increment formation is well established, but is related to diurnal feeding patterns rather than diurnal environmental cycles (Boyle & Rodhouse 2005), so periodic starvation can potentially bias age readings. The 'chalky' statoliths of octopods, by contrast, have no discernible growth increments, and those of adult cuttlefish are subject to crystallization, so direct ageing of these cephalopods has not been possible until recently (except for juvenile and immature *Sepia officinalis*; Bettencourt & Guerra 2000, 2001). Perales-Raya et al. (2018 in this Theme Section) compared the growth rates of naturally occurring and cultured octopus *Octopus vulgaris* paralarvae reared under different temperature and dietary regimes. In demonstrating the ageing potential of daily beak increments, a better understanding of the spatial dynamics of naturally occurring octopus paralarvae was also achieved.

Gastropod stock assessments have long posed difficulties due to key components of population dynamics, such as natural mortality and growth rate, remaining immeasurable. Hollyman et al. (2018 in this Theme Section) described the development and validation of statolith-based age determination in the commercially valuable whelk *Buccinum undatum*, combining field, laboratory and geochemical experiments to confirm an annual periodicity to visible

growth increments within statoliths. Natural mortality estimates and population age structures will now allow fisheries scientists to perform analytical whelk stock assessments for the first time.

The biomineralised materials derived from marine organisms can also play a role in estimating rates of natural and fishing mortality in studies of population dynamics. In a study spanning marine biology, palaeontology and zoo-archeology, Laptikhovsky et al. (2018 in this Theme Section) reviewed existing methods to evaluate applying ageing analyses to collected dead material from a range of species groups (corals, molluscs, fish and marine mammals). The application of chemical and sclerochronological analyses are discussed for key structures such as mollusc shells, coral skeletons and fish otoliths often found in thanatocoenoses. Although not all approaches and techniques are transferrable due to diverse ecology and morphology, it is suggested that cross-fertilisation amongst the methods presented could yield new approaches for population dynamics studies.

CONCLUSIONS

The 9 papers presented in this Theme Section provide a representative rather than fully exhaustive cross-section of current state-of-the art sclerochronology applications. The use of elemental and isotopic analyses in determining life-history events and population structure continues to blossom; however, an underlying lack of understanding of both sampling protocols and underlying chemistry can only be addressed through more fundamental experimental studies. Cephalopod and gastropod ageing have yet to reach the same level of maturity as fish ageing studies. A wider uptake of the results of studies using biogeochemical markers into fisheries management should help to fuel this research area. We conclude that while sclerochronological techniques continue to improve and proliferate, there is still some way to go before the full realisation of potential in this field.

Acknowledgements. We thank Yves Cherel, Stylianos Somarakis and Stephen Wing for their professional handling of the review process.

LITERATURE CITED

Anderson SC, Flemming JM, Watson R, Lotze HK (2011) Rapid global expansion of invertebrate fisheries: trends, drivers, and ecosystem effects. PLOS ONE 6:e14735

Arkhipkin AI (2005) Statoliths as 'black boxes' (life recorders) in squid. Mar Freshw Res 56:573–583

Barrow J, Ford J, Day R, Morrongiello J (2018) Environmental drivers of growth and predicted effects of climate change on a commercially important fish, *Platycephalus laevigatus.* Mar Ecol Prog Ser 598:201–212

Bettencourt V, Guerra A (2000) Growth increments and biomineralization process in cephalopod statoliths. J Exp Mar Biol Ecol 248:191–205

Bettencourt V, Guerra A (2001) Age studies based on daily growth increments in statoliths and growth lamellae in cuttlebone of cultured *Sepia officinalis.* Mar Biol 139: 327–334

Black BA, Griffin D, Sleen P, Wanamaker AD and others (2016) The value of crossdating to retain high-frequency variability, climate signals, and extreme events in environmental proxies. Glob Change Biol 22:2582–2595

Boyle PR, Rodhouse P (2005) Cephalopods: ecology and fisheries. Blackwell Science, Oxford

Darnaude AM, Hunter E (2018) Validation of otolith $\delta^{18}O$ values as effective natural tags for shelf-scale geolocation of migrating fish. Mar Ecol Prog Ser 598:167–185

Doubleday ZA, Prowse TAA, Arkhipkin A, Pierce GJ and others (2016) Global proliferation of cephalopods. Curr Biol 26:R406–R407

Doubleday ZA, Cliff J, Izzo C, Gillanders BM (2018) Untapping the potential of sulfur isotope analysis in biominerals. Mar Ecol Prog Ser 598:159–166

Fisher M, Hunter E (2018) Digital imaging techniques in otolith data capture, analysis and interpretation. Mar Ecol Prog Ser 598:213–231

Geffen AJ, Morales-Nin B, Gillanders BM (2016) Fish otoliths as indicators in ecosystem based management: results of the 5th International Otolith Symposium (IOS2014). Mar Freshw Res 67:i–iv

Grønkjær P (2016) Otoliths as individual indicators: a reappraisal of the link between fish physiology and otolith characteristics. Mar Freshw Res 67:881–888

Hollyman PR, Leng MJ, Chenery SRN, Laptikhovsky VV, Richardson CA (2018) Statoliths of the whelk *Buccinum undatum*: a novel age determination tool. Mar Ecol Prog Ser 598:261–271

ICES (2016) Theme session H. Looking backwards to move ahead—how the wider application of new technologies to interpret scale, otolith, statolith and other biomineralised age-registering structures could improve management of natural resources [Theme Session Report]. Hunter E, Laptikhovsky V, Hollyman P (convenors). ICES, Copenhagen. www.ices.dk/news-and-events/asc/ASC2016/Documents/Theme%20session%20reports/Theme%20session%20H.pdf

Izzo C, Reis-Santos P, Gillanders BM (2018) Otolith chemistry does not just reflect environmental conditions: a meta-analytic evaluation. Fish Fish, doi:10.1111/faf.12264

Laptikhovsky VV, Barrett CJ, Hollyman PR (2018) From coral reefs to whale teeth: estimating mortality from natural accumulations of skeletal materials. Mar Ecol Prog Ser 598:273–291

Morrongiello JR, Thresher RE, Smith DC (2012) Aquatic biochronologies and climate change. Nat Clim Chang 2: 849–857

Ong JJL, O'Donnell AJ, Meeuwig JJ, Zinke J and others (2016) Evidence for climate-driven synchrony of marine and terrestrial ecosystems in northwest Australia. Glob Change Biol 22:2776–2786

Ong JJL, Rountrey A, Black BA, Nguyen HM and others (2018) A boundary current drives synchronous growth of

marine fishes across tropical and temperate latitudes. Glob Change Biol, doi:10.1111/gbc.14083

Perales-Raya C, Nande M, Roura A, Bartolomé A and others (2018) Comparative study of age estimation in wild and cultured *Octopus vulgaris* paralarvae: effect of temperature and diet. Mar Ecol Prog Ser 598:247–259

Schilling HT, Reis-Santos P, Hughes JM, Smith JA and others (2018) Evaluating estuarine nursery use and life history patterns of *Pomatomus saltatrix* in eastern Australia. Mar Ecol Prog Ser 598:187–199

Seeley ME, Walther BD (2018) Facultative oligohaline habitat use in a mobile fish inferred from scale chemistry. Mar Ecol Prog Ser 598:233–245

Sturrock AM, Trueman CN, Darnaude AM, Hunter E (2012) Can otolith elemental chemistry retrospectively track migrations in fully marine fishes? J Fish Biol 81:766–795

Tanner SE, Reis-Santos P, Cabral HN (2016) Otolith chemistry in stock delineation: a brief overview, current challenges and future prospects. Fish Res 173:206–213

Tzadik OE, Curtis JS, Granneman JE, Kurth BN and others (2017) Chemical archives in fishes beyond otoliths: a review on the use of other body parts as chronological recorders of microchemical constituents for expanding interpretations of environmental, ecological, and life history changes. Limnol Oceanogr Methods 15:238–263

UNESCO (2017), Global Ocean Science Report—the current status of ocean science around the world. UNESCO, Paris

Vol. 598: 159–166, 2018
https://doi.org/10.3354/meps12605

MARINE ECOLOGY PROGRESS SERIES
Mar Ecol Prog Ser

Published June 28

Contribution to the Theme Section 'Innovative use of sclerochronology in marine resource management'

Untapping the potential of sulfur isotope analysis in biominerals

Zoë A. Doubleday[1,*], John Cliff[2,3], Christopher Izzo[1,4], Bronwyn M. Gillanders[1]

[1]School of Biological Sciences, The University of Adelaide, Adelaide, SA 5005, Australia

[2]Centre for Microscopy, Characterisation and Analysis, The University of Western Australia, Perth, WA 6009, Australia

[3]*Present address:* Environmental Molecular Sciences Laboratory, Pacific Northwest National Laboratory, Richland, WA 99354, USA

[4]*Present address:* Fisheries Research and Development Corporation, Adelaide, SA 5000, Australia

ABSTRACT: Sulfur isotope ratios are used to untangle food web dynamics, track animal movements and determine dietary provenance. Yet, their application in the biomineralised tissues of animals is relatively unexplored. These tissues are particularly useful for isotopic analyses as they can retain a permanent and temporally resolved chemical record over the lifetime of the organism. We experimentally determined whether biogenic carbonate records environmental variation in sulfur isotope ratios ($^{34}S/^{32}S$) in an aquatic system and whether such variation is influenced by the ambient water or diet. Juvenile barramundi *Lates calcarifer* were raised in 2 water treatments with differing sulfur isotope ratios, as well as 3 diet treatments with differing ratios. We subsequently analysed the calcium carbonate fish ear bones (otoliths) using secondary ion mass spectrometry, a technique that allowed the experimental growth of the otolith to be targeted. Our findings suggest that biogenic carbonate records variation in sulfur isotope ratios and that diet is not the sole source of sulfur isotope variation in aquatic consumers. Drawing from a multi-disciplinary body of literature, we also reviewed the potential ecological and environmental applications of sulfur isotope analysis in biominerals. We emphasise the extensive application of sulfur isotope ratios and that progressing this field of research to include biominerals is a worthwhile pursuit.

KEY WORDS: Carbonates · Sulfur isotopes · Diet · Fish otolith · Barramundi · *Lates calcarifer*

INTRODUCTION

The analysis of stable isotopes in plant and animal tissue is used widely in the fields of ecology and environmental science (Boecklen et al. 2011). A range of elements has been targeted, from hydrogen to lead, each with its own isotopic properties and applications (Peterson & Fry 1987, Rubenstein & Hobson 2004). For sulfur, geochemical, biological and anthropogenic processes drive relative differences in abundance between the 2 principal isotopes, ^{34}S and ^{32}S, resulting in marked isotopic variation in the environment (Thode 1991). Organisms living in marine, freshwater and terrestrial environments have distinct sulfur isotope ratios, which in turn can be influenced by local oxygen levels (aerobic versus anaerobic conditions), precipitation, geology and pollution (Rubenstein & Hobson 2004, Nehlich 2015). These properties make sulfur isotopes an attractive tool to investigate food web dynamics, movement patterns and dietary provenance (Trust & Fry 1992, Connolly et al. 2004, Fry & Chumchal 2011), and to track pollution (Barros et al. 2015), but still remain a relatively untapped resource in the field (compared to carbon, oxygen and nitrogen isotopes).

In animal studies, organic tissues, such as muscle and bone collagen, are typically used for sulfur isotope analysis. However, biominerals, such as coral

*Corresponding author: zoe.doubleday@adelaide.edu.au

Publisher: Inter-Research · www.int-res.com

skeletons, mollusc shells and fish otoliths, represent an underused alternative to organic tissue. An advantage of biomineralised tissues is that many grow incrementally, providing a time-resolved chemical record throughout the lifetime of the organism, and are preserved in the environment long after the organism has died (although taphonomic processes can alter isotope ratios over time). This enables environmental and ecological phenomena to be tracked over decadal, centennial and even millennial time scales (Rowell et al. 2010, Limburg et al. 2011, Izzo et al. 2017). Further, extensive archives of biominerals already exist in government research agencies, universities and museums, whereby data can be generated retrospectively with relatively minimal cost. Sulfur isotopes were first measured in biomineralised tissue (fish otoliths) by Weber et al. (2002) using secondary ion mass spectrometry (SIMS), a spatially resolved technique that allows the temporal properties of biominerals to be exploited. Since then, few studies have investigated sulfur isotopes in biominerals, but those that do exist have used SIMS to investigate the source and movement of hatchery salmonids (Godbout et al. 2010, Johnson et al. 2012) and to develop a tracer of hypoxia exposure (Limburg et al. 2015). Further work has also been done to develop a bulk analytical method, using isotope ratio mass spectrometry (IRMS), for biogenic apatite (Goedert et al. 2016).

In the limited studies to date, it has been assumed that sulfur isotope ratios in biominerals, specifically otolith carbonate, are influenced solely by the diet, such that the ratio of an animal's food determines the value in biomineralised tissue (Godbout et al. 2010, Johnson et al. 2012). Yet, in aquatic environments, it is suggested that sulfated macromolecules, sourced from inorganic sulfate in the water, could be incorporated into the organic matrix of the otolith (Mugiya & Iketsu 1987, Weber et al. 2002, McFadden et al. 2016). Determining the source of isotopic variation in biominerals (i.e. water or diet) has implications for how isotopic signatures are applied and interpreted (see Doubleday et al. 2013, Izzo et al. 2015 for analogous studies on elemental markers). Using an experimental approach, we explicitly determined in an aquatic system (1) whether otolith carbonate reflects environmental variation in sulfur isotope ratios, and (2) whether that variation is influenced by both the isotopic composition of the diet and the surrounding water. In addition, we reviewed relevant literature to highlight the suite of potential applications of sulfur isotope ratios to ecological and environmental science. Our aim was not to undertake an exhaustive review, but rather to focus on applications that are translatable to biominerals.

MATERIALS AND METHODS

Aquarium experiment

We raised juvenile fish in an orthogonal experimental design consisting of 2 water treatments with differing sulfur isotope ratios, as well as 3 diet treatments with differing ratios (n = 6 treatments; Table 1). Each treatment was replicated (n = 12 tanks). We selected diadromous fish for the experiment (barramundi *Lates calcarifer*), as they are adapted to both marine and freshwater environments. Juvenile fish, 1.5 to 3 g in size, were obtained from a local commercial hatchery (Robarra) and reared under experimental conditions at the University of Adelaide, South Australia. Fish were fed daily, and feeding behaviour (rate) was monitored and scored from 0 (no feeding) to 3 (high-level feeding). Fish were exposed to experimental conditions for 30 to 34 d and subsequently euthanised and weighed.

Food and water isotope analyses

To confirm that isotope ratios ($^{34}S/^{32}S$) between water and diet treatments differed, duplicate water and diet samples were analysed using IRMS. Water

Table 1. Description of experimental treatments with mean (±SE) elemental sulfur concentration (ppm) and $^{34}S/^{32}S$ values (expressed as $\delta^{34}S$ ‰, the deviation relative to Vienna Canyon Diablo Troilite) of each treatment (n = 2)

Treatment	Description	Sulfur concentration	$\delta^{34}S$ ‰
Water			
Freshwater	Borewater (0‰ salinity)	290 ± 42	11.0 ± 0.1
Seawater	Natural seawater (40‰ salinity)	3770 ± 64	20.7 ± 0.4
Diet origin			
Freshwater	Freeze-dried tubifex worms *Tubifex tubifex*	6132 ± 27	4.9 ± 0.4
Mixed	Commercial pellet food (Luckystar brand)	5887 ± 40	12.3 ± 0.3
Marine	Freeze-dried Antarctic krill *Euphausia superba*	11403 ± 49	15.6 ± 0.4

samples were analysed by a commercial provider (Environmental Isotopes, New South Wales), whereby they were evaporated (to concentrate the sulfur), acidified, heated, mixed with $BaCl_2$ solution and cooled. The $BaSO_4$ precipitate was then filtered and dried for isotope analysis. The $BaSO_4$ precipitate (approximately 0.1 mg) was mixed with V_2O_5 in tin (Sn) cups and then combusted using a modified Roboprep Elemental Analyser attached to a Finnigan Mat Conflo III and Finnigan 252 IRMS. Samples were analysed relative to an internal gas standard and solid laboratory-specific standards (Ag_2S-3: $\delta^{34}S$ = +0.4‰ Vienna Canyon Diablo Troilite [VCDT]; CSIRO-S-SO_4: $\delta^{34}S$ = +20.4‰ VCDT), which were used to correct the raw data. The internal solid laboratory standards were calibrated using international standards IAEA-S1 ($\delta^{34}S$ = −0.3‰ VCDT) and NBS-127 ($\delta^{34}S$ = +20.3‰ VCDT). The reproducibility of the sulfur isotope values of $BaSO_4$ was <0.2‰. To obtain elemental sulfur concentrations, additional water samples were analysed by a commercial provider (National Measurement Institute, Australia) using inductively coupled plasma optical emission spectrometry (Agilent / Varian 730-ES instrument).

The food samples were analysed in-house at the University of Adelaide for both isotope values and elemental sulfur concentrations. Samples were powdered and placed in Sn cups and combusted using a EuroVector Euro Elemental Analyzer in-line with a Nu Instruments CF-IRMS. Samples were analysed relative to internal laboratory standards, as above, traceable to IAEA-S2 and IAEA-S3 standards ($\delta^{34}S$ = +22.7 and −32.3 ‰ VCDT, respectively). Reproducibility was <0.1‰. Elemental concentrations were determined by comparing the peak areas of SO_2 with the known weights of sulfur in the standards. All ratios for food and water samples were expressed in per mil as $\delta^{34}S$ ‰, the deviation relative to VCDT, and elemental concentrations in ppm (Table 1).

Otolith preparation and isotope analyses

Otoliths (size: ~3 × 1 mm) were dissected from fish, cleaned in ultra-pure water and air-dried. A subsample of otoliths was cut in half at the core using a diamond saw, embedded in epoxy resin, ground until the transverse plane and core were exposed and polished to 1 µm. The sample mounts were sonicated successively in detergent, distilled deionized water and isopropyl alcohol, and then coated with 30 nm of gold (see Fig. S1 in the Supplement at www.int-res.com/articles/suppl/m598p159_supp.pdf). Otoliths were analysed in 2 consecutive sessions using SIMS (Cameca IMS 1280) at the Centre for Microscopy, Characterisation, and Analysis, University of Western Australia, Australia. Sample otoliths were sputtered with a 4nA, 20 keV Cs^+ primary ion beam and initially presputtered with a 25 × 25 µm raster. Following automatic centring in the field and contrast apertures, the analyses consisted of integrated 20 × 4 s cycles using a 20 × 20 µm rastered beam with dynamic transfer enabled. Duplicate analyses were made on the edge of each otolith cross section, representing the experimental period of otolith growth (Fig. S1). This also ensured that data were not confounded by ontogenetic effects. A normal incidence electron gun was used for charge compensation. $^{32}S^-$ ions were collected in a Faraday cup (FC) with a 10^{11} ohm amplifier resistor, and $^{34}S^-$ ions were collected simultaneously with an electron multiplier (EM). Average intensity for $^{32}S^-$ ions was ~3 × 10^6 cps. The background of the FC was characterized before each analytical session for data correction. Other parameters included an entrance slit of 120 µm, exit slit widths of 500 µm, 40 eV energy slit width with a 5 eV offset. Data correction was limited to FC background subtraction and EM deadtime correction.

Sample analyses were bracketed by 8 to 10 external standard analyses to correct for instrumental mass fractionation, which was judged to be negligible. We used an otolith section, sourced from a marine fish (snapper *Chrysophrys auratus* Sparidae), as an external standard. The standard had a homogeneous, but unknown isotopic composition, and served to estimate analysis reproducibility. Propagation of uncertainty included internal uncertainty for each analysis (SE of 20 × 4 s cycles) and the external uncertainty of the otolith standard analyses. Over the course of 2 analytical sessions, internal precision averaged 0.4‰ (1 SD) and external precision for the otolith standard for all analyses was 0.7‰ (1 SD, n = 27). Unlike the food and water analyses, which were expressed using the standardised method for reporting sulfur isotope ratios (i.e. $\delta^{34}S$ ‰, the deviation relative to the VCDT standard), otolith data were expressed as $^{34}S/^{32}S$ values, as our standard $\delta^{34}S$ composition was unknown. While this precludes data comparisons among studies, it still allows for comparisons between experimental treatments.

A proportion of the prepared samples were not analysed by SIMS (19 out of 48), because they were either completely or partially obscured by epoxy resin. The samples that were analysed were subsequently viewed under a microscope and photographed to determine whether the rasters were in the

Table 2. Number of samples analysed per treatment and number of replicate tanks represented per treatment

Treatment	Diet	Fish (n)	Tanks (n)
Freshwater	Tubifex worms	2	1
	Pellet	3	1
	Krill	6	2
Seawater	Tubifex worms	6	2
	Pellet	4	2
	Krill	4	1

correct position and the edge of the otolith was correctly targeted (Fig. S1). Otolith and epoxy material was clearly distinguishable, such that if the otolith material was coated in epoxy it was not visible. A small number of analysed samples (n = 4) were removed from the final dataset because the growing edge of the otolith was not fully exposed in the epoxy mount and the SIMS analyses did not represent experimental otolith growth (n = 25 remaining samples, see Table 2 for more details).

Statistical analyses

The mean of each duplicate otolith analysis was used as the final ratioed value for each individual (see Table S1 for raw data). Differences in otolith ratios among water and diet treatments were tested using a 2-factor permutational ANOVA with water and diet treatments as fixed factors (Primer/PERMANOVA). If significant differences were detected, post hoc pairwise tests were performed. An additional ANOVA was also conducted with tank as a nested term. No significant differences were observed between replicate tanks ($p > 0.05$), thus data from each replicate were pooled for the final analysis. One-factor ANOVAs were also performed to determine differences among water and diet treatments.

RESULTS

Water and diet samples had significantly different sulfur isotope ratios (1-factor ANOVAs: $p < 0.05$) and also matched the expected values measured in marine and freshwater environments (Table 1). Elemental sulfur concentrations also varied significantly among all treatments ($p < 0.05$), except between the pellet and tubifex diet treatments (post hoc test: $p > 0.05$).

Mean feeding scores (for all fish raised) were highest for fish fed pellets and lowest for fish raised in freshwater and fed tubifex worms and krill (Fig. S2). By the end of the experiment, fish fed commercial pellets were also approximately 6 times larger for both freshwater and seawater treatments (mean ± SE body weight of analysed samples: 12.1 ± 1.7 and 11.5 ± 1.0 g, respectively), compared to the other 2 diets (krill: 3.1 ± 0.3 and 3.3 ± 0.5 g; tubifex worms: 1.7 ± 0.3 and 2.2 ± 0.3 g, respectively).

Sulfur isotope ratios in otoliths varied significantly among fish exposed to the various experimental treatments (Fig. 1). Fish raised in freshwater and seawater had different sulfur isotope ratios (2-factor ANOVA: $F_{1,19} = 18.1$, $p < 0.001$), with fish raised in

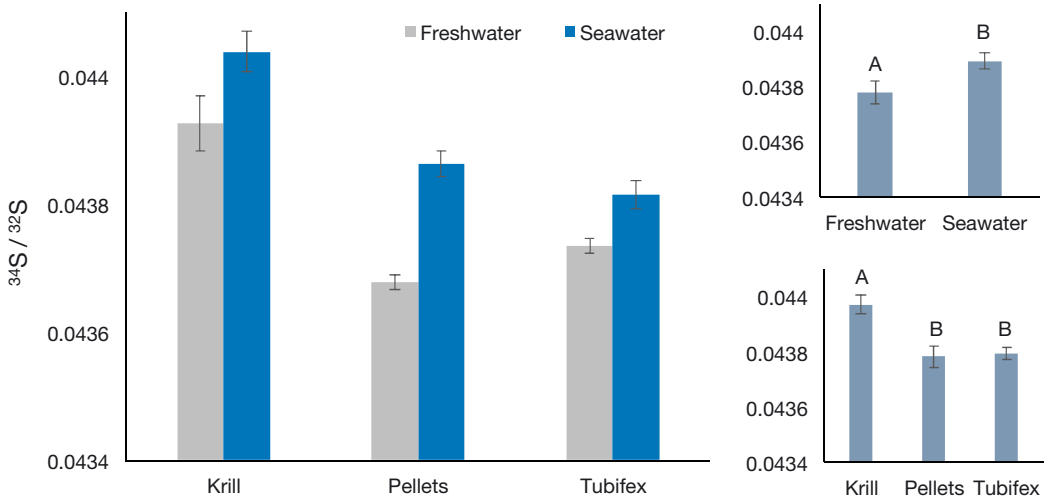

Fig. 1. Mean (±SE) otolith $^{34}S/^{32}S$ values from barramundi raised in freshwater versus seawater and fed freshwater origin (tubifex worms), mixed origin (pellets) or marine origin (krill) diets (see Table 1). Smaller graphs represent pooled otolith $^{34}S/^{32}S$ values (main effects) for water and diet, with significant differences represented by different letters ($p < 0.001$)

freshwater having lower ratios regardless of diet type. Fish fed different diets also had significantly different sulfur isotope ratios (2-factor ANOVA: $F_{2,19}$ = 25.7, p < 0.001), with fish fed krill having higher ratios compared to fish that were fed pellets or tubifex worms (post hoc tests: p < 0.001, see also Fig. 1). There were no interaction effects between water and diet treatments.

DISCUSSION

We experimentally demonstrated that otolith carbonate reflects environmental variation in sulfur isotopes. Critically, fish raised in seawater had higher sulfur isotope ratios compared to fish raised in freshwater, and fish fed marine origin diets had higher ratios than fish fed mixed- or freshwater origin diets. These findings imply that sulfur isotope ratios in otolith carbonate are not just influenced by diet, but also by water chemistry. Our 2 treatments were mainly represented by 2 different oxidation states of sulfur: the reduced form, sulfide, mainly present in the fish food (as amino acids), and the oxidised form, sulfate, mainly present in the water. Both of these forms of sulfur are thought to occur in otoliths and may explain how water and diet can both influence sulfur isotope ratios. Otoliths of teleost fish are composed of aragonite crystals, which crystallise around a protein matrix with daily periodicity (Campana 1999, Dauphin & Dufour 2008). The collagen-like protein (called otolin) makes up 2–10% of the otolith material (Murayama et al. 2002, Izzo et al. 2016), and sulfur-bearing amino acids (methionine and cysteine) in the protein are thought to be the primary source of sulfur in otoliths (Kalish 1989, McFadden et al. 2016). Methionine is essential to fish, and can only be sourced from the diet, and while cysteine can be synthesised (from methionine), dietary sources are required if utilisation exceeds synthesis (Li et al. 2009). However, sulfate may also be present in otoliths in a class of proteins called proteoglycans (Weber et al. 2002, McFadden et al. 2016), and supports previous preliminary evidence that inorganic sulfate in the water can be incorporated in the otolith under experimental conditions (Mugiya & Iketsu 1987). Sulfate has also been found in biogenic carbonates (e.g. brachiopod shells and coral skeletons) as structurally substituted ions within the carbonate lattice (Kampschulte et al. 2001, Kampschulte & Strauss 2004, Perrin et al. 2017), a process which is also thought to occur in bioapatite (Martin et al. 2017). This study provides evidence that water and diet can both influence sulfur isotope ratios in otolith carbonate, but measuring ratios in the organic and inorganic components of the otolith, as well as determining the proportional contributions of each treatment, would help unlock the potential of sulfur isotope analysis in biominerals.

Our results also support the assumption that diet does affect sulfur isotope ratios in otoliths; however, interestingly, the sulfur isotope ratios in the otoliths of the fish fed mixed and freshwater diets did not differ. This may be explained by differences in feeding and growth. Fish fed the freshwater diet (tubifex worms) were poor feeders and 5 times smaller (by the end of the experiment) than fish fed commercial pellets. This is probably associated with the enhanced palatability and nutritional quality of the commercial pellet feed, which was specifically designed for barramundi aquaculture. As such, the fish fed tubifex worms probably had a lower proportion of experimental dietary sulfur incorporated into their otoliths (even though elemental sulfur concentrations were similar between the 2 diet types). The nutritional characteristics of food may also directly influence the effect diet has on sulfur isotope ratios in the otolith. Different levels of inorganic matter in the diet, for instance, can alter the proportion of inorganic and organic sulfur in animal tissues, which in turn affects the isotope ratio (McCutchan et al. 2003). Analysing the nutritional characteristics of the diet treatments in future studies would be a critical step to clarify the mechanisms of how diet affects sulfur isotope ratios in otolith carbonate (see Nelson et al. 2011 for similar experimental work on carbon isotopes).

Only 5 known studies have investigated the use of sulfur isotopes in biominerals, with 4 based on otolith carbonate and mostly focussed on tracking the movement and life history of salmonid fish (Weber et al. 2002, Godbout et al. 2010, Johnson et al. 2012, Limburg et al. 2015). The potential application of sulfur isotopes in biominerals is much more extensive, ranging from environmental reconstruction to the study of evolution (Table 3). Sulfur isotopes are particularly useful for determining the movement patterns of animals across the land–sea–freshwater interface, and can be used to address issues in conservation and natural resource management (i.e. diet and habitat use of endangered or commercially important species). In addition, the use of biominerals allows ecological and environmental processes to be tracked over time, extending current applications (Table 3). For example, sulfur dioxide pollution, which can have serious impacts to ecosystems, human health and climate, could be potentially

Table 3. Potential ecological and environmental application of sulfur isotope signatures. *Italics* = tissue and/or mineral type

Application	Examples
Environmental reconstruction	
Provenance and loading of SO_2 emissions	Natural and anthropogenic sources of atmospheric sulfur tracked using *lichen thalli* (Barros et al. 2015) and *speleothem carbonate* (Wynn et al. 2010).
Hypoxic events in aquatic environments	Preliminary correlation of anoxic conditions to $\delta^{34}S$ values in *otolith aragonite* (Limburg et al. 2015).
Seawater $\delta^{34}S$ and paleoclimate	Carboniferous seawater $\delta^{34}S$ record reconstructed using structurally substituted sulfate in *brachiopod shells* (Kampschulte et al. 2001).
Diet and food webs	
Reconstruction of hunting, fishing and farming practises	Exploitation patterns of ancient fish populations reconstructed using archaeological fish and human *bone collagen* (Nehlich et al. 2013, Sayle et al. 2016).
Importance of different primary producers as food	Contribution of different plants and algae to marine food webs determined through analysis of *seagrass* and *saltmarsh plants* (Connolly et al. 2004).
Dietary provenance	Variations in *fish muscle* $\delta^{34}S$ related to planktonic vs. benthic feeding strategies (Fry & Chumchal 2011).
Movement and residency	
Between marine, estuarine and freshwater environments	Resident and transient fish identified across estuarine salinity zones through analysis of fish *muscle* (Fry & Chumchal 2011).
Between coastal and inland environments	Distance of sheep from coast tracked using $\delta^{34}S$ values in *wool* (Zazzo et al. 2011).
Identification of critical habitats	Freshwater identified as critical to an endangered manatee through analysis of *bone collagen* (MacAvoy et al. 2015).
Evolutionary biology	
Evolutionary transitions	Potential to define major evolutionary transitions of vertebrates between marine, freshwater and terrestrial environments through analysis of *apatite* in *bones* and *teeth* (Goedert et al. 2016).

tracked in biominerals (i.e. atmospheric sulfur is assimilated by plants and algae, through which it is then passed onto aquatic and terrestrial consumers). Understanding changes in the loading and provenance of sulfur dioxide in the atmosphere could provide critical information regarding the efficacy of legislation and mitigation measures (Wynn et al. 2010, Barros et al. 2015). Furthermore, structurally substituted sulfate in biogenic carbonates can provide an accurate record of the sulfur isotope composition of ancient oceans, helping to uncover global environmental change over geological time scales (Kampschulte & Strauss 2004, Perrin et al. 2017). Determining the presence of structurally substituted sulfate in other structures (e.g. otoliths) would further extend the potential of sulfur isotope analysis in biominerals.

The limited number of studies conducted to date, however, is telling of the challenges that may be faced when analysing sulfur isotopes in biominerals. Standard techniques (i.e. micromilling and subsequent analysis using mass spectrometry) used for the targeted analysis of light isotopes in otoliths, for instance, cannot be used due to the low concentrations of sulfur in the otolith. Although SIMS is well suited to the analysis of biominerals (high spatial resolution and low detection limits), availability of instrumentation is limited (in our experience), as well as the number of samples that can be analysed within a given time frame (small sample sizes being a limitation of this study and other studies analysing sulfur isotopes in otoliths). Further, sulfur isotope standards for otoliths and other biominerals need to be developed, commercially or in-house, so data cannot only be calibrated against the internationally accepted standard (VCDT), but also be comparable among laboratory and field studies. This calibration would also allow otolith values to be directly related to diet and water values and allow proportional contributions of diet and water to be calculated (e.g. Doubleday et al. 2013). Standards with a known isotopic value can be developed from relevant biominerals, if material with homogenous sulfur isotope distributions can be found (e.g. coral standard used for speleothem carbonate; Wynn et al. 2010), or be synthetically produced (e.g. Weber et al. 2002). Despite these challenges, sulfur isotope research crosses many disciplines, from geology to archaeology and food science; tapping into these multi-disciplinary studies will help progress analytical methods and protocols.

Biominerals allow us to reconstruct long-term ecological and environmental datasets retrospectively, which can be logistically difficult and expensive to obtain using traditional observational approaches. Such datasets are rare, particularly for aquatic environments (Richardson & Poloczanska 2008), but are vital for determining how populations and communities respond to environmental change, as well as for predicting what our future ecosystems may look like. Therefore, improving analytical methods and extending current applications of sulfur isotope analysis in biominerals is a worthwhile pursuit.

Acknowledgements. We thank Kayla Gilmore and Matthew McMillan for their assistance with fish husbandry and otolith dissections. This research was funded by an ARC Discovery grant (DP110100716) and Future Fellowship (FT100100767) awarded to B.M.G. The Nu instruments CF-IRMS and associated elemental analyzer were funded through an ARC LIEF grant (LE120100054). All animal handling and experimental procedures were approved by the Animal Ethics Committee at the University of Adelaide (permit no. S-2011-010). We acknowledge the facilities, and the scientific and technical assistance of the Australian Microscopy & Microanalysis Research Facility at the Centre for Microscopy, Characterisation & Analysis, The University of Western Australia, a facility funded by the University, State and Commonwealth Governments.

LITERATURE CITED

Barros C, Pinho P, Durão R, Augusto S, Máguas C, Pereira MJ, Branquinho C (2015) Disentangling natural and anthropogenic sources of atmospheric sulfur in an industrial region using biomonitors. Environ Sci Technol 49:2222–2229

Boecklen WJ, Yarnes CT, Cook BA, James AC (2011) On the use of stable isotopes in trophic ecology. Annu Rev Ecol Evol Syst 42:411–440

Campana SE (1999) Chemistry and composition of fish otoliths: pathways, mechanisms and applications. Mar Ecol Prog Ser 188:263–297

Connolly RM, Guest MA, Melville AJ, Oakes JM (2004) Sulfur stable isotopes separate producers in marine foodweb analysis. Oecologia 138:161–167

Dauphin Y, Dufour E (2008) Nanostructures of the aragonitic otolith of cod (*Gadus morhua*). Micron 39:891–896

Doubleday ZA, Izzo C, Woodcock SH, Gillanders BM (2013) Relative contribution of water and diet to otolith chemistry in freshwater fish. Aquat Biol 18:271–280

Fry B, Chumchal MM (2011) Sulfur stable isotope indicators of residency in estuarine fish. Limnol Oceanogr 56: 1563–1576

Godbout L, Trudel M, Irvine JR, Wood CC, Grove MJ, Schmitt AK, McKeegan KD (2010) Sulfur isotopes in otoliths allow discrimination of anadromous and non-anadromous ecotypes of sockeye salmon (*Oncorhynchus nerka*). Environ Biol Fishes 89:521–532

Goedert J, Fourel F, Amiot R, Simon L, Lécuyer C (2016) High precision $^{34}S/^{32}S$ measurements in vertebrate bioapatites using purge and trap EA IRMS technology. Rapid Commun Mass Spectrom 30:2002–2008

Izzo C, Doubleday ZA, Schultz AG, Woodcock SH, Gillanders BM (2015) Contribution of water chemistry and fish condition to otolith chemistry: comparisons across salinity environments. J Fish Biol 86:1680–1698

Izzo C, Doubleday ZA, Gillanders BM (2016) Where do elements bind within the otoliths of fish? Mar Freshw Res 67:1072–1076

Izzo C, Manetti D, Doubleday ZA, Gillanders BM (2017) Calibrating the element composition of *Donax deltoides* shells as a palaeo-salinity proxy. Palaeogeogr Palaeoclimatol Palaeoecol 484:89–96

Johnson RC, Weber PK, Wikert JD, Workman ML, MacFarlane RB, Grove MJ, Schmitt AK (2012) Managed metapopulations: Do salmon hatchery 'sources' lead to in-river 'sinks' in conservation? PLOS ONE 7:e28880

Kalish JM (1989) Otolith microchemistry: validation of the effects of physiology, age and environment on otolith composition. J Exp Mar Biol Ecol 132:151–178

Kampschulte A, Strauss H (2004) The sulfur isotopic evolution of Phanerozoic seawater based on the analysis of structurally substituted sulfate in carbonates. Chem Geol 204:255–286

Kampschulte A, Bruckschen P, Strauss H (2001) The sulphur isotopic composition of trace sulphates in Carboniferous brachiopods: implications for coeval seawater, correlation with other geochemical cycles and isotope stratigraphy. Chem Geol 175:149–173

Li P, Mai K, Trushenski J, Wu G (2009) New developments in fish amino acid nutrition: towards functional and environmentally oriented aquafeeds. Amino Acids 37: 43–53

Limburg KE, Olson C, Walther Y, Dale D, Slomp CP, Høie H (2011) Tracking Baltic hypoxia and cod migration over millennia with natural tags. Proc Natl Acad Sci USA 108: E177–E182

Limburg KE, Walther BD, Lu Z, Jackman G and others (2015) In search of the dead zone: use of otoliths for tracking fish exposure to hypoxia. J Mar Syst 141:167–178

MacAvoy SE, Bacalan V, Kazantseva M, Rhodes J, Kim K (2015) Sulfur isotopes show importance of freshwater primary production for Florida manatees. Mar Mamm Sci 31:720–725

Martin JE, Tacail T, Balter V, Smith A (2017) Non traditional isotope perspectives in vertebrate palaeobiology. Palaeontology 60:485–502

McCutchan JH, Lewis WM, Kendall C, McGrath CC (2003) Variation in trophic shift for stable isotope ratios of carbon, nitrogen, and sulfur. Oikos 102:378–390

McFadden A, Wade B, Izzo C, Gillanders B, Lenehan C, Pring A (2016) Quantitative electron microprobe mapping of otoliths suggests elemental incorporation is affected by organic matrices: implications for the interpretation of otolith chemistry. Mar Freshw Res 67:889–898

Mugiya Y, Iketsu H (1987) Uptake of asparatic acid and sulfate by calcified tissues in goldfish and tilapia. Bull Fac Fish Hokkaido Univ 38:185–190

Murayama E, Takagi Y, Ohira T, Davis JG, Greene MI, Nagasawa H (2002) Fish otolith contains a unique structural protein, otolin-1. Eur J Biochem 269:688–696

Nehlich O (2015) The application of sulphur isotope analyses in archaeological research: a review. Earth Sci Rev 142:1–17

Nehlich O, Barrett JH, Richards MP (2013) Spatial variability in sulphur isotope values of archaeological and mod-

ern cod (*Gadus morhua*). Rapid Commun Mass Spectrom 27:2255–2262

Nelson J, Hanson CW, Koenig C, Chanton J (2011) Influence of diet on stable carbon isotope composition in otoliths of juvenile red drum *Sciaenops ocellatus.* Aquat Biol 13: 89–95

Perrin J, Rivard C, Vielzeuf D, Laporte D and others (2017) The coordination of sulfur in synthetic and biogenic Mg calcites: the red coral case. Geochim Cosmochim Acta 197:226–244

Peterson BJ, Fry B (1987) Stable isotopes in ecosystem studies. Annu Rev Ecol Syst 18:293–320

Richardson AJ, Poloczanska ES (2008) Under-resourced, under threat. Science 320:1294–1295

Rowell K, Dettman DL, Dietz R (2010) Nitrogen isotopes in otoliths reconstruct ancient trophic position. Environ Biol Fishes 89:415–425

Rubenstein DR, Hobson KA (2004) From birds to butterflies: animal movement patterns and stable isotopes. Trends Ecol Evol 19:256–263

Sayle KL, Hamilton WD, Cook GT, Ascough PL, Gestsdóttir H, McGovern TH (2016) Deciphering diet and monitoring movement: multiple stable isotope analysis of the viking age settlement at Hofstaðir, Lake Mývatn, Iceland. Am J Phys Anthropol 160:126–136

Thode HG (1991) Sulfur isotopes in nature and the environment: an overview. In: Krouse HR, Grinenko VA (eds) Stable isotopes: natural and anthropogenic sulfur in the environment. John Wiley & Sons, Chichester, p 1–26

Trust BA, Fry B (1992) Stable sulphur isotopes in plants: a review. Plant Cell Environ 15:1105–1110

Weber PK, Hutcheon ID, McKeegan KD, Ingram BL (2002) Otolith sulfur isotope method to reconstruct salmon (*Oncorhynchus tshawytscha*) life history. Can J Fish Aquat Sci 59:587–591

Wynn PM, Fairchild IJ, Frisia S, Spötl C, Baker A, Borsato A (2010) High-resolution sulphur isotope analysis of speleothem carbonate by secondary ionisation mass spectrometry. Chem Geol 271:101–107

Zazzo A, Monahan F, Moloney A, Green S, Schmidt O (2011) Sulphur isotopes in animal hair track distance to sea. Rapid Commun Mass Spectrom 25:2371–2378

Editorial responsibility: Yves Cherel, Villiers-en-Bois, France

Submitted: February 28, 2017; Accepted: April 23, 2018
Proofs received from author(s): June 7, 2018

Vol. 598: 167–185, 2018
https://doi.org/10.3354/meps12302

MARINE ECOLOGY PROGRESS SERIES
Mar Ecol Prog Ser

Published June 28[§]

Contribution to the Theme Section 'Innovative use of sclerochronology in marine resource management'

Validation of otolith $\delta^{18}O$ values as effective natural tags for shelf-scale geolocation of migrating fish

Audrey M. Darnaude[1,2,*], Ewan Hunter[2,3]

[1]CNRS, UMR 9190 MARBEC, Université de Montpellier, Place Eugène Bataillon, 34095 Montpellier, France
[2]Centre for Environment, Fisheries and Aquaculture Science, Lowestoft Laboratory, Lowestoft, Suffolk NR33 0HT, UK
[3]School of Environmental Sciences, University of East Anglia, Norwich Research Park, Norwich NR4 7TJ, UK

ABSTRACT: The oxygen isotopic ratio of fish otoliths is increasingly used as a 'natural tag' to assess provenance in migratory species, with the assumption that variations in $\delta^{18}O$ values closely reflect individual ambient experience of temperature and/or salinity. We employed archival tag data and otoliths collected from a shelf-scale study of the spatial dynamics of North Sea plaice *Pleuronectes platessa* L., to examine the limits of otolith $\delta^{18}O$-based geolocation of fish during their annual migrations. Detailed intra-annual otolith $\delta^{18}O$ measurements for 1997–1999 from individuals of 3 distinct sub-stocks with different spawning locations were compared with $\delta^{18}O$ values predicted at the monthly, seasonal and annual scales, using predicted sub-stock specific temperatures and salinities over the same years. Spatio-temporal variation in expected $\delta^{18}O$ values (–0.23 to 2.94‰) mainly reflected variation in temperature, and among-zone discrimination potential using otolith $\delta^{18}O$ varied greatly by temporal scale and by time of year. Measured otolith $\delta^{18}O$ values (–0.71 to 3.09‰) largely mirrored seasonally predicted values, but occasionally fell outside expected $\delta^{18}O$ ranges. Where mismatches were observed, differences among sub-stocks were consistently greater than predicted, suggesting that in plaice, differential sub-stock growth rates and physiological effects during oxygen fractionation enhance geolocation potential using otolith $\delta^{18}O$. Comparing intra-annual $\delta^{18}O$ values over several consecutive years for individuals with contrasted migratory patterns corroborated a high degree of feeding and spawning site fidelity irrespective of the sub-stock. Informed interpretation of otolith $\delta^{18}O$ values can therefore provide relatively detailed fisheries-relevant data not readily obtained by conventional means.

KEY WORDS: Fish migration · Oxygen · Stable isotopes · Natural tag · Site fidelity · Plaice · *Pleuronectes platessa*

INTRODUCTION

The distributions of marine species are often discontinuous in time and space, usually as a consequence of spatial and temporal shifts in the physical and biological characteristics of oceanic habitats (Hixon et al. 2002). In fishes, distribution shifts further reflect ontogenetic and/or seasonal migrations driven primarily by the physiological requirements of maturation and subsequent annual reproductive cycles (Kimirei et al. 2013). Understanding them is therefore particularly important for species conservation and fisheries management (Pulliam 1988, Botsford et al. 2009).

In recent decades, sustained research focus on movement ecology has greatly improved our understanding of population structure and lifetime movements in many commercially exploited and conservation-sensitive fishes (e.g. Righton et al. 2010, Block et al. 2011, Hussey et al. 2015, Hays et al. 2016). However, direct observation of fully marine fishes in their natural environment over annual migration cycles remains challenging (Metcalfe et al. 2008). The mechanical limitations of tracking and tagging tools

*Corresponding author: audrey.darnaude@cnrs.fr

[§]Advance View was available online November 29, 2017

Publisher: Inter-Research · www.int-res.com

and hardware still largely restrict studies to shallow, mainly inshore areas, and to limited portions of the adult life in large, often predatory, fishes (Hays et al. 2016).

To describe the stock structure and spatial dynamics of fish either too small or too vulnerable to tag using satellite or archival tags, scientists increasingly apply 'natural tags', most notably the continuously accreting and physiologically inert calcified otoliths. Still a cornerstone of assessment biology, the interpretation of otoliths has long surpassed counting the annular rings to estimate fish age, and fine-scale interpretation of otolith chemistry now offers significant insights into life-history characteristics, stock structure and migratory behaviour (Morrongiello et al. 2012, Geffen et al. 2016, Grønkjær 2016). Because otoliths continuously log environmental data throughout life, and because otolith material is rarely resorbed or physiologically altered after deposition (Mugiya & Uchimura 1989, Campana 1999), otoliths provide a precisely dated and seasonally resolved record of fish lifetime environmental history (Thorrold et al. 1997). The interrogation of otolith structure and chemistry can provide coarse estimates of past geographical location ('geolocation'), at least in those species that migrate between water masses with sufficiently different characteristics (Campana 1999).

Since the isotopic ratio ^{18}O:^{16}O (expressed as $\delta^{18}O$) in biocarbonates varies with both water temperature and isotopic composition ($\delta^{18}O$) at the time of deposition (Epstein & Mayeda 1953), otolith $\delta^{18}O$ is a particularly promising marker for studying marine fish migrations. From the first estimations of seawater temperatures derived from the $\delta^{18}O$ of fish otoliths by Devereux (1967), otolith $\delta^{18}O$ has increasingly been applied to identify marine fish origin (e.g. Gao & Bean 2008, Rooker et al. 2008, Trueman et al. 2012), differentiate between residents and migrants (e.g. Northcote et al. 1992, Bastow et al. 2002, Blamart et al. 2002, Ayvazian et al. 2004) and to distinguish between mixing and non-mixing stocks (e.g. Stephenson 2001, Rooker & Secor 2004, Ashford & Jones 2007, Newman et al. 2010). However, otolith $\delta^{18}O$ heterogeneity across water temperature–$\delta^{18}O$ combinations has frequently been observed (Høie et al. 2004, Storm-Suke et al. 2007, Godiksen et al. 2010, Geffen 2012), suggesting that the isotopic fractionation between otolith aragonite and ambient water may vary between and within species. Although this might preclude identifying geographical movement using otolith $\delta^{18}O$, few attempts have been made so far to ground-truth the efficiency of this natural tag as a tool for geolocation.

As a first step toward this goal, migratory and environmental data gathered from hundreds of adult plaice *Pleuronectes platessa* L. tagged with archival tags were recently coupled with the annual $\delta^{18}O$ signatures laid down simultaneously in the otoliths of 24 tagged fish, from 3 'sub-stocks' that have discrete distributions for most of the year (Darnaude et al. 2014). Comparison between measured and expected $\delta^{18}O$ values at this temporal scale provided strong evidence that annual $\delta^{18}O$ signatures are accurate predictors of plaice sub-stock membership in the North Sea, the otolith $\delta^{18}O$ values of wild plaice largely reflecting environmental temperature and salinity at the time of deposition. However, variation in adult physiology among local sub-stocks and at certain seasons could also be partly responsible for the observed $\delta^{18}O$ differences.

Here, we draw on the same sets of otolith and environmental data to further explore the spatial and temporal limits of otolith $\delta^{18}O$ values as a geolocation tool. For individuals representative of the same 3 sub-stocks and their main migration routes, we reanalysed a subset of the original otoliths for intra-annual $\delta^{18}O$ values gathered over multiple years, including those prior to the commencement of tag recording. By comparing these intra-annual $\delta^{18}O$ signatures with detailed multi-annual predictions of $\delta^{18}O$ (from tag-derived bottom temperatures and salinities) across the full geographical range of the sampled plaice, we investigated (1) how precisely intra-annual variations in temperature and salinity predicted seasonal otolith $\delta^{18}O$ differences among the 3 sub-stocks, (2) areas and seasons where otolith $\delta^{18}O$ could be used for geolocation in the North Sea and English Channel, and (3) whether seasonal differences in otolith $\delta^{18}O$ could identify site fidelity to geographically discrete local summer feeding grounds and winter spawning areas. This *in situ* validation approach, although still novel, is an essential pre-requisite if otolith $\delta^{18}O$ is ever to be meaningfully applied as an alternative natural tag for describing fish population dynamics for application in fisheries management.

MATERIALS AND METHODS

The otoliths and environmental data used in this work derive from an extensive study of plaice tagged with archival tags and released at various locations in the North Sea between 1993 and 2000 (see Hunter et al. 2004 for full details, including hardware deployed and tagging methodology). Of 785 mature, predomi-

nantly female plaice released, 194 individuals were recovered, with tag-recorded environmental data of between 2 and 512 d. The archival tags recorded ambient water temperatures (±0.2°C) and pressures at 10 min intervals throughout the period during which the fish were at liberty, providing detailed information on the environmental conditions experienced, but also allowing reconstruction of fish movements. When tagged plaice remained on the seabed for one or more tidal cycles, the times of high water and accompanying tidal ranges measured were used to identify fish geographical position using the tidal location method (see Hunter et al. 2003b for full details). For each individual, a best-fit track was then reconstructed by fitting a piece-wise linear curve through the release position, and any sequential geolocations and the recapture position (full details in Hunter et al. 2003b). This allowed the generation of daily geolocations for every tagged fish, providing long-term knowledge on the local stock structure and adult annual migrations (see Hunter et al. 2004) but also access to location-specific concomitant otolith records and environmental data.

Intact otoliths were returned along with the archival tags for 83 fish, amongst which individuals with data records ≥3 mo were released and recaptured mainly between 1997 and 1999 (Darnaude et al. 2014). Consequently, we chose these 3 successive years to reconstruct multi-annual environmental conditions prevailing over the full observed distribution range to compare with the seasonal $\delta^{18}O$ signal simultaneously laid down in the otoliths of the same fish (see section 'Prediction of expected otolith $\delta^{18}O$ values per substock or area').

Plaice distribution and behaviour in relation to environmental conditions experienced

Plaice are not randomly distributed in the North Sea, but form 3 separate feeding aggregations ('sub-stocks') which remain geographically discrete from May to October each year (Hunter et al. 2004): sub-stock A in the Northern (NNS), sub-stock B in the Eastern (ENS) and sub-stock C in the Western (WNS) North Sea (Fig. 1). Between November and April, all 3 sub-stocks migrate to and from predominantly southerly located spawning areas where they mix. However, the timing and extent of the spawning migration varies both among and between sub-stocks (Fig. 1). Most plaice remain in the North Sea throughout the year (Hunter et al. 2004). The small

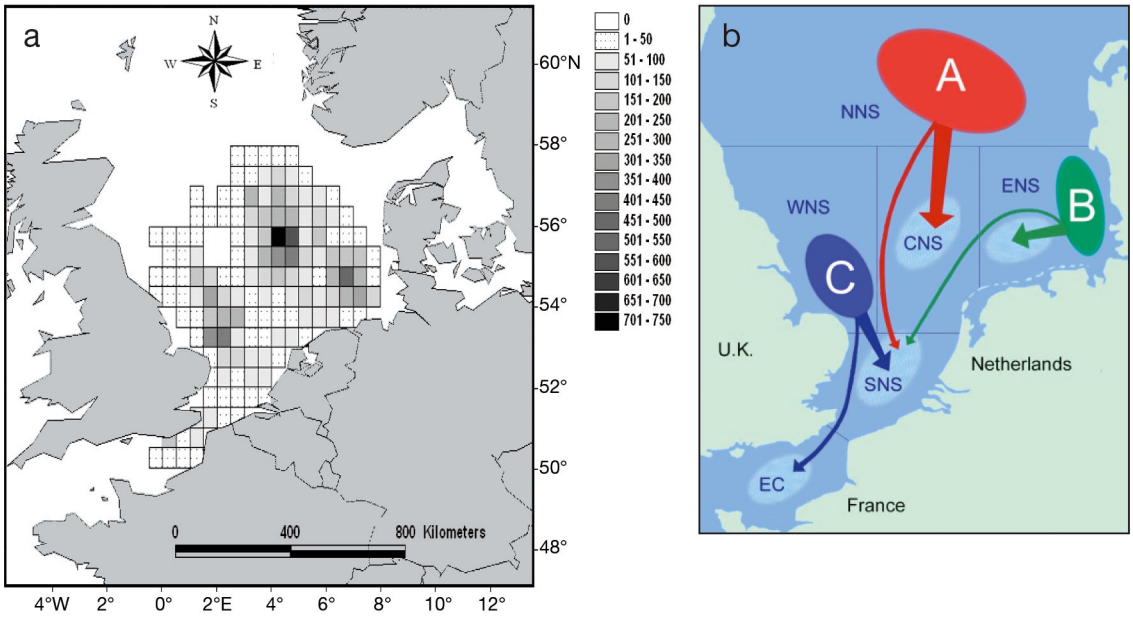

Fig. 1. North Sea areas and plaice *Pleuronectes platessa* sub-stocks studied. (a) The global area over which plaice adults migrate (non-empty grid cells on the map) between their (b) summer feeding aggregations (sub-stocks A, B and C) and winter spawning grounds (light blue areas: Van Neer et al. 2004) was divided into 6 regions: English Channel (EC: <51.00° N), Southern North Sea (SNS: 51.00–52.49° N), Western North Sea (WNS: 52.50–55.49° N; <2.50° E), Central North Sea (CNS: 52.50–55.49° N, 2.50–4.99° E), Eastern North Sea (ENS: 52.50–55.49° N, ≥5.00° E) and Northern North Sea (NNS: ≥55.50° N). The legend in panel a shows the total number of geolocations obtained per grid cell during the 1993–2000 tagging experiment (Hunter et al. 2004), while in b, coloured arrows show migration routes typical of each sub-stock (Fig. 1b modified from Darnaude et al. 2014)

proportion of plaice from sub-stock C that spawn in the English Channel (EC) do so only in December or in January, spending the remainder of the winter in the Southern North Sea (SNS) (Hunter et al. 2004). There, they mix with the individuals of the same sub-stock that spawn in the SNS (mainly in January), but also with fish of sub-stocks A and B that also spawn in this area (in February and March). Similarly, in transit to their spawning grounds in the SNS, the fish from sub-stock A mix with those of sub-stock B in the ENS (from December to April), and some fish from all sub-stocks mix in the Central North Sea (CNS) from January to March, either because they spawn there (sub-stock A) or because their spawning migration takes them through this area (sub-stocks B and C spawning in the SNS or the EC). The environmental conditions encountered should therefore mostly differ among all 3 sub-stocks from May to October. During the rest of the year, environmental conditions are migration-type dependent, but will not necessarily reflect the final location of spawning since the time spent on the spawning grounds (in the EC, SNS, ENS or CNS, depending on the migration type) is limited when compared to the time spent migrating between them (through NNS, CNS and sometimes SNS for sub-stock A; through ENS and sometimes CNS and SNS for sub-stock B; through WNS, SNS and sometimes EC for sub-stock C).

Otolith selection, preparation and analysis

The 2 biggest otoliths (paired sagittae) are not identical in plaice: the left sagitta is symmetric, the right asymmetric. Although the paired otoliths exhibit differential growth from metamorphosis (Lychakov et al. 2008), this does not induce differences in seasonal oxygen isotope signature between them (Geffen 2012). Therefore, to maximize time-resolution when sampling the distal area laid down during tag recording time, frontal sections of right sagittae were used, the fine-scale (intra-annual) $\delta^{18}O$ signatures obtained being used to evaluate the potential for otolith $\delta^{18}O$-based seasonal estimates of geolocation. For this, the right otoliths of 24 mature females (8 from each sub-stock), with individual data records ≥78 d (Table 1), were selected. This sub-sample of fish was representative of the principal migration types observed for each sub-stock (Fig. 1). Each individual data record allowed unequivocal identification of spawning areas and feeding grounds for at least one annual cycle, sometimes two (Table 1). Furthermore, for 12 fish representative of all migration types (2 each, Fig. 1), tag data records allowed unequivocal identification of both the winter spawning areas and the summer feeding grounds in 1998 (Table 1). The comparison of their otolith $\delta^{18}O$ signatures, in particular those for the winters 1997–98 and 1998–99, allowed testing of the extent to which otolith $\delta^{18}O$ could identify differences in spawning location within and among sub-stocks.

Otolith preparation was similar for all fish. The right otoliths (sagittae) were cleaned of organic surface debris, embedded in clear epoxy resin and cut along the frontal plane containing the core. Each otolith section (~1000 µm thick) was then ground down to 500–600 µm until the otolith edge was perpendicular to the section surface, and polished until superficial scratches were removed on both sides. All sections were glued onto glass slides using epoxy resin, and their ventral side (facing up) was photographed under reflected light. Glass slides supporting the sections were then rinsed with distilled water, dried overnight in a clean vertical laminar flow workstation and stored in acid-washed plastic envelopes prior to powder sampling for analysis. More details about these initial steps of otolith preparation can be found in Darnaude et al. (2014).

Seasonality of opaque-translucent otolith banding fluctuates with fish age and latitude in North Sea plaice (Van Neer et al. 2004), implying the potential for geographic and individual variation in otolith growth during the year. However, the opaque zone is largely accreted during April to September, and the hyaline (or translucent) zone from October to March (Van Neer et al. 2004, authors' pers. obs.). Therefore, in order to facilitate assessment of otolith $\delta^{18}O$ potential for sub-stock discrimination at the sub-annual scale, the year was divided into 4 periods ('seasons'), each of 3 mo: February to April (late winter/early spring: LW/ES), May to July (late spring/early summer: LS/ES), August to October (late summer/early autumn: LS/EA) and November to January (late autumn/early winter: LA/EW). Environmental $\delta^{18}O$ records during these 4 seasons are easy to locate on the otoliths, the material laid down during LW/ES being positioned at the translucent–opaque border each year, that for LS/EA occurring on the opaque–translucent border, and those for LS/ES and LA/EW sitting intermediate between these two.

Individual ages for all fish were assessed previously from transverse sections made on the left otoliths (Darnaude et al. 2014). Powder samples corresponding to the 4 seasons (see above) were then

Table 1. Details of female plaice *Pleuronectes platessa* assessed for intra-annual variations in otolith $\delta^{18}O$ signatures. CNS: Central North Sea; ENS: Eastern North Sea; SNS: Southern North Sea; EC: English Channel. For each sub-stock (see Fig. 1), individuals highlighted in grey were used to investigate fidelity to summer feeding grounds and spawning sites. DST: data storage tag. For all fish, the year and age (in yr) analyzed for otholith $\delta^{18}O$ signatures are indicated in **bold** and x2 indicates when the breeding area was identified for 2 consecutive years in the same fish

ID	Recapture date	Size (cm)	Age (yr)	No. days of DST record (start & end dates)	Breeding area (breeding month) identified from DST records	Year(s) analysed for $\delta^{18}O$ (age)
Sub-stock A						
A-1	Jul 99	40	12	386 (Dec 97–Dec 98)	CNS (December)	1995–**1998** (9–**11**)
A-2	May 99	44	14	512 (Dec 97–Apr 99)	CNS (January) x2	1997 & **1998** (12–**13**)
A-3	Jan 99	40	5	398 (Dec 97–Jan 99)	CNS (January)	**1998** (**5**)
A-4	Dec 98	40	8	365 (Dec 97–Dec 98)	CNS (January)	1997 & **1998** (7–**8**)
A-5	Sep 98	38	6	272 (Dec 97–Aug 98)	CNS (February)	**1997** (**5**)
A-6	Mar 98	38	9	134 (Oct 97–Mar 98)	CNS (January)	1996 & **1997** (7–**8**)
A-7	Jun 00	37	6	354 (Feb 99–Feb 00)	SNS (February)	1998–**1999** (5–**6**)
A-8	Sep 98	40	6	78 (Oct 97–Jan 98)	SNS (February)	1997 & **1998** (5–**6**)
Sub-stock B						
B-1	Dec 98	48	7	382 (Oct 97–Nov 98)	SNS (January) x2	1996 – **1998** (5–**7**)
B-2	Feb 99	46	12	317 (Oct 97–Aug 98)	SNS (January)	1997 & **1998** (10–**11**)
B-3	Oct 99	38	7	194 (Feb–Aug 99)	SNS (February)	**1999** (**7**)
B-4	Feb 98	36	6	104 (Nov 97 – Feb 98)	SNS (January)	**1997** (**5**)
B-5	Jan 99	41	7	262 (Oct 97–Jul 98)	ENS (January)	1996 & **1997** (6–**7**)
B-6	Jun 98	41	5	202 (Nov 97–May 98)	ENS (February)	1997 & **1998** (4–**5**)
B-7	Apr 98	39	6	153 (Nov 97–Apr 98)	ENS (February)	**1997** (**5**)
B-8	Feb 98	40	7	97 (Oct 97–Jan 98)	ENS (January)	**1997** (**6**)
Sub-stock C						
C-1	Apr 99	52	9	411 (Feb 98–Apr 99)	EC (December) x2	1996– **1998** (6–**8**)
C-2	Nov 99	36	7	384 (Oct 98–Oct 99)	EC (January)	1998 & **1999** (6–**7**)
C-3	Mar 00	39	12	303 (Feb 98–Dec 99)	EC (January)	**1999** (**11**)
C-8	Jun 98	39	11	109 (Feb–May 98)	EC (December)	**1997** (**10**)
C-4	Aug 99	38	5	231 (Oct 98–May 99)	SNS (January)	**1999** (**5**)
C-5	Oct 99	41	10	223 (Feb–Sep 99)	SNS (January)	1998 & **1999** (9–**10**)
C-6	Sep 98	44	10	221 (Dec 97–Jul 98)	SNS (December)	1997 & **1998** (9–**10**)
C-7	Sep 99	41	9	182 (Feb–Aug 98)	SNS (January)	**1998** (**9**)

collected from the otolith frontal section, using a computer-controlled micro-milling system (New Wave Research 'MicroMill'). Sampling always covered the annual growth band(s), reflecting the life of the fish throughout the archival tag data recording period. For the 12 individuals with tag records allowing unequivocal identification of both spawning area and feeding grounds in 1998 (2 for each migration type, Table 1), seasonal powder samples were also gathered for the 2 yr preceding initial capture to investigate fish multi-annual fidelity to spawning and feeding grounds.

The positions of opaque and translucent zones on magnified images of the sections were used to identify data storage tag (DST) recording periods in the otoliths, and were digitized to provide navigational input to the instrument. Depending on the fish and the year of life sampled, the respective widths of the opaque and translucent bands allowed extraction of 1 to 3 otolith powder samples between the opaque–translucent borders. Therefore, 1 to 12 sequential layers (of ~50–80 µm width and 450 µm depth) were milled per otolith, from the distal edge (most recent growth) inwards. The respective positions of the samples on the otoliths were used to assign them retrospectively to seasons. The corresponding powder samples (40–50 µg in weight) were collected separately and analysed at the Woods Hole Oceanographic Institution, MA, USA, using a Finnigan MAT252 mass spectrometer system with a Kiel III carbonate device. All isotopic values were reported relative to the international carbonate standard Vienna Pee Dee Belemnite (VPDB), using the international standard delta notation:

$$\delta^{18}O = [(R_{sample}/R_{standard}) - 1] \times 1000\ (‰) \quad (1)$$

where R is the ^{18}O:^{16}O ratio in the sample or standard. Analytical precision for $\delta^{18}O$ values, based on the SD of daily analysis of NBS-19 carbonate standard, was ±0.07‰.

Prediction of expected otolith $\delta^{18}O$ values per sub-stock or area

Using all geolocations derived from the 194 tagged fish recaptured between 1993 and 2000 (n = 13 512), monthly distributions of adult plaice were summarized using grid-maps, showing the cells (0.5° latitude × 0.5° longitude) containing 80% of geolocations for each sub-stock (Fig. 1). Daily seabed temperatures and salinities in 1997, 1998 and 1999 were generated for corresponding grid cells using the general estuarine transport model (GETM), developed and validated for realistic 3-dimensional simulations of temperature and salinity in the North Sea (Stips et al. 2004). The model domain extends from a boundary in the western English Channel (–5° E) into the North Sea with an eastern boundary in the Baltic (16° E) and then northwards as far as the Shetland Isles (60° N) at a resolution of ~6 nautical miles and with 25 terrain-following vertical levels. Meteorological forcing in the model for the 3 studied years was derived from the European Centre for Medium-range Weather Forecasting ERA datasets. Tidal boundaries were calculated from Topex-Poseidon satellite altimetry, and temperature and salinity boundary conditions were taken from the climatologic predictions of the POLCOMS S12 model (http://cobs.pol.ac.uk/modl/metfcst/POLCOMS_DOCUMENTATION/).

For each sub-stock or area in the study zone (Fig. 1), daily GETM temperature and salinity estimates for each grid cell and year were used to predict corresponding otolith $\delta^{18}O$ values. For this, ambient water (w) $\delta^{18}O$ values relative to the Vienna Pee Dee Belemnite standard (VSMOW) were derived from salinity (S) estimates using the equation of Harwood et al. (2008) for the North Sea:

$$\delta^{18}O_w\,(\text{VSMOW}) = 0.274 \times S - 9.3 \quad (2)$$

then converted into $\delta^{18}O_w$ relative to the Vienna Pee Dee Belemnite standard (VPDB) using the equation of Coplen et al. (1983):

$$\delta^{18}O_w\,(\text{VPDB}) = 0.97002 \times \delta^{18}O_w\,(\text{VSMOW}) - 29.98 \quad (3)$$

Finally, the corresponding temperature estimates (T, in K) were incorporated in order to predict otolith $\delta^{18}O$ values ($\delta^{18}O_o$) using the theoretical equation for inorganic aragonite deposition (Kim et al. 2007):

$$1000\ \ln\alpha = \left(17.88 \times \frac{1000}{T}\right) - 31.14, \quad \text{with } \alpha = \frac{1000 + \delta^{18}O_o}{1000 + \delta^{18}O_w} \quad (4)$$

The resulting daily maps of otolith $\delta^{18}O$ values were used to simulate specific range of monthly otolith $\delta^{18}O$ signatures for each sub-stock or area.

Prediction of individual otolith $\delta^{18}O$ values during tag recording time

For the 12 fish representative of the 6 main migration types in 1998 (Table 1), specific daily otolith $\delta^{18}O$ values between release and recapture were predicted using the tag-recorded temperatures. Equivalent ambient salinities at all successive individual daily geolocations were extracted from the CEFAS database for North Sea bottom salinity, where available (16%), or were predicted using the GETM. Water salinities were converted into $\delta^{18}O_w$ (VPDB) values using Eqs. (2) & (3). Daily otolith $\delta^{18}O$ values were predicted from tag-recorded temperatures using Eq. (4) from Kim et al. (2007). Intra-annual otolith growth was assumed to vary slightly among individuals and years. To display predicted and measured otolith $\delta^{18}O$ values over time, therefore, calendar dates were estimated for measured $\delta^{18}O$ values by graphically adjusting profile shape and inflection points to best match the corresponding predicted annual $\delta^{18}O$ profile using Analyseries 2.0 (Paillard et al. 1996).

Data analysis

All statistical analyses and simulations were performed in R (R Development Core Team 2011), taking 0.05 as the limit for statistical significance. For all variables tested (salinity, temperature, predicted and measured otholith $\delta^{18}O$), data homoscedasticity and the normality and independence of residuals after parametric ANOVAs were investigated using Shapiro-Wilk normality tests, Studentized Breusch-Pagan tests and Durbin-Watson tests of residuals, respectively. When these conditions were not met, even after data transformation, non-parametric statistics were used (see below).

Inter-annual differences in the temperatures, salinities and otolith $\delta^{18}O$ values predicted over the full distributional area of plaice during the study period were tested by a non-parametric 1-way, fixed-effects, unbalanced ANOVA (Kruskal-Wallis tests), followed by post hoc multiple comparisons tests (Wilcoxon-Mann-Whitney tests) with Bonferroni corrections for statistical significance. Since no significant year effect could be detected on either the environmental

data (temperature: $\chi^2 = 3.24$, p = 0.81; df = 2; salinity: $\chi^2 = 2.06$, p > 0.66; df = 2) or the predicted $\delta^{18}O$ signal at this scale ($\chi^2 = 5.54$, p > 0.92; df = 2), the values predicted in each grid cell for all 3 study years (1997, 1998 and 1999) were considered grouped for the rest of the analyses.

Predicted intra-annual variations of salinity, temperature and otolith $\delta^{18}O$ among areas over the 1997–1999 period were investigated at different temporal scales using 2-way (area × month or area × season) fixed-effects, unbalanced ANOVAs with permutations (PERMANOVAs, n = 999 permutations, Anderson 2001) followed by separate Kruskal-Wallis 1-way ANOVAs and post hoc multiple comparisons tests (Wilcoxon-Mann-Whitney tests with Bonferroni corrections for statistical significance) for identifying areas with significantly different conditions at each temporal scale (year, season or month).

To verify the pertinence of the 4 seasons chosen to describe seasonal $\delta^{18}O$ changes in North Sea plaice (see 'Otolith selection, preparation and analysis' above), monthly variations of the predicted otolith $\delta^{18}O$ signals for all sub-stocks were investigated using a 2-way (sub-stock × month) unbalanced PERMANOVA. This was later supplemented by non-parametric Kruskal-Wallis ANOVAs (1 per factor) and post hoc multiple comparison tests (Wilcoxon-Mann-Whitney tests, with Bonferroni corrections) to identify the months expected to produce maximum differences among sub-stocks and those responsible for the maximum and minimum $\delta^{18}O$ signatures recorded during the year for each sub-stock. The same approach (2-way PERMANOVAs, followed by Kruskal-Wallis ANOVAs and post hoc Wilcoxon-Mann-Whitney tests) was used to investigate seasonal differences in predicted and measured otolith $\delta^{18}O$ values among sub-stocks. Lastly, differences between observed and predicted values for each sub-stock and season were tested separately using non-parametric Wilcoxon tests for paired samples.

In the following sections, all average values are provided with corresponding standard deviations (SD).

RESULTS

In addition to providing a detailed description of the distribution area and the spatio-temporal movements of plaice in the North Sea (Fig. 1), the data gathered during the 1993–2000 tagging experiment allowed the generation of 136 875 daily estimates of bottom temperature and salinity over the entire distribution range of our tagged fish for 1997–1999. Fine-scale analysis of the right-hand sagittae of 24 of the tagged fish returned with intact otoliths generated 117 measures of intra-annual $\delta^{18}O$ to be compared with the $\delta^{18}O$ values calculated from expected temperatures and salinities. The comparison was performed at various temporal scales, for each of the 3 sub-stocks, and for the areas seasonally occupied by the fish within the North Sea and the English Channel.

Environmental conditions and predicted geolocation success

In the areas frequented by adult plaice (Fig. 1), bottom temperatures and salinities were predicted to fluctuate from 1.62 to 21.65°C and from 24.10 to 35.28 over the year, around respective global annual averages of 10.41 ± 3.85°C and 34.58 ± 0.98. Otolith $\delta^{18}O$ signatures in this zone were predicted to range from −2.08 to 3.03‰, around a global annual average of 1.6 ± 0.91‰ (see Table S1 in the Supplement at www.int-res.com/articles/suppl/m598p167_supp.pdf). The ambient environmental conditions encountered varied greatly over time and space, with major consequences for the expected area discrimination success using corresponding otolith $\delta^{18}O$ values.

Spatio-temporal variations in environmental conditions

Temperature and salinity conditions were predicted to differ significantly both by month (temperature: p < 0.001, $F = 49863.96$, df = 11; salinity: p < 0.001, $F = 22.46$, df = 11) and by area (temperature: p < 0.001, $F = 26301.12$, df = 5; salinity: p < 0.001, $F = 14395.20$, df = 5), the interaction between the 2 factors also being significant (temperature: p < 0.001, $F = 1738.22$, df = 55; salinity: p < 0.001, $F = 8.49$, df = 55), as the intra-annual patterns of variations differed among areas (Fig. 2).

Spatial differences in salinity were more consistent than those for temperature. Average salinities for all months differed significantly (p < 0.05) among all areas but the WNS and CNS, with consistently lower (p < 0.05) salinities in the ENS (annual average: 33.45 ± 1.52) and in the SNS (annual average: 34.48 ± 0.97) than in the rest of the study area. Salinities in the EC (annual average: 35.12 ± 0.07) and the NNS (annual average: 34.98 ± 0.25) also differed significantly from October to March (p < 0.05)

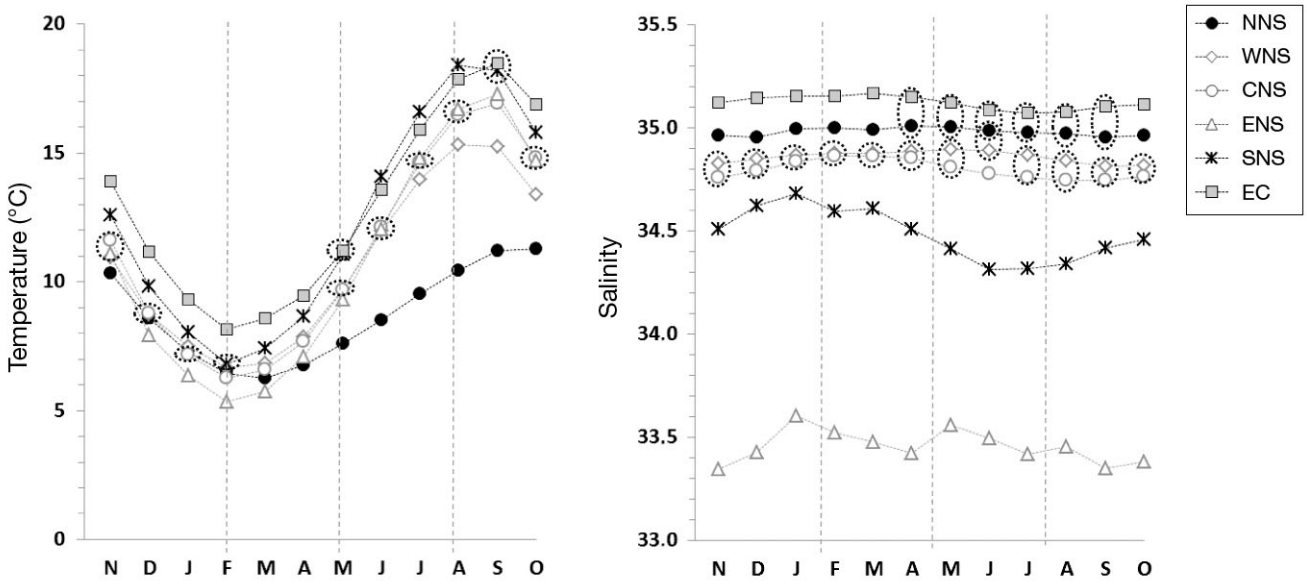

Fig. 2. Intra-annual variations in temperature and salinity within the study zone. For each of the 6 areas defined in Fig. 1 (NNS, WNS, CNS, ENS, SNS and EC), monthly means were calculated from the daily values predicted by the general estuarine transport model (GETM; see 'Materials and methods') in 1997, 1998 and 1999 over the full distribution of plaice *Pleuronectes platessa* in the area. For each month, dotted ellipses regroup areas with average values that did not differ significantly ($p \geq 0.05$)

and were always higher ($p < 0.05$) than those in the WNS (annual average: 34.86 ± 0.17) and CNS (annual average: 34.80 ± 0.45). Intra-annual variations in salinity were significant only in the SNS, with significantly ($p < 0.05$) lower average salinities from June to August (<34.32), and higher average salinities from December to March (>34.59), than during the rest of the year (34.42–34.51; Fig. 2). In the ENS, the average salinity also fluctuated throughout the year (minimum = 33.35 ± 1.53 in November, maximum = 33.60 ± 1.50 in January) but differences among months were not significant due to the high year-round variability in the salinity range (6.29–10.96) within the ENS.

Intra-annual temperature profiles were more similar among areas than salinities, with significant temporal variations ($p < 0.05$) irrespective of zone (Fig. 2). However, the amplitude of intra-annual variation varied among areas, being maximum in the ENS (total range: 1.62–21.65°C) and minimum in the NNS (total range: 4.02–18.00°C). The most contrasted thermal conditions were observed in the NNS (annual average: 8.69 ± 1.54°C), where average monthly temperatures were at least 1.74 to 4.87°C lower than in the rest of the study zone from May to October. Intra-annual variations in water temperature in the NNS, although significant ($p < 0.05$), were less marked, with minima around 6.5°C in February to April and maxima around 11.2°C in September to October (Fig. 2). For the 5 other areas, intra-annual patterns of variation were alike and more pronounced, with minima consistently observed in February to March, and maxima in August to September (Fig. 2). However, average temperatures between areas differed significantly ($p < 0.05$) for most of the year, with minimum monthly values generally observed in the WNS (annual average: 10.70 ± 1.70°C) or the ENS (annual average: 10.73 ± 4.43°C) and maxima in the EC (annual average: 12.91 ± 2.09°C) or the SNS (annual average: 12.32 ± 2.25°C). The CNS (annual average: 11.08 ± 2.15°C) always had intermediate average temperatures (Fig. 2). Among-area differences depended on the period of the year. Thus, monthly temperatures were at the least 0.82 to 1.35°C greater on average in the EC than in the North Sea, but only from October to April. Similarly, in the WNS, they were at least 2.12 to 4.97°C higher on average than in the NNS and 1.17 to 1.41°C lower on average than in the rest of the study area, but only from August to October.

Area discrimination based on intra-annual otolith $\delta^{18}O$ values

As a result of variations in environmental conditions in the study zone, significant differences in

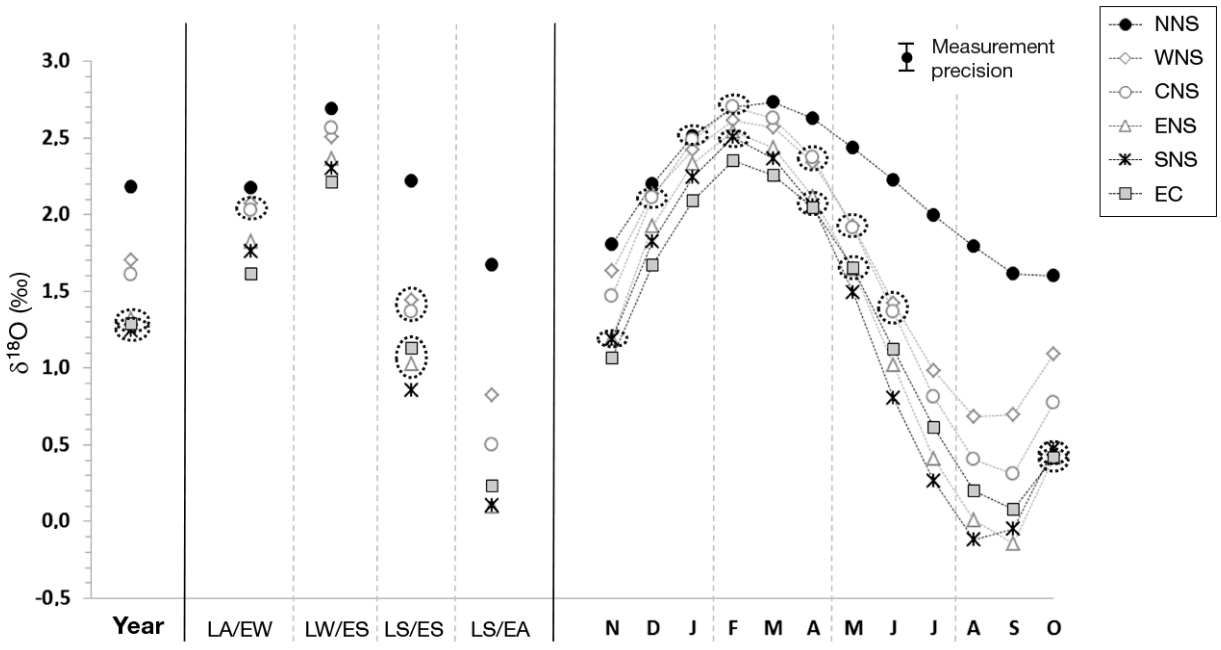

Fig. 3. Regional $\delta^{18}O$ values expected for North Sea plaice *Pleuronectes platessa* at annual, seasonal or monthly temporal scales for the 3 years investigated. For each area defined in Fig. 1, $\delta^{18}O$ means at the annual, 'seasonal' and monthly scales were calculated from the temperature and salinity data gathered for all cells with at least 10 geolocations. For each temporal scale, dotted ellipses regroup areas with average values that did not differ significantly ($p \geq 0.05$), when present. LW/ES: late winter/early spring, LS/EA: late summer/early autumn, LS/ES: late spring/early summer, LA/EW: late autumn/early winter

otolith $\delta^{18}O$ signatures were expected by area ($p < 0.001$, $F = 26\,328.18$, df = 5) and by month ($p < 0.001$, $F = 32\,419.57$, df = 11), the significant interaction of the 2 factors ($p < 0.001$, $F = 1126.69$, df = 55) indicating different patterns of intra-annual variation among areas.

With the exception of December, $\delta^{18}O$ signatures were predicted to differ significantly ($p < 0.05$) all year round among at least the NNS, the WNS and the ENS (Fig. 3). Consistently higher $\delta^{18}O$ values were predicted in the NNS (annual average: 2.18 ± 0.53‰) and lower $\delta^{18}O$ values in the ENS (annual average: 1.32 ± 0.77‰) than in the WNS (annual average: 1.71 ± 1.07‰). The difference in average $\delta^{18}O$ values among these 3 areas was predicted to be greater than 0.4‰ from June to October (Table S1), and seasonal otolith $\delta^{18}O$ signatures were expected to differ significantly ($p < 0.01$) in both LS/ES (with respective means of 1.03 ± 0.88‰ for ENS, 1.44 ± 0.56‰ for WNS and 2.22 ± 0.36‰ for NNS) and LS/EA (with respective means of 0.10 ± 0.88‰ for ENS, 0.83 ± 0.52‰ for WNS and 1.67 ± 0.57‰ for NNS). Seasonal otolith $\delta^{18}O$ values, especially those in LS/EA, were therefore predicted to allow confident area discrimination throughout the period of feeding ground 'residency' (in the NNS, WNS and ENS).

During the spawning migration (from November to April), constant discrimination only of the CNS (annual average: 1.61 ± 0.90‰) was predicted ($p < 0.05$) against the other areas where the spawning occurs (Fig. 3). Monthly $\delta^{18}O$ values in the CNS were always expected to be at least 0.15, 0.20 and 0.32‰ higher than those for the SNS, ENS and EC, respectively (Table S1). Monthly $\delta^{18}O$ signatures were also predicted to differ significantly from November to March between the SNS and the EC ($p < 0.05$), with average values in the EC being 0.11 to 0.16‰ lower, and between the ENS and the SNS ($p < 0.05$) in December, January and March, although average differences in $\delta^{18}O$ signatures for these months were only 0.07–0.10‰ (Fig. 3, Table S1). Consequently, expected seasonal otolith signatures for the 4 potential spawning zones were predicted to differ significantly both in LA/EW ($p < 0.05$) and LW/ES ($p < 0.05$), with mean values increasing from the EC (1.61 ± 0.46‰ in LA/EW and 2.22 ± 0.15‰ in LW/ES) to the CNS (2.03 ± 0.50‰ in LA/EW and 2.57 ± 0.22‰ in LW/ES), with the SNS and ENS having intermediate values (1.76 ± 0.51‰ and 1.82 ± 0.57‰ in LA/EW and 2.30 ± 0.30‰ and 2.38 ± 0.46‰ in LW/ES, respectively). However, otolith $\delta^{18}O$ signatures were expected to differ among all areas only in LW/ES, with the highest

Table 2. Monthly mean (range in parentheses) otolith $\delta^{18}O$ values predicted for each North Sea plaice *Pleuronectes platessa* sub-stock over the 3 yr period investigated (1997–1999) with corresponding temperature and salinity data

Month	Temperature (°C)	Salinity	$\delta^{18}O$ (‰)
Sub-stock A			
1	7.27 (5.16–9.95)	34.94 (34.14–35.17)	2.46 (2.25–2.59)
2	6.31 (3.43–8.12)	34.80 (31.82–35.17)	2.64 (2.34–2.75)
3	6.34 (3.96–7.88)	34.85 (31.27–35.21)	2.64 (2.05–2.79)
4	7.06 (5.81–9.10)	35.01 (34.31–35.18)	2.52 (2.31–2.64)
5	7.65 (6.15–10.47)	35.05 (34.80–35.17)	2.40 (2.05–2.56)
6	8.55 (7.13–11.38)	35.06 (34.82–35.17)	2.20 (1.83–2.42)
7	9.47 (7.03–14.09)	35.02 (34.82–35.16)	1.98 (1.48–2.43)
8	10.76 (7.47–16.43)	35.00 (34.61–35.17)	1.69 (0.76–2.32)
9	12.01 (8.69–16.23)	34.98 (34.64–35.17)	1.41 (0.77–2.06)
10	11.57 (8.69–15.91)	35.04 (34.72–35.17)	1.52 (0.93–2.08)
11	11.18 (8.65–13.95)	34.94 (33.90–35.16)	1.58 (1.32–1.85)
12	8.76 (6.49–11.62)	34.89 (33.67–35.18)	2.11 (1.94–2.35)
Global	8.22 (3.43–16.49)	34.94 (31.27–35.21)	2.58 (0.76–2.79)
Sub-stock B			
1	7.13 (3.25–10.72)	33.43 (31.65–35.15)	2.35 (2.04–2.59)
2	5.67 (1.93–8.07)	33.56 (28.40–35.14)	2.45 (1.81–2.70)
3	6.10 (3.98–7.90)	33.75 (29.67–35.11)	2.40 (1.79–2.71)
4	7.45 (4.87–10.38)	33.28 (25.23–35.13)	1.96 (0.54–2.47)
5	9.40 (6.70–13.25)	33.81 (31.10–34.99)	1.67 (1.13–2.07)
6	11.87 (9.02–15.99)	33.85 (32.15–34.97)	1.13 (0.76–1.60)
7	14.42 (10.42–18.21)	33.49 (30.57–35.00)	0.47 (–0.39–1.11)
8	16.82 (12.93–18.96)	33.45 (30.71–34.82)	–0.06 (–0.77– 0.21)
9	17.29 (15.09–19.04)	32.84 (30.70–34.82)	–0.32 (–0.73– 0.04)
10	14.69 (10.77–18.09)	33.29 (30.88–34.78)	0.36 (0.06–0.65)
11	11.10 (6.61–13.98)	33.32 (30.89–34.82)	1.15 (0.91–1.30)
12	8.44 (5.13–12.24)	34.00 (30.43–35.11)	1.93 (1.73–2.04)
Global	9.42 (1.93–19.04)	33.66 (25.23–35.15)	1.10 (–0.77 –2.71)
Sub-stock C			
1	8.35 (5.08–10.93)	34.99 (34.46–35.26)	2.22 (2.00–2.44)
2	6.97 (5.08–8.88)	34.87 (34.29–35.15)	2.51 (2.37–2.65)
3	6.97 (5.78–8.53)	34.78 (32.53–35.21)	2.48 (2.15–2.63)
4	8.08 (6.68–10.12)	34.89 (34.42–35.14)	2.26 (2.06–2.36)
5	10.17 (8.23–12.97)	34.88 (34.58–35.18)	1.79 (1.62–1.99)
6	15.43 (10.43–15.65)	34.86 (34.61–35.08)	1.21 (0.98–1.39)
7	16.58 (12.85–18.30)	34.85 (34.60–35.11)	0.63 (0.42–0.91)
8	15.77 (12.78–19.40)	34.83 (34.60–35.05)	0.38 (0.03–0.83)
9	12.01 (10.11–18.94)	34.84 (34.57–35.06)	0.57 (0.16–1.61)
10	14.08 (9.41–17.89)	34.83 (34.57–35.12)	0.91 (0.55–1.77)
11	12.60 (899–15.79)	34.90 (33.52–35.18)	1.26 (1.00–1.52)
12	9.06 (6.87–13.26)	34.76 (33.52–35.19)	2.00 (1.64–2.10)
Global	10.96 (5.08–19.40)	34.87 (33.67–35.26)	1.66 (0.03–2.65)

($p < 0.05$) average predicted for the NNS (2.69 ± 0.12‰) and intermediate yet significantly different ($p < 0.05$) values in the WNS (2.51 ± 0.46‰) and the CNS (2.57 ± 0.22‰). In LA/EW, differences in average $\delta^{18}O$ signatures between these 2 latter areas (CNS = 2.03 ± 0.50‰; WNS = 2.07 ± 0.57‰) were too low to be significant (Fig. 3).

Sub-stock discrimination based on intra-annual otolith $\delta^{18}O$ values

Expected discrimination success at monthly and seasonal scales

Due to migration among areas during the year, the predicted intra-annual variations in otolith $\delta^{18}O$ signatures of the 3 sub-stocks never fully matched those of any single area in the study zone. Nonetheless, the reconstructed environmental conditions experienced by the 3 sub-stocks differed markedly (Table 2), as predicted from their geographically discrete summer feeding locations and winter migration routes (Fig. 1). Annual temperature profiles were comparable for sub-stocks B and C, with important seasonal variations and minima around 6–7°C in February–March while maxima around 16–17°C were observed in August–September (Table 2). By contrast, the average temperatures experienced by sub-stock A peaked at 12°C in September and very rarely exceeded 14°C. Annual salinity profiles were similar for sub-stocks A and C, with relatively constant average salinities (34.8–35.1) throughout the year (Table 2). This contrasted with sub-stock B, for which monthly salinities were <34.0 on average and more variable overall.

Consequently, predicted intra-annual otolith $\delta^{18}O$ values varied greatly among sub-stocks (Table S2A), ranging from 0.76 to 2.79‰ in sub-stock A, from –0.77 to 2.71‰ in sub-stock B and from 0.03 to 2.65‰ in sub-stock C, around average values of 2.58 ± 0.23‰, 1.10 ± 0.17‰ and 1.66 ± 0.16‰, respectively (Table 2). They varied significantly ($p < 0.001$) by month irrespective of sub-stock (Table S2C) and largely mirrored the seasonal temperature signal observed across the entire study area (Fig. 2): average monthly otolith $\delta^{18}O$ values were consistently expected to be highest (>2.40‰) in February–March (i.e. during the coldest months of the year) and lowest (<1.69‰) in August or September (i.e. during the warmest months), irrespective of the sub-stock (Table 2, Table S2C). However, intra-annual patterns of $\delta^{18}O$ variation (mean value and

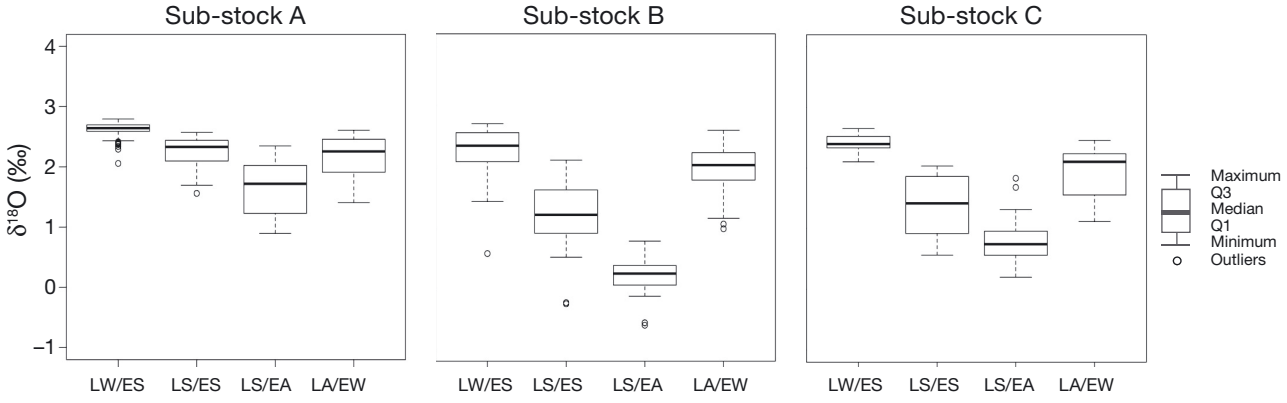

Fig. 4. Seasonal expected $\delta^{18}O$ values for each of the 3 North Sea plaice *Pleuronectes platessa* sub-stocks (A, B and C; see Fig. 1). In each case, $\delta^{18}O$ values were predicted from the environmental temperature and salinity ranges experienced by the fish using the equations of Kim et al. (2007) and Harwood et al. (2008). Seasons on the *x*-axis defined as in Fig. 3

amplitude) differed among sub-stocks (Table 2), mainly due to differences in the temperatures and salinities they experienced on their respective feeding grounds, in the NNS, ENS or WNS (Figs. 2 & 3). Consequently, predicted otolith $\delta^{18}O$ values varied significantly ($p < 0.001$) among sub-stocks irrespective of the month (Table S2B). However, they differed among all 3 sub-stocks only in April ($p < 0.05$), August ($p < 0.05$), September ($p < 0.01$) and October ($p < 0.001$). During the rest of the year, predicted otolith $\delta^{18}O$ values allowed constant discrimination between the northern and the 2 southern sub-stocks ($p < 0.01$), except during December, when predicted values were similar for sub-stocks A and C but differed significantly between the 2 southern sub-stocks ($p < 0.05$).

As a result of these differences, predicted otolith $\delta^{18}O$ values varied significantly ($p < 0.001$) by both season and sub-stock (Table S3A). With the exception of LS/ES and LA/EW for sub-stock A (Table S3C), otolith $\delta^{18}O$ values were consistently predicted to differ ($p < 0.01$) among seasons for a given sub-stock. Irrespective of sub-stock, $\delta^{18}O$ values were consistently the highest ($p < 0.001$) in LW/ES and the lowest ($p < 0.001$) in LS/EA, the other 2 seasons having intermediate values (Fig. 4, Table S3C). Otolith $\delta^{18}O$ signatures were also predicted to differ significantly ($p < 0.01$) by sub-stock, irrespective of season (Table S3B). However, they differed among all 3 sub-stocks only in LS/EA ($p < 0.01$). During the other 3 seasons, discrimination only of the northern from the 2 southern sub-stocks was predicted ($p < 0.05$) (Fig. 4, Table S3B).

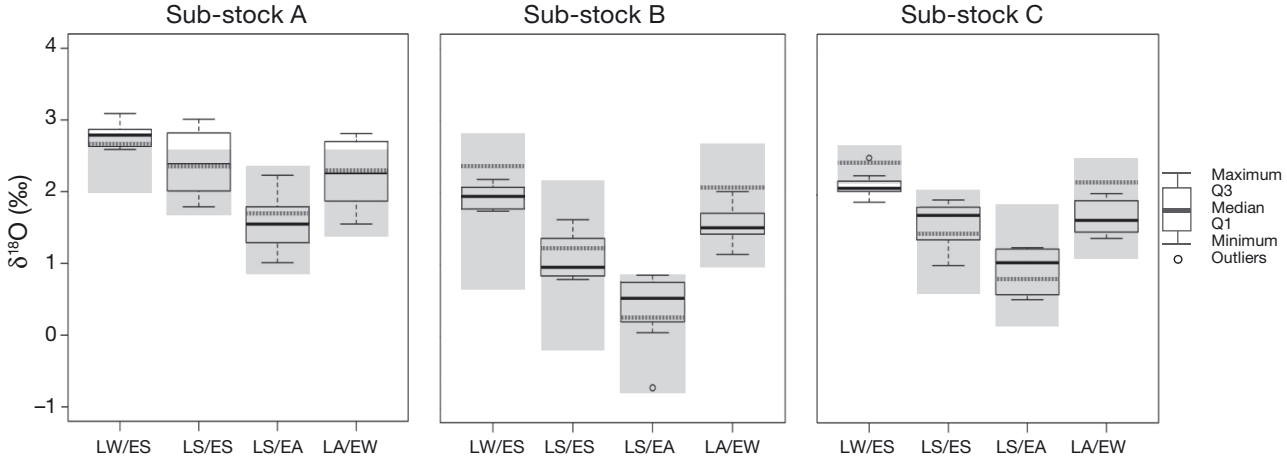

Fig. 5. Potential for 'seasonal' sub-stock discrimination using otolith $\delta^{18}O$ in North Sea plaice *Pleuronectes platessa*. In each case, the boxplot shows the otolith $\delta^{18}O$ values measured for each sub-stock (minimum, Q1, median, Q3 and maximum values, outliers; see Fig. 1 for sub-stocks), and the range of otolith $\delta^{18}O$ values predicted from the corresponding environmental data is indicated (grey shade), the dotted grey line showing the median predicted value. Seasons on the *x*-axis defined as in Fig. 3

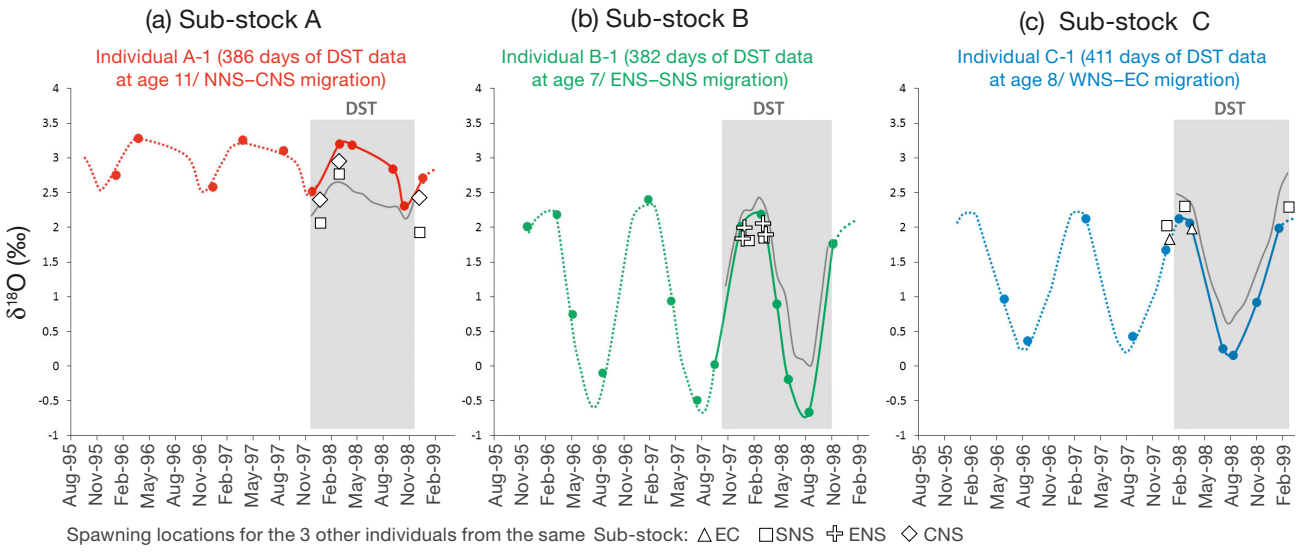

Fig. 6. Potential for seasonal geolocation using otolith $\delta^{18}O$ signatures in plaice *Pleuronectes platessa* from sub-stocks (a) A, (b) B and (c) C (see Fig. 1). Solid circles represent the intra-annual otolith $\delta^{18}O$ values measured during the final 3 yr of life in 3 individuals (1 sub-stock^{-1}) with known spawning locations in 2 successive winters (Table 1). To investigate fidelity to migration routes, intra-annual values are plotted above the repeated 'typical' annual pattern derived from otolith $\delta^{18}O$ values measured during data storage tag (DST) recording time (coloured curve, solid during tag recording time, dotted for the pre-tag recording period). The predicted $\delta^{18}O$ signal based on tag data is plotted as the solid grey line. Open symbols represent otolith $\delta^{18}O$ values measured during the spawning migrations in the same winters (1997–98 or 1998–99) for 3 other individuals from the same sub-stock (Table 1), 1 from each migration type (see legend for spawning locations, defined in Fig. 1)

Consistency between predicted and observed 'seasonal' otolith $\delta^{18}O$ values

For the majority of our observations, measured and predicted seasonal otolith $\delta^{18}O$ values were consistent (Fig. 5); however, small differences between them were observed. For several individuals, $\delta^{18}O$ measures fell outside the expected ranges, with values 0.20‰ lower than the minimum predicted in the LW/ES for sub-stock C, and values 0.21–0.44‰ higher than the maxima predicted for all seasons but LS/EA for sub-stock A. Nonetheless, when observed $\delta^{18}O$ values did not match the predictions for a given season (e.g. in the LW/ES for sub-stocks A and C), the differences in $\delta^{18}O$ among stocks were consistently above the expected values, maintaining the potential for sub-stock discrimination.

As predicted, measured otolith $\delta^{18}O$ values differed significantly by sub-stock irrespective of season (Table S4B), allowing constant discrimination of the northern from the 2 southern sub-stocks during the year ($p < 0.05$) and robust differentiation of all 3 sub-stocks in LS/EA ($p < 0.001$). In LS/EA, the differences in average measured otolith $\delta^{18}O$ values among sub-stocks were even greater than expected (Fig. 5). Intra-annual variations in measured $\delta^{18}O$ values also followed those predicted from temperature and salinity conditions irrespective of the sub-stock (Fig. 5). The $\delta^{18}O$ values were consistently predicted to be the greatest ($p < 0.01$) in LW/ES and the lowest ($p < 0.001$) in LS/EA (Fig. 5, Table S4C). Moreover, measured $\delta^{18}O$ signatures differed among all seasons ($p < 0.01$) for a given sub-stock, except for LS/ES and LA/EW in sub-stock A (Table S4C).

Discriminating migratory behaviours based on otolith $\delta^{18}O$ signatures

By matching the intra-annual $\delta^{18}O$ profiles predicted for 1998 with sampled values from the corresponding annual otolith growth rings (Fig. 6), we were able to confirm the broad timing of deposition of the opaque and translucent bands, irrespective of the sub-stock. Indeed, otolith samples taken at the translucent to opaque transition (deposited in LW/ES, Van Neer et al. 2004) consistently had the highest $\delta^{18}O$ values, matching the maximum values predicted for February–March. The lowest $\delta^{18}O$ values were consistently taken from the opaque to translucent transition (deposited in LS/EA; Van Neer et al. 2004), matching the minimum values predicted for August–October. However, the respective widths of the opaque and translucent bands varied among individuals, depending on the age of the fish at the time of deposition but also, apparently, by sub-stock.

Matching the growth band signatures to predicted monthly $\delta^{18}O$ values for the corresponding sub-stock confirmed this pattern, and suggested more rapid growth over the autumn and winter months in sub-stock A, over the spring and summer months in sub-stock C and constant growth all year long in sub-stock B. Depending on the sub-stock, the measured $\delta^{18}O$ signal was also consistently lower (sub-stocks B and C) or higher (sub-stock A) than that predicted from the environmental conditions, with mismatches between predicted and measured signatures ranging from 0.04 to 0.51‰ (Fig. 6).

In spite of the observed mismatches, the different intra-annual $\delta^{18}O$ profiles observed for 1998 in the 12 fish investigated suggest that otolith oxygen signatures can confidently discriminate most migratory behaviours in North Sea plaice (Fig. 6). The $\delta^{18}O$ signatures recorded in 1998 confirmed the value of LS/EA $\delta^{18}O$ values for geolocation of plaice among the NNS (1.92 to 3.15‰), the WNS (0.33 to 0.89‰) and the ENS (−0.78 to 0.29‰) within the period corresponding to feeding ground residency. Analysis of the $\delta^{18}O$ signatures obtained for all 6 migration types in the migration period in 1997–98 and 1998–99 (N = 27 from 12 fish) further suggested that the fish from sub-stocks A and C with different spawning locations have discriminable otolith signatures in LA/EW and LW/ES (Fig. 6). This observation is consistent with the $\delta^{18}O$ values predicted from the environmental conditions prevailing in the areas traversed for each spawning migration. Consequently, based on the predicted differences in otolith signatures at this time of the year between the CNS (2.03 ± 0.50‰ in LA/EW and 2.57 ± 0.22‰ in LW/ES) and the SNS (1.76 ± 0.51‰ in LA/EW and 2.30 ± 0.30‰ in LW/ES), observed signatures for these 2 seasons were higher in the fish of sub-stock A spawning in the CNS (2.30–2.59‰ and 2.87–3.29‰ for LA/EW and LW/ES, respectively) than for those spawning in the SNS (1.87–2.27‰ and 2.67–3.02‰, respectively). Similarly, the differences in expected otolith signatures in the EC (1.61 ± 0.46‰ in LA/EW and 2.22 ± 0.15‰ in LW/ES) and in the SNS (1.76 ± 0.51‰ in LA/EW and 2.30 ± 0.30‰ in LW/ES) could explain the slightly different otolith signatures recorded by the fish from sub-stock C spawning in the EC (1.77–1.92‰ in LA/EW and 2.02–2.11‰ in LW/ES) and in the SNS (2.02–2.27‰ in LA/EW and 2.27–2.51‰ in LW/ES). Finally, the comparable values predicted for both seasons in the SNS and the ENS (1.76 ± 0.51‰ and 1.82 ± 0.57‰ in LA/EW and 2.30 ± 0.30‰ and 2.38 ± 0.46‰ in LW/ES, respectively) resulted in non-distinguishable $\delta^{18}O$ values for both seasons in the fish of sub-stock B, with values of 1.71–1.95‰ for LA/EW and of 1.80–2.18‰ for LW/ES.

Site fidelity and repeated patterns of behaviour

Analysis of the $\delta^{18}O$ values in the years prior to tagging suggested a high degree of fidelity to summer feeding and winter spawning grounds (Fig. 6). The pre-tagging summer signatures (N = 25) indicate feeding ground (sub-stock) fidelity for at least 2 successive years in all of our sampled fish. Indeed, the LS/EA pre-tagging $\delta^{18}O$ values measured (all comprised between 1.59 and 2.39‰, −0.46 and 1.24‰ and 0.45 and 1.40‰ in the fish assigned to sub-stocks A, B and C, respectively) remained relatively constant, irrespective of the individual, inter-annual differences for a given fish ranging from 0.02 to 0.28‰.

Fidelity to spawning site was more complicated to interpret, as average differences in $\delta^{18}O$ seasonal signatures between spawning migration types for sub-stocks A and C were only of ~0.2‰, i.e. close to the detection limit (0.07‰). However, observed signatures for pre-tagging LA/EW seasons in fish assigned to sub-stock A and spawning sites in the CNS or in the SNS ranged from 2.21 to 2.70‰ and from 1.87 to 2.27‰, respectively. For sub-stock C fish, signatures ranged between 2.11 and 2.32‰ and between 1.87 and 2.27‰ depending on whether, in 1998, the fish had spawned in the SNS or in the EC, respectively. For sub-stock B fish assigned, signatures ranged between 1.78 and 2.01‰ irrespective of the spawning location identified during DST recording time.

DISCUSSION

Otolith $\delta^{18}O$ signatures have widely been used to infer past environmental and/or migratory histories of fish (e.g. Surge & Walker 2005, Shephard et al. 2007, Rooker et al. 2008, Imsland et al. 2014), and scientists are increasingly seeking applications for tracking fish geographical movements based on oxygen isoscapes (e.g. Wunder 2010, Trueman et al. 2012, Torniainen et al. 2017). Individual experience and environmental variation, however, have not previously been considered to any significant extent in fish studies involving otolith $\delta^{18}O$ (e.g. Stephenson 2001, Imsland et al. 2014, Torniainen et al. 2017). This results primarily from the difficulties in obtaining accurate corresponding positional and environmental data (Begg et al. 2005, Tanner et al. 2016). The first attempt to address this shortcoming (Dar-

naude et al. 2014) demonstrated that otolith $\delta^{18}O$ in adult North Sea plaice largely reflected the differences in ambient temperatures and salinities experienced by wild fish. Furthermore, annual $\delta^{18}O$ values allowed robust re-assignment of the same fish to their 3 local sub-stocks. The data presented here greatly extend the previous study, as location-specific daily estimates of temperature and salinity for the migrations of individual, free-swimming fish in their natural environment have for the first time been matched with oxygen isotope data from the same individuals at a sub-annular scale, linking environmental variation and otolith $\delta^{18}O$ to fish geographical distribution. As far as we are aware, our results provide the first example documenting the scope and limits for applying otolith $\delta^{18}O$ values to reconstruct the past migration histories of a wild marine fish.

Likely causes of mismatches between expected and observed otolith $\delta^{18}O$ values

As in Darnaude et al. (2014), we used measured and modelled environmental data in our study to predict otolith $\delta^{18}O$ values from fish positions estimated from archival tag data. Although this approach generates robust predictions of otolith $\delta^{18}O$ values, both for individual fish and for sub-stocks (Darnaude et al. 2014), we acknowledge 2 inherent and largely unavoidable potential sources of error in this process. The first relates to the estimation of fish location (geolocation) and to the estimation of complementary environmental data in those locations where *in situ* measurements were unavailable. However, these 2 sources of bias have only limited impact (<0.2‰), even when combined, on the majority of monthly otolith $\delta^{18}O$ predictions across the North Sea area (Darnaude et al. 2014). Another potential source of error lies in the estimation of water $\delta^{18}O$ from salinity. However, by applying the North Sea-specific equation developed by Harwood et al. (2008), again we are confident that our dataset is predominantly accurate. Unavoidably, localised inputs from the Rhine and Elbe Rivers can influence the $\delta^{18}O$ salinity relationship (Harwood et al. 2008), but any resulting errors in our estimations would be localised primarily to sub-stock B.

A third possible, and more likely, source of error in our seasonal predictions is linked to sub-stock-specific variation in plaice otolith growth rate during the year. The incorporation of such variations in growth when calculating expected otolith annual $\delta^{18}O$ values by sub-stock, from monthly, environmental-based $\delta^{18}O$ estimates, has already been shown to have a marked influence on the prediction accuracy (Darnaude et al. 2014). Like the few additional studies that have investigated sub-annual variation in otolith $\delta^{18}O$ signatures (e.g. Høie & Folkvord 2006, Kastelle et al. 2017), we did not apply differential monthly weighting when calculating seasonal $\delta^{18}O$ signals expected from the fish position-linked environmental data. This may have slightly biased our predictions, as some of our observations suggested more rapid growth over autumn and winter in sub-stock A, spring and summer in sub-stock C and constant year-long growth in sub-stock B. An explanation for these differences lies in the distinct annual ambient temperature profiles for sub-stock A (Darnaude et al. 2014) and variation in the timing and duration of migration among the sub-stocks (Hunter et al. 2004). Because otolith growth rate has been shown to reflect fish metabolic rates (Grønkjær 2016) it should reflect the variation in metabolism documented for female plaice (Rijnsdorp & Ibelings 1989, Fonds et al. 1992, Bromley 2000). In plaice, metabolism is mainly related to temperature and feeding (Fonds et al. 1992). Maximum otolith growth is therefore expected in the warmest months for each sub-stock (i.e. from June to October in sub-stocks B and C, but from September to November in sub-stock A). However, female plaice feed intensely during spring to build reserves for gametogenesis commencing in July (Rijnsdorp 1989), then cease feeding and reduce their metabolic rates during their spawning migrations, due to limited metabolic scope that precludes the simultaneous oxygen demands for spawning and feeding (Rijnsdorp & Ibelings 1989). Although no study has yet investigated temporal variation in feeding levels or metabolic rates among the 3 sub-stocks studied here, the timing of otolith edge deposition in North Sea plaice varies by the area of capture, in relation to the interruption of somatic growth in winter (Van Neer et al. 2004). Several studies (e.g. Harding et al. 1978, Bromley 2000) have also shown that spawning occurs progressively later with latitude, with peak spawning generally observed in December–January in the EC, in January–February in the SNS and in February–March in the CNS and ENS. Fish from sub-stock A, which spawn either in the SNS or CNS, are therefore more likely to cease otolith accretion in spring, while those of sub-stock C, which spawn either in the EC or SNS, are more likely to exhibit reduced otolith growth in autumn and winter. Almost constant otolith growth is most likely in sub-stock B otoliths since, as many sub-stock B fish spawn in the ENS (Hunter et al. 2004), in areas

relatively close to their summer feeding grounds, their fasting duration during spawning may be more limited. For individual fish, therefore, we are unable to entirely exclude possible errors in the positioning of some seasonal growth bands on the otolith. Given the 3-dimensional structure of the otoliths, the drilling depth (450 µm) used in this study might also have resulted in partial contamination of our sub-seasonal samples with material from earlier or later periods in the year, particularly since we used frontal sections for this. However, all otoliths in the present study were cut and polished down with the specific aim to obtain 500 to 600 µm thick sections along this plane with the otolith edge (and its most outer growth bands) as perpendicular to the section surface as possible. Therefore we are confident that the bias in sub-seasonal $\delta^{18}O$ induced by such contamination, when present, was limited.

This having been said, position-based errors do not fully explain the divergence between measured and predicted seasonal otolith $\delta^{18}O$ values. Indeed, they would only result in an attenuation of the $\delta^{18}O$ signal when, conversely, some of the $\delta^{18}O$ values measured (for example those observed for sub-stock A in LW/ES) were greater than any of those predicted in the study area, even at the monthly scale. Our intra-annual measured $\delta^{18}O$ values repeatedly diverged from predicted values, even when using *in situ* temperature tag records from the same fish (Fig. 6). This mismatch was previously identified in Darnaude et al. (2014), where it is discussed at length. In North Sea plaice, vital effects appear to alter the $\delta^{18}O$ signal ultimately recorded in otoliths, both through variations in the otolith deposition rate during the year and through changes in the water-otolith oxygen isotopic fractionation, at least during certain seasons. Ideally, multi-stock validation studies across a wide range of ontogenies are required to establish a more comprehensive understanding of the relationship between fish metabolism and otolith $\delta^{18}O$.

Optimizing $\delta^{18}O$ values to reconstruct environmental and migratory histories

Our results demonstrate how sub-annual otolith $\delta^{18}O$ signatures can successfully reveal the spatial and temporal details of annual migration cycles. Such otolith $\delta^{18}O$-based geolocation can be achieved only by a comprehensive understanding of the spatial dynamics of the target species, coupled with an adequately detailed accumulation of matching data mapping environmental variation across the species range. This cross-referencing of datasets further allows optimization of the temporal scale to be adopted for otolith sampling in order to maximize discrimination/geolocation potential. In our case, partitioning the calendar year into LW/ES, (February to April), LS/ES (May to July), LS/EA (August to October) and LA/EW (November to January) instead of traditional seasons optimized our ability to apply otolith $\delta^{18}O$ signatures to discriminate among sub-stocks and spawning migration types, and to capture the maximal amplitude of $\delta^{18}O$ intra-annual fluctuations irrespective of the fish.

$\delta^{18}O$ signatures for LS/EA, LW/ES and LA/EW were the most valuable for characterizing differences in both environmental and migratory histories. In particular, LS/EA included the 3 months (August–October) with the lowest predicted $\delta^{18}O$ values, irrespective of sub-stock. Monthly values in this season were also consistently expected to differ significantly among all sub-stocks (B < C < A) due to their residency, at this time, in discrete areas with contrasted temperatures (especially in the colder NNS) and different salinities (mainly in the ENS). The measured $\delta^{18}O$ values for LS/EA therefore allowed robust discrimination of all 3 sub-stocks, ranging mostly (>75%) between 1.3 and 2.2‰ in sub-stock A, between 0.2 and 0.8‰ in sub-stock B, and between 0.6 and 1.2‰ in sub-stock C. LW/ES included the 2 months (February and March) with the highest expected monthly $\delta^{18}O$ values during the year, irrespective of sub-stock, and 1 month (April) where the expected $\delta^{18}O$ values differed significantly between all sub-stocks (B < C < A). Accordingly, measured otolith $\delta^{18}O$ values for this season allowed discrimination of fish from sub-stock A (>2.5‰) from those of sub-stocks B and C (1.7–2.2‰ and 1.9–2.3‰, respectively). Measured $\delta^{18}O$ signatures for the 6 migration types examined in 1998 further suggest that fish from sub-stocks A and C with different spawning locations have discriminable LA/EW signatures, as predicted from prevailing environmental conditions in their respective migration transit areas. Our results require further validation with larger sample sizes, but suggest LA/EW otolith $\delta^{18}O$ signatures of 1.8–2.3‰ and 2.3–2.6‰ in sub-stock A fish spawning in the SNS and the CNS, respectively. In sub-stock C fish spawning in the EC and the SNS, concomitant signatures appear to range from 1.7 to 2.0‰ and from 2.0 to 2.3‰, respectively, while in sub-stock B fish, they seem to range from 1.7 to 2.0‰, irrespective of the spawning locations (SNS or ENS). We are therefore confident that feeding site location will be identifiable for all plaice females using LS/EA otolith $\delta^{18}O$

values, and 4 out of the 6 spawning migration types should equally be recognizable using LA/EW and LW/ES ones. Given the fine-scale spatial and temporal variations in $\delta^{18}O$ observed, higher otolith sampling resolution, e.g. by using a secondary ion mass spectrometer (SIMS) ion microprobe (Matta et al. 2013), could further improve this categorisation. However, the time and cost of SIMS is often currently impractical for large sample sizes.

The ground-truth validation approach applied here shows that seasonal samples derived from high-resolution micro-milling represent a non-negligible addition to the information on plaice migratory behaviour in the North Sea beyond the results obtained using annual otolith signatures only (Darnaude et al. 2014). The seasonal otolith $\delta^{18}O$ values laid down during and prior to tagging confirmed inter-annual fidelity to summer feeding sites (N = 25), as previously suggested from multi-annual archival tag records (Hunter et al. 2003a). Otolith $\delta^{18}O$ values further allowed multiple-year evidence of spawning site fidelity, at least in sub-stocks A and C. This is an important observation in that the vulnerability of fish stocks to exploitation by fisheries is often related to the degree of site fidelity exhibited by fish stocks (Sadovy de Mitcheson et al. 2008, Erisman et al. 2017), but this characteristic is often inferred, rather than directly measured.

Otolith $\delta^{18}O$ as a natural tag

As well as providing significant insights into plaice population structure and spatial dynamics (Hunter et al. 2004), the hundreds of plaice released bearing archival tags allowed us to test whether measurement of otolith $\delta^{18}O$ could provide similar population-level information. We were able to correctly identify sub-stock membership for most plaice using otolith $\delta^{18}O$ values, and achieved broad-scale geolocation on a finer temporal scale than is currently applied to most offshore fisheries area-based management (Kell et al. 2004). This fully validates $\delta^{18}O$ as an alternative natural tag for fish geolocation and stock identification in offshore environments, and we suggest that the technique can be applied to study other shelf-species in well-described systems.

Our results emphasize that geolocation accuracy using otolith $\delta^{18}O$ is dependent on the variability of the water masses frequented both in terms of temperature and of salinity. The low assumed variability in offshore salinity in marine studies has led to an assumption in previous studies that otolith $\delta^{18}O$ variations in marine fish otoliths reflect movements between water masses with distinct temperatures (e.g. Dorval et al. 2011, Imsland et al. 2014, Javor & Dorval 2014). However, local variation in sea salinity, especially in the coastal zone (Harwood et al. 2008), can affect otolith $\delta^{18}O$, as already shown for species migrating to coastal brackish or hypersaline habitats (Northcote et al. 1992, Bastow et al. 2002, Walther et al. 2011, Stanley et al. 2015). Our results demonstrate that in regions with very similar salinities, such as the CNS and WNS, differences in temperature of just 2°C induce significant differences in predicted otolith $\delta^{18}O$ values. Spatial differences in salinity of just 1 psu can however result in mismatches in regional classification between temperature and otolith $\delta^{18}O$. We emphasize therefore that a basic knowledge of apparently stable local salinities is imperative for the successful assessment of marine fish spatial movements or stock membership using otolith $\delta^{18}O$.

Because most commercially exploited marine fish are poikilotherms (Carey et al. 1971) that may experience high variability of ocean temperatures (Levitus & Antonov 1995) and often exist as discontinuous sub-stocks (Metcalfe 2006), otolith $\delta^{18}O$ use could have widespread application. However, geolocation efficiency using otolith $\delta^{18}O$ is likely to be species-specific (Stanley et al. 2015). In pelagic thermoregulating fishes such as tunas, where variations in internal temperature are low (Block & Finnerty 1994, Block et al. 2001), otolith $\delta^{18}O$ is thus unlikely to be practicable as a tag. Vertical migrations are also likely to bias otolith $\delta^{18}O$-based estimates of fish geolocation, making the technique difficult to apply to mesopelagic or vertically active species (e.g. Righton et al. 2016). Because plaice, like other flatfish, spend much of their life on or close to the seabed (Hunter et al. 2009), the risk of confounding effects due to vertical movements with geographical migrations is limited. Other potential candidates include cod *Gadus morhua*, which can spend protracted periods of time resting on the seabed (Righton et al. 2001). Cod otolith $\delta^{18}O$ values are already applied in ageing (Kastelle et al. 2017), but broader baseline knowledge of bottom temperature and salinities should be sufficient to produce geographical isoscapes of expected otolith $\delta^{18}O$, in turn allowing the efficacy of otolith $\delta^{18}O$ for fish geolocation to be predicted for the area. Finally, our results support the existence of inter-stock differences in physiology that could sometimes affect the environmental signal recorded in fish otoliths (Darnaude et al. 2014), by shifting $\delta^{18}O$ values upward (like here in sub-stock A) or downward (in sub-stocks B and C), depending on the stock.

The ability to successfully gauge temporal resolution in otolith sampling is also essential for the successful exploitation of otolith $\delta^{18}O$ as a natural tag. With few exceptions (e.g. Zazzo et al. 2006, Dufour et al. 2008, Torniainen et al. 2017), previous isotopic studies examining otolith $\delta^{18}O$ have been based, at best, on results from annual otolith samples. Our results demonstrate, for plaice at least, that geolocation potential is high at a broad spatial scale, but that spatial discrimination based on annual otolith $\delta^{18}O$ is poor when compared to monthly or even seasonal values. Furthermore, because the spatial discriminatory power of otolith $\delta^{18}O$ varies over the course of the year, the timing and extent of spatial movements in migrating fish will inevitably bias assessments of spatial distribution based on annual $\delta^{18}O$ alone. In our study, the season with maximal inter-regional differences in otolith $\delta^{18}O$ (here the summer) corresponded with the period of fish residency in geographically distinct areas (here from June to October), greatly enhancing sub-stock discrimination, even from annual $\delta^{18}O$ values. Where no prior knowledge of seasonal movements and environmental histories is available, otolith analysis at the highest possible level of resolution will clearly be of benefit for accurate stock separation or geolocation studies.

CONCLUSION

Beyond sub-stock discrimination based on annual otolith $\delta^{18}O$, sub-annual sampling of the otolith allows regional geolocation with a seasonally dependent, but relatively accurate degree of resolution, commensurate to the scale of migration in our study species. This technique can potentially yield simple geo-referenced data that may be valuable for fish stock conservation and sustainable fisheries management. Successful application of $\delta^{18}O$ values as a natural tag does, however, require baseline knowledge of temperature and salinity across the geographical range of the target species and of potential population-specific vital effects during oxygen uptake/incorporation into otolith aragonite. For plaice, otolith $\delta^{18}O$ values act as an effective low-cost natural tag, the results from which can complement and extend observations from other methodologies used to describe population structure. These data have an immediate application for the description of stock movements and management areas occupied, for example to predict the potential impacts of management strategies, such as area closures to fishing.

Acknowledgements. We thank Paul McCloghrie for the provision of GETM data, and Steven Campana, Linda Marks and Warren Joyce at BIO (Canada) for providing access to their MicroMill and for technical assistance during otolith analyses. This work was funded primarily by the European Commission Marie-Curie Intra-European Fellowship Program (MEIF-CT-2003-501391 'PlaiceLifeLine'). The release of DST-tagged plaice was funded by the UK Department of Environment, Food and Rural Affairs, and the Commission of European Communities Agriculture and Fisheries specific RTD program, PL96-2079, 'Migration, distribution and spatial dynamics of plaice and sole in the North Sea and adjacent areas'. It does not necessarily reflect their views and in no way anticipates the Commission's future policy in this area.

LITERATURE CITED

Anderson MJ (2001) A new method for non-parametric multivariate analysis of variance. Austral Ecol 26:32–46

Ashford J, Jones C (2007) Oxygen and carbon stable isotopes in otoliths record spatial isolation of Patagonian toothfish (*Dissostichus eleginoides*). Geochim Cosmochim Acta 71:87–94

Ayvazian SG, Bastow TP, Edmonds JS, How J, Nowara GB (2004) Stock structure of Australian herring (*Arripis georgiana*) in southwestern Australia. Fish Res 67:39–53

Bastow TP, Jackson G, Edmonds JS (2002) Elevated salinity and isotopic composition of fish otolith carbonate: stock delineation of pink snapper, *Pagrus auratus*, in Shark Bay, Western Australia. Mar Biol 141:801–806

Begg GA, Campana SE, Fowler AJ, Suthers IM (2005) Otolith research and application: current directions in innovation and implementation. Mar Freshw Res 56:477–483

Blamart D, Escoubeyrou K, Juillet-Leclerc A, Ouahdi R (2002) Composition isotopique $\delta^{18}O$ – $\delta^{13}C$ des otolithes des populations de poissons récifaux de Taiaro (Tuamotu, Polynésie française): implications isotopiques et biologiques. C R Biol 325:99–106

Block BA, Finnerty JR (1994) Endothermy in fishes: a phylogenetic analysis of constraints, predispositions, and selection pressures. Environ Biol Fishes 40:283–302

Block BA, Dewar H, Blackwell SB, Williams TD and others (2001) Migratory movements, depth preferences, and thermal biology of Atlantic bluefin tuna. Science 293: 1310–1314

Block BA, Jonsen ID, Jorgensen SJ, Winship AJ and others (2011) Tracking apex marine predator movements in a dynamic ocean. Nature 475:86–90

Botsford LW, Brumbaugh DR, Grimes C, Kellner JB and others (2009) Connectivity, sustainability, and yield: bridging the gap between conventional fisheries management and marine protected areas. Rev Fish Biol Fish 19:69–95

Bromley PJ (2000) Growth, sexual maturation and spawning in central North Sea plaice (*Pleuronectes platessa* L.), and the generation of maturity ogives from commercial catch data. J Sea Res 44:27–43

Campana SE (1999) Chemistry and composition of fish otoliths: pathways, mechanisms and applications. Mar Ecol Prog Ser 188:263–297

Carey FG, Teal JM, Kanwisher JW, Lawson KD (1971) Warm-bodied fish. Am Zool 11:137–145

Coplen TB, Kendall C, Hopple J (1983) Comparison of stable isotope reference material. Nature 302:236–238

Darnaude AM, Sturrock A, Trueman CN, Mouillot D, Craven JA, Campana SE, Hunter E (2014) Listening in on the past: What can otolith $\delta^{18}O$ values really tell us about the environmental history of fishes? PLOS ONE 9:e108539

Devereux I (1967) Temperature measurements from oxygen isotope ratios of fish otoliths. Science 155:1684–1685

Dorval E, Piner K, Robertson L, Reiss CS, Javor B, Vetter R (2011) Temperature record in the oxygen stable isotopes of Pacific sardine otoliths: experimental vs. wild stocks from the Southern California Bight. J Exp Mar Biol Ecol 397:136–143

Dufour E, Höök TO, Patterson WP, Rutherford ES (2008) High-resolution isotope analysis of young alewife *Alosa pseudoharengus* otoliths: assessment of temporal resolution and reconstruction of habitat occupancy and thermal history. J Fish Biol 73:2434–2451

Epstein S, Mayeda T (1953) Variations in ^{18}O contents of waters from natural sources. Geochim Cosmochim Acta 4:213–224

Erisman B, Heyman W, Kobara S, Ezer T, Pittman S, Aburto-Oropeza O, Nemeth RS (2017) Fish spawning aggregations: where well-placed management actions can yield big benefits for fisheries and conservation. Fish Fish 18: 128–144

Fonds M, Cronie R, Vethaak AD, Van Der Puyl P (1992) Metabolism, food consumption and growth of plaice (*Pleuronectes platessa*) and flounder (*Platichthys flesus*) in relation to fish size and temperature. J Sea Res 29: 127–143

Gao YW, Bean D (2008) Stable isotope analyses of otoliths in identification of hatchery origin of Atlantic salmon (*Salmo salar*) in Maine. Environ Biol Fishes 83:429–437

Geffen AJ (2012) Otolith oxygen and carbon stable isotopes in wild and laboratory-reared plaice (*Pleuronectes platessa*). Environ Biol Fishes 95:419–430

Geffen AJ, Morales-Nin B, Gillanders BM (2016) Fish otoliths as indicators in ecosystem based management: results of the 5th International Otolith Symposium (IOS2014). Mar Freshw Res 67:i–iv

Godiksen JA, Svenning MA, Dempson JB, Marttila M, Storm-Suke A, Power M (2010) Development of a species-specific fractionation equation for Arctic charr (*Salvelinus alpinus* (L.)): an experimental approach. Hydrobiologia 650:67–77

Grønkjær P (2016) Otoliths as individual indicators: a reappraisal of the link between fish physiology and otolith characteristics. Mar Freshw Res 67:881–888

Harding J, Nichols JH, Tungate DS (1978) The spawning of plaice (*Pleuronectes platessa* L.) in the southern North Sea and English Channel. Rapp P-V Réun Cons Int Explor Mer 172:102–113

Harwood AJP, Dennis PF, Marca AD, Pilling GM, Millner RS (2008) The oxygen isotope composition of water masses within the North Sea. Estuar Coast Shelf Sci 78:353–359

Hays GC, Ferreira LC, Sequeira AMM, Meekan MG and others (2016) Key questions in marine megafauna movement ecology. Trends Ecol Evol 31:463–475

Hixon MA, Pacala SW, Sandin SA (2002) Population regulation: historical context and contemporary challenges of open vs. closed systems. Ecology 83:1490–1508

Høie H, Folkvord A (2006) Estimating the timing of growth rings in Atlantic cod otoliths using stable oxygen isotopes. J Fish Biol 68:826–837

Høie H, Andersson C, Folkvord A, Karlsen O (2004) Precision and accuracy of stable isotope signals in otoliths of pen-reared cod (*Gadus morhua*) when sampled with a high-resolution micromill. Mar Biol 144:1039–1049

Hunter E, Metcalfe JD, Reynolds JD (2003a) Migration route and spawning area fidelity by North Sea plaice migration. Proc Biol Sci 270:2097–2103

Hunter E, Aldridge JN, Metcalfe JD, Arnold GP (2003b) Geolocation of free-ranging fish on the European continental shelf as determined from environmental variables. I. tidal location method. Mar Biol 142:601–609

Hunter E, Metcalfe JD, Arnold GP, Reynolds JD (2004) Impacts of migratory behaviour on population structure in North Sea plaice. J Anim Ecol 73:377–385

Hunter E, Cotton RJ, Metcalfe JD, Reynolds JD (2009) Large-scale variation in seasonal swimming patterns of plaice in the North Sea. Mar Ecol Prog Ser 392:167–178

Hussey NE, Kessel ST, Aarestrup K, Cooke SJ and others (2015) Aquatic animal telemetry: a panoramic window into the underwater world. Science 348:1255642

Imsland AK, Ólafsson K, Skírnisdóttir S, Gunnarsson S and others (2014) Life history of turbot in Icelandic waters: intra- and inter-population genetic diversity and otolith tracking of environmental temperatures. Fish Res 155: 185–193

Javor B, Dorval E (2014) Geography and ontogeny influence the stable oxygen and carbon isotopes of otoliths of Pacific sardine in the California Current. Fish Res 154:1–10

Kastelle CR, Helser TE, McKay JL, Johnston CG, Anderl DM, Matta ME, Nichol DG (2017) Age validation of Pacific cod (*Gadus macrocephalus*) using high-resolution stable oxygen isotope ($\delta^{18}O$) chronologies in otoliths. Fish Res 185:43–53

Kell LT, Scott R, Hunter E (2004) Implications for current management advice for North Sea plaice: Part I. Migration between the North Sea and English Channel. J Sea Res 51:287–299

Kim ST, O'Neil JR, Hillaire-Marcel C, Mucci A (2007) Oxygen isotope fractionation between synthetic aragonite and water: influence of temperature and Mg^{2+} concentration. Geochim Cosmochim Acta 71:4704–4715

Kimirei IA, Nagelkerken I, Trommelen M, Blankers P and others (2013) What drives ontogenetic niche shifts of fishes in coral reef ecosystems? Ecosystems 16:783–796

Levitus S, Antonov J (1995) Observational evidence of interannual to decadal-scale variability of the subsurface temperature-salinity structure of the World Ocean. Clim Change 31:495–514

Lychakov DV, Rebane YT, Lombarte A, Demestre M, Fuiman LA (2008) Saccular otolith mass asymmetry in adult flatfishes. J Fish Biol 72:2579–2594

Matta ME, Orland IJ, Ushikubo T, Helser TE, Black BA, Valley JW (2013) Otolith oxygen isotopes measured by high-precision secondary ion mass spectrometry reflect life history of a yellowfin sole (*Limanda aspera*). Rapid Commun Mass Spectrom 27:691–699

Metcalfe JD (2006) Fish population structuring in the North Sea: understanding processes and mechanisms from studies of the movements of adults. J Fish Biol 69: 48–65

Metcalfe JD, Righton D, Eastwood P, Hunter E (2008) Migration and habitat choice in marine fishes. In: Magnhagen C, Braithwaite VA, Forsgren E, Kapoor BG (eds) Fish behaviour. Science Publishers, Enfield, NH, p 187–133

Morrongiello JR, Thresher RE, Smith DC (2012) Aquatic biochronologies and climate change. Nat Clim Chang 2: 849–857

Mugiya Y, Uchimura T (1989) Otolith resorption induced by anaerobic stress in the goldfish, *Carassius auratus*. J Fish Biol 35:813–818

Newman SJ, Wright IW, Rome BM, Mackie MC and others (2010) Stock structure of grey mackerel, *Scomberomorus semifasciatus* (Pisces: Scombridae) across northern Australia, based on otolith stable isotope chemistry. Environ Biol Fishes 89:357–367

Northcote TG, Hendy CH, Nelson CS, Boubee JAT (1992) Tests for migratory history of the New Zealand common smelt (*Retropinna retropinna* (Richardson)) using otolith isotopic composition. Ecol Freshw Fish 1:61–72

Paillard D, Labeyrie L, Yiou P (1996) Macintosh program performs time-series analysis. EOS Trans Am Geophys Union 77:379

Pulliam HR (1988) Sources, sinks, and population regulation. Am Nat 132:652–661

R Development Core Team (2011) R: a language and environment for statistical computing. R Foundation for Statistical Computing, Vienna

Righton D, Metcalfe J, Connolly P (2001) Fisheries: different behaviour of North and Irish Sea cod. Nature 411:156

Righton DA, Andersen KH, Neat F, Thorsteinsson V and others (2010) Thermal niche of Atlantic cod *Gadus morhua*: limits, tolerance and optima. Mar Ecol Prog Ser 420:1–13

Righton D, Westerberg H, Feunteun E, Økland F and others (2016) Empirical observations of the spawning migration of European eels: the long and dangerous road to the Sargasso Sea. Sci Adv 2:e1501694

Rijnsdorp AD (1989) Maturation of male and female North Sea plaice (*Pleuronectes platessa* L.). ICES J Mar Sci 46: 35–51

Rijnsdorp AD, Ibelings B (1989) Sexual dimorphism in the energetics of reproduction and growth of North Sea plaice, *Pleuronectes platessa* L. J Fish Biol 35:401–415

Rooker JR, Secor DH (2004) Stock structure and mixing of Atlantic bluefin tuna: evidence from stable $\delta^{13}C$ and $\delta^{18}O$ isotopes in otoliths. Collect Vol Sci Pap ICCAT 56: 1115–1120

Rooker JR, Secor DH, DeMetrio G (2008) Natal homing and connectivity in Atlantic bluefin tuna populations. Science 322:742–744

Sadovy de Mitcheson Y, Cornish A, Domeier M, Colin PL, Russell M, Lindeman KC (2008) A global baseline for spawning aggregations of reef fishes. Conserv Biol 22: 1233–1244

Shephard S, Trueman C, Rickaby R, Rogan E (2007) Juvenile life history of NE Atlantic orange roughy from otolith stable isotopes. Deep Sea Res I 54:1221–1230

Stanley RRE, Bradbury IR, DiBacco C, Snelgrove PVR, Thorrold SR, Killen SS (2015) Environmentally mediated trends in otolith composition of juvenile Atlantic cod (*Gadus morhua*). ICES J Mar Sci 72:2350–2363

Stephenson P (2001) Analysis of stable isotope ratios to investigate stock structure of red emperor and Rankin cod in northern Western Australia. J Fish Biol 58:126–144

Stips A, Bolding K, Pohlmann T, Burchard H (2004) Simulating the temporal and spatial dynamics of the North Sea using the new model GETM (general estuarine transport model). Ocean Dyn 54:266–283

Storm-Suke A, Dempson JB, Reist JD, Power M (2007) A field-derived oxygen isotope fractionation equation for *Salvelinus* species. Rapid Commun Mass Spectrom 21: 4109–4116

Surge D, Walker KJ (2005) Oxygen isotope composition of modern and archaeological otoliths from the estuarine hardhead catfish (*Ariopsis felis*) and their potential to record low-latitude climate change. Palaeogeogr Palaeoclimatol Palaeoecol 228:179–191

Tanner SE, Reis-Santos P, Cabral HN (2016) Otolith chemistry in stock delineation: a brief overview, current challenges and future prospects. Fish Res 173:206–213

Thorrold SR, Jones CM, Campana SE (1997) Response of otolith microchemistry to environmental variations experienced by larval and juvenile Atlantic croaker (*Micropogonias undulatus*). Limnol Oceanogr 42:102–111

Torniainen J, Lensu A, Vuorinen PJ, Sonninen E and others (2017) Oxygen and carbon isoscapes for the Baltic Sea: testing their applicability in fish migration studies. Ecol Evol 7:2255–2267

Trueman CN, MacKenzie KM, Palmer MR (2012) Identifying migrations in marine fishes through stable-isotope analysis. J Fish Biol 81:826–847

Van Neer W, Ervynck A, Bolle LJ, Millner RS (2004) Seasonality only works in certain parts of the year: the reconstruction of fishing seasons through otolith analysis. Int J Osteoarchaeol 14:457–474

Walther BD, Dempster T, Letnic M, McCulloch MT (2011) Movements of diadromous fish in large unregulated tropical rivers inferred from geochemical tracers. PLOS ONE 6:e18351

Wunder MB (2010) Using isoscapes to model probability surfaces for determining geographic origins. In: West JB, Bowen GJ, Dawson TE, Tu KP (eds) Isoscapes: understanding movement, pattern, and process on Earth through isotope mapping. Springer Netherlands, Dordrecht, p 251–270

Zazzo A, Smith GR, Patterson WP, Dufour E (2006) Life history reconstruction of modern and fossil sockeye salmon (*Oncorhynchus nerka*) by oxygen isotopic analysis of otoliths, vertebrae, and teeth: implication for paleoenvironmental reconstructions. Earth Planet Sci Lett 249: 200–215

Editorial responsibility: Stephen Wing, Dunedin, New Zealand

Submitted: April 4, 2017; Accepted: August 9, 2017
Proofs received from author(s): November 2, 2017

Vol. 598: 187–199, 2018
https://doi.org/10.3354/meps12495

MARINE ECOLOGY PROGRESS SERIES
Mar Ecol Prog Ser

Published June 28[§]

Contribution to the Theme Section 'Innovative use of sclerochronology in marine resource management'

Evaluating estuarine nursery use and life history patterns of *Pomatomus saltatrix* in eastern Australia

H. T. Schilling[1,2,*], P. Reis-Santos[3,4], J. M. Hughes[5], J. A. Smith[1,2], J. D. Everett[1,2], J. Stewart[5], B. M. Gillanders[4], I. M. Suthers[1,2]

[1]Evolution and Ecology Research Centre, University of New South Wales, Sydney, NSW 2052, Australia
[2]Sydney Institute of Marine Science, Building 19, Chowder Bay Road, Mosman, NSW 2088, Australia
[3]MARE – Marine and Environmental Sciences Centre, Faculdade de Ciências, Universidade de Lisboa, 1749-016 Campo Grande, Lisboa, Portugal
[4]Southern Seas Ecology Laboratories, School of Biological Sciences, The University of Adelaide, SA 5005, Australia
[5]New South Wales Department of Primary Industries, Chowder Bay Road, Mosman, NSW 2088, Australia

ABSTRACT: Estuaries provide important nursery habitats for juvenile fish, but many species move between estuarine and coastal habitats throughout their life. We used otolith chemistry to evaluate the use of estuaries and the coastal marine environment by juvenile *Pomatomus saltatrix* in eastern Australia. Otolith chemical signatures of juveniles from 12 estuaries, spanning 10° of latitude, were characterised using laser ablation-inductively coupled plasma-mass spectrometry. Based upon multivariate otolith elemental signatures, fish collected from most estuaries could not be successfully discriminated from one another. This was attributed to the varying influence of marine water on otolith elemental composition in fish from all estuaries. Using a reduced number of estuarine groups, the multivariate juvenile otolith elemental signatures and univariate Sr:Ca ratio suggest that between 24 and 52% of adult *P. saltatrix* had a juvenile period influenced by the marine environment. Elemental profiles across adult (age-1) otoliths highlighted a variety of life history patterns, not all consistent with a juvenile estuarine phase. Furthermore, the presence of age-0 juveniles in coastal waters was confirmed from historical length-frequency data from coastal trawls. Combining multiple lines of evidence suggests considerable plasticity in juvenile life history for *P. saltatrix* in eastern Australia through their utilisation of both estuarine and coastal nurseries. Knowledge of juvenile life history is important for the management of coastal species of commercial and recreational importance such as *P. saltatrix*.

KEY WORDS: Otolith chemistry · Elemental profiles · Bluefish · Tailor · Strontium · Barium

INTRODUCTION

Estuaries function as nursery grounds for juveniles of many coastal fish species, providing refuge, food and habitat (Beck et al. 2001, Able 2005). Many species subsequently emigrate from estuaries to join adult populations in coastal waters, with the duration of the estuarine life history stage ranging from months to years (Gillanders et al. 2003, Fodrie & Herzka 2008). Assessing connectivity between estuarine and coastal environments is critical for the management of coastal species, but is a complex task, due to the constraints and logistical difficulties of mark-recapture studies using juvenile fish. An alternative approach is to use the elemental composition of fish otoliths or other calcified structures, which allows insights into how species use estuarine and coastal environments throughout their life history (Gillanders et al. 2003, Brown 2006, Izzo et al. 2016).

In recent decades, otolith chemistry has become an increasingly popular tool to investigate multiple aspects of fish life history. As fish otoliths are biolog-

*Corresponding author: h.schilling@unsw.edu.au
[§]Advance View was available online April 17, 2018

ically inert and grow continuously, trace elements from the surrounding environment are incorporated on the growing surface of the otolith (Campana & Thorrold 2001). Since water masses are known to vary in their environmental conditions over time and space, fish collected in different environments are expected to have different otolith elemental composition (Campana et al. 2000). These elemental 'signatures' or 'fingerprints' have been used to successfully identify natal origins and nursery estuaries of adult fish (Gillanders & Kingsford 1996, Gillanders 2002a, Vasconcelos et al. 2011, Reis-Santos et al. 2013), discriminate between populations (Rooker et al. 2001, Tanner et al. 2016) and determine mixed stock composition (Munch & Clarke 2008, Geffen et al. 2011).

Otoliths are also used as environmental chronometers of temporal variation in elemental concentrations. Through analysis of elemental profiles from the core to the edge of otoliths, a continuous record of how elements change in concentration throughout the life of a fish may be revealed (Campana & Thorrold 2001). In particular, profiles of strontium and barium have been used successfully in reconstructing environmental and estuary–ocean migration histories for individual fish (Elsdon & Gillanders 2005a, Fowler et al. 2016), as concentrations of these elements are strongly influenced by salinity (Secor & Rooker 2000, Walther & Limburg 2012). If fish movement occurs over a large salinity gradient, it is more likely to be detected, and hence most research has focused on migrations between freshwater and marine environments. However, studies reconstructing habitat use and environmental life histories along narrow salinity gradients are becoming more common (Tanner et al. 2013, Williams et al. 2018).

Tailor or bluefish (*Pomatomus saltatrix*) is a globally distributed pelagic mesopredator that is fished commercially and recreationally throughout its range. Stark differences in life history patterns exist between populations (Juanes et al. 1996), particularly in growth rates and average maximum size (L_∞). For example, L_∞ in the west Atlantic Ocean is more than double that in the Mediterranean (Ceyhan et al. 2007, Robillard et al. 2009). In general, adult *P. saltatrix* undertake annual migrations along the coast before spawning at sea, with larvae that are then distributed by ocean currents to downstream areas (Juanes et al. 1996). While larvae recruit to both estuarine and coastal areas in most global populations, in eastern Australia, larvae have only been documented to recruit to estuaries (Miskiewicz et al. 1996), where they remain until they emigrate to coastal marine waters at approximately 27 cm fork length (FL) (Morton et al. 1993, Zeller et al. 1996), corresponding to approximately 1 yr of age (Dodt et al. 2006, H.T.S. unpubl. data). This contrasts with the life history of other populations, namely the eastern Indian Ocean and western Atlantic Ocean populations, which have both coastal and estuarine recruitment (Lenanton et al. 1996, Able et al. 2003, Callihan et al. 2008). It is likely that juvenile tailor in eastern Australia use both estuarine and coastal habitat, and this discrepancy in juvenile habitat use has previously been identified as warranting further attention (Juanes et al. 1996).

Otolith chemistry is an ideal tool with which to investigate life history plasticity and the use of estuarine and coastal juvenile habitats by *P. saltatrix*. The broad goal of this study was to use otolith chemistry techniques to gain insight into the life history of *P. saltatrix* in eastern Australia, specifically estuarine–ocean movements, and to compare these to the life history patterns exhibited by populations elsewhere. Specifically, we tested whether: (1) otoliths of juvenile *P. saltatrix* from different estuaries had characteristic elemental signatures; (2) adult *P. saltatrix* could be assigned to juvenile habitats types based on the elemental signatures from the juvenile area of their otoliths; and (3) elemental profiles from the core to the edge of adult *P. saltatrix* support movement between estuarine and oceanic habitats.

MATERIALS AND METHODS

Fish collection

Juvenile *Pomatomus saltatrix* (n = 360, age-0) were collected from 12 estuaries along the east coast of Australia over 2 southern hemisphere summers (2014/15 and 2015/16; Fig. 1; see Table S1 in the Supplement at www.int-res.com/articles/suppl/m598p187_supp.pdf). Fish were collected from 2 haphazardly selected sites at least 1 km apart within each estuary. As *P. saltatrix* were not found in all estuaries in both years, some estuaries only had fish collected from one summer. Fish were collected with baited handlines and frozen prior to dissection in the laboratory.

Adult *P. saltatrix* (n = 121, age-1) were also collected from both estuarine and coastal habitats along the east coast of Australia during the 2015–2016 summer (to match the 2014–2015 juvenile cohort; Table S1 in the supplement). These fish were collected by commercial fishers or donated by recreational fishers. All fish were frozen prior to dissection. To confirm fish were from the correct cohort, the

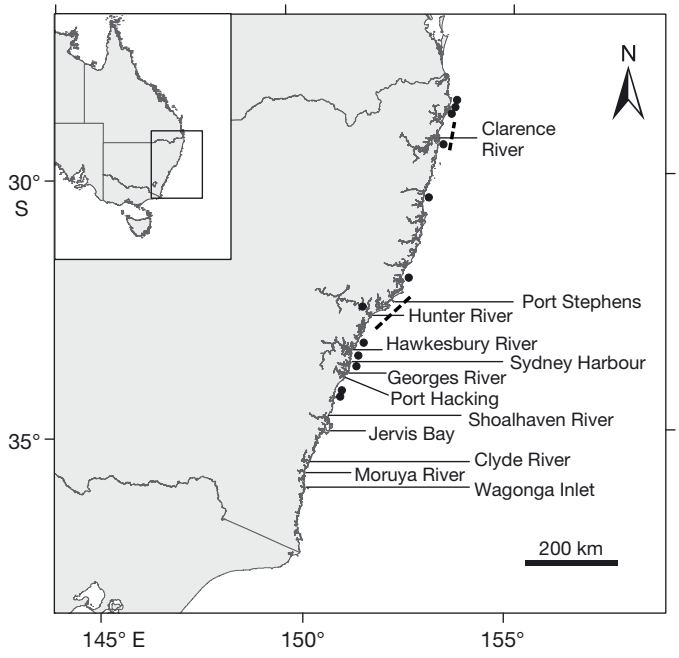

Fig. 1. Locations of the estuaries where juvenile *Pomatomus saltatrix* were collected. The dashed lines represent the regions where offshore trawl samples were conducted during the 1990s. These trawls were conducted at 2 depths: 5–27 m and 64–77 m (Graham et al. 1993a,b, Graham & Wood 1997). Each black circle represents the capture location of a 1-yr-old *P. saltatrix* used in the elemental profile analysis

ages of all fish were estimated from whole otoliths viewed using a light microscope under water with reflected light. This estimated age was subsequently confirmed after transverse sectioning for otolith chemical analysis (see below) and viewing the section under reflected light (H.T.S. unpubl. data, Robillard et al. 2009). Only fish aged 1 yr were selected for subsequent analysis. The age and size at sexual maturity of *P. saltatrix* in eastern Australia are 1 yr and approximately 27 cm FL, respectively (Bade 1977, H.T.S. unpubl. data).

Otolith element analysis

To characterise the elemental signatures of *P. saltatrix* from each estuary, sagittal otoliths were embedded in indium-spiked (^{115}In) resin (~40 ppm) and sectioned transversely. The sections were then polished using fine lapping paper and fixed to microscope slides with ^{115}In-spiked thermoplastic glue (~200 ppm; Hughes et al. 2016), and subsequently cleaned and sonicated with ultrapure water. Otolith sections were analysed at Adelaide Microscopy (The University of Adelaide) using a New Wave UP-213-nm laser ablation system connected to an Agilent 7500cs inductively coupled plasma-mass spectrometer (LA-ICP-MS). The laser was run using a spot size of 30 µm, at a frequency of 5 Hz and fluence of 7 J cm^{-2}. A single spot was ablated on the outer edge of each otolith along the proximal surface, beside the sulcal groove. Spots at the outer edge of the juvenile otoliths were used to characterise the elemental fingerprint of each estuary (i.e. representative of collection site) as this is the material most recently incorporated into the otolith (Elsdon et al. 2008). An inner spot was also ablated on otoliths of adult (age 1) fish along the same axis as the outer spot, and corresponded to ablation of material accreted when these fish were juveniles. These inner spots were located ca. 250 µm from the core, which was the average distance that the corresponding edge spots in juveniles were from the core. The elemental signature of these inner spots should be indicative of the habitat adult fish used as juveniles. The element concentrations measured (and their associated dwell times) were ^{7}Li (150 ms), ^{24}Mg (100 ms), ^{43}Ca (100 ms), ^{55}Mn (150 ms), ^{63}Cu (100 ms), ^{66}Zn (100 ms), ^{88}Sr (100 ms), ^{115}In (10 ms), ^{138}Ba (100 ms) and ^{208}Pb (150 ms). ^{43}Ca was used as an internal standard and ^{115}In was analysed solely to detect any contamination by resin or thermoplastic glue.

Otolith sections of 12 adult fish were randomly selected for analysis of elemental profiles from the core to the edge. The profiles were run at a scan speed of 3 µm s^{-1} using the same instrument settings described above but only for the elements ^{43}Ca, ^{55}Mn, ^{88}Sr, ^{115}In and ^{138}Ba. There is no experimental validation of the relationship between salinity and otolith elemental concentrations for *P. saltatrix*, so it was assumed that the element:Ca ratios on the edges of otoliths represent capture environment, and the average Sr:Ca ratios of the edges of otoliths from adults collected from coastal marine waters were used as reference criteria to characterise the estuarine or coastal marine environments (Milton et al. 2008). The resulting average Sr:Ca ratio from fish captured in coastal marine environments was 2.18 mmol mol^{-1}. We therefore defined Sr:Ca ratios greater than this value as representing coastal marine environments and any value below this value as representing estuarine or brackish environments. Ba:Ca thresholds were calculated in the same way, but there was no difference between edge otolith Ba:Ca of fish from estuarine and coastal collection areas (Welch two-sample *t*-test: $t_{28} = 1.42$, $p = 0.176$); therefore, Ba:Ca was not used to characterise environments fish had spent time in.

Periodic ablations on certified reference materials (glass standard NIST 612 and carbonate standard MACS-3) were used to calibrate elemental concentrations, correct mass bias and instrument drift, and assess external precision. Prior to data collection and before each ablation, background concentrations of elements within the sample chamber were measured for 40 s. A washout delay of 30 s was used between each ablation to allow the chamber to purge and prevent samples from becoming cross-contaminated. Raw count data for the spot analyses were processed using the GLITTER software program (Griffin et al. 2008). Profile data reductions were performed manually using spreadsheet software (Microsoft Excel). All elemental data were expressed as ratios to ^{43}Ca (in mmol mol^{-1}) to account for fluctuations in the ablation yield (Munro et al. 2008). In the few cases where data fell below the limit of detection, the raw data were used because substituting values with an arbitrary number has been shown to bias data owing to non-random patterns in the distribution of small values (Helsel 2006, Schaffler et al. 2014, Lazartigues et al. 2016).

Statistical analysis

PERMANOVA and canonical analysis of principal coordinates (CAP) were used to analyse the elemental data, using PERMANOVA+ for PRIMER software (Anderson et al. 2008). Prior to analysis, the elemental variables in each dataset were normalised and assumptions were checked using shade plots, which confirmed the equal spread of variance within each dataset (Clarke et al. 2014).

The factors in the PERMANOVA analysis were 'estuary' (fixed), 'year' (fixed) and 'site' (random, nested within estuary), and 'fork length' was included as a covariate because otolith chemistry can vary with ontogeny (Beer et al. 2011). Euclidean distances were used to calculate the resemblance matrix. Type I sum of squares was used in the analysis so that the factor 'estuary' was fitted to the data after the covariate. Permutations were conducted on residuals under a reduced model, rather than on raw data, to avoid inflated Type 1 error rates associated with covariates in multivariate analyses (Anderson et al. 2008). P-values were generated using 9999 permutations. This PERMANOVA analysis was performed on the multivariate (elemental 'signature') data as well as univariate element data.

CAP was used to visualise multivariate differences in otolith elemental signatures between estuaries, and to determine how accurately juvenile individuals could be allocated to their collection estuary. The goal of this was to assign juveniles of known estuaries back to the area of collection; therefore a full baseline of all estuaries in which tailor may be found was unnecessary. Following initial analysis, which found that most estuaries could not be discriminated accurately (see 'Results' for details), 3 groups were formed to improve discrimination accuracy. These groups represent the most marine-dominated estuary in NSW (highest salinity; Jervis Bay; mean = 35.0, min = 32.5, max = 36.0, SD = 0.7; CSIRO 1994), the estuary with the largest freshwater input in NSW (lowest salinity; Clarence River; mean = 22.7, min = 5.4, max = 35.7, SD = 9.2; NSW Office of Environment and Heritage 2012) and 'Other estuaries', which were a mix of smaller estuaries of variable freshwater input and size (mean = 30.8, min = 6.4, max = 35.7, SD = 3.7; NSW Office of Environment and Heritage 2012). These 3 groups were selected as a parsimonious representation of the potential types of estuarine habitat used by juvenile *P. saltatrix*. CAP allows additional samples to be placed onto the canonical axes of an existing CAP model and thereby classifies each of the new unknown origin samples to an existing group. Using this procedure, the elemental signatures from the juvenile section of otoliths of 121 adult fish were added onto the existing CAP model to identify the most likely nursery origins of the adult fish [i.e. whether they had a marine influenced signature (Jervis Bay) or an estuarine influenced signature (Clarence River or 'Other estuaries')]. Fish that had signatures that placed them outside the boundaries of the current CAP analysis were removed (n = 3), as this suggests that they came from areas that were not characterised in our analysis.

As an additional concurrent univariate analysis, the Sr:Ca values from the spot analyses of the juvenile section of adult otoliths were arranged to visualise the spectrum of Sr:Ca values observed within juvenile regions, aiming at representing sites used by juveniles relative to the 2.18 mmol mol^{-1} Sr:Ca break between coastal marine and estuarine environments.

Otolith elemental profile data from age-1 tailor were smoothed with a 7-point moving average and plotted relative to distance from the primordium. Fish with similar profiles of both Sr:Ca and Ba:Ca were considered to be representative of different *P. saltatrix* life histories. Despite no difference in Ba:Ca being observed in our saline estuarine and coastal samples described above, high Ba:Ca values were still interpreted as indicative of high freshwater influence.

Historical offshore length frequency analysis

To provide additional support for the findings from the otolith chemistry analyses regarding habitat use and life history patterns, a re-analysis of historical trawl data was undertaken. Length-frequency and abundance data for *P. saltatrix* were compiled from a multi-species dataset from 2 sets of research voyages conducted by the RV 'Kapala' between 1990–1992 and 1995–1996. The original aim of the research voyages was to determine the relative abundances and size composition of prawns and associated bycatch species on trawling grounds in the Newcastle and Clarence River regions (Graham et al. 1993a,b, Graham & Wood 1997). The trawls were conducted in coastal waters of 2 regions, near the Clarence River (northern NSW; 28.5–29.5° S; Fig. 1) and near Newcastle/Tuncurry (central NSW; 32–33° S; Fig. 1). Within these regions, both inshore (5–27 m depth) and offshore (64–77 m depth) trawl transects were conducted. The trawling was conducted with three 22 m headline Florida Flyer prawn nets towed in a triple-rig arrangement. Fish were measured onboard the RV 'Kapala' for fork length.

RESULTS

Juvenile elemental signatures by estuary

Variations in juvenile otolith element:Ca ratios among estuaries were evident (Fig. 2). For instance, higher Ba:Ca and Mn:Ca ratios were found in otoliths from Clarence River than from the other estuaries sampled. Using multivariate PERMANOVA, significant differences were found between estuaries as well as between sites (nested within estuary; Table 1).

Table 1. Summary of PERMANOVA results for the multivariate analysis of edge otolith elemental compositions of juvenile *Pomatomus saltatrix* collected in different estuaries. There were >9000 unique permutations for each term in the model

	df	MS	Pseudo-*F*	p(perm)
Fork length	1	106.46	8.2391	0.0001
Estuary	11	26.595	1.6642	0.0479
Year	1	18.699	2.6345	0.1735
Site(Estuary)	14	13.174	1.9321	0.0012
Estuary × Year	3	10.657	2.3534	0.2458
Year × Site(Estuary)	2	4.159	0.60998	0.6741
Residuals	327	6.8183		
Total	359			

Fork length as a covariate was also significant. Pairwise tests of estuaries revealed that only some estuaries were significantly different to each other (Table S2 in the Supplement). The significant effects of estuary and site show that variation in otolith chemistry of *Pomatomus saltatrix* could be used for discrimination of groups in some situations. Overall, univariate PERMANOVAs found a significant effect of estuary for Mg, significant site (nested within estuary) effects for Mn, Sr and Ba, and a significant estuary × year interaction for Sr (see Table S3 in the Supplement for full univariate PERMANOVA results).

This study was unable to successfully classify fish to estuaries of capture based on their multivariate otolith elemental signatures (with only 31% of individuals correctly classified), but classification success varied greatly among estuaries (Table 2). Classification accuracies for Jervis Bay, Wagonga Inlet and Clarence River were the highest (68.4, 52.0 and 50.0% accuracy respectively), and as Jervis Bay and Clarence River correspond to estuaries with different freshwater flow (highest and lowest salinity), further classification analysis was undertaken (see 'Materials and methods' for full justification). Classification analysis using only 3 groups (Jervis Bay, Clarence River and 'Other estuaries') had an improved overall classification rate of 86%. Individual classification success for each group was 73% for Jervis Bay, 62% for Clarence River and 89% for 'Other estuaries'. While the overall classification accuracy for both the CAP analysis with 12 groups and the CAP analysis with 3 groups was approximately 3 times better than random, the higher allocation

Table 2. Summary of total correct cross-validated individuals of juvenile *Pomatomus saltatrix* classified back to the estuary in which they were caught, based upon otolith elemental chemistry and canonical analysis of principal coordinates (CAP). The % allocation to each estuary in a random assignment would be ~8%

Estuary	% Allocated correctly
Clarence River (Cla)	50.0
Port Stephens (PS)	14.3
Hunter River (HR)	32.0
Hawkesbury River (HB)	31.0
Sydney Harbour (SH)	4.4
Georges River (GR)	36.7
Port Hacking (PH)	20.0
Shoalhaven River (SR)	4.8
Jervis Bay (JB)	68.4
Clyde River (Cly)	38.1
Moruya River (MR)	21.1
Wagonga Inlet (WI)	52.1

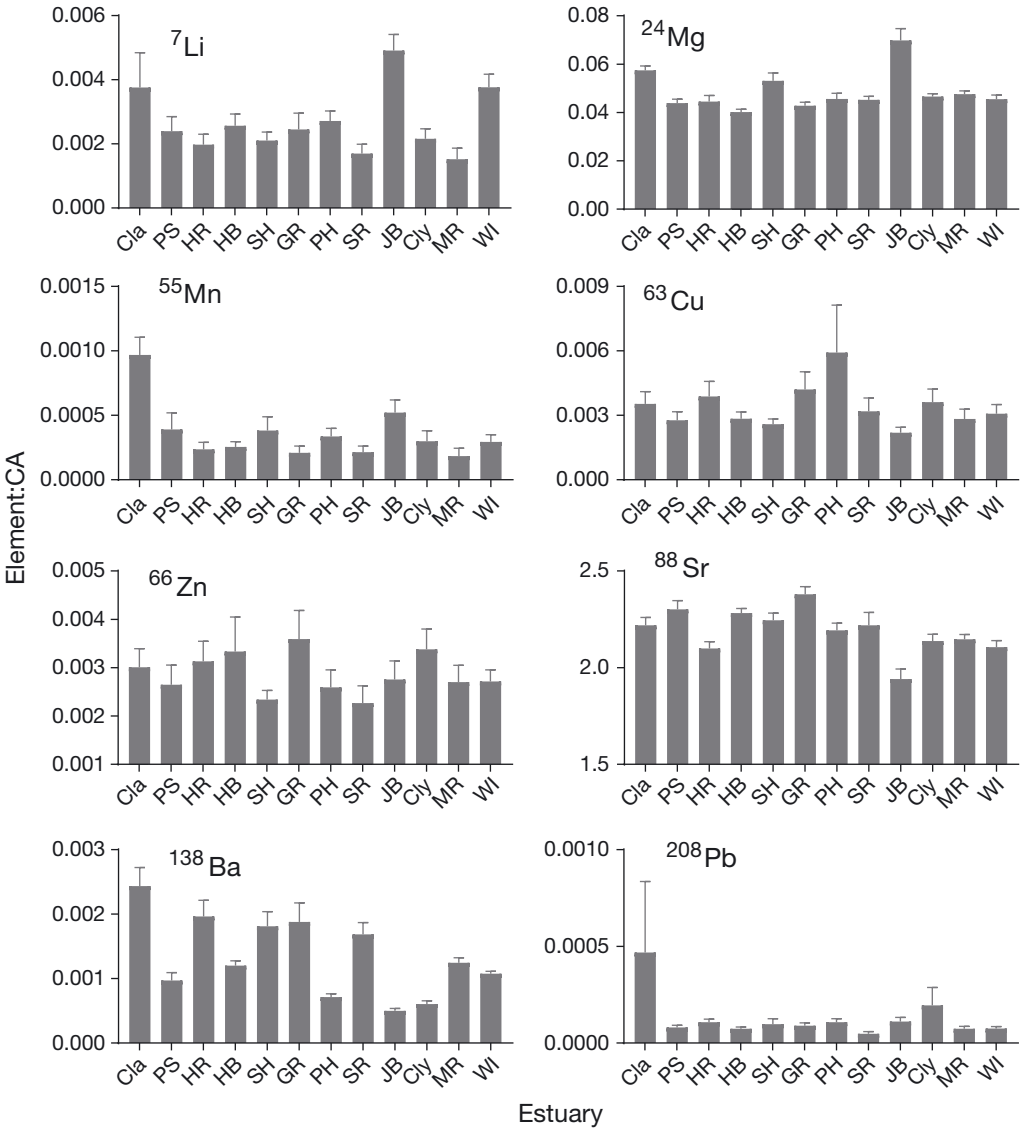

Fig. 2. Element:Ca ratios (mean ± 1 SE) from a spot analysis at the edge of otoliths from juvenile (age-0) *Pomatomus saltatrix* collected in different estuaries. All units are in mmol mol^{-1}. Estuaries are arranged by latitude; abbreviations are given in Table 2. These otolith elemental ratios may represent contributions from a variety of sources, including the water, diet and other physiological influences

accuracies from the 3-group analysis allowed the results to be interpreted in a more biologically meaningful way.

Juvenile life period chemical signatures from adult otoliths

Using the CAP analysis, the chemical composition of the juvenile area of each adult's otolith was used to classify fish to the 3 major estuary groups (Jervis Bay, Clarence River and 'Other estuaries'). A random classification of fish would result in ~33% assigned to each group. Assuming that most estuaries available for *P. saltatrix* would have signatures similar to those of the Clarence River (high freshwater) or 'Other estuaries' groups, classification of fish from estuarine nursery areas would likely result in more fish assigned to these 2 groups. However, the majority of the adult fish were classified as having juvenile otolith elemental 'signatures' most similar to those of the Jervis Bay group, and thus most resembling the marine environment (51.6% Jervis Bay, 30.3% Clarence River and 18.0% 'Other estuaries'). This suggests that both coastal and estuarine environments are important juvenile habitats.

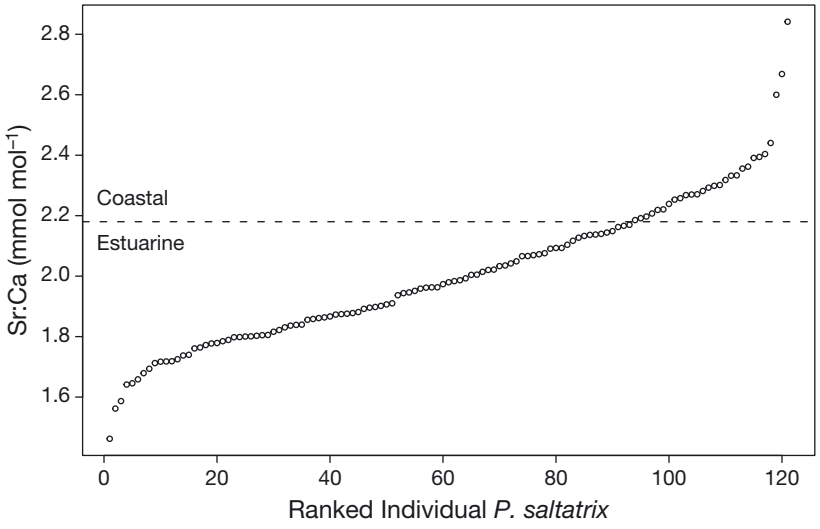

Fig. 3. A visual representation of the continuum of Sr:Ca (mmol mol^{-1}) values observed in the spot analyses of the juvenile section from adult otoliths. The numbers on the *x*-axis indicate ranked individual *Pomatomus saltatrix*. The dashed line shows the calculated threshold between estuarine and coastal waters (2.18 mmol mol^{-1})

The spot analysis of juvenile regions within the adult otoliths revealed a range of Sr:Ca values (1.46–2.84; Fig. 3). These spots provide a snapshot of the juvenile phase of many fish and also suggest that juvenile *P. saltatrix* utilise a wide range of salinity environments. A total of 24% of the spots from the juvenile section of the adult otoliths were above the 2.18 mmol mol^{-1} ratio marine water threshold for Sr:Ca. This was less than the percentage of spots considered to have a signature most similar to the marine environment from the multivariate analysis (52%), but it corroborates evidence that a substantial proportion of the fish sampled were influenced by the marine environment during their juvenile period.

Otolith elemental profiles

All elemental profiles of adult *P. saltatrix* showed elevated levels of manganese at the start (Fig. S1 in the Supplement), indicating that the profile started at the core of the otolith (Brophy et al. 2004). Distinct shifts in elemental concentration were observed in the profiles of some otoliths. Sr and Ba profiles showed variation between individual fish, but 4 main patterns were evident (Fig. 4). While over half of the profiles showed a pat-

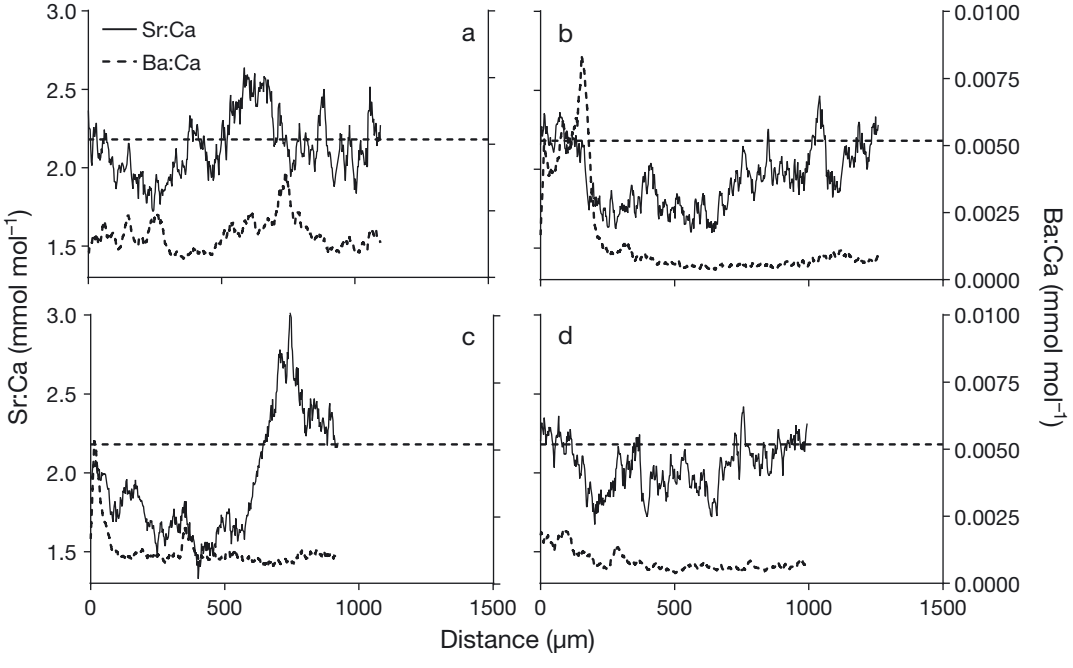

Fig. 4. Examples of profiles of Sr:Ca and Ba:Ca from 1-yr-old *Pomatomus saltatrix* from the core to the edge of otoliths, showing different life history patterns. Profiles were created using a 7-point moving average. The dashed horizontal line represents the calculated reference criteria for Sr:Ca in coastal environments based upon the end points of the profiles from adults caught in coastal environments (2.18 mmol mol^{-1}). These otolith elemental ratios may represent contributions from a variety of sources, including the water, diet and other physiological influences

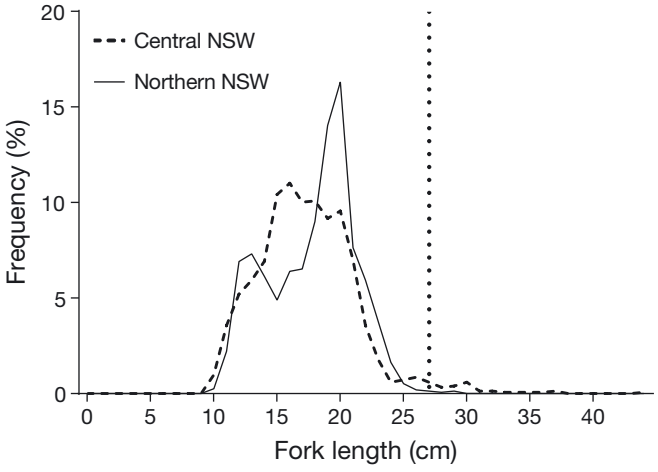

Fig. 5. Compiled length-frequency data of *Pomatomus saltatrix* in coastal trawls from surveys conducted by the RV 'Kapala' in central NSW (dashed line; n = 1533) and northern NSW (solid line; n = 1517) during 1990–1992 and 1995–1996 (Graham et al. 1993a,b, Graham & Wood 1997). The vertical dotted line represents size at age-1, when *P. saltatrix* were previously assumed to emigrate to coastal marine waters (Morton et al. 1993, Zeller et al. 1996)

tern of initially high Ba concentration, which then progressively declined along the profile until approximately 350 µm from the otolith core (Fig. 4B,C), other fish did not have this initial spike of Ba (Fig. 4A,D; Fig. S2 in the Supplement). Sr concentrations initially declined in all fish (until approximately 350 µm from the otolith core) before subsequently increasing again once (Fig. 4B) or twice (Fig. 4A; Fig. S2) throughout the life history at approximately 650 and 900–1000 µm from the core.

Historical coastal trawl data

The RV 'Kapala' voyages collected 3050 *P. saltatrix*. The fish ranged in size from 9 to 37 cm FL, with the majority being between 11 and 20 cm FL (Fig. 5), smaller than the age-1 size of 27 cm at which fish would emigrate from estuaries (Morton et al. 1993). These juvenile fish were only caught in the nearshore coastal trawls and not the deeper offshore trawls.

DISCUSSION

Pomatomus saltatrix in eastern Australia show greater life history plasticity than previously hypothesised. Otolith chemistry analysis of both juveniles and adults revealed a more complex and variable life history than expected, which highlights the use of both coastal and estuarine environments during the juvenile phase of *P. saltatrix* in this region. The multiple lines of evidence, including the better than random assignment of fish to estuary of capture, the range of Sr:Ca values in the juvenile region of adult otoliths, the evidence of estuary–coast movement in some profiles, and the presence of juvenile tailor in offshore trawls, show that *P. saltatrix* use a mix of estuarine and coastal areas during their juvenile stage, with some individuals potentially only using coastal habitats, as seen in other *P. saltatrix* populations globally (Lenanton et al. 1996, Callihan et al. 2008). This further highlights the importance of both estuaries and coastal regions as habitats for juvenile fish (Able 2005, Nagelkerken et al. 2015, Sheaves et al. 2015).

Juvenile otolith chemistry differences

The elemental signatures in *P. saltatrix* otoliths differed significantly among estuaries and among sites within estuaries, indicating that there are inter-individual patterns in habitat use at various spatial scales. The lack of consistent differences between all estuaries concurs with previous research in the region (including for the same set of estuaries), which found differences in the otolith chemistry of *Pagrus auratus* and *Pelates sexlineatus* from some but not all estuaries (Gillanders 2002a, Sanchez-Jerez et al. 2002). Estuaries are variable environments, influenced by both terrestrial and marine inputs (Roy et al. 2001), and the consequent variation in water chemistry is often reflected in otolith chemistry (Elsdon & Gillanders 2003, 2004). Water quality and chemistry within an estuary can vary temporally and spatially, and this variability influences the estuarine signatures from the otoliths. Nonetheless, it is not uncommon for otoliths from some estuaries to have similar elemental signatures, particularly in studies with larger numbers of source sites (Gillanders 2002a, Marriott et al. 2016). It is possible that the lack of distinct otolith chemistry signatures between estuaries found in this study is due to *P. saltatrix* visiting multiple source estuaries. While this study suggests movement of juveniles between estuarine and coastal habitats, previous tag-recapture work suggests there is no evidence for movements between estuaries (Morton et al. 1993). Recapture studies are often biased by high sampling effort in close proximity to release locations (Gillanders et al. 2001). However due to the high popularity of *P. saltatrix* with fishers, fishing effort in this region is uniformly high, and no tag was returned from an estuary other than the estu-

ary in which a fish was tagged. It is thus considered unlikely that the otolith elemental signature of juvenile *P. saltatrix* is being influenced by individuals spending time in multiple estuaries.

It is noted that Jervis Bay, the most marine-dominated estuary, had the lowest average Sr:Ca ratio in the juvenile otoliths. While there was no significant effect of fish length found in the univariate Sr PERMANOVA (Table S3), the fish from Jervis Bay were, on average, the smallest (Table S1) and there were therefore possibly some size-related intrinsic effects on otolith chemistry here such as ontogenetic changes in diet (Buckel et al. 2004, Engstedt et al. 2012) or differing physiology in small *P.saltatrix* (Grammer et al. 2017). Indeed, decreases in Ba:Ca and Sr:Ca ratios have previously been demonstrated in *P. saltatrix* when switching diet from prawns to fish (Buckel et al. 2004). Fish from Clarence River may have had a higher proportion of crustaceans in their diet (due to their small size) than the fish from some of the other estuaries (Schilling et al. 2017), and this may have been reflected by the high Ba:Ca ratios found for this group. However, this pattern was not seen in similarly small fish collected from Jervis Bay, suggesting, conversely, that diet had a limited impact on Ba:Ca ratios in this group (Izzo et al. 2018). Nevertheless, these patterns could simply reflect the higher freshwater input in Clarence River compared with in Jervis Bay.

Due to the large variation in the otolith chemistry of individual *P. saltatrix* within all the estuaries sampled, it was not possible to link *P. saltatrix* individuals to a particular source estuary, and we rejected our initial hypothesis that *P. saltatrix* otoliths have estuary-specific elemental signatures.

Within-estuary variation has previously been observed in multiple estuaries (Dorval et al. 2005), including some of the same estuaries sampled in this study (Gillanders 2002b, Sanchez-Jerez et al. 2002). There are 2 possible explanations for the within-estuary (site) differences observed in the present study. First, perhaps the highly mobile nature of *P. saltatrix* may result in groups of individuals spending enough time in different areas within an estuary to pick up different chemical signatures. Alternatively, it is possible that there are multiple distinct *P. saltatrix* schools within an estuary which do not mix with one another and thus pick up different chemical signatures. Although juvenile *P. saltatrix* are pelagic predators (Schilling et al. 2017), and are known to roam widely around estuaries (Morton et al. 1993), differences in chemical composition resulting from pollutants have been observed in *P. saltatrix* at various sites within a single estuary (Sydney Harbour; Manning et al. 2017). These spatial differences support the idea that juvenile *P. saltatrix* are resident enough that the bioaccumulation of chemicals is different between areas within a single estuary and thus intra-estuary differences in otolith chemistry could be observed in some circumstances.

Assigning adults to estuaries

The ability to assign individual fish back to specific juvenile sites requires a site-specific baseline of elemental fingerprints. To subsequently discern the contribution of individual nursery habitats to adult populations would require a library of otolith chemistry signatures of all potential source sites (Elsdon et al. 2008). While this study did not have such a library, we were able to test the ability to discriminate *P. saltatrix* source sites using our sampled sites. Although the ability to discriminate individual estuaries based upon juvenile *P. saltatrix* otolith elemental signatures was generally poor, it was still possible to distinguish between 3 main groups: Jervis Bay (the most 'marine' estuary), Clarence River (the estuary with the largest freshwater input) and 'Other estuaries' (other estuaries influenced by variable freshwater flows and marine influences). The allocation of signatures from the juvenile section of adult otoliths back to these groups showed that more than half of these fish had juvenile life stage signatures most similar to the Jervis Bay group (51.6%). This indicates that a large proportion of adult *P. saltatrix* have multi-elemental signatures in the juvenile section of their otoliths that are most similar to those found in juveniles from a marine-dominated estuary. The 3 fish that were unable to be allocated to any of our 3 groups may indicate that there was a missing juvenile habitat not sampled; if so, it is likely to be another coastal marine group (possibly a northern group) as our estuary groups encompassed many types of estuaries. We believe it is unlikely that there is another marine group, as a previous study showed that the eastern Australian population is a well-mixed stock along the coast (Nurthen et al. 1992). It is likely that these 3 fish (< 2% of analysed fish) were outliers in the LA-ICP-MS analysis. The univariate analysis of Sr:Ca ratios from the spots in the juvenile section of adult otoliths suggested that 24% of the sampled fish had a significant marine influence in their juvenile life history stage. Combined, the univariate (Sr) and multi-element analysis of the spots suggest that a large proportion (24–52%) of fish were subject to high marine influence at the time that portion of the otolith was being laid down.

The sizes of *P. saltatrix* collected by the RV 'Kapala' from coastal marine waters confirm that juvenile (age-0, <27 cm) *P. saltatrix* inhabit coastal marine environments, providing the first documented evidence of juveniles in coastal environments. The presence of juveniles in the coastal marine environment is also consistent with the strong marine-influenced signature in *P. saltatrix* otoliths demonstrated by the spot analyses in their juvenile section. This re-affirms the suggestion that a large portion of juvenile *P. saltatrix* spend sufficient time in marine-dominated waters to possess a marine-influenced signature, either in coastal waters or near the entrances to estuaries where coastal water is present. This is particularly clear in the wide range of Sr:Ca ratios observed in the juvenile section of adult otoliths. These findings conform with the life history patterns observed in other populations of *P. saltatrix* worldwide that indicate the use of both estuarine and coastal nursery habitats (Lenanton et al. 1996, Able et al. 2003, Callihan et al. 2008), and are further supported by our elemental profile analyses.

Elemental profiles

Our exploratory analysis to determine the suitability of elemental profiles on *P. saltatrix* otoliths revealed multiple patterns in 1-yr-old fish. Assuming the general relationship of increasing Sr and decreasing Ba with salinity (Campana 1999, Elsdon et al. 2008), some of the observed patterns correspond to the previously documented life history of *P. saltatrix* in eastern Australia: that they spawn in marine environments (high Sr and low Ba) before recruiting to estuaries (lower Sr and higher Ba) and then, after a period of time, return to the marine environment (rising Sr and lower Ba; Bade 1977, Morton et al. 1993, Zeller et al. 1996). Only 58% of the fish showed Ba rising to a high level initially, while the remaining 42% only showed a small or negligible rise, suggesting some fish may never enter the less saline regions of estuaries. While the Ba peaks only encompassed a short time period, indicating that lower-salinity estuarine use is limited, the higher Ba concentrations are similar to those recorded in previous research on estuarine fish (Milton et al. 2008, Macdonald & Crook 2010). The Sr profiles show numerous spikes during the juvenile phase, which suggests movement between estuarine/brackish waters and the coastal marine environments. Overall, results indicate that while some juvenile *P. saltatrix* recruit to estuarine or more freshwater environments, others do not, and they may stay in waters of approximately marine salinity or move between estuaries and the coastal marine environment. This is consistent with the results from the spot analyses and historical trawl samples discussed above, which showed that juveniles are not restricted to estuarine environments. All fish except one (fish 3; Fig. S2) were caught in coastal environments, and as such, the end point of the profiles should represent a marine environment.

Low Ba concentrations at the end of the profile, reflecting the marine environment when the fish was caught, would be expected, and this pattern was observed. Conversely, high Sr concentrations would be expected at the end point of the profiles, and was observed, although there were exceptions. As there is a lag between otolith chemistry and fish movement as new otolith material forms, these 2 exceptions may be due to recent movement between estuarine and coastal environments (Elsdon et al. 2008). The lag in incorporating elements such as Sr into the otolith can be over 20 d in some species (Elsdon & Gillanders 2005b, Engstedt et al. 2012), which makes it possible that short temporal scales or recent movements between different environments are missed or not fully represented in the elemental profiles.

It is increasingly being shown that otolith chemistry is influenced by numerous intrinsic (e.g. growth and diet) and extrinsic (e.g. temperature, salinity) factors in addition to a simple relationship with water chemistry (Sturrock et al. 2014, 2015, Grammer et al. 2017). A recent meta-analysis highlighted this by demonstrating that whilst salinity was the primary driver of both Ba and Sr, Sr was also influenced by factors including the ecological niche, condition, diet and ontogeny of individual species (Izzo et al. 2018). As such, it is important to note that factors such as diet may be influencing the Sr:Ca profiles presented here (Engstedt et al. 2012). While experimental validation of the variation in otolith Sr and Ba concentrations is important in order to determine the resolution at which movement between the coast and estuaries (or even within estuaries) can be effectively determined, it is possible to use wild-caught fish from known environments to define reference chemical composition thresholds, assuming the otolith edge is representative of capture location. Sr:Ca ratios of *P. saltatrix* from both estuarine and coastal environments have previously been used to generate reference criteria representative of estuarine (3–12 salinity; 1.68 mmol mol^{-1}) and coastal environments (~35 salinity; 2.2 mmol mol^{-1}) around Chesapeake Bay, USA (Takata 2004). The coastal reference value from that study was similar to that in ours, and suggests that a

Sr:Ca ratio of ~2.2 mmol mol^{-1} is an appropriate reference level for coastal environments. Sr:Ca ratios lower than 1.68 mmol mol^{-1} were rarely observed in our study, probably because the salinity in the estuaries sampled in the present study (NSW Office of Environment and Heritage 2012) is rarely as low as that observed in Chesapeake Bay (Takata 2004). The lack of difference in Ba concentrations between the coastal- and estuarine-caught fish in the present study is possibly because the estuarine regions where *P. saltatrix* were collected were higher in salinity (>25) than regions where salinity is low enough to produce the high Ba:Ca signal commonly observed in other studies (Macdonald & Crook 2010). Overall, analysis of otolith Sr:Ca and Ba:Ca profiles can be used to trace estuarine–ocean movement in *P. saltatrix*, and concur with both the spot analyses and re-analysis of historical coastal length frequencies to indicate that the life history of *P. saltatrix* in eastern Australia is more facultative than previously thought, a finding shared with several studies that have investigated life history patterns in fish (Milton et al. 2008, Gillanders et al. 2015, Condini et al. 2016).

Conclusions

Analysis of the otolith chemistry of *Pomatomus saltatrix* from eastern Australia revealed a more plastic life history than previously hypothesised. Due to the weight of evidence from the otolith chemistry analysis, we rejected our initial hypothesis that the juvenile life history region of adult otoliths would have characteristic estuarine signatures. The present study has shown that *P. saltatrix* in eastern Australia use both estuarine and coastal habitats as part of their juvenile development. Furthermore, the use of coastal habitats by juvenile *P. saltatrix* was supported by both otolith elemental profiles and historical length frequencies. These findings further corroborate the applicability of otolith chemistry to evaluate life history patterns and confirm previously undocumented complexity within fish species life histories.

Acknowledgements. We thank Ashley Fowler (NSW DPI) for providing many helpful ideas during the data analysis process, and Aoife Mcfadden for providing assistance with the LA-ICP-MS. Many volunteers, including Chris Stanley, Chris Setio, Matthew Hyatt, Alexandra Milne-Muller, Koren Fang, Gareth Deacon, Chris Lawson, Aaron Puckeridge, Georgia Brook, Dylan van der Meulen and Matthew Broadhurst, helped to collect the juvenile tailor. Many thanks to the fishers who donated fish as part of the NSW Research Angler Program, in particular Ben van der Woude and Australian Surfcaster. We also thank the Fay family for looking after H.T.S. in Adelaide. This research was supported by an Australian Research Council Linkage Grant (LP150100923), the NSW Recreational Fishing Trust, an Ecological Society of Australia student research award and Hornsby Council. H.T.S. was supported by a Research Training Scholarship. P.R.S. was funded with a Fundação para a Ciência e Tecnologia (FCT) postdoctoral grant (SFRH/BPD/95784/2013). Fish were collected under NSW DPI Scientific Collection Permit no. P03/0086(F)-8.1 and the research was conducted with approval from the NSW DPI Animal Care and Ethics Committee (approval no. SIMS 14/14). This is contribution no. 219 of the Sydney Institute of Marine Science. Thanks also to the 3 anonymous reviewers, who provided many helpful comments.

LITERATURE CITED

Able KW (2005) A re-examination of fish estuarine dependence: evidence for connectivity between estuarine and ocean habitats. Estuar Coast Shelf Sci 64:5–17

Able KW, Rowe P, Burlas M, Byrne D (2003) Use of ocean and estuarine habitats by young-of-year bluefish (*Pomatomus saltatrix*) in the New York Bight. Fish Bull 101: 201–214

Anderson M, Gorley RN, Clarke RK (2008) Permanova+ for Primer: guide to software and statistical methods. Primer-E, Plymouth

Bade TM (1977) The biology of tailor (*Pomatomus saltatrix* Linn.) from the east coast of Australia. MSc thesis, University of Queensland, Brisbane

Beck MW, Heck KL Jr, Able KW, Childers DL and others (2001) The identification, conservation, and management of estuarine and marine nurseries for fish and invertebrates: a better understanding of the habitats that serve as nurseries for marine species and the factors that create site-specific variability in nursery quality will improve conservation and management of these areas. Bioscience 51:633–641

Beer NA, Wing SR, Swearer SE (2011) Otolith elemental evidence for spatial structuring in a temperate reef fish population. Mar Ecol Prog Ser 442:217–227

Brophy D, Jeffries TE, Danilowicz BS (2004) Elevated manganese concentrations at the cores of clupeid otoliths: possible environmental, physiological, or structural origins. Mar Biol 144:779–786

Brown JA (2006) Using the chemical composition of otoliths to evaluate the nursery role of estuaries for English sole *Pleuronectes vetulus* populations. Mar Ecol Prog Ser 306: 269–281

Buckel JA, Sharack BL, Zdanowicz VS (2004) Effect of diet on otolith composition in *Pomatomus saltatrix*, an estuarine piscivore. J Fish Biol 64:1469–1484

Callihan JL, Takata LT, Woodland RJ, Secor DH (2008) Cohort splitting in bluefish, *Pomatomus saltatrix*, in the US mid-Atlantic Bight. Fish Oceanogr 17:191–205

Campana SE (1999) Chemistry and composition of fish otoliths: pathways, mechanisms and applications. Mar Ecol Prog Ser 188:263–297

Campana SE, Thorrold SR (2001) Otoliths, increments, and elements: keys to a comprehensive understanding of fish populations? Can J Fish Aquat Sci 58:30–38

Campana SE, Chouinard GA, Hanson JM, Fréchet A, Brattey J (2000) Otolith elemental fingerprints as biolog-

ical tracers of fish stocks. Fish Res 46:343–357

Ceyhan T, Akyol O, Ayaz A, Juanes F (2007) Age, growth, and reproductive season of bluefish (*Pomatomus saltatrix*) in the Marmara region, Turkey. ICES J Mar Sci 64: 531–536

Clarke KR, Tweedley JR, Valesini FJ (2014) Simple shade plots aid better long-term choices of data pre-treatment in multivariate assemblage studies. J Mar Biol Assoc UK 94:1–16

Condini MV, Tanner SE, Reis-Santos P, Albuquerque CQ and others (2016) Prolonged estuarine habitat use by dusky grouper *Epinephelus marginatus* at subtropical latitudes revealed by otolith microchemistry. Endang Species Res 29:271–277

CSIRO (Commonwealth Scientific and Industrial Research Organisation) (1994) Jervis Bay Baseline Studies, Final Report. Book 2. CSIRO Division of Fisheries

Dodt N, O'Sullivan S, McGilvray J, Jebreen E, Smallwood D, Breddin I (2006) Fisheries long term monitoring program—summary of tailor (*Pomatomus saltatrix*) survey results: 1999–2004. Department of Primary Industries, Brisbane, Australia

Dorval E, Jones CM, Hannigan R, van Montfrans J (2005) Can otolith chemistry be used for identifying essential seagrass habitats for juvenile spotted seatrout, *Cynoscion nebulosus*, in Chesapeake Bay? Mar Freshw Res 56:645–653

Elsdon TS, Gillanders BM (2003) Relationship between water and otolith elemental concentrations in juvenile black bream *Acanthopagrus butcheri*. Mar Ecol Prog Ser 260:263–272

Elsdon TS, Gillanders BM (2004) Fish otolith chemistry influenced by exposure to multiple environmental variables. J Exp Mar Biol Ecol 313:269–284

Elsdon TS, Gillanders BM (2005a) Alternative life-history patterns of estuarine fish: barium in otoliths elucidates freshwater residency. Can J Fish Aquat Sci 62:1143–1152

Elsdon TS, Gillanders BM (2005b) Strontium incorporation into calcified structures: separating the effects of ambient water concentration and exposure time. Mar Ecol Prog Ser 285:233–243

Elsdon TS, Wells BK, Campana SE, Gillanders BM and others (2008) Otolith chemistry to describe movements and life-history parameters of fishes: hypotheses, assumptions, limitations and inferences. Oceanogr Mar Biol Annu Rev 46:297–330

Engstedt O, Koch-Schmidt P, Larsson P (2012) Strontium (Sr) uptake from water and food in otoliths of juvenile pike (*Esox lucius* L.). J Exp Mar Biol Ecol 418-419:69–74

Fodrie FJ, Herzka SZ (2008) Tracking juvenile fish movement and nursery contribution within arid coastal embayments via otolith microchemistry. Mar Ecol Prog Ser 361:253–265

Fowler AM, Smith SM, Booth DJ, Stewart J (2016) Partial migration of grey mullet (*Mugil cephalus*) on Australia's east coast revealed by otolith chemistry. Mar Environ Res 119:238–244

Geffen AJ, Nash RDM, Dickey-Collas M (2011) Characterization of herring populations west of the British Isles: an investigation of mixing based on otolith microchemistry. ICES J Mar Sci 68:1447–1458

Gillanders BM (2002a) Connectivity between juvenile and adult fish populations: do adults remain near their recruitment estuaries? Mar Ecol Prog Ser 240:215–223

Gillanders BM (2002b) Temporal and spatial variability in elemental composition of otoliths: implications for determining stock identity and connectivity of populations. Can J Fish Aquat Sci 59:669–679

Gillanders BM, Kingsford MJ (1996) Elements in otoliths may elucidate the contribution of estuarine recruitment to sustaining coastal reef populations of a temperate reef fish. Mar Ecol Prog Ser 141:13–20

Gillanders BM, Ferrell DJ, Andrew NL (2001) Estimates of movement and life-history parameters of yellowtail kingfish (*Seriola lalandi*): how useful are data from a cooperative tagging programme? Mar Freshw Res 52:179–192

Gillanders BM, Able KW, Brown JA, Eggleston DB, Sheridan PF (2003) Evidence of connectivity between juvenile and adult habitats for mobile marine fauna: an important component of nurseries. Mar Ecol Prog Ser 247:281–295

Gillanders BM, Izzo C, Doubleday ZA, Ye Q (2015) Partial migration: growth varies between resident and migratory fish. Biol Lett 11: 20140850

Graham KJ, Wood BR (1997) Kapala Cruise Report No. 116: the 1995-96 survey of Newcastle and Clarence River prawn grounds. Fisheries Research Institute, Cronulla, NSW

Graham KJ, Liggins GW, Wildforster J, Kennelly SJ (1993a) Kapala Cruise Report No. 110: report for cruises 90-08 to 91-05 conducted between May 1990 and April 1991. Fisheries Research Institute, Cronulla, NSW

Graham KJ, Liggins GW, Wildforster J, Kennelly SJ (1993b) Kapala Cruise Report No. 112: relative abundances and size compositions of prawns and by-catch species on New South Wales prawn grounds during surveys V-VIII (May 1991—May 1992). Fisheries Research Institute, Cronulla, NSW

Grammer GL, Morrongiello JR, Izzo C, Hawthorne PJ, Middleton JF, Gillanders BM (2017) Coupling biogeochemical tracers with fish growth reveals physiological and environmental controls on otolith chemistry. Ecol Monogr 87:487–507

Griffin W, Powell W, Pearson N, O'Reilly S (2008) GLITTER: data reduction software for laser ablation ICP-MS. Laser Ablation-ICP-MS in the Earth Sciences. Mineralogical Association of Canada Short Course Series 40:204–207

Helsel DR (2006) Fabricating data: How substituting values for nondetects can ruin results, and what can be done about it. Chemosphere 65:2434–2439

Hughes JM, Stewart J, Gillanders BM, Collins D, Suthers IM (2016) Relationship between otolith chemistry and age in a widespread pelagic teleost *Arripis trutta*: influence of adult movements on stock structure and implications for management. Mar Freshw Res 67:224–237

Izzo C, Doubleday ZA, Grammer GL, Gilmore KL and others (2016) Fish as proxies of ecological and environmental change. Rev Fish Biol Fish 26:265–286

Izzo C, Reis-Santos P, Gillanders BM (2018) Otolith chemistry does not just reflect environmental conditions: a meta-analytic evaluation. Fish Fish, https://doi.org/10.1111/faf.12264

Juanes F, Hare JA, Miskiewicz AG (1996) Comparing early life history strategies of *Pomatomus saltatrix*: a global approach. Mar Freshw Res 47:365–379

Lazartigues AV, Plourde S, Dodson JJ, Morissette O, Ouellet P, Sirois P (2016) Determining natal sources of capelin in a boreal marine park using otolith microchemistry. ICES J Mar Sci 73:2644–2652

Lenanton R, Ayvazian S, Pearce A, Steckis R, Young G (1996) Tailor (*Pomatomus saltatrix*) off Western Australia:

where does it spawn and how are the larvae distributed? Mar Freshw Res 47:337–346

Macdonald JI, Crook DA (2010) Variability in Sr:Ca and Ba:Ca ratios in water and fish otoliths across an estuarine salinity gradient. Mar Ecol Prog Ser 413:147–161

Manning TM, Roach AC, Edge KJ, Ferrell DJ (2017) Levels of PCDD/Fs and dioxin-like PCBs in seafood from Sydney Harbour, Australia. Environ Pollut 224:590–596

Marriott AL, McCarthy ID, Ramsay AL, Chenery SRN (2016) Discriminating nursery grounds of juvenile plaice (*Pleuronectes platessa*) in the south-eastern Irish Sea using otolith microchemistry. Mar Ecol Prog Ser 546:183–195

Milton D, Halliday I, Sellin M, Marsh R, Staunton-Smith J, Woodhead J (2008) The effect of habitat and environmental history on otolith chemistry of barramundi *Lates calcarifer* in estuarine populations of a regulated tropical river. Estuar Coast Shelf Sci 78:301–315

Miskiewicz AG, Bruce BD, Dixon P (1996) Distribution of tailor (*Pomatomus saltatrix*) larvae along the coast of New South Wales, Australia. Mar Freshw Res 47:331–336

Morton RM, Halliday I, Cameron D (1993) Movement of tagged juvenile tailor (*Pomatomus Saltatrix*) in Moreton bay, Queensland. Aust J Mar Freshwater Res 44:811–816

Munch SB, Clarke LM (2008) A bayesian approach to identifying mixtures from otolith chemistry data. Can J Fish Aquat Sci 65:2742–2751

Munro AR, Gillanders BM, Elsdon TS, Crook DA, Sanger AC (2008) Enriched stable isotope marking of juvenile golden perch (*Macquaria ambigua*) otoliths. Can J Fish Aquat Sci 65:276–285

Nagelkerken I, Sheaves M, Baker R, Connolly RM (2015) The seascape nursery: a novel spatial approach to identify and manage nurseries for coastal marine fauna. Fish Fish 16:362–371

NSW Office of Environment and Heritage (2012) OEH NSW estuaries salinity data compilation 1992 to 2011. NSW Government Public Works, Manly Hydraulic Laboratory, Manly Vale

Nurthen R, Cameron R, Briscoe D (1992) Population genetics of tailor, *Pomatomus saltatrix* (Linnaeus) (Pisces: Pomatomidae) in Australia. Mar Freshw Res 43:1481–1486

Reis-Santos P, Tanner SE, Vasconcelos RP, Elsdon TS, Cabral HN, Gillanders BM (2013) Connectivity between estuarine and coastal fish populations: contributions of estuaries are not consistent over time. Mar Ecol Prog Ser 491:177–186

Robillard E, Reiss CS, Jones CM (2009) Age-validation and growth of bluefish (*Pomatomus saltatrix*) along the East Coast of the United States. Fish Res 95:65–75

Rooker JR, Secor DH, Zdanowicz VS, Itoh T (2001) Discrimination of northern bluefin tuna from nursery areas in the Pacific Ocean using otolith chemistry. Mar Ecol Prog Ser 218:275–282

Roy PS, Williams RJ, Jones AR, Yassini I and others (2001) Structure and Function of South-east Australian Estuaries. Estuar Coast Shelf Sci 53:351–384

Sanchez-Jerez P, Gillanders BM, Kingsford MJ (2002) Spatial variability of trace elements in fish otoliths: comparison with dietary items and habitat constituents in seagrass meadows. J Fish Biol 61:801–821

Schaffler JJ, Miller TJ, Jones CM (2014) Spatial and temporal variation in otolith chemistry of juvenile Atlantic menhaden in the Chesapeake Bay. Trans Am Fish Soc 143:1061–1071

Schilling HT, Hughes JM, Smith JA, Everett JD, Stewart J, Suthers IM (2017) Latitudinal and ontogenetic variation in the diet of a pelagic mesopredator (*Pomatomus saltatrix*), assessed with a classification tree analysis. Mar Biol 164:75

Secor DH, Rooker JR (2000) Is otolith strontium a useful scalar of life cycles in estuarine fishes? Fish Res 46:359–371

Sheaves M, Baker R, Nagelkerken I, Connolly RM (2015) True value of estuarine and coastal nurseries for fish: incorporating complexity and dynamics. Estuar Coast 38:401–414

Sturrock AM, Trueman CN, Milton JA, Waring CP, Cooper MJ, Hunter E (2014) Physiological influences can outweigh environmental signals in otolith microchemistry research. Mar Ecol Prog Ser 500:245–264

Sturrock AM, Hunter E, Milton JA, EIMF, Johnson RC, Waring CP, Trueman CN (2015) Quantifying physiological influences on otolith microchemistry. Methods Ecol Evol 6:806–816

Takata LT (2004) Habitat use and cohort recruitment patterns of juvenile bluefish (*Pomatomus saltatrix*) in diverse Maryland nursery systems. MSc thesis, University of Maryland

Tanner SE, Reis-Santos P, Cabral HN (2016) Otolith chemistry in stock delineation: a brief overview, current challenges and future prospects. Fish Res 173:206–213

Tanner SE, Reis-Santos P, Vasconcelos RP, Fonseca VF, França S, Cabral HN, Thorrold SR (2013) Does otolith geochemistry record ambient environmental conditions in a temperate tidal estuary? J Exp Mar Biol Ecol 441:7–15

Vasconcelos RP, Reis-Santos P, Costa MJ, Cabral HN (2011) Connectivity between estuaries and marine environment: Integrating metrics to assess estuarine nursery function. Ecol Indic 11:1123–1133

Walther BD, Limburg KE (2012) The use of otolith chemistry to characterize diadromous migrations. J Fish Biol 81:796–825

Williams J, Jenkins GP, Hindell JS, Swearer SE (2018) Fine-scale variability in elemental composition of estuarine water and otoliths: developing environmental markers for determining larval fish dispersal histories within estuaries. Limnol Oceanogr 63:262–277

Zeller BM, Pollock BR, Williams LE (1996) Aspects of the life history and management of tailor (*Pomatomus saltatrix*) in Queensland. Mar Freshw Res 47:323–329

Editorial responsibility: Stylianos Somarakis, Heraklion, Greece

Submitted: June 19, 2017; Accepted: January 22, 2018
Proofs received from author(s): March 15, 2018

Vol. 598: 201–212, 2018
https://doi.org/10.3354/meps12234

MARINE ECOLOGY PROGRESS SERIES
Mar Ecol Prog Ser

Published June 28[§]

Contribution to the Theme Section 'Innovative use of sclerochronology in marine resource management'

Environmental drivers of growth and predicted effects of climate change on a commercially important fish, *Platycephalus laevigatus*

Joshua Barrow[1,*], John Ford[1,2], Rob Day[1], John Morrongiello[1]

[1]School of BioSciences, University of Melbourne, Parkville 3010, Victoria, Australia
[2]Mezo Research, 28 Freshwater Place, Southbank, Melbourne 3006, Victoria, Australia

ABSTRACT: Human-driven climate change and habitat modification are negatively impacting coastal ecosystems and the species that reside within them. Uncovering how individuals of key species respond to environmental influences is crucial for effective and responsive coastal resource and fisheries management. Here, using an otolith based analysis, we recreated the growth history of rock flathead *Platycephalus laevigatus* from Corner Inlet, Victoria, Australia, over a 32 yr timeframe and related growth variation to changes in key environmental variables. Growth increased with higher temperatures during the fish growing season (December–May) and also increased with higher freshwater flow during the period important for seagrass growth (July–February). We hypothesise that fish are responding to enhanced productivity in the seagrass food web, driven by increased nutrient input from freshwater flows. Fish also appear to be responding to higher temperatures via a direct physiological pathway. We then predicted fish growth under 3 plausible climate change scenarios. Growth is predicted to increase across all our projections, because any predicted decrease in river flow will likely be offset by rapid predicted increases in temperature. Our results highlight the value of understanding the drivers of long-term growth variation in harvested fishes as this allows for the prediction of future productivity under a range of environmental and management scenarios.

KEY WORDS: Climate change · Coastal ecosystems · Ecosystem resilience · Fisheries productivity · Fish growth · Variable growth · Otolith · Sclerochronology

INTRODUCTION

Coastal areas are dynamic and complex environments that support valuable fisheries around the world (FAO 2016). Occurring at the interface of land and sea, they are naturally affected by both terrestrial and marine processes that together play a fundamental role in driving variation in abiotic conditions (Alongi 1998). Coastal waters are, however, heavily affected by human activity (Halpern et al. 2008) and climate change (Harley et al. 2006). The growth information naturally archived in fish otoliths provides a unique opportunity to recreate multi-decadal time series in regions where monitoring data does not exist (Morrongiello et al. 2012, Poloczanska et al. 2016). This valuable longer-term perspective is vital to understanding and managing the impacts of natural and anthropogenic change on fisheries productivity.

Habitat forming species such as seagrass play a fundamental role in underpinning the productivity of coastal fisheries (Butler & Jernakoff 1999, Ellison et al. 2005). For example, seagrass provides protection and resources for newly settled larvae and juvenile fishes (Jenkins et al. 1997, Ford et al. 2010), as well as feeding and spawning opportunities for adults (Klumpp & Nichols 1983). The health and productivity of seagrass itself is driven by both terrestrial and marine processes that are increasingly being modi-

*Corresponding author: j.barrow@student.unimelb.edu.au

[§]Advance View was available online September 5, 2017

Publisher: Inter-Research · www.int-res.com

fied by humans (Orth et al. 2006). Terrestrial runoff, marine currents, and wind-driven mixing provide nutrients that fertilise seagrass beds. However, in urbanised and agricultural catchments, nutrient loads can exceed natural levels and result in phytoplankton blooms and excessive algal growth that reduce light penetration or smother seagrass (Thomsen et al. 2012). Likewise, catchment erosion increases water turbidity which can also retard seagrass growth. Globally, seagrasses are declining at an accelerating rate (Waycott et al. 2009) with consequent detrimental impacts to many species that depend on them.

Coastal fishery productivity is also directly affected by freshwater inflows. For example, Morrongiello et al. (2014) found that recruitment success and growth rate of an estuarine fish was strongly related to high freshwater flows during the spawning season and during the growing year. These results suggest that flows play an important role in providing both a spawning cue and favourable conditions for larval survival and juvenile and adult growth. Increased recruitment success and somatic growth subsequently impacts the biomass of adults, and therefore fishery productivity (Bardos et al. 2006, Whitten et al. 2013). While increased nutrients often positively influence ecosystem productivity, excessive nutrient inputs can promote harmful algal blooms (McComb et al. 1995). Further, sediment and phytoplankton-related increases in turbidity can negatively affect the foraging success of visual predators (Abrahams & Kattenfeld 1997, Sohel et al. 2017). Reduced prey encounter rates and food acquisition can subsequently affect individual growth and fitness. River flow can therefore affect the primary productivity of the foundation species, and drive the abundances and reproductive success of all trophic levels, including key fisheries species.

Fishes have physiological tolerances that allow them to live within a specific range of variation in environmental factors (Barton et al. 2002). Changes in environmental conditions, such as temperature, beyond this range can influence abundances and distributions, and can be stressful or even fatal to fish (Roessig et al. 2004). In many species, a slight temperature increase may be initially beneficial as it results in increased energy and therefore increased growth (Takasuka & Aoki 2006). However, if temperature exceeds the optimal range for a particular species, it can be deleterious to growth (Wang & Overgaard 2007). In coastal environments many fishes may also be completely dependent on specific habitat, so their persistence in that ecosystem will depend on the response of that habitat to fluctuations in temperature. Rainfall, nutrient upwelling and temperature will all vary with wind patterns and ocean circulation, so average wind direction and oceanic indices can also be important predictors of these 3 key environmental parameters affecting fish growth.

The effects of environmental change on coastal ecosystem productivity, and in particular the growth rates and production of commercial resources in coastal ecosystems, have seldom been examined at longer time-scales, probably due to the lack of good long-term monitoring in most such systems. Similarly, the importance of juvenile growth rates for fisheries dynamics is increasingly understood (Cowan et al. 2000, Whitten et al. 2013), but the factors controlling it have seldom been investigated at the time scales relevant to both fishery management and predicting future climate change effects. A novel way to overcome the lack of longer term monitoring is to use fish otoliths as records of growth rates (Thresher et al. 2007, Black 2009, Matta et al. 2010, Morrongiello & Thresher 2015), and then relate these to available environmental data records.

This study investigates the influence of 4 environmental factors — freshwater flows, temperature, wind, and the Southern Oscillation Index (SOI) — on the growth of the commercially important fish, rock flathead *Platycephalus laevigatus*, in Corner Inlet, Victoria, Australia. We explore the environmental drivers of growth variation in this species using mixed effects models to analyse otolith samples from 1982 to 2014. We recreate a 32 yr growth biochronology and partition growth into its intrinsic and extrinsic components (Weisberg et al. 2010 Morrongiello & Thresher 2015). We then use these models to predict fish growth under a range of plausible future climate scenarios.

We expect that the growth of flathead will reflect a complex integration of different physical processes and causal pathways (Fig. 1). We predict that freshwater flow can affect growth via 2 distinct and opposing mechanisms: increased flow during the period July–February will provide critical nutrients for seagrass and thus result in habitat expansion, which in turn will promote flathead growth. Conversely, higher flows during the period December–May (the fish growing period) will increase turbidity and limit the efficacy of feeding, as flathead are ambush predators. We expect that increased temperatures during the growing season will promote fish growth via a direct physiological pathway (this population is approximately in the middle of its range, so should be favoured by warming), or via an indirect promotion

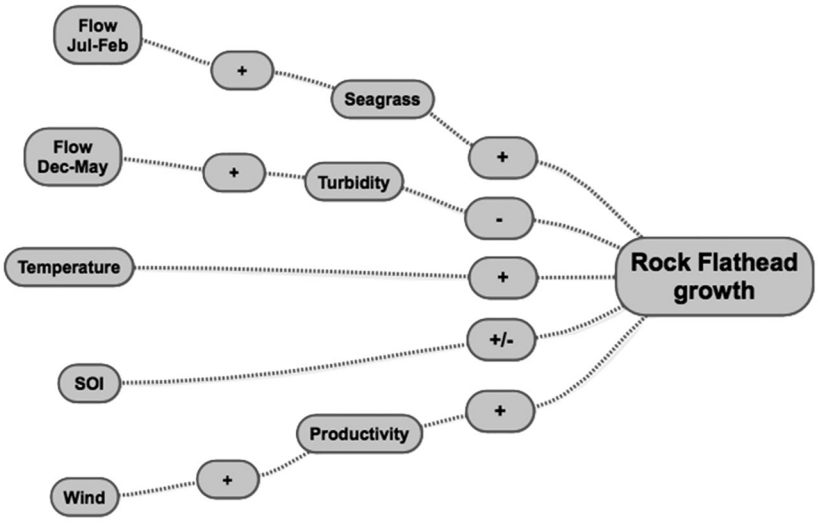

Fig. 1. Conceptual model of the predicted effects of environmental factors on rock flathead *Platycephalus laevigatus* growth. Plus (+) and minus (–) signs indicate that there could be a positive or negative influence of the environmental factor on the subsequent effect or habitat. For example, higher river flow in July–February could increase seagrass cover, and subsequently increase rock flathead growth

of primary productivity that has a positive cascading effect through the food web. This effect would be consistent with a previous growth study on rock flathead from Western Australia (Coulson et al. 2014). We hypothesise that zonal westerly winds will increase nutrient upwelling and thus promote system productivity, whilst we also expect that fish growth will be positively correlated with positive SOI values (La Niña events), which affects local rainfall and thus stream flows.

MATERIALS AND METHODS

Study site

Corner Inlet Marine and Coastal Park (38° 45′ 57″ S, 146° 20′ 21″ E) is a large embayment (18 500 ha) in Victoria, approximately 180 km southeast of Melbourne (Fig. 2). The inlet comprises extensive shallow sand and mudflats at <2 m depth fragmented by deeper tidal channels. Subtidal seagrass beds are abundant on the shallow areas and composed mainly of *Posidonia australis* and *Zostera nigracaulis*. These seagrass beds are vital habitat for many fish and invertebrate species within Corner Inlet, including a number of commercially important fish species (Kemp et al. 2013). The main growth window for both seagrass species is the late winter to early summer period (July–February), when epiphyte growth is depressed due to low water temperatures (Ford et al. 2016). Seagrass cover in Corner Inlet has declined 23 % in the past 48 yr, at a rate of 0.5 km^2 yr^{-1} (Ford 2014, Ford et al. 2016). This seagrass decline, attributed to algal blooms and turbidity, may have affected the productivity of the ecosystem and its reliant species.

Study species

Rock flathead *Platycephalus laevigatus* is a seagrass-associated fish inhabiting shallow water throughout southern Australia (Koopman et al. 2004). The Corner Inlet population is approximately in the middle of this species' distribution, and contains both spawning and recruited individuals; however, linkages with other populations are currently unknown (Koopman et al. 2004, Kemp et al.

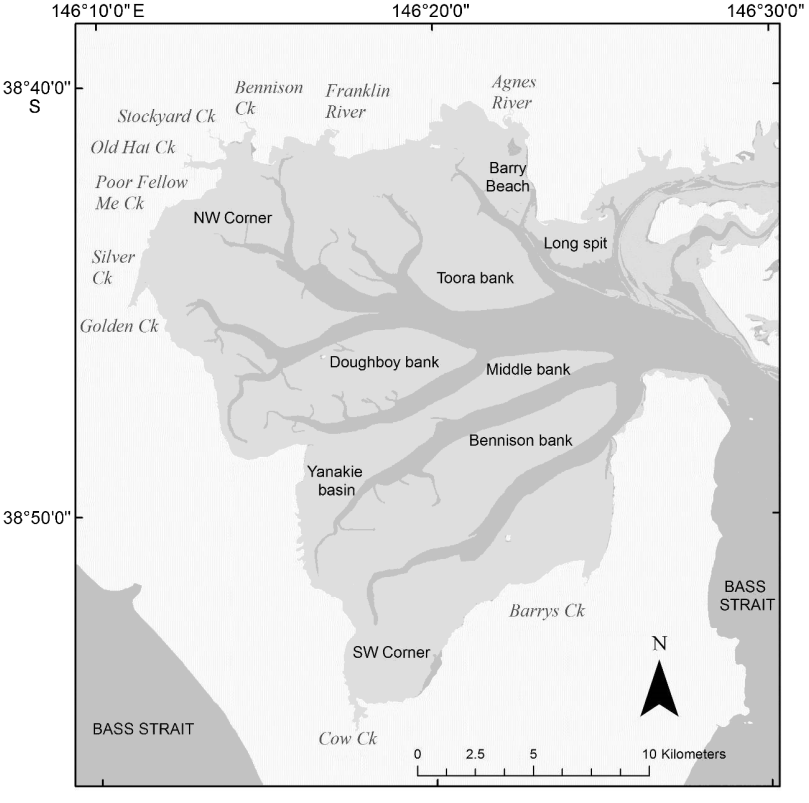

Fig. 2. Corner Inlet, Victoria, Australia (from Ford et al. 2016)

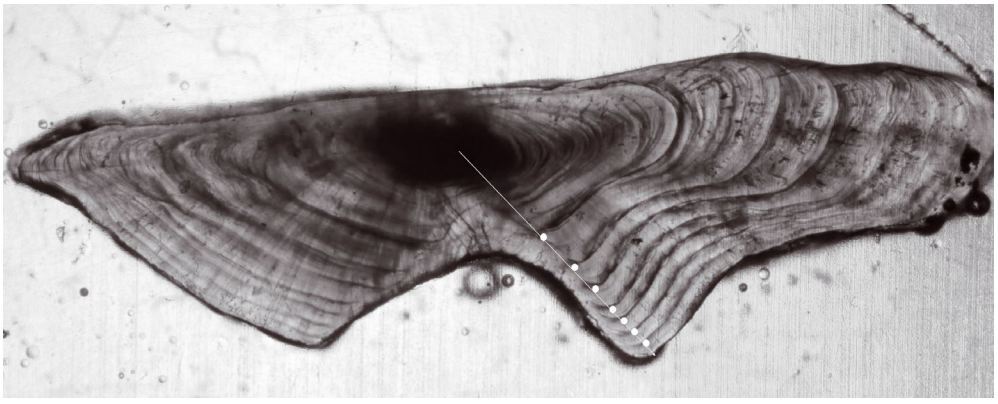

Fig. 3. Sectioned *Platycephalus laevigatus* otolith with 7 opaque zones, taken with transmitted light. The white line identifies the axis along which the age of the otolith was estimated, and the circles identify where measurements between opaque zones were taken

2013). Newly settled *P. laevigatus* spend the first part of their life on bare sand flats before moving into the seagrass beds as older juveniles and remaining there as adults (Jenkins et al. 1993). In Corner Inlet, rock flathead constitutes approximately 23% by weight of the total fishery, and is one of the most valuable species along with King George whiting *Sillaginodes punctatus* and southern calamari *Sepioteuthis australis* (Kemp et al. 2013). Rock flathead, King George whiting and southern calamari together contribute over AU$1.6 million of the total 'off the boat' value of the fishery, and are also important recreationally targeted species (Department of Primary Industries 2012).

Sample collection and estimation of age and growth

Otoliths from 526 fish were collected from the commercial fishery over the period 1994–2014. One otolith from each fish was embedded in clear epoxy resin (EpoFix) in embedding moulds (14 × 5 × 6 mm). Using a low speed diamond saw (South Bay Technology Model 650) we cut a transverse section (~0.3 mm) through the core of the otolith (previously marked with pencil under a microscope). The sections were ground and polished (using a South Bay Technology Model 920 lapping and polishing machine), then mounted on a microscope slide. Digital images of each section were captured using a Canon EOS 60D digital camera attached to a compound microscope at ×40 magnification.

Coulson et al. (2014) used marginal increment analysis to show that a single opaque zone is laid down annually in otoliths of *P. laevigatus* throughout its life. Therefore, opaque zones can be used to determine the age of fish from this species. Using the same method, Koopman et al. (2004) established that opaque zones are laid down in December in Corner Inlet rock flathead. We counted the opaque zones on the dorsal side of the otolith to determine the age of each fish, taking into consideration the date that the fish were caught and the birth date of the species. Despite individuals being found in spawning condition in most months throughout the year, the main spawning period of *P. laevigatus* in Victoria is between September and February (Koopman et al. 2004). Therefore an arbitrary birthdate of December 1 was chosen to correspond with the middle of the spawning period and the period of new increment formation.

We used Image Pro Plus software (v.6.3, Mediacybernetics) to measure growth increments on the sectioned otoliths. Measurements were taken of the distances between the outer edges of each opaque zone, to determine the width of each consecutive growth increment (Fig. 3). We also measured the distance between the otolith core and the periphery (outermost edge of the otolith). We used this measurement to compare otolith size and total fish length, ensuring that otolith growth is an appropriate proxy for fish somatic growth (Fig. S1 in the Supplement at www.int-res.com/articles/suppl/m598p201_supp.pdf). Measurements were restricted to increments after the second growth ring because the location of the first growth ring can reflect 8–14 mo of growth depending on when an individual was spawned.

Statistical analyses

We investigated the sources of variation in annual growth of rock flathead (increment width in mm) using a mixed effects modelling framework. Models contained different combinations of fixed intrinsic predictors (within-individual), fixed extrinsic predictors (environmental), and their interactions. Each increment width was treated as a separate response sample, which resulted in 2145 total increment meas-

Table 1. Descriptions of intrinsic (within-individual), extrinsic (environmental) and random factors used in rock flathead *Platycephalus laevigatus* growth analysis, with ranges and means of measured values (where applicable)

Parameter	Description		Range	Mean
Intrinsic factors				
AOG	Age at which the year of growth occurred		2–17 yr	4.5 yr
AAC	Age at which the fish was captured		2–17 yr	6.9 yr
Sex	Male or female			
Extrinsic factors				
Temperature	Average maximum temperature during the main growth period (Dec–May)		20.9–25.3°C	23.2°C
Flow	River flow from the Agnes and Franklin rivers during seagrass growth (Jul–Feb) and flathead growth (Dec–May) of the previous year. Calculated as mean of highest 10% of flows per year, and median flow.	July–Feb highest 10%:	100.8–1912.3 Ml	646.9 Ml
		July–Feb median:	18.8–125.1 Ml	74.8 Ml
		Dec–May highest 10%:	44.7–1173.5 Ml	341.94 Ml
		Dec–May median:	8.1–29.7 Ml	29.7 Ml
Wind	Zonal westerly wind index, based on direction and strength of winds		−70.4–465.4	184.7
SOI	Monthly Southern Oscillation Index		−1.2–19.7	−1.2
Random factors				
1|Year	Year that the increment was formed			
1|FishID	Unique code which identifies each fish			
AOG|X	Random age slope for X (FishID and Year random intercepts)			

urements. The issue of non-independence of increments from the same fish was dealt with in the model structure as described below.

Intrinsic predictors

Fixed intrinsic predictors were sex, age of the fish at the time the growth increment was formed (AOG), and age at capture (AAC) (Table 1). Age at capture was included in the data to test for any bias associated with age selectivity in the samples (Morrongiello et al. 2012). We introduced a random intercept for FishID to induce a correlation among increment measurements and allow each fish to have higher or lower growth than the model's intercept, and to account for non-independence of the response data (Morrongiello & Thresher 2015). Similarly, increments formed by different fish in a given year are also non-independent as the sampled fish were exposed to the same environmental conditions. We included a random intercept for Year to induce a correlation among increments at this level. We also investigated whether including a random age slope for FishID (AOG|FishID) and Year (AOG|Year), would improve the fit of the model (Table 2). These random slopes allow for individual-specific differences in the growth–age relationship, and year-dependent differences in age-specific growth.

Extrinsic predictors

We developed 4 environmental variables to test our hypotheses about the drivers of variation in fish growth (Fig. 1). These fixed extrinsic factors included the temperature in that year (Temperature), nutrient input from freshwater flows in the corresponding year and the months leading up to that year (Flow), wind strength and direction in that year (Wind), and the southern oscillation index for that year (SOI) (Table 1; Figs. S2 & S3 in the Supplement). Mean maximum temperature was available from a nearby weather station for the period between December and May, from 1982–2014 (Bureau of Meteorology 2017). Air temperature was used as a proxy for sea temperature as the

Table 2. Model selection results for random effects structures of rock flathead *Platycephalus laevigatus* annual growth. Models included the maximal fixed effect structure of AOG × Sex. Columns are: degrees of freedom (df), difference in Akaike's information criterion (AIC) value (ΔAIC), AIC weight, and restricted log likelihood (LL)

Random effects models	df	ΔAIC	AIC weight	LL
AOG|FishID + AOG|Year	11	0	1	753.49
AOG|FishID + 1|Year	9	82.16	0	710.39
1|FishID + 1|Year	9	127.23	0	687.86
1|FishID + AOG|Year	7	199.76	0	649.58

latter data were not available (correlation between air temperature and sea surface temperature in nearby Port Phillip Bay; r = 0.71) (NOAA 2015). Daily temperature data were then averaged over the fish growing season (December–May).

Daily river flows (Ml) were available for the Franklin River and Agnes River, the main tributaries into Corner Inlet (Department of Environment, Land, Water and Planning 2015). Higher freshwater flows deliver nutrients to estuaries and coastal waters used by seagrasses, encouraging frond rejuvenation. Seagrass growth typically occurs when the temperature begins to warm in spring (Ford et al. 2016). The mean of the top 10% of river flows per year (representing the quantity of water during large flow events), and the median flows (representing annual variation in average flow conditions) were calculated for 2 time periods: from July when the seagrass has declined over the winter until the end of February when the seagrass is typically rejuvenated, and also over the main fish growing period (December–May). We used the mean of the top 10% as an arbitrary high percentage of flows instead of a Q10 value (flow which is exceeded 10% of the time), as it was a more accurate representation of the extent of large flow events that were not as well captured by the Q10 value.

Wind can have an important influence on ocean current patterns off the Victorian coast, and therefore the ocean input into bays and inlets along the southern coast (Hamer et al. 2010). The methods for developing a zonal westerly wind (ZWW) index are outlined in Hamer et al. (2010). In this study, we used average ZWW from the main fish growing period (December–May) as the environmental indicator.

The Southern Oscillation Index (SOI) is a measure of El Niño Southern Oscillation events that represents regional climate variability by quantifying El Niño and La Niña events in the Pacific Ocean (Bureau of Meteorology 2017). Negative values (El Niño events) are typically associated with warmer sea surface temperatures and drier regional conditions. Positive values (La Niña events) are typically associated with cooler sea surface temperatures and higher probability of rainfall (Bureau of Meteorology 2017).

Model comparisons

To satisfy model assumptions, we log-transformed the growth (increment width), AOG and AAC data. The predictor variables were centered to facilitate model convergence and interpretation of interaction and polynomial terms (Morrongiello & Thresher 2015). Firstly, we created a base model including AOG and AAC and explored different random effect structures (using restricted maximum likelihood estimation, REML). We then compared models with and without AAC using maximum likelihood (ML). Competing random effect and then intrinsic effect models were then ranked using Akaike's information criterion corrected for small sample size (AICc), and the difference between the best model (lowest AICc) and each other model (ΔAIC) (Morrongiello & Thresher 2015). The best fitting of these models would become the base model for introducing the fixed extrinsic factors (Morrongiello et al. 2014).

Building on this base model, we fitted a series of models with different combinations of extrinsic factors and their interactions with AOG. These interaction terms allow for age-dependent growth responses to environmental variables. Competing models were fit using ML and ranked using AICc and ΔAICc values. The best model was then refitted with REML to produce unbiased parameter estimates (Zuur et al. 2009). In addition, we calculated conditional (all factors) R^2 values for the best models. This R^2 value describes the proportion of variation in growth described by all factors in the model (Nakagawa & Schielzeth 2013). Models were fit using the lme4 package (Bates et al. 2015) in the program R (v. 0.98.977) (R Core Team 2014). Models were compared using the AICcmodavg package (Mazerolle 2015), and predictions and confidence intervals generated using the arm and Effects packages (Fox 2003, Gelman & Hill 2006).

Climate change scenarios

We predicted rock flathead growth, using the best fitting model under 3 possible climate change scenarios: 2030, 2055/70 (high emissions), 2055/70 (low emissions) (Stocker 2014). Projections were estimated as a change relative to the baseline period 1986–2005. We used the median values of predicted temperature change for Gippsland, Victoria, for 2030, 2070 (high emissions) and 2070 (low emissions). The ranges exclude the upper and lower 10% of results (CSIRO & Bureau of Meteorology 2015). Changes to river flow were estimated using the mean of our flow parameter values (top 10% July–February) from between 1986–2005 as a baseline. We used the flow estimation model for South Gippsland, Victoria, from Jones & Durack (2005) to estimate the median percentage change to mean flows for 2030 and 2055. We used the third lowest and third highest

values of 10 climate model predictions for 2030 and 2055 to indicate the range of values (Jones & Durack 2005). We converted the percentage change in flows predicted by the model to estimate actual changes to flow relative to our 1986–2005 baseline flow.

RESULTS

Intrinsic and random factors

The increment widths on a total of 526 otoliths were measured, resulting in 2145 individual increment measurements, dating from 1982 to 2014. The best intrinsic effect model included an AOG × Sex interaction, with random AOG slopes for Year and FishID (Table 2). Growth declined with age, with females having faster growth later in life than males (>5 yr old) (Fig. 4). We plotted the Year random intercepts from the best model to visualise temporal patterns in growth (Fig. 5). Rock flathead displayed a high variation in growth over time. There was a period of strong growth from 1995 to 2001, then a poor growth period between 2002 and 2006. 2010 was a strong growth year, but it was immediately followed by a poor growing year in 2011.

Extrinsic factors

The best extrinsic effects model included additive effects of temperature in the fish growing seasons (December–May) and high flow during the seagrass growing season (highest 10% flows in July–February) (Table 3). This model had an AIC weight of 0.41, compared to weights of 0.11, 0.06 and 0.05 of the next best fitting models (Table 4). The best fitting model reflects that rock flathead growth increased as freshwater inflows increased in the months that the seagrass rejuvenates with rising tem-

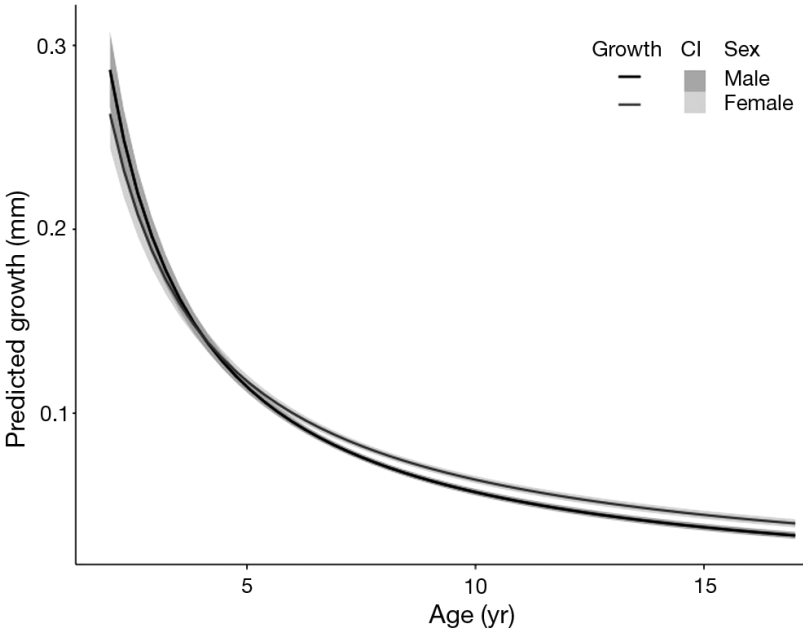

Fig. 4. Predicted growth of male (dark grey) and female (light grey) rock flathead *Platycephalus laevigatus* otolith increments (mm) at each age of growth (years). Shaded areas are 95% confidence intervals

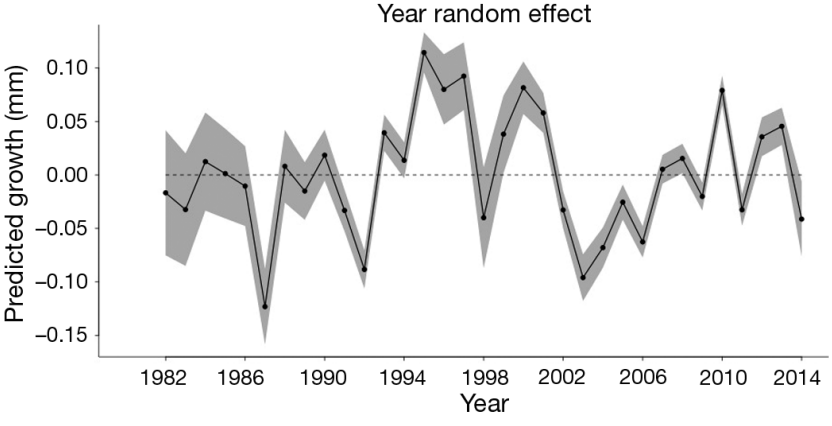

Fig. 5. Variation in predicted annual growth (accounting for intrinsic effects) of rock flathead *Platycephalus laevigatus*, represented by year random effect

Table 3. Parameter estimates (with SE), 95% confidence intervals and test statistic (*t*) from the best-fit model of rock flathead *Platycephalus laevigatus* annual growth

Parameter	Estimate	SE	5% CI	95% CI	*t*
Intrinsic factors					
Intercept	−2.672	0.0129	−2.694	−2.651	−206.28
Age	−1.004	0.0286	−1.051	−0.958	**−35.07**
Sex (F)	0.0889	0.0127	0.068	0.110	**6.99**
Age × Sex	0.124	0.0225	0.086	0.163	**5.51**
Extrinsic factors					
Temperature	0.0298	0.0111	0.011	0.049	**2.68**
Flow (Highest 10% Jul–Feb)	0.00008	0.00003	0.00003	0.0001	**2.83**

Table 4. Overall best fitting models of rock flathead *Platycephalus laevigatus* annual growth including intrinsic, random and extrinsic factors, after a comparison of AICc values. Columns are degrees of freedom (df), difference in AIC value (ΔAIC), AIC weight, maximised log likelihood (LL) and the R^2 value

Model's extrinsic factors	df	ΔAIC	AIC weight	LL	R^2
Temperature + Flow (highest 10% Jul–Feb)	13	0	0.41	770.39	0.938
Flow (highest 10% Jul–Feb) + Wind	13	2.70	0.11	769.04	0.938
Wind	12	3.89	0.06	767.44	0.938
Flow (highest 10% Jul–Feb)	12	4.07	0.05	767.34	0.938

peratures (July–February) (Fig. 6). Rock flathead growth also increased in warmer fish growing seasons (December–May) (Fig. 7). Temperature and river flow were negatively correlated (r = –0.63), yet growth appears to be enhanced by increases in both factors, which suggests that any correlation has not obscured the influence of either factor.

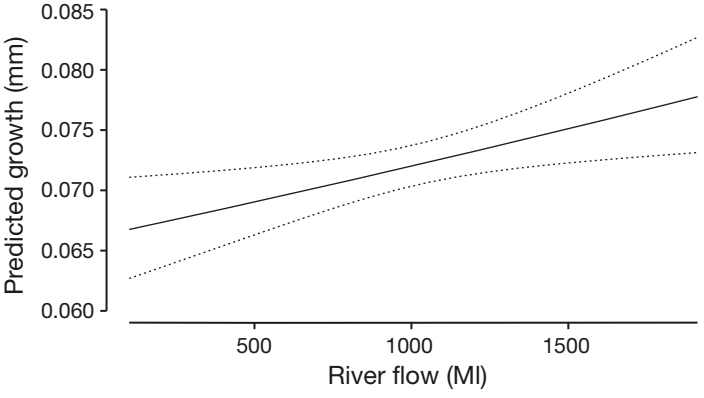

Fig. 6. Predicted otolith incremental growth (mm) and confidence intervals of rock flathead *Platycephalus laevigatus* with freshwater river flows

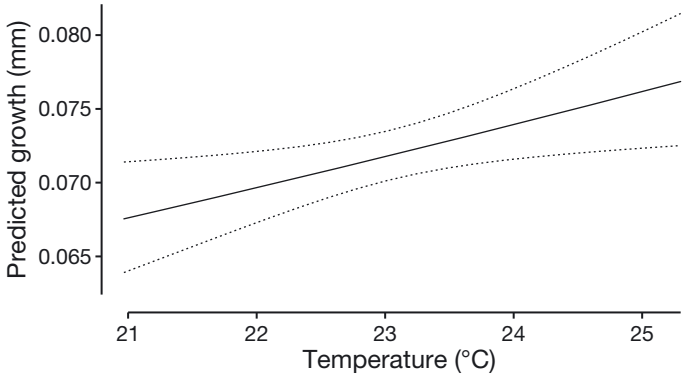

Fig. 7. Predicted otolith incremental growth (mm) and confidence intervals of rock flathead *Platycephalus laevigatus* in increasing temperatures (°C)

Climate change scenarios

We predict that mean annual growth of 2 yr old rock flathead in 2030 will increase by 2.46% as temperature increases and river flow decreases. In 2070 under a low emissions scenario, we predict that growth will increase by 3.58%. In 2070 under a high emissions scenario, we predict that growth will increase by 6.67% (Fig. 8).

DISCUSSION

Annual growth of rock flathead in Corner Inlet was significantly influenced by environmental factors. Growth was higher in periods following larger river flows and likely represents a response to nutrient-rich river flow stimulating productivity through the seagrass food web. High temperatures during summer and autumn also increased the growth of all individuals in the population. Our model explicitly incorporates both intrinsic and extrinsic sources of growth variation and allows managers to identify whether changes in fish stocks are likely to be related to environmental or fishing factors.

Intrinsic factors

Age (AOG) explained a substantial amount of the variation in growth and reflects the commonly observed pattern of fish growth decreasing when individuals get older. The significant interaction between age and sex was also expected. There was no effect of sex on growth in young individuals (<5 yr), but in older fish (>5 yr) females exhibited significantly larger growth than males. This is consistent with previous studies on *P. laevigatus* and tiger flathead *P. richardsoni* (Koopman et al. 2004, Morrongiello & Thresher 2015). It is beneficial for female fish to grow faster and larger than male fish so that they can accommodate more eggs during the spawning period (Koopman et al. 2004). In most fish the growth of males and their growth efficiency declines more than females after maturity, perhaps because they are more active in finding and displaying to mates (Henderson et al. 2003, Pauly 2010). These behaviours have been observed in other related species in the Platycephalidae family (Shinomiya et al. 2003).

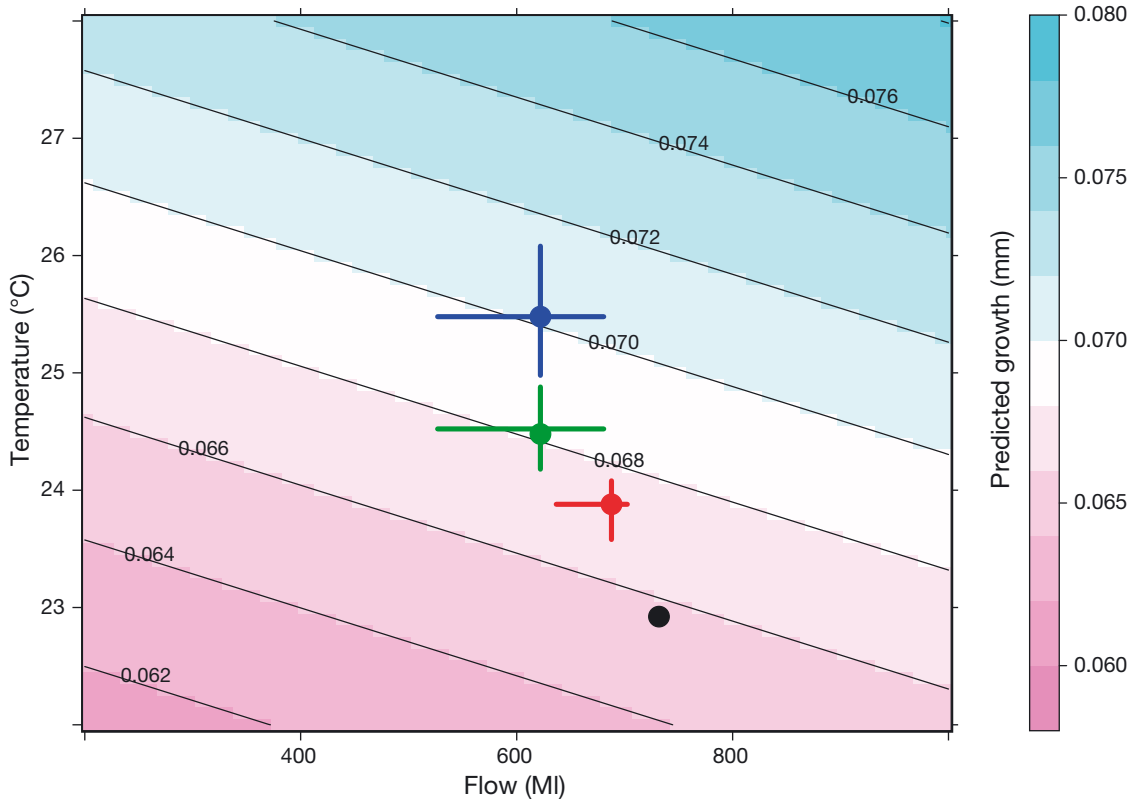

Fig. 8. Predicted otolith incremental growth (mm) and confidence intervals of rock flathead *Platycephalus laevigatus* in current temperatures and productivity (1986–2005) and under 3 climate change scenarios: current baseline (black), 2030 (red), 2070 + low emissions (green), 2070 + high emissions (blue)

Environmental influences on fish growth

Rock flathead growth was positively influenced by increased river flow which we hypothesise stimulates productivity in the seagrass ecosystem. It is well understood that estuarine and coastal ecosystems are more productive than areas distant from the coast (Whitfield 1996). This productivity is often driven by the availability of nutrients from nutrient-rich river flows (Caddy & Bakun 1994) and subsequently cascades up the food web to predators such as rock flathead (Edgar & Shaw 1995). Corner Inlet is a seagrass dominated environment. This seagrass predominantly grows during spring and summer, so increased nutrient input from the rivers at this time may especially enhance productivity of the seagrass ecosystem and increase abundances of prey. Excessive nutrient input from river inflows, however, is suspected to lead to algal blooms and thus seagrass decline (Ford et al. 2016). In spite of this, we found no evidence of a negative impact of higher flow levels on rock flathead growth, and thus a hump-shaped relation of growth to flow. One possibility is that the fishery catches were focused on areas that retained good seagrass habitat. The impacts of high nutrients on the health of seagrass and consequently on species inhabiting the seagrass deserve further investigation.

Increased temperatures during the main growth period (December–May) resulted in increased fish growth. As fish are ectothermic, their metabolic rate varies with the external water temperature. Within the range of temperatures that fish are exposed to, species will have an optimal range in which their metabolism is enhanced (Christie & Regier 1988). Increases in temperature (within the optimal range) can result in a direct increase in growth, through allocation of enhanced energy (Fry 1971). Our results are consistent with those from a previous growth study on rock flathead (Coulson et al. 2014). As Corner Inlet is in the middle of rock flathead's distribution, we expect that warming water will promote fish growth. Similar patterns have been observed in a multi-population analysis of the related tiger flathead *P. richarsoni* (Morrongiello & Thresher 2015). Increased temperatures can also improve the productivity of the seagrass ecosystem (Masini et al. 1995), and thus indirectly promote rock flathead growth via

increases in food. It is possible that increases in rock flathead growth with warming water represents a combination of both direct metabolic and indirect food web mechanisms.

Climate change scenarios

We predict that rock flathead growth rates will increase in the future. Warmer temperatures associated with climate change may be slightly offset by a simultaneous decrease in flow, though in general the magnitude of the temperature effect is greater and would be expected to have a stronger impact on growth (Fig. 8) (Jones & Durack 2005, CSIRO & Bureau of Meteorology 2015). While the future productivity of the fishery may be enhanced by increased fish growth, it is important to remember that rock flathead are reliant on the seagrass ecosystem for both habitat and nutrition. Future seagrass declines that occur due to changes in flow or even independently of climate (Ford et al. 2016), will likely have strong impact on fish growth. Further study is required to understand the cumulative impacts that anthropogenic and climate driven environmental change have on the seagrass ecosystem.

Whilst we think our predictions of enhanced growth with warming are robust, they do not account for changed frequency and intensity of extreme events (e.g. marine heatwaves and unpredictable flooding events; Hobday et al. 2016) that can impact biological systems (Wernberg et al. 2013). Predicted changes in mean temperature for 2030 and 2070 (low emissions) are both within the observed temperature range of the study, while the predicted temperature for 2070 (high emissions) exceeds the highest yearly mean temperature by 0.82°C. Nonetheless, daily temperatures often exceed this value, so that we are confident that predicted temperatures will not exceed physiological tolerances for rock flathead. The values for predicted changes in river flow, and therefore nutrient input into Corner Inlet, are well within the observed range of river flows. Rock flathead have therefore already been exposed to all of the predicted temperatures and river flow scenarios.

Implications for the fishery and ecosystem management

Our study indicates that freshwater flows that enhance the productivity of the seagrass ecosystem stimulate the growth of rock flathead. This information is important for fisheries and ecosystem managers because it provides clear empirical evidence for the need to appropriately manage catchment processes and water extraction to ensure fisheries production is maintained. Such an ecosystem-based management approach is increasingly being employed to ensure the ongoing sustainable management of fisheries worldwide. Future work needs to focus on understanding the drivers of poor water quality, seagrass declines and how seagrass-inhabiting species are impacted, so that practical strategies can be put in place to promote recovery (e.g. managing the terrestrial impacts on the content of freshwater flows, seagrass transplantation). We also need to understand the mechanisms driving growth and successful recruitment of other commercially important species in Corner Inlet, to make informed decisions that will benefit all major species within the fishery.

Acknowledgements. All collection of specimens and field survey methods were carried out with the permission of the Department of Environment, Land, Water and Planning National Parks Act 1975 Research Permit (permit no. 10007406) and the Department of Environment and Primary Industries Fisheries Act 1995 Permit (permit no. RP1135). We thank Fisheries Victoria for their help supplying us with historical samples. We thank Gary Cripps and Ray Dunstone for boating support and providing some recent samples. We also thank Neville Clarke, Brett Cripps, Wayne Cripps, and Lachie and Alice from Foster Seafood for providing additional recent samples for this project.

LITERATURE CITED

Abrahams MV, Kattenfeld MG (1997) The role of turbidity as a constraint on predator–prey interactions in aquatic environments. Behav Ecol Sociobiol 40:169–174

Alongi DM (1998) Coastal ecosystems processes. CRC Press, Boca Raton, FL

Bardos DC, Day RW, Lawson NT, Linacre NA (2006) Dynamical response to fishing varies with compensatory mechanism: an abalone population model. Ecol Model 192: 523–542

Barton BA, Morgan JD, Vijayan MM (2002) Physiological and condition related indicators of environmental stress in fish. In: Adams SM (ed) Biological indicators of ecosystem stress. American Fisheries Society, Bethesda, MD, p 111–148

Bates D, Maechler M, Bolker B, Walker S (2015) Fitting linear mixed-effects models using lme4. J Stat Softw 67: 1–48

Black BA (2009) Climate-driven synchrony across tree, bivalve, and rockfish growth-increment chronologies of the northeast Pacific. Mar Ecol Prog Ser 378:37–46

Bureau of Meteorology (2017) Climate data online. Bureau of Meteorology. www.bom.gov.au/climate/data/ (accessed 25 May 2017)

Butler A, Jernakoff P (1999) Seagrass in Australia. Strategic

review and development of an R&D plan. CSIRO Publishing, Collingwood

Caddy JF, Bakun A (1994) A tentative classification of coastal marine ecosystems based on dominant processes of nutrient supply. Ocean Coast Manage 23:201–211

Christie GC, Regier HA (1988) Measures of optimal thermal habitat and their relationship to yields for four commercial fish species. Can J Fish Aquat Sci 45:301–314

Coulson PG, Black BA, Potter IC, Hall NG (2014) Sclerochronological studies reveal that patterns of otolith growth of adults of two co-occurring species of Platycephalidae are synchronized by water temperature variations. Mar Biol 161:383–393

Cowan JH Jr, Rose KA, De Vries DR (2000) Is density-dependent growth of young-of-the-year fishes a question of critical weight? Rev Fish Biol Fish 10:61–89

CSIRO and Bureau of Meteorology (2015) Climate change in Australia: information for Australia's Natural Resource Management Regions. Technical Report, CSIRO and Bureau of Meteorology. https://www.environment.gov.au/system/files/pages/61971ba0-0847-4fef-846e-36d6b706a7a5/files/corner-inlet-fishery-corner-inlet-nooramunga-fishery-assessment.pdf

Department of Environment, Land, Water and Planning (2015) Water Measurement Information System, Department of Environment, Land, Water and Planning, Melbourne. http://data.water.vic.gov.au/monitoring.htm (accessed 1 August 2015)

Department of Primary Industries (2012) Fisheries Victoria commercial fish production information bulletin 2012. Fisheries Victoria, Queenscliff

Edgar GJ, Shaw C (1995) The production and trophic ecology of shallow-water fish assemblages in southern Australia II. Diets of fishes and trophic relationships between fishes and benthos at Western Port, Victoria. J Exp Mar Biol Ecol 194:83–106

Ellison AM, Bank MS, Clinton BD, Colburn EA and others (2005) Loss of foundation species: consequences for the structure and dynamics of forested ecosystems. Front Ecol Environ 3:479–486

FAO (2016) The state of world fisheries and aquaculture 2016. FAO, Rome

Ford JR (2014) A review of the chemical toxicant threats to seagrass in Corner Inlettoria. Report to the West Gippsland Catchment Management Authority, as part of Fisheries Research Development Corporation Project 13/021, Melbourne

Ford JR, Williams RJ, Fowler AM, Cox DR, Suthers IM (2010) Identifying critical estuarine seagrass habitat for settlement of coastally spawned fish. Mar Ecol Prog Ser 408:181–193

Ford JR, Barclay K, Day RW (2016) Using local knowledge to understand and manage ecosystem-related decline in fisheries productivity. Fisheries Research and Development Corporation Final Project Report, Melbourne. http://frdc.com.au/research/Final_reports/2013-021-DLD.pdf

Fox J (2003) Effect displays in R for generalised linear models. J Stat Softw 8:1–27

Fry FEJ (1971) 1—The effect of environmental factors on the physiology of fish. Fish Physiol 6:1–98

Gelman A, Hill J (2006) Data analysis using regression and multilevel/hierarchical models. Cambridge University Press, New York, NY

Halpern BS, Walbridge S, Selkoe KA, Kappel CV and others (2008) A global map of human impact on marine ecosystems. Science 319:948–952

Hamer P, Jenkins G, Kemp J (2010) Linking key environmental and life history indicators for monitoring and assessment of bay and inlet fisheries in Victoria. Fisheries Victoria Research Report Series No. 44, Melbourne

Harley CD, Randall Hughes A, Hultgren KM, Miner BG and others (2006) The impacts of climate change in coastal marine systems. Ecol Lett 9:228–241

Henderson BA, Collins N, Morgan GE, Vaillancourt A (2003) Sexual size dimorphism of walleye (*Stizostedion vitreum vitreum*). Can J Fish Aquat Sci 60:1345–1352

Hobday AJ, Alexander LV, Perkins SE, Smale DA and others (2016) A hierarchical approach to defining marine heatwaves. Prog Oceanogr 141:227–238

Jenkins GP, Hammond LS, Watson GF (1993) Patterns of utilisation of seagrass (*Heterozostera*) dominated habitats as nursery areas by commercially important fish. Victorian Institute of Marine Sciences, Report No. 19. Queenscliff

Jenkins GP, May HMA, Wheatley MJ, Holloway MG (1997) Comparison of fish assemblages associated with seagrass and adjacent unvegetated habitats of Port Phillip Bay and Corner Inlet, Victoria, Australia, with emphasis on commercial species. Estuar Coast Shelf Sci 44:569–588

Jones RN, Durack PJ (2005) Estimating the impacts of climate change on Victoria's runoff using a hydrological sensitivity model. CSIRO Atmospheric Research, Melbourne

Kemp J, Brown L, Bruce T, Bridge N, Conron S (2013) Corner Inlet and Nooramunga Fishery Assessment 2012. Fisheries Victoria Assessment Report Series No. 68. Department of Primary Industries, Queenscliff

Klumpp DW, Nichols PD (1983) A study of food chains in seagrass communities II. Food of the rock flathead, *Platycephalus laevigatus* Cuvier, a major predator in a *Posidonia australis* seagrass bed. Mar Freshw Res 34: 745–754

Koopman M, Morison AK, Troynikov VS (2004) Population dynamics and assessment of sand and rock flathead in Victorian waters. FRDC Report 2000/120. Department of Primary Industries, Queenscliff

Masini RJ, Cary JL, Simpson CJ, McComb AJ (1995) Effects of light and temperature on the photosynthesis of temperate meadow-forming seagrasses in Western Australia. Aquat Bot 49:239–254

Matta ME, Black BA, Wilderbuer TK (2010) Climate-driven synchrony in otolith growth-increment chronologies for three Bering Sea flatfish species. Mar Ecol Prog Ser 413: 137–145

Mazerolle MJ (2015) AICcmodavg: Model selection and multimodel inference based on (Q)AIC(c). R package version 2.0-3. https://cran.r-project.org/web/packages/AICcmodavg/AICcmodavg.pdf

McComb AJ, Atkins RP, Birch PB, Gordon DM, Lukatelich RJ (1995) The Peel–Harvey estuarine system, Western Australia. In: McComb AJ (ed) Eutrophic shallow estuaries and lagoons. CRC Press, London, p 5–17

Morrongiello JR, Thresher RE (2015) A statistical framework to explore ontogenetic growth variation among individuals and populations: a marine fish example. Ecol Monogr 85:93–115

Morrongiello JR, Thresher RE, Smith DC (2012) Aquatic biochronologies and climate change. Nat Clim Chang 2: 849–857

Morrongiello JR, Walsh CT, Gray CA, Stocks JR, Crook DA

(2014) Environmental change drives long term recruitment and growth variation in an estuarine fish. Glob Change Biol 20:1844–1860

Nakagawa S, Schielzeth H (2013) A general and simple method for obtaining R^2 from generalized linear mixed effects models. Methods Ecol Evol 4:133–142

NOAA (2015) NOAA high resolution SST data. NOAA/OAT/ESRL PSD, Boulder, CO. http://www.esrl.noaa.gov/psd/

Orth RJ, Carruthers TJ, Dennison WC, Duarte CM and others (2006) A global crisis for seagrass ecosystems. Bioscience 56:987–996

Pauly D (2010) Gasping fish and panting squids: oxygen, temperature and the growth of water-breathing animals. In: Kinne O (ed) Excellence in ecology, Book 22. International Ecology Institute, Oldendorf/Luhe

Poloczanska ES, Burrows MT, Brown CJ, García Molinos J and others (2016) Responses of marine organisms to climate change across oceans. Front Mar Sci 3:62

R Core Team (2014) R: A language and environment for statistical computing. R Foundation for Statistical Computing, Vienna

Roessig JM, Woodley CM, Cech JJ Jr, Hansen LJ (2004) Effects of global climate change on marine and estuarine fishes and fisheries. Rev Fish Biol Fish 14:251–275

Shinomiya A, Yamada M, Sunobe T (2003) Mating system and protandrous sex change in the lizard flathead, *Inegocia japonica* (Platycephalidae). Ichthyol Res 50: 383–386

Sohel S, Mattila J, Lindström K (2017) Effects of turbidity on prey choice of three-spined stickleback *Gasterosteus aculeatus*. Mar Ecol Prog Ser 566:159–167

Stocker T (ed) (2014) Climate change 2013: the physical science basis: Working Group I contribution to the Fifth assessment report of the Intergovernmental Panel on Climate Change. Cambridge University Press, Cambridge

Takasuka A, Aoki I (2006) Environmental determinants of growth rates for larval Japanese anchovy *Engraulis japonicus* in different waters. Fish Oceanogr 15:139–149

Thomsen MS, Wernberg T, Engelen AH, Tuya F and others (2012) A meta-analysis of seaweed impacts on seagrasses: generalities and knowledge gaps. PLOS ONE 7: e28595

Thresher RE, Koslow JA, Morison AK, Smith DC (2007) Depth-mediated reversal of the effects of climate change on long-term growth rates of exploited marine fish. Proc Natl Acad Sci USA 104:7461–7465

Wang T, Overgaard J (2007) The heartbreak of adapting to global warming. Science 315:49–50

Waycott M, Duarte CM, Carruthers TJ, Orth RJ and others (2009) Accelerating loss of seagrasses across the globe threatens coastal ecosystems. Proc Natl Acad Sci USA 106:12377–12381

Weisberg S, Spangler G, Richmond LS (2010) Mixed effects models for fish growth. Can J Fish Aquat Sci 67:269–277

Wernberg T, Smale DA, Tuya F, Thomsen MS and others (2013) An extreme climatic event alters marine ecosystem structure in a global biodiversity hotspot. Nat Clim Chang 3:78–82

Whitfield AK (1996) Fishes and the environmental status of South African estuaries. Fish Manag Ecol 3:45–57

Whitten AR, Klaer NL, Tuck GN, Day RW (2013) Accounting for cohort-specific variable growth in fisheries stock assessments: a case study from south-eastern Australia. Fish Res 142:27–36

Zuur AF, Ieno EN, Walker NJ, Saveliev AA, Smith GM (2009) Mixed effects models and extensions in ecology with R. Springer, New York, NY

Editorial responsibility: Stylianos Somarakis, Heraklion, Greece

Submitted: March 17, 2017; Accepted: June 21, 2017
Proofs received from author(s): August 25, 2017

Vol. 598: 213–231, 2018
https://doi.org/10.3354/meps12531

MARINE ECOLOGY PROGRESS SERIES
Mar Ecol Prog Ser

Published June 28

Contribution to the Theme Section 'Innovative use of sclerochronology in marine resource management'

REVIEW

Digital imaging techniques in otolith data capture, analysis and interpretation

Mark Fisher[1,*], Ewan Hunter[2,3]

[1]School of Computing Sciences, University of East Anglia, Norwich Research Park, Norwich NR4 7TJ, UK
[2]Centre for the Environment, Fisheries and Aquaculture Sciences (CEFAS), Lowestoft, Suffolk NR33 0HT, UK
[3]School of Environmental Sciences, University of East Anglia, Norwich Research Park, Norwich NR4 7TJ, UK

ABSTRACT: Otoliths or ear-stones are hard, calcium carbonate structures located within the inner ear of bony fishes. Counts of rings and measurements of seasonal growth increments from otoliths are important metrics for assessment and management of fish stocks, and the preparation and microscopic analysis of otoliths forms an essential part of the routine work undertaken by fisheries scientists worldwide. Otolith analysis is a skilled task requiring accuracy and precision, but it is laborious, time-consuming to perform, and represents a significant cost to fisheries management. In the last 2 decades, several attempts to apply 'computer vision' (systems that perform high-level tasks and exhibit intelligent behaviour) in otolith analysis have been reported. Although considerable progress has been made and several prototype systems developed, laboratories have been reluctant to adopt image-based computer-assisted age and growth estimation (CAAGE) systems. This paper surveys applications of CAAGE, focusing on their utility for automated ageing using images of otolith macrostructure. A cost–benefit analysis of CAAGE of cod, plaice and anchovy shows that computer vision performs relatively poorly compared with morphometric techniques. However, there is evidence that information from visual features can boost the performance of morphometric CAAGE, and further work is needed to develop effective frameworks for this integrated approach. The cost benefit of these systems might be attractive to smaller laboratories that are already using age–length keys derived from otolith morphometrics for management of smaller artisanal fisheries.

KEY WORDS: Otolith · Computer-assisted age and growth estimation · CAAGE · Image analysis · Computational model

INTRODUCTION

The population models used in fisheries management require age data to define stock characteristics (Cadima 2003, Cadrin & Dickey-Collas 2015). For most commercially exploited fish stocks, this information is determined from an analysis of seasonally accreted growth marks in the calcified structures (scales, bones, fin rays, otoliths) of fish (Welch et al. 1993, Panfili et al. 2002, Brophy 2014, Zhu et al. 2015). The calcified inner ear-stones of bony fishes, or otoliths, have been a cornerstone of fish ageing methodology for over a century, as otolith rings are formed with regular periodicity (Williams & Bedford 1974, Mendoza 2006). The literature on ageing of fish stocks continues to grow; however, the approach is essentially subjective. While expert otolith readers can enumerate the annual increments for many stocks with a good degree of accuracy and high precision, ageing certain stocks and older individuals can be very challenging (Campana 2001, Morison et al. 2005, de Pontual et al. 2006, Fey & Linkowski

*Corresponding author: mark.fisher@uea.ac.uk

Publisher: Inter-Research · www.int-res.com

2006, Smith 2014, Hüssy et al. 2016a). Otoliths act as endolymphatic infillings (masses) within the saccule of the inner ear and function as auditory, balance, movement, and direction receptors in all vertebrates and some aquatic invertebrates (Popper & Hoxter 1981, Popper et al. 2005, Schulz-Mirbach et al. 2015). Bony fish (teleosts) possess 3 pairs of otoliths (sagittae, lapilli and asterisci), and in most species, the saccular sagitta is the largest otolith and the focus of most scientific inquiries (Fig. 1). Otoliths grow according to an accretionary process of calcium carbonate deposition that builds as a succession of concentric layers from an inner core. Inter-specific variability in the shapes and proportional sizes of otoliths is substantial, and often diagnostic (Schmidt 1969, Messieh 1972, Campana & Casselman 1993, Friedland & Reddin 1994, Lombarte & Morales-Nin 1995). Considerable research effort has been expended examining the biomineralisation process that drives otolith growth and factors affecting the seasonal formation of annuli and other growth marks, but our understanding is currently incomplete and the mechanics of the otolith structure and composition continues to be an active topic of research (Jolivet et al. 2008, 2013, Morales-Nin & Geffen 2015). The individual biochronologies encoded as growth marks are thought to reflect environmental experience, since the composite calcium carbonate is primarily derived from the ambient water, but recent research suggests that physiological factors also play an important role (Darnaude et al. 2014, Sturrock et al. 2015, Hüssy et al. 2016a, Smolinski & Mirny 2017). Typically, there is more growth in summer, less in winter, and this annual cycle manifests as a macrostructure (MaS) exhibiting translucent rings, somewhat similar to tree rings. In many species, the accretion of calcium carbonate and glutinous matrix alternates on a daily cycle, and this periodicity is particularly evident in microscope examinations of otolith microstructure (MiS) in juvenile fish (Campana & Neilson 1985). As otolith shape is indicative of fish species and related to life history and behaviour (Popper & Lu 2000), this structure has attracted the interest of fisheries scientists since at least 1899 (Ricker 1975).

Consequently, data gathered from otoliths has been applied in fisheries science worldwide for over a century, with otoliths forming the basis of routine assessment of age and structure of fish stocks. Cam-

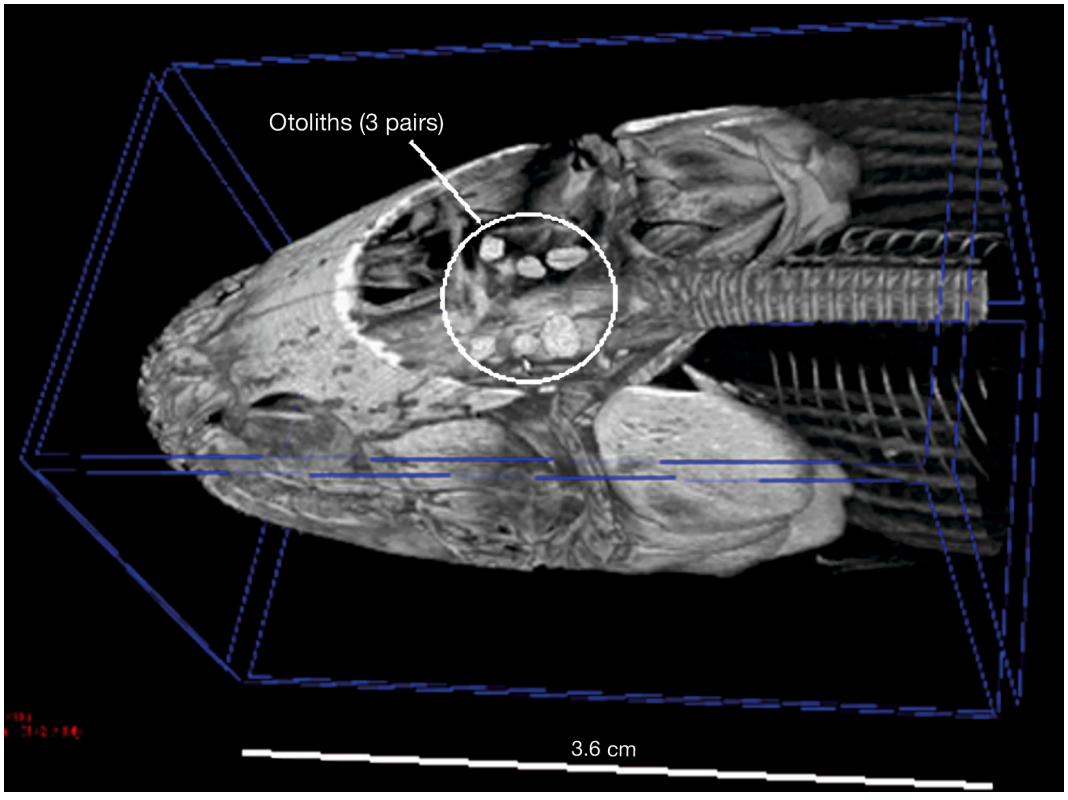

Fig. 1. Micro-computed tomography (micro-CT) image of bowfin *Amia calva* showing the *in situ* location of otoliths (sagittae, lapilli and asterisci), representative of all bony fish (teleosts). Data comprises 1071 slices (1024 × 1024 pixels) along the coronal axis; each slice is 0.1237 mm thick, with an interslice spacing of 0.1237 mm

pana & Thorrold (2001) estimated the minimum number of otoliths examined worldwide to be between 800 000 and 2 000 000 per annum, underlining their importance in monitoring and characterising fish populations. Fish have indeterminate growth patterns that are influenced by environmental conditions, and as such, fish growth and production require frequent measurement to monitor productivity and population characteristics in response to varying levels of exploitation and environmental change. Campana (2001) discusses the importance of this work and highlights several examples where inaccuracies in age determination have led to age estimates that differ by up to a factor of 3, leading in turn to overly optimistic estimates of growth and mortality in certain species that have contributed to overexploitation (e.g. de Pontual et al. 2006). In addition to annual ageing and otolith MiS, more recent reviews (Begg et al. 2005, Campana 2005) highlight emerging applications such as otolith chemistry, and the literature continues to grow (Geffen 2012, Sturrock et al. 2012), underlining the ongoing relevance of otoliths to innovations in fisheries science.

The feasibility of using digital imaging in fish ageing studies has been investigated since Fawel (1974) first reported results using a video camera and digital frame store. Further use of computer-assisted ageing techniques followed (Methot 1981, Frei 1982, Messieh & McDougall 1985, Campana 1987, McGowen et al. 1987, Panfili et al. 1990) with the availability of cheaper personal computers. Protocols and potential advantages of computer-assisted analysis of MiS and MaS were investigated by Campana (1992) and King (1993). Routine tasks which have attracted the attention of the image-processing community are fish age determination and the measurement of inter-annual growth increments (Troadec 1991, Morales-Nin et al. 1998, Takashima et al. 2000, Campana & Thorrold 2001, Troadec & Benzinou 2002, Begg et al. 2005, Black et al. 2005). Other areas where image analysis has played an important role are otolith allometry and morphometrics for distinguishing between fish stocks (Cardinale et al. 2004, Burke et al. 2008a,b, Parisi-Baradad et al. 2010), quality assurance (Morison et al. 1998, 2005, Palmer et al. 2005) and environmental reconstruction (Millner et al. 2011, Morrongiello et al. 2012).

Routine capture and analysis of otolith images has formed an important component of European Union (EU)-funded collaborative fisheries research since 1996, with projects focused on improving the accuracy of otolith ageing (Moksness 2000, Appelberg et al. 2005), age determination by otolith shape (Arneri et al. 2002) and automatic age determination and growth analysis (Mahé 2009, Mahé et al. 2017). Digital imaging offers a number of potential advantages, including the development of online scientific archives and historical records (Lombarte et al. 2006), the rapid calculation of biological and life history information (Carbini et al. 2008), and the automated capture and seamless storage of associated information (Morison et al. 1998). Some EU projects have delivered specialised algorithms and spawned bespoke software environments for otolith imaging, such as IMAGIC (Image Science Software) and TNPC (Mahé 2009, Mahé et al. 2011). Two hundred copies of TPNC are licenced and it is cited in research (e.g. de Pontual et al. 2006, Mille et al. 2016) and used in routine survey analysis. However, much of the literature on computer-assisted sclerochronology is dominated by generic proprietary microscopy tools such as ImagePro (Media Cybernetics®), Lucia (Laboratory Imaging®) and open-source systems such as ImageJ (formerly NIH image) (Abràmoff et al. 2004). Examples include Whitman & Johnson's (2016) tutorial featuring ImagePro and an ImageJ plug-in for otolith and tree ring counting resulted from research sponsored by the Norwegian Institute of Marine Research, but there is no evidence that this has been evaluated (Vischer & Nastase 2015).

Panfili et al. (1990) originally coined the phrase 'computer-assisted age and growth estimation' (CAAGE) to describe interactive imaging tools, and this name is still used to describe more recent systems that operate completely autonomously. Such systems are attractive in that they seem to offer the possibility of moving from subjective estimates of age towards objective measures. However, these systems have been very difficult to implement. In an observation that remains true to this day, Morison et al. (2005) observed,

> 'it is a recognition of the complexity of the process that no age estimation laboratories have been able to replace their human readers' (Morison et al. 2005, p. 777).

This review aims to provide an overview of imaging and pattern recognition systems for routine automated ageing through computerised analysis of growth marks that present in the otolith MaS. The work builds on a previous tutorial introduction by Troadec & Benzinou (2002) and conference presentation by Carbini et al. (2008). We highlight results of the most comprehensive evaluation of CAAGE techniques and methodology undertaken by an EU-funded project entitled Automated FISh Ageing

(AFISA) (Mahé 2009). In reviewing this work and attempts by others to develop automatic image-based ageing tools, we try to explain why there has been relatively little activity in this area since a flurry of articles were published in the 2000s. We highlight an existing approach to integrating information from otolith images within existing morphometric CAAGE systems which we believe could be further developed and exploited more widely. We also signpost future frameworks that could be developed to enable experts and computers to work cooperatively, and we believe that these systems may have a role in training and quality assurance.

REVIEW OF TECHNIQUES

Image processing has been used in sclerochronology since the 1980s and initially focused on low-level image-processing tasks aimed at facilitating interactive systems to assist scientists in making measurements and recording results (Campana 1987, McGowen et al. 1987, Small & Hirschhorn 1987, Panfili et al. 1990). In the 1990s, scientists considered high-level tasks such as classification of otolith shape (for discrimination between stocks), and CAAGE systems were designed to analyse 1-dimensional (1-D) opacity signals recovered from a ray (transect) originating at the nucleus and extending to the otolith edge (Troadec 1991, Macy 1995, Welleman & Storbeck 1995, Cailliet et al. 1996) (Table 1). Later, CAAGE advanced to take advantage of 2-dimensional (2-D) algorithms and growth models. We consider these in the section 'Image processing', after first reviewing the important step of image acquisition.

Image acquisition

Age-related studies of otoliths can be broadly divided into those involving MaS, such as routine age determination from annual rings or species identification (Morales-Nin & Panfili 2002, Courbin et al. 2007), or those involving MiS, for example nucleus or daily incremental width and primordia studies (Campana & Neilson 1985, Geffen 2002, Neat et al. 2008). Although all researchers agree that the method used for otolith preparation and examination with microscopy is key in obtaining high-quality images, the imaging techniques employed vary depending on established protocols within each laboratory. A survey by Morison et al. (2005) concludes that in general there is great diversity in attention to quality and no consensus on desirable standards. The diversity of techniques applied for otolith preparation (Christensen 1984, Miller & Simenstead 1994, Estep et al. 1995, Casselman & Scott 2000, Easey & Millner 2008) and microscopy has hampered the adoption of widely agreed protocols with respect to studies of otolith MaS, and the guidelines for image acquisition are typically quite imprecise (e.g. Clausen 2006). While this represents a problem for human interpretation, it is of vital significance for CAAGE systems (Mahé 2009).

It is tempting to think that image acquisition is mainly concerned with camera and sensor technologies, but the considerable improvements in image quality and widespread availability of colour images (e.g. Fig. 2) over the last 2 decades have not translated into similar improvements in overall system accuracies. Some articles demonstrate that surprisingly good images can be obtained at low cost (Campana 1987, Rypel 2008). Modern digital cameras are not prohibitively expensive, and for fisheries that are well resourced, it is unlikely that camera technology will be a limiting factor. Studies undertaken by AFISA used Leica 300/320 digital cameras (3.3 Megapixels, up to 36-bit colour depth) and a stereomicroscope (Leica MZ6). However, they found that factors such as consistent illumination geometry and otolith preparation were important in achieving good overall performance.

Images are essentially just the visual rendering of an array of numbers, representing pixel (picture element) intensities. Computers running image-processing programs make decisions based on individual values in the array. It is essential that these values are reproducible; for example, the same otolith, imaged at a different time, with the same equipment, should yield the same, or *very similar* values. Even if the computer program interprets relative differences between pixel values, rather than absolute values, it is important that differences in intensities across the image are consistent. Microscopy in most otolith labs tends to be optimised for human readers and the lighting geometry is flexible, allowing it to be easily adjusted for personal preference, per otolith. In contrast, automated systems go to great lengths to ensure lighting geometry is fixed and this is often addressed by establishing calibration protocols. There is some evidence that fisheries science is addressing these issues, driven by a need to meet quality assurance standards. The AFISA project (Mahé 2009) took great care to measure light intensities and adopted a consistent setup protocol.

Table 1. Computerised age and growth estimation (CAAGE) of otolith macrostructure (MaS) from the published literature (1990 onwards). 1-D = 1-dimensional, 2-D = 2-dimensional, ML = machine learning, Prep = otolith preparation, W = whole, S = section, APE = average percent error; dashes indicate data not available. VI-A: ICES area

CAAGE classification	Method			Species	Area	N	Evaluation		
	1-D	2-D	ML				Age or size	Prep	APE (%)
Interactive systems									
Panfili et al. (1990)	✓			Mediterranean eel *Anguilla anguilla*	–	–	–	W	–
Cailliet et al. (1996), King (1993)	✓	✓		Bank rockfish *Sebastes rufus*	–	60	–	S	4.0
Benzinou et al. (1997)		✓		Plaice *Pleuronectes platessa* L.	–	–	–	–	–
Formella et al. (2007)	✓	✓		Cod *Gadus morhua*	<55° N	17	3–5 yr	S	14.0
Fully automatic systems									
Troadec (1991)	✓			Saithe *Pollachius virens*	VI-A	58	3–10 yr	W	4.3
Welleman & Storbeck (1995)	✓			Plaice *Pleuronectes platessa* L.	–	334	2–5 yr	W	3.0–18.0
Robertson & Morison (2001)	✓		✓	King George whiting *Sillaginodes punctate*	–	378	2–5 yr	S	3.5
	✓		✓	School whiting *Sillago flindersi*	–	514	1–6 yr	S	12.3
	✓		✓	Ling *Genypterus blacodes*	–	2226	0–17 yr	S	18.0
	✓		✓	Snapper *Pagrus auratus*	–	987	0–28 yr	S	22.2
	✓		✓	Black bream *Acanthopagrus butcheri*	–	913	1–37 yr	S	17.2
	✓		✓	Sand flathead *Platycephalus bassensis*	–	963	0–20 yr	S	18.2
	✓		✓	Blue grenadier *Macruronus novaezelandiae*	–	1531	1–19 yr	S	15.6
	✓		✓	Ocean perch *Heliocolenus* sp.	–	573	4–60 yr	S	21.8
Troadec et al. (2000)		✓		Plaice *Pleuronectes platessa* L.	–	102	2–5 yr	W	20.0
Takashima et al. (2000)	✓		✓	White-spotted char *Salvilinus leucomaenis*	–	439	2–6 yr	W	–
Fablet et al. (2003)	✓			Plaice *Pleuronectes platessa* L.	Eastern Channel	116	0–6 yr	–	40.0
				Plaice *Pleuronectes platessa* L.	Eastern Channel	116	7–11 yr	–	10.0
Fablet et al. (2004)	✓		✓	Plaice *Pleuronectes platessa* L.	Eastern Channel	300	1–6 yr	–	14.0
Fablet (2006b), Fablet & Le Josse (2005)	✓		✓	Plaice *Pleuronectes platessa* L.	Eastern Channel	320	1–6 yr	–	12.0
Fablet (2006a)	✓		✓	Plaice *Pleuronectes platessa* L.	Eastern Channel	200	1–6 yr	–	11.0
Palmer et al. (2005)		✓		Plaice *Pleuronectes platessa* L.	–	–	–	–	–
		✓		Cod *Gadus morhua*	–	–	–	–	–
Courbin et al. (2007)	✓	✓	✓	Hake *Merluccius merluccius*	–	628	8–50 cm	W	–
Mahé (2009)	✓	✓	✓	Cod *Gadus morhua*	North Sea	311	1 to 3+ yr	S	13.8
	✓	✓	✓	Cod *Gadus morhua*	Northeast Arctic	527	2 to 7+ yr	S	25.48
	✓	✓	✓	Cod *Gadus morhua*	Faroe Plateau	254	1–6 yr	S	–
	✓	✓	✓	Plaice *Pleuronectes platessa* L.	Eastern Channel	237	2 to 6+ yr	S	34.16
	✓	✓	✓	Plaice *Pleuronectes platessa* L.	Iceland	251	4 to 7+ yr	W	13.06
	✓	✓	✓	Anchovy *Engraulis encrasicolus*	Bay of Biscay	312	1 to 2+ yr	W	9.35
Sória Pérez (2012)	✓		✓	Plaice *Pleuronectes platessa* L.		189	2–6 yr		11.5

Fisheries scientists making measurements of opacity using images go to great lengths to ensure their otolith preparation and imaging protocols deliver precise measurements. They favour thinly ground otolith sections under transmitted light (Hüssy & Mosegaard 2004, Jolivet et al. 2013). The need for consistent lighting geometry mitigates against using whole otoliths, as due to their irregular surface and crystalline structure, the appearance of growth marks is very sensitive to small variations in the lighting geometry. Imaging thin sections has been shown to enhance the contrast between opaque and hyaline zones, illuminated by reflected light (Panfili et al. 1990). AFISA tested their system with both whole otoliths (under reflected light) and transverse and sagittal sections (under both reflected and transmitted light). They used one magnification setting and carefully configured the lighting and ensured consistency by making measurements on a 'calibration otolith'. AFISA found that

> 'the set-up concerning light settings were [sic] highly influential on the opacity measure and were [sic] very well defined and all measurements of opacity were done using a standard set-up in which the magnification, the light settings, position of light-source and otolith under the light and the setting of the frame-grabber system was [sic] kept constant between all otoliths' (Mahé 2009, p. 15).

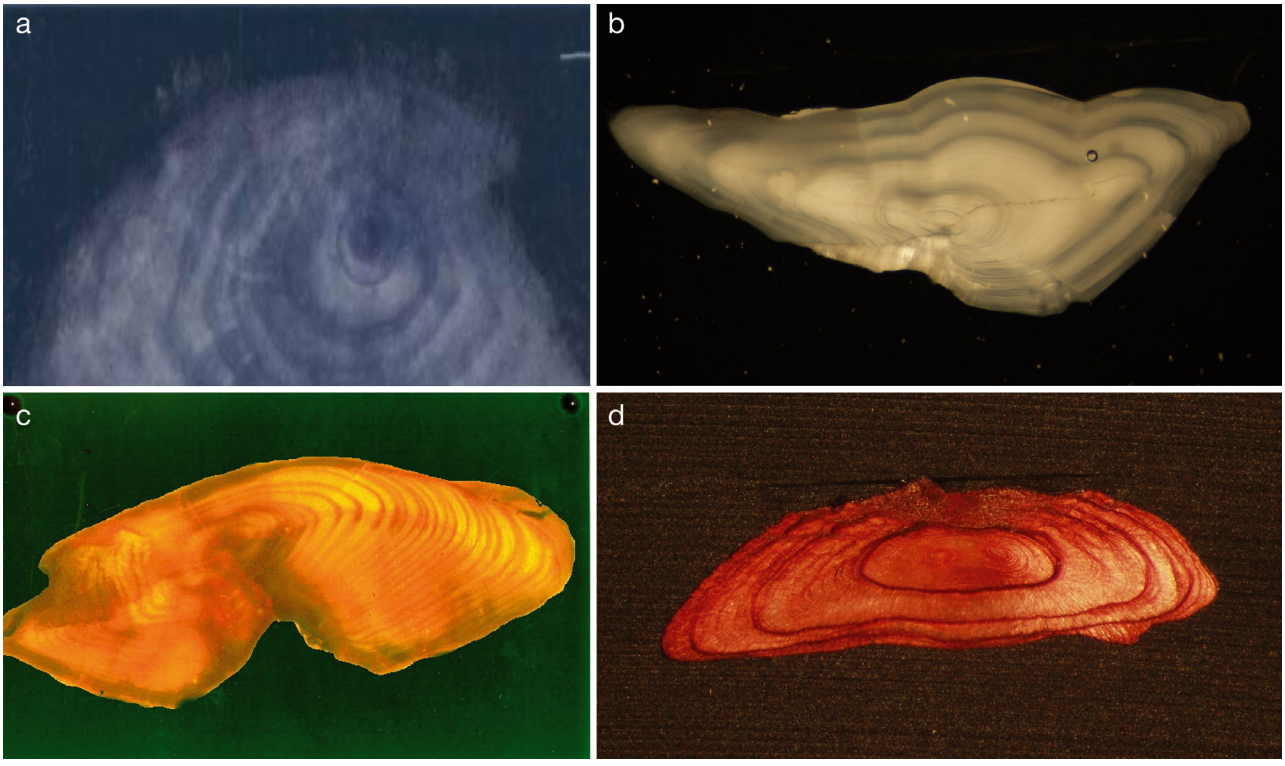

Fig. 2. Example otolith images illustrate improvement in image capture technology: (a) eel *Anguilla anguilla*, sectioned otolith (Panfili et al. 1990); (b) cod *Gadus morhua*, sectioned otolith (2013 image from Cefas); (c) eel, sectioned otolith stained with neutral red (2013 image from Cefas); (d) sole *Solea solea*, sectioned otolith stained with neutral red (2013 image from Cefas)

Image processing

Image processing is mostly concerned with digital processing of signals derived from images. The techniques employed can be classified as low-level, e.g. enhancement of contrast, noise removal, and thresholding; and high-level, e.g. image/object classification, and scene understanding (Sonka et al. 2008, Gonzalez & Woods 2008). The term 'computer vision' is used to describe systems that perform high-level tasks and exhibit intelligent behaviour. Computer vision systems often take advantage of temporal coherence between video frames rather than working with one isolated image. Almost all computer vision systems employ computer software, and developing efficient pattern-recognition algorithms is very much a focus of current research. Image-based CAAGE techniques can be broadly classified as 1-D or 2-D, and a good overview of these is provided by Troadec & Benzinou (2002). 1-D approaches measure the opacity profile along a line originating at the otolith core and ending at the edge (Panfili et al. 1990, Troadec 1991, Welleman & Storbeck 1995). This line is called a ray or transect and is usually taken in the direction of maximal growth; an example is shown in Fig. 3. In contrast, 2-D approaches consider all the otolith's pixels rather than just those that underlie one (or a small number of) transect(s). A 2-D approach is essential for some algorithms, such as finding the position of the core or nucleus, but other operations such as filtering the image may be accomplished equivalently in 1-D or 2-D. One of the most common image-processing operators used in CAAGE is a smoothing filter. Many otolith readers interactively apply filters to improve the distinction between increments and will be familiar with the names used to identify the kernels (e.g. 'Laplacian', 'unsharp' etc.). These enhance fine detail, but often amplify image noise. Fortunately, humans are good at discriminating between structured and unstructured visual information and can discount the noise. But, unlike humans, computers are unable to discriminate between structured high-frequency information and noise, so high frequencies are usually suppressed by applying a smoothing filter prior to processing. AFISA highlighted some challenges in applying smoothing filters to otolith images. Firstly, the ring structures are clearly oriented, and secondly,

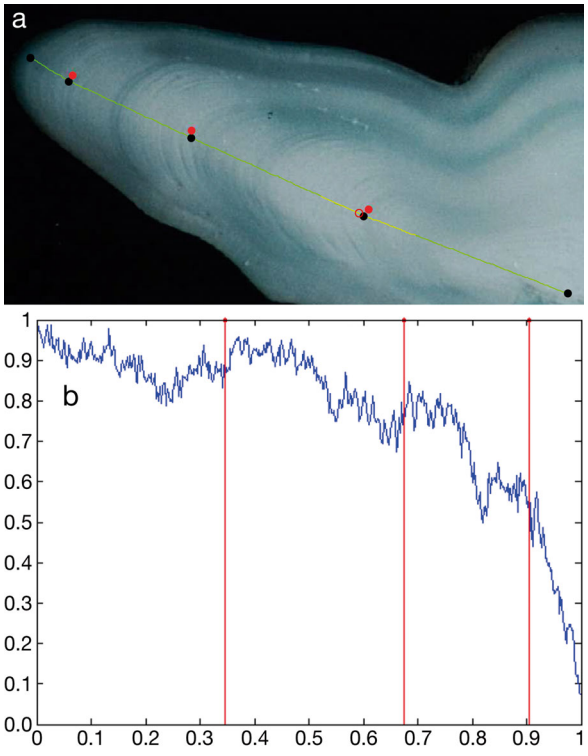

Fig. 3. (a) Section of a 3 yr old cod otolith. Red dots, from left to right: the nucleus and successive year marks, placed manually by an expert. Yellow/green line: the radial transect used to extract the intensity profile. Black dots denote positions where growth marks identified by red dots intersect the radial transect. Open red circle: position of the computed first annual ring along this intensity profile. (b) Intensity profile along the radial growth axis. Note: *x*-axis shows relative distance from otolith nucleus, *y*-axis shows pixel intensity (0.0 = black, 1.0 = white). Vertical red lines denote positions of black dots shown in panel (a). From Mahé (2009)

their width is modulated by the growth function. Further, the opaque and translucent rings are also associated with different scales. These factors make optimising the filter parameters very difficult. AFISA addressed this by employing a novel filter that used a 2-D otolith growth model (discussed in the section '2-D analysis') to automatically adapt its parameters in different regions of the otolith image.

1-D analysis

The first algorithms for automatically ageing otoliths simply enumerated the peaks in a 1-D transect opacity signal (Panfili et al. 1990), but more robust results are obtained using Fourier analysis to digitally process the signal (Troadec 1991). Troadec demodulates the transect signal by assuming otolith growth to be modelled by a 1-D growth function and then uses Fourier analysis to establish the fish age. Welleman & Storbeck (1995) consider the problem of automatically identifying the nucleus and evaluate their system for routine ageing of 334 plaice *Pleuronectes platessa* individuals. Extending this work, other researchers have exploited alternative signal processing techniques such as wavelet decomposition (Morales-Nin et al. 1998, Palmer et al. 2005) and bilinear transforms (Fablet et al. 2003) to study the time-frequency signal behaviour. Both Troadec (1991) and Formella et al. (2007) apply coordinate transformations before processing; an example is shown Fig. 4. Fig. 4b,c illustrates problems associated with non-uniform growth that in turn give rise to local discontinuities. To address problems that arise due to differences in accretion rates that (in extreme cases) can give rise to local discontinuities in 1-D signals representing growth rings, Troadec (1991) integrates profiles using a median estimator to improve robustness and Campana (1992) proposed combining measurements from different sources. Takashima et al. (2000) combine information from 1-D transects in a statistical model, while Guillaud et al. (2002a,b), Rodin et al. (1996) and Palmer et al. (2005) describe algorithms linking growth features in adjacent transects, thereby providing a step towards 2-D analysis.

2-D analysis

In the late 1990s, researchers attempted to use 2-D image segmentation tools called active contour models to recover complete growth rings. The approach is inspired by a computational analogue of an elastic band that is seeded in the image and allowed to deform due to external forces generated by image features (e.g. annular rings). The contour is free to move, finally reaching equilibrium when the internal elastic force in the model and the external image features are balanced. The internal force comprises several parameterised components that can be tuned to ensure the contour remains smooth and unbroken even when the external image features are weak, so that the contour is robust to cases where the annular growth marks are incomplete. Sethian's work on evolving interfaces (Sethian 1996) provides an efficient mathematical framework for this type of model, and Troadec et al. (2000) use this to recover 2-D growth features. The model aims to generate the arrival time surface, $T(x,y)$, shown in Fig. 5, that in turn is interpreted as a forward model of growth. Using this surface, the otolith ring structures are predicted by solving the equation

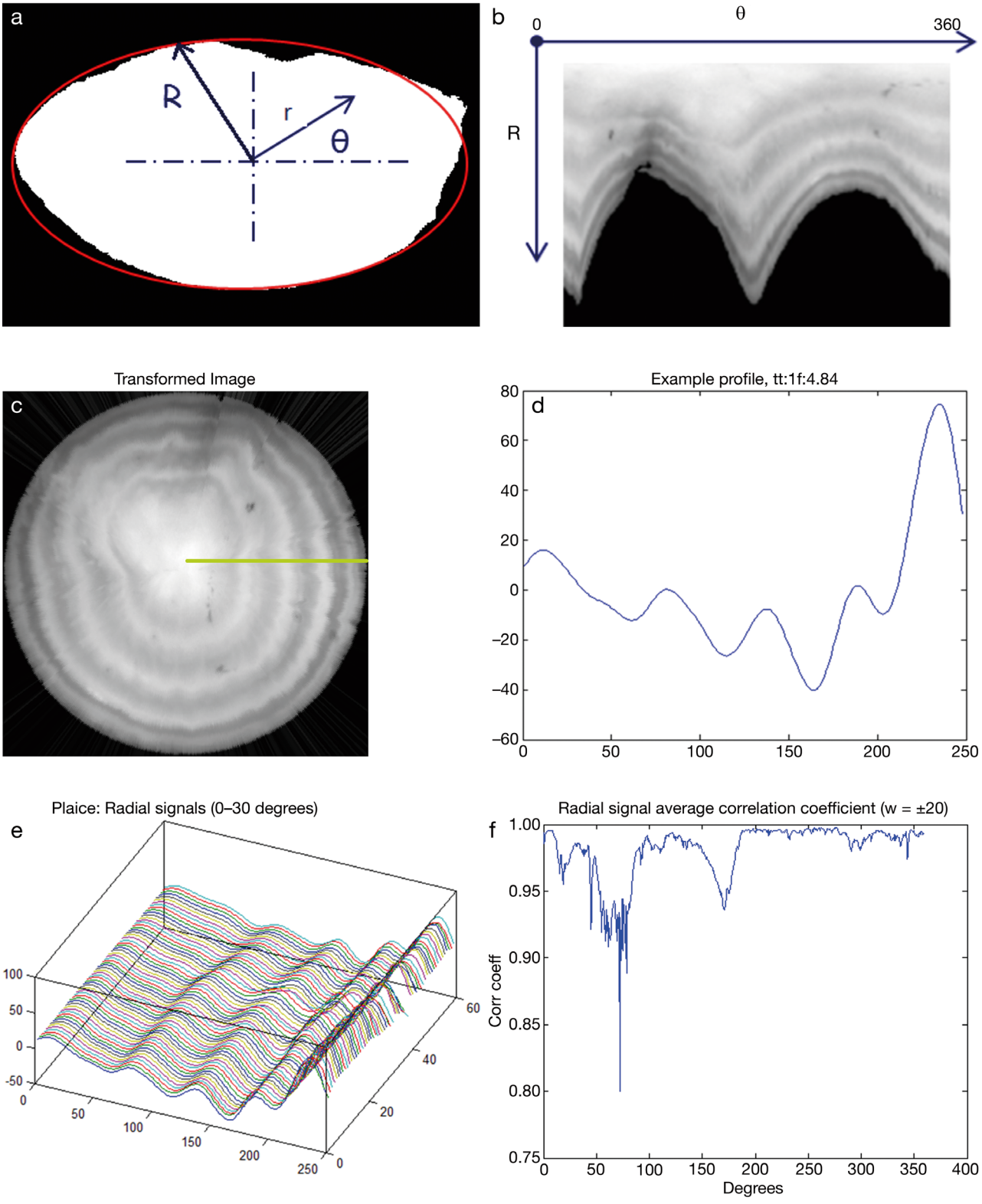

Fig. 4. (a) Plaice (*Pleuronectes platessa*) otolith binary image illustrating Cartesian to polar transform $P(r,\theta)$ where $r = \sqrt{x^2+y^2}, \theta = \tan^{-1} y/x$; (b) transformed plaice otolith $P(r,\theta)$; (c) rescaled polar transformation $P(r^t,\theta)$ where $r^t = r/R$; (d) filtered radial 1-dimensional (1-D) transect signal (path highlighted in green in (c)); (e) ensemble of 1-D transects (0–30°); (f) covariance between neighbouring 1-D transects

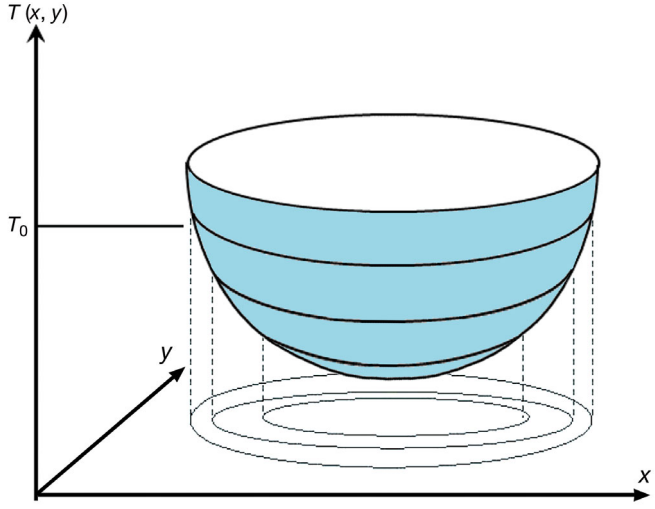

Fig. 5. The arrival time surface $T(x,y)$ in relation to observed otolith ring structures

$$T(x,y) = T_0 \quad (1)$$

for any T_0. The solution of this equation corresponds to the otolith surface at time T_0, and further embedded growth layers at $t > T_0$, thereby allowing a time series of otolith shapes to be synthesised. AFISA (Mahé 2009) adopted and extended this model by combining low-level growth cues derived from the local orientation and shape of growth marks (Álvarez et al. 2008, Chessel et al. 2008, Fablet et al. 2008, 2009). The accuracy of this forward model of accretionary otolith morphogenesis in space and time is illustrated in Fig. 6. The model is used by AFISA to drive the adaptive smoothing filter introduced in the section 'Image processing' above, but more recently it has been extended to form the basis for more complex bioenergetic models (Fablet et al. 2011).

An important subproblem for both 1-D and 2-D approaches is that of detecting the otolith nucleus or core; this is the focus of work by Cao & Fablet (2006). They combine morphological features recovered from the otolith image and a statistical model trained on expert readers to automatically locate the otolith core. Machine learning is a paradigm that seems to deliver the best results in terms of performance for automatic ageing, and neural network and statistical frameworks are popular implementations. Approaches that use machine learning paradigms often derive features from spatial and frequency domain analysis of 1-D transect signals, sometimes combined with 2-D features extracted from the image (Robertson & Morison 1999, Fablet et al. 2004, Fablet & Le Josse 2005, Fablet 2006a) and other measurements such as weight (Fablet 2006b, Bermejo 2007).

Since 2010, there has been a noticeable shift towards computational modelling of otolith increment formation through integration of visual and chemical analysis. These efforts have attempted to answer questions relating to the coupling between otolith growth and fish growth through metabolism and the formation of opaque and translucent growth zones in relation to the physiology of the individual (Grønkjaer 2016).

VALIDATION OF COMPUTER-ASSISTED OTOLITH ANALYSIS

Troadec & Benzinou (2002) review the motivation for pursuing research into CAAGE systems, citing improvements in accuracy, precision, and productivity. While early research tended to evaluate the accuracy of computer-assisted and automatic ageing systems with reference to human interpretation and give results in terms of absolute error (Δ), more recent studies use methods that report errors in the context of amongst-reader variability. A recent evaluation by Fablet (2006b) (plaice *Pleuronectes platessa* otoliths, N = 320) reported 95% of automatic age estimates were identical to those of human readers, and Takashima et al. (2000) claimed the performance of automated counting to be indistinguishable

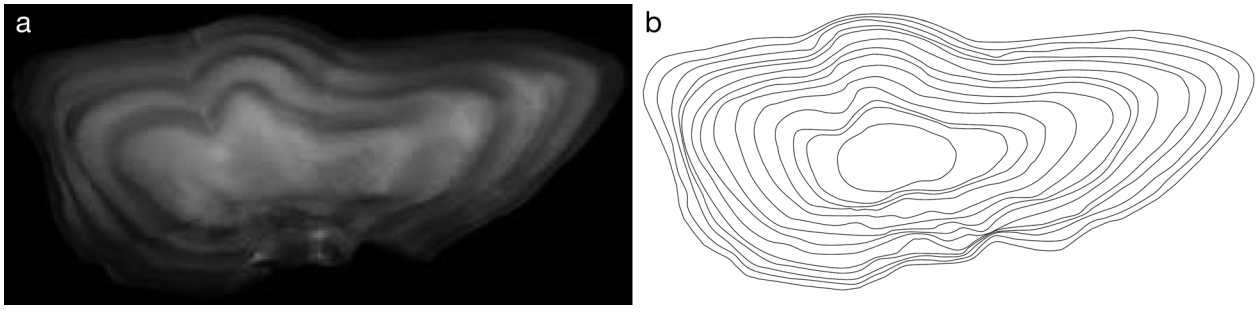

Fig. 6. (a) Cod otolith image (transverse section) rendered by overlaying annular growth rings, generated by forward growth model (b)

to that of expert readers. The precision (the ability of a system to produce repeatable measurements) of computer-assisted techniques has been reported to be similar to that of human interpretation (Cailliet et al. 1996), and broad agreement exists that the benefit from computational recording of results lies in the elimination of minor errors in the process. Troadec & Benzinou (2002) argue that using a computerised process forces readers to focus their attention on a defined protocol, and this in turn produces benefits in terms of quality assurance. With this in mind, some laboratories have written species-specific protocols for age analysis that require the users to execute (ImagePro) macros defining sequences of image-processing functions. An ImagePro plug-in developed by Alaska fisheries is available from www.mediacy.com/resources/appcenter/otolith-application--27-detail. The question of productivity is frequently addressed. Developers of interactive systems claim a benefit (from 30–300% depending on the task) in using computer-assisted techniques, while developers of fully automated systems (e.g. Troadec & Benzinou 2002) conclude that the prospect of fully automated unsupervised processing (of a subset of fish species) is entirely feasible. AFISA (Mahé 2009) undertook a very detailed evaluation of the technology, and their findings are summarised in the next section.

Since 2010, most work on automated ageing has been focused on evaluating and improving models that use otolith morphology, sometimes combined with biological measurements, for stock assessment (Smith & Campana 2010, Matic-Skoko et al. 2011, Campana & Fowler 2012, Bermejo 2014, Williams et al. 2015). Some of this work is motivated by a need to manage stock in artisanal fisheries located in areas where there is a shortage of trained readers. Although the accuracy of morphometric approaches is poorer than estimates provided by human readers, some scientists conclude that, with hindsight, there would have been little difference in stock management strategies, had previous decisions been based on ages derived from morphometric rather than expert estimates (Williams et al. 2015).

COST–BENEFIT ANALYSIS

The most significant research effort in recent years to assess CAAGE applications in otolith reading was the AFISA project (Mahé 2009). AFISA attempted to address the cost of using age-based models based on age estimations using otolith readings, considered to be several million euros annually, by using automated computerised techniques. In this context, the project aimed to provide a means of standardising ageing amongst laboratories and to build interpreted image databases that could, in turn, be used for quality assurance as well as reducing the cost of acquiring age data. AFISA developed and tested a suite of algorithms for image-based CAAGE. Some of these have been reviewed earlier in this article, but although results testing the accuracy of various systems ageing plaice were published (Table 1), the wider picture resulting from a detailed cost–benefit analysis comparing the performance of several different CAAGE systems and otolith reading across a range of fisheries has until now only been accessible as a final project report (Mahé 2009). The project evaluation focused on 3 case studies (Table 2): cod *Gadus morhua* (Faroe Plateau, North Sea, and northeast Arctic); anchovy *Engraulis encrasicolus* (Bay of Biscay); and plaice *Pleuronectes platessa* (Eastern Channel and Iceland). A total of 6729 otoliths were collated from surveys and commercial landings, and the following associated data were recorded: area, year, quarter, total length, weight, sex, and maturity. Two different approaches delivering automated age estimates were evaluated (Table 3): using 1-D opacity profiles along radial transects, and a conditional model using morphologic descriptors together with a nearest-neighbour classifier. These were compared with another morphologic approach using a mixture model (Francis & Campana 2004) and estimates by expert readers. The evaluation method built age–length keys for each approach based on a subset of each fish stock from the database. The efficiency or precision of a method is determined by the goodness-of-fit of the age–length key built from a subset compared to the true age distribution of the sample. Results from 3 case studies (cod, plaice, and anchovy) undertaken by AFISA are presented in Table 3. The analysis only considered a homogeneous subset of fish (i.e. individual fish data for which the relationship between age, length, otolith weight and other otolith characteristics is the same) caught in the same year and quarter (Table 2). The costs (Table 4) were estimated from work undertaken within the project. As all the automatic methods required experts to prepare training sets of otoliths, manual age reading remained an essential component. The cost of both the morphological and image-based automated methods are considered as equivalent, the major component of cost being due to the preparation of otolith samples. The accuracy

Table 2. Automated FISh Ageing (AFISA) case study samples (Mahé 2009). Cefas = Centre for Environment, Fisheries and Aquaculture Science (UK), IMR = Institute of Marine Research (Norway), Difres = Danish Institute for Fisheries Research, Ifremer = Institut Français de Recherche pour l'Exploitation de la Mer (France), MRI = Marine Research Institute (Iceland), AZTI = AZTI Technology Centre (Spain), NS = North Sea, NEA = northeast Arctic, FP = Faroe Plateau, EC = Eastern Channel (ICES area VIId), Biscay = Bay of Biscay, Prep = otolith preparation, W = whole, S = section. Faroe samples collected by the Fish Ageing by Otolith Shape Analysis (FAbOSA) project (Arneri et al. 2002)

Institute	Species	Area	Year	Quarter	Source	Prep	N
Cefas	Cod	NS	1998	3	Survey	S	400
Cefas	Cod	NS	1999	3	Survey	S	347
Cefas	Cod	NS	2000	3	Survey	S	400
Cefas	Cod	NS	2001	3	Survey	S	400
IMR	Cod	NEA	2000	1–4	Survey	S	494
IMR	Cod	NEA	2001	1–4	Survey	S	498
IMR	Cod	NEA	2004	1–4	Survey	S	500
IMR	Cod	NEA	2005	1–4	Survey	S	500
Difres	Cod	FP	1996–2001	1–4	Tag/recapture	S	255
Ifremer	Plaice	EC	2006	1	Survey/market	W/S	248
Ifremer	Plaice	EC	2006	2	Survey/market	W/S	249
Ifremer	Plaice	EC	2006	3	Survey/market	W/S	195
Ifremer	Plaice	EC	2006	4	Survey/market	W/S	237
MRI	Plaice	Iceland	2006	1–4	Market	W	1000
AZTI	Anchovy	Biscay	1998	1–3	Market	W	500
AZTI	Anchovy	Biscay	1999	1–3	Market	W	500
AZTI	Anchovy	Biscay	2004	2	Market	W	500
AZTI	Anchovy	Biscay	2005	1–3	Market	W	500

of each method is given in terms of mean-squared error (MSE) and relative bias (Table 3), computed as follows:

> 'For a given stock and period, usually a quarter, data on fish length and weight, otolith characteristics such as weight, area etc. and the age determined by expert readers were available for a random sample of fish. This sample was randomly divided into two groups of equal size, for which one group was used as learning data with the age included and the second was used as testing data for which the age information were [sic] excluded. For each of the three methods the age distribution in the combined learning and testing sample (i.e. the original random sample available) was estimated based on these data. This procedure was repeated 100 times and thus resulting [sic] in 100 estimates of the age distribution in the combined learning and testing sample. As the 'true' age distribution is known in this combined sample the goodness of the methods can be evaluated' (Mahé 2009, p 120).

Since the true age–length key is built using otolith ages provided by expert readings for the whole sample, the results for age–length key (i.e. age determined by expert readers) given in Table 3 reflect the sampling error. MSE is the most important since it measures the mean error across all ages. Relative bias provides information about how the errors are distributed. For example, a high relative bias indicates that the error is not normally distributed and the system shows a tendency to under- or over-estimate a particular year group. It is important to note that bias can exist for the age estimation among international readers. For example, exchanges of Arctic cod otoliths have also reported inter-reader bias, indicating that there are significant differences in age estimates among readers from different institutions (Yaragina et al. 2009, Healey et al. 2011).

The results presented in Table 3 show that the mixture model (Francis & Campana 2004) outperforms the nearest-neighbour classifier built on morphometric features and gives an MSE close to that of expert readers. The performance of image-based CAAGE gives at best an MSE between 5 and 10 times greater than expert readers (often more for particular year groups). We discuss these results in the next section.

DISCUSSION

Computer vision, image processing and image quality

Computer vision technology has matured over the last 3 decades and is now commonly deployed by manufacturing industries to guide robotic systems, inspect component parts or complete assemblies, etc. These will usually have been precisely manufactured often by numerically controlled machines using data derived from computer-aided design (CAD) software. The lighting within manufacturing cells that use these systems is tightly controlled and conventional camera images are often supplemented by additional sensors (e.g. lasers). More challenging scenarios for computer vision lie in specific applications that are less constrained but which are the subject of well-documented domain ontologies. Otolith ageing represents an important application and an opportunity to benchmark intelligent systems that integrate computer vision and machine learning. The importance of this research within the image analysis and machine learning community is evidenced by the many articles published in relevant computer-

Table 3. Automated FISh Ageing (AFISA) case study: mean squared error (MSE) and relative bias (RB) by method, stock and age (Mahé 2009). Note: MSE and RB are calculated using the methodology described by Mahé 2009 (p. 121). (–) not determined (Mahé 2009)

Stock	Age (yr)	Method							
		Automated		Conditional		Francis & Campana (2004)		Age–length key	
		MSE (×100)	Bias (%)	MSE (×100)	Bias (%)	MSE (×100)	Bias (%)	MSE (×100)	Bias (%)
North Sea cod (N = 311)	1	0.40	4.47	0.66	1.65	0.23	−0.88	0.31	−0.22
	2	4.04	8.68	0.71	0.92	0.36	−0.34	0.36	−0.25
	3+	4.44	−100.0	0.21	−14.77	0.12	5.67	0.12	2.92
Northeast Arctic cod (N = 527)	2–	1.02	−67.64	0.58	−46.84	0.06	10.73	0.02	1.06
	3	1.47	−18.39	0.32	−1.02	0.17	−3.14	0.16	1.04
	4	8.32	31.35	0.87	7.86	0.34	2.6	0.25	−0.42
	5	2.83	19.54	1.09	11.52	0.22	−1.12	0.33	−0.81
	6	0.70	−1.37	0.41	−2.51	0.16	−0.77	0.22	0.13
	7+	4.12	−51.58	0.69	−13.74	0.09	−1.61	0.15	0.15
Faroe Plateau cod[a,b] (N = 254)	1	–	–	0.93	−17.31	–	–	9.32	1.48
	2	–	–	2.52	−13.81	–	–	3.47	0.67
	3	–	–	1.25	12.03	–	–	1.25	0.07
	4	–	–	1.65	−16.68	–	–	6.71	−0.27
	5	–	–	2.62	35.29	–	–	1.30	−0.70
	6	–	–	2.17	31.63	–	–	1.30	−0.17
Eastern Channel plaice (N = 237)	2–	0.45	−12.81	2.69	−38.69	0.19	6.36	0.28	0.37
	3	2.13	21.96	2.27	13.36	0.47	−2.44	0.52	−0.51
	4	2.24	−6.19	1.93	−11.01	0.56	−3.33	0.58	−1.08
	5	21.3	53.73	6.20	24.71	0.74	−0.79	0.78	0.92
	6+	21.1	−49.91	2.25	−10.13	0.56	1.85	0.59	−0.02
Icelandic plaice (N = 251)	4–	1.28	−35.56	1.68	−31.00	0.28	−3.26	0.21	1.14
	5	0.63	−6.77	2.62	−19.57	0.59	3.86	0.43	−0.31
	6	6.09	16.70	2.88	7.88	0.89	−0.30	1.09	0.72
	7+	1.96	−5.83	2.26	5.30	0.71	−0.49	1.09	−0.84
Bay of Biscay anchovy (N = 312)	1	3.44	7.23	29.26	23.22	0.43	−1.69	0.32	0.35
	2+	2.94	−13.94	29.26	−53.60	0.43	3.92	0.32	−0.82

[a]The contrast between transparent and opaque zones was too low for automatic zone detection
[b]A requirement for the Mixture analysis (Francis & Campana 2004) is that otolith weight and fish length data are normally distributed within ages. Data from the Faeroe cod stock violated this requirement and Mixture analysis was therefore not possible

vision journals (Caselles et al. 1998, Guillaud et al. 2002a,b, Cao & Fablet 2006) and presented at conferences (Rodin et al. 1996, Benzinou et al. 1997, Fablet et al. 2003, Fablet 2005, Chessel et al. 2006). Most research into automated image-based CAAGE undertaken in the 2000s was funded by the European Union, and the emphasis probably reflected the broader information and communication technology (ICT) research and development (R&D) agenda that existed at that time in the EU.

Image quality is a decisive factor for image-based automatic ageing systems. Attempts to acquire and measure growth rings using other sensors have either failed, or are too costly to use in production

Table 4. Automated FISh Ageing (AFISA) case study: costs in euros (⇔) per fish for measuring fish characteristics (Mahé 2009). NS = North Sea, NEA = northeast Arctic, FP = Faroe Plateau, EC = Eastern Channel, Biscay = Bay of Biscay, (–) not determined

Process	Cost (€) per otolith					
	Cod			Plaice		Anchovy
	NS	NEA	FP	EC	Iceland	Biscay
Measuring length and weight and manual age reading	2.81	5.88	2.85	2.13	5.37	6.5
Automated age determination and manual age reading	3.93	10.46	5.61	2.47	6.24	9.71
Automated age determination	–	–	–	1.38	3.03	7.74
Tag/recapture and pen rearing	–	–	17.0	–	–	–

(Hamrin et al. 1999, Jolivet et al. 2008, 2013, Mapp et al. 2016). AFISA's (Mahé 2009) image acquisition protocol used otolith sections for cod and Eastern Channel plaice and whole otoliths for Icelandic plaice and anchovy, consistently imaged at one magnification. They tested using reflected and transmitted light and carefully set up their system with a calibration otolith. AFISA were unable to obtain age estimates for some stocks due to poor contrast (e.g. Faroe Plateau cod), and found that although images recovered from whole otoliths suffer from instability due to lighting inconsistencies, ages could be automatically estimated from 1-D transects (Mahé 2009). However, more successful outcomes were obtained from digitised images exhibiting clear annual growth structures, such as those acquired from North Sea cod, Icelandic plaice and Eastern Channel plaice (year groups <5 yr).

The need for further work

The literature on image-based CAAGE of otolith MaS since 1990 is summarised in Table 1. While many authors describe image-processing approaches and algorithms for image-based CAAGE of otolith MaS, few studies evaluate performance on a significant cohort of fish (N > 30). The most comprehensive studies involving multiple species have been undertaken by Morison et al. (1998), Robertson & Morison (1999, 2001) and Mahé (2009). Both use information from 1-D transects. Robertson and colleagues (Morison et al. 1998, Robertson & Morison 1999, 2001) include this information as an additional feature and show that its inclusion slightly improves the performance of a neural network trained using only morphological and biological features. They use Fourier transforms to encode features of 5 transect signals and test 3 neural network architectures, showing that all deliver similar performance (note: results shown in Table 1 are obtained from a simple back-propagation network trained using only transect signals, i.e. morphological or biological features have been excluded).

The results from AFISA have been published in the form of an EU report only (Mahé 2009), although a subset of the work concerning Eastern Channel plaice feature widely in publications by Fablet and colleagues (Fablet 2005, 2006b, Fablet & Le Josse 2005). AFISA also analyse transect signals but employ a statistical framework and more complex pre-processing than do Robertson and colleagues (Morison et al. 1998, Robertson & Morison 1999, 2001). Both systems are automatic, but adopt different strategies for choosing a suitable set of transects and finding the otolith nucleus. Overall, AFISA's results are consistent with those of Morison et al., but evaluations often highlight problems of undercounting and coping with marginal rings, and this seems to be reflected in high bias for year groups > 3 yr. AFISA also highlight problems due to under-represented year groups in the training set for some stocks, resulting in high relative bias. North Sea cod, Icelandic plaice and Bay of Biscay anchovy exhibit the lowest average percent errors. Results from image-based CAAGE using whole otoliths are surprisingly good (e.g. Icelandic plaice and Bay of Biscay anchovy), and could potentially deliver a cost benefit. Although Eastern Channel plaice exhibit high-contrast growth marks, the results suffer from high relative bias (year groups 5 to 6+), and the average percent error found by AFISA is much poorer than that reported in previous studies published by Fablet and colleagues, which seems to suggest that some of these systems combine image-based and morphological information (Fablet 2006b).

While Morison et al. aim to integrate visual and morphological features, AFISA's primary focus is on visual analysis. However, their tests benchmarking against other approaches employing morphological features show that age estimates produced using the mixture model proposed by Francis & Campana (2004) are consistently better than either of the 2 CAAGE approaches developed by AFISA, and deliver estimates close to those achieved by experts. However, neither technique is applicable for Faroe Plateau cod due to either poor contrast or non-normally distributed data. This may be because the Faroe Plateau cod data were derived from a tag/recapture sample, i.e. fish were reared in captivity, tagged, released and subsequently recaptured at different times of the year (Doering-Arjes et al. 2008).

In other domains such as medicine and remote sensing, the availability of open-access, online databases, ground-truthed data and algorithms has motivated considerable interest amongst the computer-vision research community and has generated a valuable and voluminous portfolio of published studies. We suggest therefore that publication of the AFISA database as an online resource could act as a significant catalyst to progress CAAGE-based otolith research.

Cost

Costs for human and machine ageing systems are broadly similar since a large part of the cost is associ-

ated with preparing the otolith sections. Some costs shown in Table 4 assume that the cost for both morphometric and image-based systems are equal and that they do not include capital equipment. This is an oversimplification, and it may be reasonably expected that costs for imaging may be slightly higher, given that the process developed by AFISA is computationally demanding. All methods need to be trained using expert reader estimates and assume that there are an equal number of otolith samples in training and production samples. Further work is needed to evaluate the relationship between performance and training. The power of an automated approach lies in the ability to scale, and in a successful system, an adequate performance using as few as <10% of the number of production otoliths might be anticipated.

Is age reading too difficult a problem?

At first sight, otolith reading represents an ideal candidate for a computer vision system, since the application offers a natural progression for state-of-the-art algorithms, which by the early 2000s had chalked up some successes on similar but less demanding applications. But, some features of otolith reading present difficulties to the designer of an image-processing algorithm. Firstly, the task is much more challenging than a naïve description in terms of a cyclic pattern of rings suggests. For example, Chauvelon & Bach (1993) observe that many otoliths are difficult for expert readers to interpret and it is not always possible to age fish along a predefined axis. Secondly, the structure of visual features comprising internal growth marks is complex, comprising check or stress marks in addition to opaque and translucent bands (e.g. Smith 2014, Hüssy et al. 2016b), and although the domain ontology is well defined (Kalish et al. 1995), the expertise needed to successfully interpret growth marks is sometimes related to specific stocks and held within specific institutes. For example, Faroe Plateau cod form a transparent 'winter ring' which is out of phase with the annual cycle, and depending on the time of year that the fish was captured, the final ring has either to be counted or neglected. The accuracy of age estimates from a reader unfamiliar with the Faroe cod stock is only 40–50%, while the equivalent figure is 95–99% for expert Faroe readers (Doering-Arjes et al. 2008).

AFISA represents the most recent comprehensive attempt to implement and evaluate a CAAGE system. Here we provide a glimpse only of AFISA's case studies; however, the project report describes >15 separate algorithms, tested in MATLAB and implemented in C code within Ifremer's TNPC platform (Fablet & Ogor 2005). The executive summary of the AFISA project highlights the success of the project and concludes:

> 'the AFISA project resulted in advances in computer vision which provide more reliable methods to extract information from otoliths in order to estimate the individual age and the age structure. These methods are operational using TNPC software. However, such methods should not be seen as being able to fully substitute to experts. They should rather be seen as tools to provide automatically extracted information that requires a subsequent control by experts for the estimations of individual age and age structure. For some species such as plaice, these methods could be usable from the perspective of bias and costs' (Mahé 2009, p. 7).

With hindsight, perhaps AFISA's goals were overambitious and the decision to include species such as Faroe Plateau cod unwise, since the challenges of reading these stocks are well documented. As a rule of thumb, automated image analysis systems rarely outperform human experts and one would anticipate problems for tasks that attract a high degree of inter-expert variation. The study concludes that results obtained from plaice and North Sea cod which exhibit higher-contrast annular rings would be usable and highlights the importance of ensuring all year groups are equally represented in the training set. Anchovy is also highlighted as a possible candidate for further work due to the potential cost saving. The performance achieved by the mixture model is a major problem for CAAGE and perhaps the reason why this has been the focus of much of the work since 2010.

Future directions for image-based CAAGE

With the above in mind, there are 2 possible directions for future image-based CAAGE developments in relation to fisheries management and assessment. The first of these lies in adapting the integrated system proposed by Robertson & Morison (2001) and exploring frameworks for fusing morphological and image-based otolith features. Robertson & Morison (2001) show this approach boosts performance in the context of a neural network classifier, and if the information from a transect, perhaps positioned interactively, was integrated with the mixture model proposed by Francis & Campana (2004), then for plaice and cod (Table 3) it could conceivably deliver accuracies that are indistinguishable from those of human expert readers.

The second direction addresses a more general problem that affects all existing machine-learning frameworks to some extent, in that for most users, the system is a 'black box'. The priority for software designers is to produce systems with equivalent performance to that of human experts, and the requirement to explain decisions made, particularly within an operational context, is a secondary concern. Building systems that can be trained by domain experts rather than by computer programmers might offer a solution. With intelligent system applications ranging from clinical decision-making, autonomous driving, financial services, and predictive policing comes the growing need for accountability. In this context, the exposure of the decision-making logic is not just a legal necessity but can prevent system errors and build trust amongst users. Details of a potential 'right to explanation' were debated in the most recent revision of the EU's General Data Protection Regulation (GDPR) (Goodman & Flaxman 2016). While current legislation requires explanations only in very limited contexts, questions around operational explanation are expected to become more important in the future. In fisheries management, the development of appropriate computational frameworks that support explanations could begin by exposing the human–computer interactions that occur when the system is trained. Open-access logging of this decision process could be used to reduce inter-reader variation, improve quality assurance and perhaps play a role in training future generations of otolith readers.

CONCLUSIONS

Digital otolith imagery is easy to acquire and relatively cheap to store compared with physical specimens, which may degrade with age; its use in otolith science is already well established and will become increasingly important, particularly for projects involving long chronological time-series. Fisheries management has benefitted from CAAGE systems that exploit both fully automatic and interactive paradigms. However, the cost–benefit analysis reviewed in this paper shows that imaging systems are currently unable to deliver accuracies comparable with systems using models built on morphologic features or age–length keys based on estimates from expert readers, and using current systems, any associated cost-savings will be marginal at best. However, image-based information has been shown to improve age estimates using morphological features, and in the short term, future research should focus on refining this approach.

Acknowledgements. We thank Prof. Duncan Bell, School of Science, Technology and Health, University Campus Suffolk, UK, and David Mortimer, Newbourne Solutions Ltd. for their help creating Fig. 1. We also thank Dr. Timothy Rowe (www.digimorph.org) for permission to use the 3-D micro-CT data set. This review was inspired by a pilot study undertaken by Joe Scutt Phillips at Cefas and we would like to acknowledge the support of Wendy Dawson and Mark Etherton in securing funding for this work. We also thank Sally Songer for her help in recovering and interpreting otolith images. A recently established strategic alliance between Cefas and the University of East Anglia (UEA) provided a framework supporting further interdisciplinary research in the area and we thank both partners for their financial support. We are also grateful to Kelig Mahé and the anonymous referees whose comments greatly improved an earlier version of this review.

LITERATURE CITED

Abràmoff M, Magalhães P, Ram S (2004) Image processing with ImageJ. Biophoton Int 11:36–42

Álvarez A, Morales-Nin B, Palmer M, Tomás J, Sastre J (2008) A two-dimension otolith growth inverse model. J Fish Biol 72:512–522

Appelberg M, Formigo N, Geffen A, Hammer C and others (2005) A cooperative effort to exchange age reading experience and protocols between European fish institutes. Fish Res 76:167–173

Arneri E, Bergstrom N, Cardinale M, Claes E and others (2002) FAbOSA: Fish Ageing by Otolith Shape Analysis: final report to the European Commission. EC contract no. FAIR CT97 3402. www.ices.dk/community/Documents/PGCCDBS/fabosa_rapp02_hel.pdf (accessed 26 April 2018)

Begg G, Campana S, Fowler A, Suthers I (2005) Otolith research and application: current directions in innovation and implementation. Mar Freshw Res 56:477–483

Benzinou A, Troadec H, Binhant JL, Rodin V, de Pontual H, Tisseau J (1997) A locally deformable B-Bubble model: an application to growth ring detection on fish otoliths. In: Proc 10th Scand Conf Image Analysis, p 181–187

Bermejo S (2007) Fish age classification based on length, weight, sex and otolith morphological features. Fish Res 84:270–274

Bermejo S (2014) The benefits of using otolith weight in statistical fish age classification: a case study of Atlantic cod species. Comput Electron Agric 107:1–7

Black BA, Boehlert GW, Yoklavich MM (2005) Using tree-ring crossdating techniques to validate annual growth increments in long-lived fishes. Can J Fish Aquat Sci 62: 2277–2284

Brophy D (2014) Chapter eight – Analysis of growth marks in calcified structures: insights into stock structure and migration pathways. In: Cadrin SX, Kerr LA, Mariani S (eds) Stock identification methods, 2nd edn. Academic Press, San Diego, CA, p 141–170

Burke N, Brophy D, King P (2008a) Otolith shape analysis: its application for discriminating between stocks of Irish Sea and Celtic Sea herring (*Clupea harengus*) in the Irish Sea. ICES J Mar Sci 65:1670–1675

Burke N, Brophy D, King PA (2008b) Shape analysis of otolith annuli in Atlantic herring (*Clupea harengus*); a new method for tracking fish populations. Fish Res 91:133–143

Cadima EL (2003) Fish stock assessment manual. FAO Fish Tech Pap No. 393. www.fao.org/3/a-x8498e.pdf (accessed 26 April 2018)

Cadrin SX, Dickey-Collas M (2015) Stock assessment methods for sustainable fisheries. ICES J Mar Sci 72:1–6

Cailliet GM, Botsford LW, Brittnacher JG, Ford G and others (1996) Development of a computer-aided age determination system: evaluation based on otoliths of bank rockfish off California. Trans Am Fish Soc 125:874–888

Campana S (1987) Image analysis for microscope based observation: an inexpensive configuration. Can Tech Rep Fish Aquat Sci No. 1569

Campana SE (1992) Measurement and interpretation of the microstructure of fish otoliths. In: Stevenson D, Campana S (eds) Otolith microstructure examination and analysis. Can Spec Publ Fish Aquat Sci 117:59–71

Campana S (2001) Accuracy, precision and quality control in age determination, including a review of the use and abuse of age validation methods. J Fish Biol 59: 197–242

Campana S (2005) Otolith science entering the 21st century. Mar Freshw Res 56:485–495

Campana S, Casselman J (1993) Stock discrimination using otolith shape analysis. Can J Fish Aquat Sci 50: 1062–1083

Campana S, Fowler G (2012) Age determination without tears: statistical estimation of silver hake (*Merluccius bilinearis*) age composition on the basis of otolith weight and fish length. DFO Can Sci Advis Sec Res Doc 2012/079

Campana S, Neilson J (1985) Microstructure of fish otoliths. Can J Fish Aquat Sci 42:1014–1032

Campana S, Thorrold S (2001) Otoliths, increments, and elements: keys to a comprehensive understanding of fish populations. Can J Fish Aquat Sci 58:30–38

Cao F, Fablet R (2006) Automatic morphological detection of otolith nucleus. Pattern Recognit Lett 27:658–666

Carbini S, Chessel A, Benzinou A, Fablet R (2008) A review of image-based tools for automatic fish ageing from otolith features. In: Proc Approche Systémique des Pêches, Boulogne-sur-Mer, p 1

Cardinale M, Doering-Arjes P, Kastowsky M, Mosegaard H (2004) Effects of sex, stock, and environment on the shape of known-age Atlantic cod (*Gadus morhua*) otoliths. Can J Fish Aquat Sci 61:158–167

Caselles V, Morel J, Sbert C (1998) An axiomatic approach to image interpolation. IEEE Trans Image Process 7: 376–386

Casselman J, Scott K (2000) A general procedures manual for CSAGES-Calcified Structure Age-Growth data Extraction Software (version 5.2). Spec Publ Glenora Fisheries Stn. Ontario Ministry of Natural Resources, Picton

Chauvelon P, Bach P (1993) Modelling the otolith shape as an ellipse: an attempt for back-calculation purposes. ICES J Mar Sci 50:121–128

Chessel A, Cao F, Fablet R (2006) Interpolating orientation fields: an axiomatic approach. In: Proc 9th Eur Conf Computer Vision, Part IV, ECCV'06. Springer-Verlag, Berlin, p 241–254

Chessel A, Fablet R, Kervrann C, Cao F (2008) Otolith image analysis by computer vision: extraction of growth rings and recovering shape evolution of acretionary structures. In: Proc Int Conf Bio-Insp Signal Process Syst Biosignal 2008, p 490–497

Christensen JM (1984) Burning of otoliths, a technique for age determination of soles and other fish. J Cons Int Explor Mer 29:73–81

Clausen LW, Davis CG, Hansen S (2006) Report of the Sand Eel Otolith Ageing Workshop, DIFRES Charlottenlund, Denmark 11–13 September 2006. www.ices.dk/community/Documents/PGCCDBS/ReportSandEelAgeWK0906.pdf (accessed 26 April 2018)

Courbin N, Fablet R, Mellon C, de Pontual H (2007) Are hake otolith macrostructures randomly deposited? Insights from an unsupervised statistical and qualitative approach applied to Mediterranean hake otoliths. ICES J Mar Sci 64:1191–1201

Darnaude AM, Sturrock A, Trueman CN, Mouillot D, Campana SE, Hunter E (2014) Listening in on the past: What can otolith ^{18}O values really tell us about the environmental history of fishes? PLOS ONE 9:e114951

de Pontual H, Groison AL, Piñeiro C, Bertignac M (2006) Evidence of underestimation of European hake growth in the Bay of Biscay, and its relationship with bias in the agreed method of age estimation. ICES J Mar Sci 63: 1674–1681

Doering-Arjes P, Cardinale M, Mosegaard H (2008) Estimating population age structure using otolith morphometrics: a test with known-age Atlantic cod (*Gadus morhua*) individuals. Can J Fish Aquat Sci 65:2342–2350

Easey M, Millner R (2008) Improved methods for the preparation and staining of thin sections of fish otoliths for age determination. Sci Ser Tech Rep 143. Cefas, Lowestoft

Estep K, Nedreaas K, MacIntyre F (1995) Computer image enhancement and presentation of otoliths. In: Secor D, Dean J, Campana S (eds) Recent developments in fish otolith research. Belle W. Baruch Institute for Marine Biology and Coastal Research. University of South Carolina Press, Columbia, SC, p 303–317

Fablet R (2005) Extraction and interpretation of ring structures in images of biological hard tissues: application to fish age and growth estimation. In: Proc IEEE Int Conf Image Processing, Vol 2, p 830–833

Fablet R (2006a) Semi-local extraction of ring structures in images of biological hard tissues: application to the Bayesian interpretation of fish otoliths for age and growth estimation. Can J Fish Aquat Sci 63:1414–1428

Fablet R (2006b) Statistical learning applied to computer-assisted fish age and growth estimation from otolith images. Fish Res 81:219–228

Fablet R, Le Josse N (2005) Automatic fish age estimation from otolith images using statistical learning. Fish Res 72:279–290

Fablet R, Ogor A (2005) TNPC: digital processing for calcified structures. www.ifremer.fr/lasaa/TNPC/manuel_tnpc4.pdf

Fablet R, Benzinou A, Doncarli C (2003) Robust time-frequency model estimation in otolith images for fish age and growth analysis. In: Proc IEEE Int Conf Image Processing, Vol 3, p 593–596

Fablet R, Le Josse N, Benzinou A (2004) Automatic fish age estimation from otolith images using statistical learning. In: Proc 17th Int Conf Pattern Recognition, Vol 4, p 503–506

Fablet R, Pujolle S, Chessel A, Benzinou A, Cao F (2008) 2D image-based reconstruction of shape deformation of biological structures using a level-set representation. Comput Vis Image Underst 111:295–306

Fablet R, Chessel A, Carbini S, Benzinou A, de Pontual H (2009) Reconstructing individual shape histories of fish

otoliths: a new image-based tool for otolith growth analysis and modelling. Fish Res 96:148–159

Fablet R, Pecquerie L, de Pontual H, Høie H, Millner R, Mosegaard H, Kooijman S (2011) Shedding light on fish otolith biomineralization using a bioenergetic approach. PLOS ONE 6:e27055

Fawel J (1974) The use of image analysis in the ageing of fish. In: Bagenal T (ed) The ageing of fish. Unwin Brothers, London, p 103–107

Fey D P, Linkowski TB (2006) Predicting juvenile Baltic cod (*Gadus morhua*) age from body and otolith size measurements. ICES J Mar Sci 63:1045–1052

Formella A, Vázquez JM, Carrión P, Cernadas E, Vázquez A, Pérez-Gándaras G (2007) Age reading of cod otoliths based on image morphing, filtering and Fourier analysis. In: 7th IASTED Int Conf Visualization, Imaging and Image Processing, VIIP '07. ACTA Press, Anaheim, CA, p 207–212. http://dl.acm.org/citation.cfm?id=1659167.1659207 (accessed 26 April 2018)

Francis RC, Campana SE (2004) Inferring age from otolith measurements: a review and a new approach. Can J Fish Aquat Sci 61:1269–1284

Frei R (1982) Measurements of fish scales and back-calculation of body lengths using a digitizing pad and microcomputer. Fisheries 7:5–8

Friedland KD, Reddin DG (1994) Use of otolith morphology in stock discriminations of Atlantic salmon (*Salmo salar*). Can J Fish Aquat Sci 51:91–98

Geffen A (2002) Length of herring larvae in relation to age and time of hatching. J Fish Biol 60:479–485

Geffen AJ (2012) Otolith oxygen and carbon stable isotopes in wild and laboratory-reared plaice (*Pleuronectes platessa*). Environ Biol Fishes 95:419–430

Gonzalez RC, Woods RE (2008) Digital image processing, 3rd edn. Pearson Education, Upper Saddle River, NJ

Goodman B, Flaxman S (2016) EU regulations on algorithmic decision-making and a 'right to explanation'. In: ICML workshop on human interpretability in machine learning. WHI 2016, New York, NY. https://pdfs.semanticscholar.org/f051/55c4d7d77f32855b80a86bb987818838d50d.pdf (accessed 27 April 2018)

Grønkjaer P (2016) Otoliths as individual indicators: a reappraisal of the link between fish physiology and otolith characteristics. Mar Freshw Res 67:881–888

Guillaud A, Benzinou A, Troadec H, Rodin V, Bihan JL (2002a) Autonomous agents for edge detection and continuity perception on otolith images. Image Vis Comput 20:955–968

Guillaud A, Troadec H, Benzinou A, Le Bihan J, Rodin V (2002b) A multiagent system for edge detection and continuity perception on fish otolith images. EURASIP J Adv Signal Process 2002:756043

Hamrin SF, Arneri E, Doering-Arjes P, Mosegaard H and others (1999) A new method for three-dimensional otolith analysis. J Fish Biol 54:223–225

Healey B, Mahe K, Cossitt G, Dufour JL and others (2011) Age determination of Atlantic cod *Gadus morhua*: results from an otolith exchange between Canada and France. Tech Rep Can Sci Advis Sec Res Doc 2011/015. http://archimer.ifremer.fr/doc/00035/14627/ (accessed 26 April 2018)

Hüssy K, Mosegaard H (2004) Atlantic cod (*Gadus morhua*) growth and otolith accretion characteristics modelled in a bioenergetics context. Can J Fish Aquat Sci 61:1021–1030

Hüssy K, Radtke K, Plikshs M, Oeberst R and others (2016a) Challenging ICES age estimation protocols: lessons learned from the eastern Baltic cod stock. ICES J Mar Sci 73:2138–2149

Hüssy K, Mosegaard H, Albertsen CM, Nielsen EE, Hemmer-Hansen J, Eero M (2016b) Evaluation of otolith shape as a tool for stock discrimination in marine fishes using Baltic Sea cod as a case study. Fish Res 174:210–218

Jolivet A, Bardeau JF, Fablet R, Paulet YM, de Pontual H (2008) Understanding otolith biomineralization processes: new insights into microscale spatial distribution of organic and mineral fractions from Raman microspectrometry. Anal Bioanal Chem 392:551–560

Jolivet A, Bardeau JF, Fablet R, Paulet YM, de Pontual H (2013) How do the organic and mineral fractions drive the opacity of fish otoliths? Insights using Raman microspectrometry. Can J Fish Aquat Sci 70:711–719

Kalish JM, Beamish RJ, Brothers EB, Casselman JM and others (1995) Glossary for otolith studies. In: Secor DH, Dean JM, Campana SE (eds) Recent developments in fish otolith research. University of South Carolina Press, Columbia, SC, p 723–729. http://horizon.documentation.ird.fr/exl-doc/pleins_textes/pleins_textes_6/b_fdi_35-36/42209.pdf (accessed 26 April 2018)

King AE (1993) Determination of bank rockfish age and growth: a comparison of traditional and computer-aided techniques. MSc thesis, San Jose State University, San Jose, CA. http://scholarworks.sjsu.edu/etd_theses/687/ (accessed Sep 25, 2013)

Lombarte A, Morales-Nin B (1995) Morphology and ultrastructure of saccular otoliths from five species of the genus *Coelorinchus* (Gadiformes: Macrouridae) from the Southeast Atlantic. J Morphol 225:179–192

Lombarte A, Chic Ò, Parisi-Baradad V, Olivella R, Piera J, García-Ladona E (2006) A web-based environment for shape analysis of fish otoliths. The AFORO database. Sci Mar 70:147–152

Macy WI (1995) The application of digital image processing to aging of long-finned squid, *Loligo pealei*, using the statolith. In: Secor D, Dean J, Campana S (eds) Recent developments in fish otolith research. University of South Carolina Press, Columbia, SC, p 283–302

Mahé K (2009) Project no. 044132 Automated FISh Ageing (AFISA): final activity report. www.ices.dk/explore-us/projects/EU-RFP/EU%20Repository/AFISA/FP6%20AFISA%20Final%20Activity%20Report.pdf (accessed 26 April 2018)

Mahé K, Fave S, Couteau J (2011) TNPC User guide. http://archimer.ifremer.fr/doc/00032/14288/ (accessed 26 April 2018)

Mahé K, Aumond Y, Rabhi K, Elleboode R and others (2017) Relationship between somatic growth and otolith growth: a case study of the ornate jobfish *Pristipomoides argyrogrammicus* from the coast of Réunion (SW Indian Ocean), Afr J Mar Sci 39:145–151

Mapp JJI, Fisher MH, Atwood RC, Bell GD, Greco MK, Songer S, Hunter E (2016) Three-dimensional rendering of otolith growth using phase contrast synchrotron tomography. J Fish Biol 88:2075–2080

Matic-Skoko S, Ferri J, Skeljo F, Bartulovic V, Glavic K, Glamuzina B (2011) Age, growth and validation of otolith morphometrics as predictors of age in the forkbeard, *Phycis phycis* (Gadidae). Fish Res 112:52–58

McGowen M, Prince E, Lee D (1987) An inexpensive micro-

computer-based system for making rapid and precise counts and measurements of zonations in video displayed skeletal structures of fish. In: Summerfelt R, Hall G (eds) Age and growth of fish. Iowa State University Press, Ames, IA, p 385–395

Mendoza RR (2006) Otoliths and their applications in fishery science. Ribarstvo 64:89–102

Messieh SN (1972) Use of otoliths in identifying herring stocks in the southern Gulf of St. Lawrence and adjacent waters. J Fish Res Board Can 29:1113–1118

Messieh S, McDougall C (1985) A computer based method for separating herring spawning groups using digitized otolith morphometrics. Can Atl Fish Sci Advis Comm (CAFSAC) Res Doc 85/106

Methot RD Jr (1981) Spatial covariation of daily growth rates of larval northern anchovy, (*Engraulis mordax*), and northern lampfish, (*Stenobrachius leucopsarus*). Rapp P-V Reun Cons Int Explor Mer 178:424–431

Mille T, Mahé K, Cachera M, Villanueva M, de Pontual H, Ernande B (2016) Diet is correlated with otolith shape in marine fish. Mar Ecol Prog Ser 555:167–184

Miller J, Simenstead C (1994) Otolith microstructure preparation, analysis and interpretation: procedures for a potential habitat assessment methodology. Fish Res Inst Tech Rep FRI-UW-9406. School of Fisheries, University of Washington, Seattle, WA

Millner R, Pilling G, McCully S, Høie H (2011) Changes in the timing of otolith zone formation in North Sea cod from otolith records: an early indicator of climate-induced temperature stress? Mar Biol 158:21–30

Moksness E (2000) FAIR-CT 96.1304 European Fish Aging Network (EFAN): final report. ftp://ftp.imr.no/tobi/Efan/ (accessed 26 April 2018)

Morales-Nin B, Geffen AJ (2015) The use of calcified tissues as tools to support management: the view from the 5th International Otolith Symposium. ICES J Mar Sci 72: 2073–2078

Morales-Nin B, Panfili J (2002) Sclerochronological studies: age estimation. In: Panfili J, de Pontual H, Troadec H, Wright P (eds) Manual of fish sclerochronology. IFREMER-IRD, Brest, p 91–98

Morales-Nin B, Lombarte A, Japòn B (1998) Approaches to otolith age determination: image signal treatment and age attribution. Sci Mar 62:247–256

Morison A, Robertson S, Smith D (1998) An integrated system for production fish aging: image analysis and quality assurance. N Am J Fish Manage 18:587–598

Morison AK, Burnett J, McCurdy WJ, Moksness E (2005) Quality issues in the use of otoliths for fish age estimation. Mar Freshw Res 56:773–782

Morrongiello JR, Thresher RE, Smith DC (2012) Aquatic biochronologies and climate change. Nat Clim Change 2:849–857

Neat F, Wright P, Fryer R (2008) Temperature effects on otolith pattern formation in Atlantic cod *Gadus morhua*. J Fish Biol 73:2527–2541

Palmer M, Àlvarez A, Tomàs J, Morales-Nin B (2005) A new method for robust feature extraction of otolith growth marks using fingerprint recognition methods. Mar Freshw Res 56:791–794

Panfili J, Ximenes MC, Do Chi T (1990) Age determination of eels in the French Mediterranean lagoons using classical methods and an image analysis system. Int Rev Gesamten Hydrobiol Hydrograph 75:745–754

Panfili J, de Pontual H, Troadec H, Wright P (eds) (2002) Manual of fish sclerochronology. Ifremer-IRD, Brest

Parisi-Baradad V, Manjabacas A, Lombarte A, Olivella R, Chic Ò, Piera J, García-Ladona E (2010) Automated taxon identification of teleost fishes using an otolith online database AFORO. Fish Res 105:13–20

Popper A, Hoxter B (1981) The fine structure of the sacculus and lagena of a teleost fish. Hear Res 5:245–263

Popper A, Lu Z (2000) Structure–function relationships in fish otolith organs. Fish Res 5:245–263

Popper AN, Ramcharitar J, Campana SE (2005) Why otoliths? Insights from inner ear physiology and fisheries biology. Mar Freshw Res 56:497–504

Ricker W (1975) Computation and interpretation of biological statistics of fish populations. Bull Fish Res Board Can 191:382

Robertson SG, Morison AK (1999) A trial of artificial neural networks for automatically estimating the age of fish. Mar Freshw Res 50:73–82

Robertson S, Morison A (2001) Development of an artificial neural network for automated age estimation. Tech Rep 98/105. Marine and Freshwater Resources Institute

Rodin V, Troadec H, de Pontual H, Benzinou A, Tisseau J, Le Bihan J (1996) Growth ring detection on fish otoliths by a graph construction. In: Proc IEEE Int Conf Image Processing, Vol 2, p 685–688

Rypel A (2008) An inexpensive image analysis system for fish otoliths. N Am J Fish Manage 28:193–197

Schmidt W (1969) The otoliths as a means for differentiation between species of fish of very similar appearance. In: Proc Symp Oceanogr Fish Resour Trop Atlantic, p 393–396

Schulz-Mirbach T, Ladich F, Plath M, Hess M (2015) The role of otolith size in hearing – insights from cichlid fishes. Front Mar Sci 34

Sethian J (1996) Level set methods. Cambridge University Press, Cambridge

Small G, Hirschhorn G (1987) Computer-assisted age and growth pattern recognition of fish scales using a digitizing tablet. In: Summerfelt G (ed) Age and growth of fish. Iowa State University Press, Ames, IA, p 397–410

Smith J (2014) Age validation of lemon sole (*Microstomus kitt*), using marginal increment analysis. Fish Res 157: 41–46

Smith SJ, Campana SE (2010) Integrated stock mixture analysis for continous and categorical data, with application to genetic–otolith combinations. Can J Fish Aquat Sci 67:1533–1548

Smolinski S, Mirny Z (2017) Otolith biochronology as an indicator of marine fish responses to hydroclimatic conditions and ecosystem regime shifts. Ecol Indic 79: 286–294

Sonka M, Hlavac V, Boyle R (2008) Image processing, analysis and machine vision, 3rd edn. Cengage Learning, Stamford, CT

Sória Pérez JA (2012) On the automatic detection of otolith features for fish species identification and their age estimation. PhD thesis, Universitat Politècnica de Catalunya, Barcelona

Sturrock AM, Trueman CN, Darnaude AM, Hunter E (2012) Can otolith elemental chemistry retrospectively track migrations in fully marine fishes? J Fish Biol 81:766–795

Sturrock AM, Hunter E, Milton JA, EIMF, Johnson RC, Waring CP, Trueman CN (2015) Quantifying physiological influences on otolith microchemistry. Methods Ecol Evol 6:806–816

Takashima Y, Takada T, Matsuishi T, Kanno Y (2000) Validation of auto-counting method by NIH image using otoliths of white-spotted char *Salvelinus leucomaenis*. Fish Sci 66:515–520

Troadec H (1991) Frequency demodulation on otolith numerical images for the automation of fish age estimation. Aquat Living Resour 4:207–219

Troadec H, Benzinou A (2002) Computer-assisted age estimation. In: Panfili J, de Pontual H, Troadec H, Wright P (eds) Manual of fish sclerochronology. Ifremer-IRD, Brest, p 199–241

Troadec H, Benzinou A, Rodin V, Bihan JL (2000) Use of deformable templates for otolith 2D growth ring detection by digital image processing. Fish Res 46:155–163

Vischer N, Nastase S (2015) ObjectJ otolith and tree ring counter. https://sils.fnwi.uva.nl/bcb/objectj/examples/TreeRings/TreeRings-9.htm

Welch TJ, van den Avyle MJ, Betsill RK, Driebe EM (1993) Precision and relative accuracy of striped bass age estimates from otoliths, scales, and anal fin rays and spines. N Am J Fish Manage 13:616–620

Welleman H, Storbeck F (1995) Automatic ageing of plaice (*Pleuronectes platessa* L.) otoliths by means of image analysis. In: Secor D, Dean J, Campana S (eds) Recent developments in fish otolith research. University of South Carolina Press, Columbia, SC, p 271–282

Whitman G, Johnson RC (2016) Imaging of otoliths for analysis of fish age and growth: a guide for measuring daily increments in adult and juvenile otoliths using Image-Pro Premier ®, University of California Davis, Center for Watershed Sciences. www.barnett-johnson.com/uploads/1/9/9/0/1990941/increment_measurement_sop_v2.0_final.pdf (accessed 27 April 2018)

Williams T, Bedford B (1974) The use of otoliths for age determination. In: Bagenal T (ed) The ageing of fish. Unwin Brothers, Surrey, p 114–123

Williams AJ, Newman SJ, Wakefield CB, Bunel M, Halafihi T, Kaltavara J, Nicol SJ (2015) Evaluating the performance of otolith morphometrics in deriving age compositions and mortality rates for assessment of data-poor tropical fisheries. ICES J Mar Sci 72:2098–2109

Yaragina NA, Nedreaas KH, Koloskova VP, Mjanger H, Senneset H, Zuykova NV, Gotnes P (2009) Fifteen years of annual Norwegian–Russian cod comparative age readings. Mar Biol Res 5:54–65

Zhu X, Wastle RJ, Howland KL, Leonard DJ, Mann S, Carmichael TJ, Tallman RF (2015) A comparison of three anatomical structures for estimating age in a slow-growing subarctic population of lake whitefish. N Am J Fish Manage 35:262–270

Editorial responsibility: Stylianos Somarakis, Heraklion, Greece

Submitted: June 28, 2017; Accepted: February 14, 2018
Proofs received from author(s): April 27, 2018

Vol. 598: 233–245, 2018
https://doi.org/10.3354/meps12223

MARINE ECOLOGY PROGRESS SERIES
Mar Ecol Prog Ser

Published June 28[§]

Contribution to the Theme Section 'Innovative use of sclerochronology in marine resource management'

Facultative oligohaline habitat use in a mobile fish inferred from scale chemistry

M. E. Seeley[1], B. D. Walther[2,*]

[1]University of Texas at Austin, Marine Science Institute, Port Aransas, Texas 78373, USA
[2]Texas A&M University–Corpus Christi, Corpus Christi, Texas 78412, USA

ABSTRACT: Reconstructing fish movements is critical to understand the diversity of habitats required to sustain mobile species. Chemical constituents in otoliths have been invaluable for the field of fish migration ecology to track natal origins and reconstruct lifetime movement patterns. However, alternative non-lethal structures, such as scales, are preferred for imperiled species to avoid mortality. We analyzed 29 individual scales from highly migratory and vulnerable Atlantic tarpon *Megalops atlanticus* (hereafter referred to as tarpon) in the Gulf of Mexico to identify migrations across salinity gradients and associated trophic shifts using paired measurements of elemental (Sr/Ca) and isotopic ($\delta^{13}C$ and $\delta^{15}N$) proxies. Although tarpon can inhabit freshwater, the specific patterns of facultative oligohaline habitat use are unknown. Individual scale-based salinity and diet histories were highly variable, with 4 contingents identified depending on the presence and sequence of movements. Scale salinity proxies (Sr/Ca and $\delta^{13}C$) indicated that tarpon spent on average 42 ± 34% of their scale-based life histories within oligohaline habitats. Transhaline movements were accompanied by shifts in $\delta^{15}N$ that indicated putative trophic shifts between marine or estuarine and oligohaline food webs. Oligohaline habitat use is common yet individually facultative for tarpon. This information is critical to devise sustainable fisheries management plans that account for the full range of diverse habitats used by this species throughout its life. Chemical analyses of scales have the potential to be broadly informative about migrations and trophic interactions in species where lethal methods must be avoided.

KEY WORDS: Migration · Scales · Elements · Stable isotopes · *Megalops atlanticus* · Contingents

INTRODUCTION

> 'There is considerable movement in and out of streams by these fishes. If there is any regularity to it we have not been able to determine such.'
>
> Breder (1944), p. 233

Migration allows species to increase fitness by seeking out optimal environments for growth and reproduction at different life history stages (Dingle & Drake 2007). While migratory movements can be obligate, a growing number of species are now recognized to have subgroups, or contingents, that display distinct migratory behaviors. This diversity includes partial migration, wherein one contingent displays migratory behavior while another contingent is resident (Chapman et al. 2011, 2012) and differential migration, wherein migratory behaviors diverge among life history stages or sexes (Terrill & Able 1988). These contingents themselves may be obligate or facultative. Such intraspecific diversity in migratory behavior may confer resilience to the population in the face of environmental variability (Secor 1999, Kerr et al. 2010). As a result, species with intraspecific migratory diversity may respond differently to altered fitness landscapes induced by human activities, including habitat loss, altered environmental conditions, and fisheries harvest. Further, quantifying whether and to what extent facultative migrations in predators

*Corresponding author: benjamin.walther@tamucc.edu

[§]Advance View was available online September 5, 2017

Publisher: Inter-Research · www.int-res.com

occur is an important step towards understanding the relative impact of transient predators to local food webs (Bond et al. 2015). In addition, understanding variable habitat use by highly migratory fishes is an essential prerequisite for effective spatially explicit management and conservation (Hobson 1999). However, the degree to which movements are obligate or facultative and the specific patterns of habitat use for many mobile taxa are unknown.

There are a range of potential tools available to characterize movement and habitat use in mobile fishes, each of which has inherent advantages and limitations. Acoustic and satellite tagging have the potential to reveal high-resolution information about movements and environmental parameters experienced by the individual; however, tag size, receiver array coverage, and battery life limit the life history stages with which tags can be used and the duration and spatial extent of collected data (Bégout et al. 2016, Schaefer & Fuller 2016). In recent decades, the use of otolith chemistry has grown as a powerful method that can provide lifelong records of environmental and habitat use histories, particularly for fishes that traverse significant chemical gradients, such as diadromous taxa (Campana & Thorrold 2001, Elsdon et al. 2008, Walther & Limburg 2012). An inevitable disadvantage of otolith analysis is lethal sampling, which renders it unsuitable for use with imperiled species where mortality must be minimized or avoided completely. For this reason, interest in the use of non-lethal otolith 'analogues' has grown considerably in recent years.

Researchers have capitalized on both stable isotope ratios and elemental markers in fish scales to reconstruct diet and habitat histories in a wide range of taxa (Seeley et al. 2015, Tzadik et al. 2017). Scales share many properties with otoliths that allow them to be used as a non-lethal analogue. Both structures have incremental growth and incorporate chemical constituents from the surrounding environment and diet (Wells et al. 2000, Holá et al. 2011). Scales have a bipartite architecture composed of an external layer underlain by a basal plate. The external layer is well calcified and can be assayed for proxies such as Sr/Ca, while the basal plate is a hydroxyapatite matrix that can be assayed for stable isotope values such as $\delta^{13}C$ and $\delta^{15}N$ (Seeley et al. 2015). Although both types of proxies can be successfully obtained from scales, few studies combine stable isotope and elemental assays due in part to size and architectural limitations that render it difficult to extract time series of both types of proxies from individual scales (Hutchinson & Trueman 2006, Trueman & Moore 2007). However, for species with sufficiently large scales that allow subsampling from interior scale increments and which are less subject to increment underplating that causes bias in isotope values, paired elemental and isotopic measurements across individual scales are possible (Woodcock & Walther 2014).

We applied paired assays of stable isotope ratios and elemental values in scales to infer migratory movements and dietary histories of Atlantic tarpon *Megalops atlanticus* (hereafter referred to as tarpon). Tarpon are highly migratory euryhaline predators that inhabit subtropical to tropical waters throughout the Atlantic Ocean (Ault et al. 2008). Their ability to tolerate a wide range of salinities, temperatures, and dissolved oxygen concentrations allow them to occupy diverse coastal, estuarine, and freshwater habitats over the course of their lives (Harrington 1958, Crabtree et al. 1995, Luo et al. 2008). Tarpon are generalist feeders, and juveniles inhabiting coastal, estuarine, and riverine habitats consume diverse prey items, including copepods, fishes, and terrestrial insects (Jud et al. 2011). Tarpon are thought to inhabit estuarine and oligohaline habitats primarily during juvenile phases, although migrations into rivers have been observed in older individuals (Luo et al. 2008). The duration and frequency of migrations across these salinity gradients into oligohaline habitats at different life stages are not well known. Characterizing the degree of facultative use of oligohaline habitats is critical to devise effective management strategies that account for all required habitats that support different life history stages of tarpon, which are currently listed as 'Vulnerable' by the IUCN (Adams et al. 2014).

A few studies have investigated the ability of chemical proxies in structures such as otoliths to reveal tarpon migrations across salinity gradients (Brown & Severin 2007, Rohtla & Vetemaa 2016). However, because of their Vulnerable status, a non-lethal examination of scale chemistry is preferable to otoliths in this species. Tarpon scales are particularly suitable as an otolith analogue because their size (>6 cm diameter in mature fish) enables detailed chemical analyses (Harrington 1958). This size allows subsampling of interior increments for stable isotope values across scales as well as paired laser ablation analysis of the exterior calcified surface layer of the same scale. While discrete paired subsample analyses of tarpon scales have suggested individually diverse migratory and trophic interactions (Woodcock & Walther 2014), a recently developed cross-sectional laser ablation technique for obtaining con-

tinuous elemental transects in these large scales allows more detailed assessments of migratory histories (Seeley et al. 2015). A paired analysis approach therefore allows putative dietary and migratory histories to be reconstructed for individual fish, providing significant insight into life history variability, facultative habitat use, and trophic interactions.

The aims of this study were to use isotopic and elemental signatures in tarpon scales to: (1) identify migratory contingents and lifetime patterns of oligohaline habitat use; and (2) assess whether movements across salinity gradients are accompanied by shifts in food web interactions. Together, these analyses provide novel insight into the migratory behavior and trophic structure of these imperiled fish.

MATERIALS AND METHODS

Scale collection and preparation

Tarpon scales were opportunistically collected along the Texas coast during fishing tournaments and from donations by local anglers. Scales were placed in water-resistant envelopes on which estimated length, weight, and capture location were recorded by anglers. From 2013 to 2015, scales were collected from 29 individual tarpon from 2 locations (Fig. 1). Collections occurred in Port Aransas (n = 7, with 2 collected in 2013, 4 in 2014, and 1 in 2015), Matagorda Bay (n = 22, with 9 in 2013 and 13 in 2014). Fish ranged from 0.91 to 90.72 kg and were considered sexually immature when <18.2 kg (n = 11) and sexually mature at >18.2 kg (n = 18) (Crabtree et al. 1997, Ault & Luo 2013). Scales were inspected under a microscope to ensure regular increments were present from the focus, or center of the scale, to the edge. Scales with disorganized interiors that lacked increments for a portion of scale growth were taken to be indicative of regenerated scales, and these were excluded from further analyses (Seeley et al. 2017).

Scale preparation for elemental analysis followed established methods. Methods for removing sequential subsamples for isotope analyses are detailed in Woodcock & Walther (2014) and methods and diagrams detailing the cross-sectional laser ablation approach are described in Seeley et al. (2015). Methods and diagrams describing stable isotope subsampling and cross-sectioning for laser ablation are further elaborated on in Seeley et al. (2017). Briefly, a rectangle containing all increments from the focus to the edge of each scale was excised and embedded in epoxy. This rectangle was cross-sectioned to expose a smooth plane of the surficial calcified external layer, which was targeted for laser ablation inductively coupled plasma mass spectrometry (ICP-MS). Thus, continuous ICP-MS transects from focus to edge in the surficial calcified external layer were obtained for each scale. In addition, subsamples 0.5–2.0 mg in mass were removed from the focus to the edge of each scale from an alternative transect offset radially approximately 90° from the rectangle removed for ICP-MS analyses. Dimensions of subsamples were chosen to obtain sufficient material per subsample for reliable analyses on an isotope ratio mass spectrometer. A total of 2–10 subsamples were removed per scale depending on scale diameter. Samples were spaced regularly across increments unless laser ablation elemental analyses indicated a major transition in Sr/Ca values occurred at a known location on the scale. Where such major elemental transitions were identified, scale subsamples were chosen to bracket the elemental shift to determine whether isotope shifts were concurrent. Each of these subsamples was analyzed separately with isotope ratio mass spectrometry (IR-MS) to obtain individual time series of $\delta^{13}C$ and $\delta^{15}N$ values that corresponded to the same time series obtained for elemental ratios via ICP-MS for each scale.

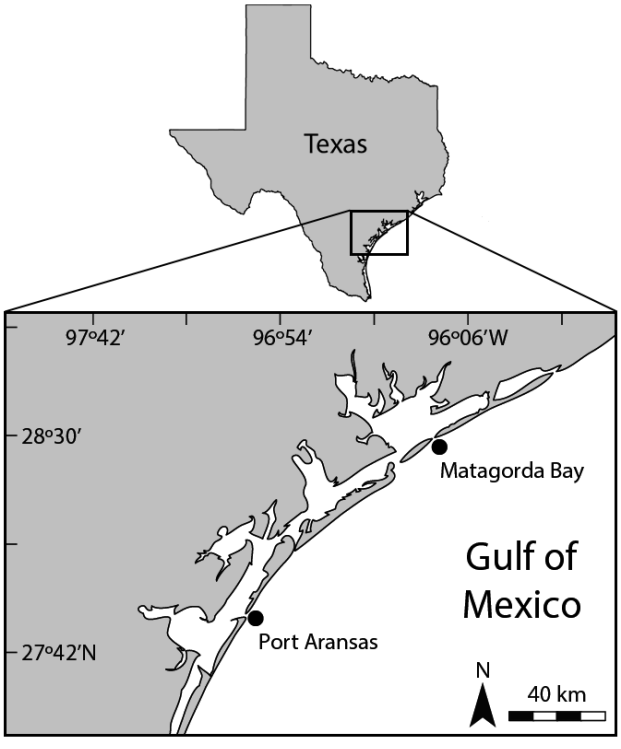

Fig. 1. Collection locations where scales were removed from wild tarpon (Matagorda Bay and Port Aransas)

Elemental analyses

Scale analyses using ICP-MS were conducted at the Jackson School of Geosciences at the University of Texas with a New Wave Research UP193-FX fast excimer 193-nm-wavelength laser system coupled to an Agilent 7500ce ICP-MS to quantify ^{43}Ca and ^{88}Sr. Preablation was conducted on all samples to remove any potential surface contaminants. Scales were ablated from the focus to edge within the calcified external layer following the methods outlined by Seeley et al. (2015). The laser ablation speed was 25 µm s^{-1}, the laser spot diameter was 25 µm, the power was 30%, and the repetition rate was 10 Hz. The laser spot diameter was chosen so that transects from focus to edge could be completely contained within the exterior calcified layer of cross-sectioned scales. Laser energy densities (fluences) obtained for the analytical session ranged from 2.5 to 3.25 J cm^{-2}. Certified reference materials NIST 612, NIST 610, and MAPS4 bracketed scale runs, while ^{43}Ca was used as an internal standard assuming a concentration of 39.89% Ca in the sampled outer calcium phosphate layer, corresponding to an assumed composition of $Ca_{10}(PO_4)_6(OH)_2$. Analyses took place over 2 sessions in 2015. In spring 2015, the percent residual standard deviations (RSDs) for Sr were 2.13% and 2.32% for NIST 612 and 610 against MAPS4, respectively. In fall 2015, the RSDs for Sr were 4.51% and 6.67% for NIST 612 and 610 against MAPS4, respectively.

Occasionally, high magnitude Sr counts were observed on individual transects. These points occurred because the laser spot drifted out of the external layer and into the epoxy, or due to major cracks in the scale. Laser transect misplacement and cracks in the scale were confirmed visually by microscope subsequent to analytical sessions, and where confirmed, these sections of the elemental transects were removed and data were linearly interpolated to replace these missing portions of individual transects.

Stable isotope analyses

Analyses of $\delta^{13}C$ and $\delta^{15}N$ values from scale subsamples were conducted twice in 2015. Each subsample was encapsulated in tin and analyzed at the University of California, Davis, Stable Isotope Facility using a PDZ Europa ANCA-GSL elemental analyzer interfaced to a PDZ Europa 20-20 isotope ratio mass spectrometer (Sercon). In the first sampling, samples were run against 4 reference materials (nylon: $\delta^{15}N$ = −10.31‰, $\delta^{13}C$ = −27.72‰; bovine liver: $\delta^{15}N$ = 7.72‰, $\delta^{13}C$ = −21.69‰; glutamic acid (USGS-41): $\delta^{15}N$ = 47.6‰, $\delta^{13}C$ = 37.63‰; and glutamic acid: N = 9.52%, $\delta^{15}N$ = −6.8‰, C = 40.81%, $\delta^{13}C$ = −16.65‰). In the second sampling, samples were run against 4 reference materials (nylon: $\delta^{15}N$ = −10.31‰, $\delta^{13}C$ = −27.72‰; bovine liver: $\delta^{15}N$ = 7.72‰, $\delta^{13}C$ = −21.69‰; glutamic acid: N = 9.52%, $\delta^{15}N$ = −6.8‰, C = 40.81%, $\delta^{13}C$ = −16.65‰; and enriched alanine: $\delta^{15}N$ = 41.13‰, $\delta^{13}C$ = 43.02‰). Scales were not decalcified prior to analysis as previous investigations found no significant effect of decalcification on isotope values in tarpon scales (Woodcock & Walther 2014).

Oligohaline threshold estimation

The proportion of dissolved ambient elemental concentrations in water that are taken up and incorporated into scales is defined by the partition coefficient D, calculated as $D_{Sr/Ca} = [(Sr/Ca)_{scale}] / [(Sr/Ca)_{water}]$ (Morse & Bender 1990). The $D_{Sr/Ca}$ can be used to estimate expected scale Sr/Ca values in oligohaline waters given measured Sr/Ca water values. To calculate the $D_{Sr/Ca}$, the exterior portion (last 1000 µm) of Sr/Ca transects in scales from the 22 fish captured in marine environments was averaged to represent expected scale Sr/Ca values in marine habitats and parameterize the numerator of the $D_{Sr/Ca}$ equation. Scales from fish captured in estuarine habitats or scales containing a major shift in Sr/Ca values within the exterior 1000 µm of their transects were excluded from this calculation. The denominator of the $D_{Sr/Ca}$ equation was parameterized with the globally homogeneous Sr/Ca value of 8.54 mmol mol^{-1} (de Villiers 1999). This value is stable in marine waters worldwide due to the large reservoir and long residence time (2–5 million yr) of Sr in the ocean (Banner 2004), and therefore a robust value to use as a marine endmember.

Mean values of Sr/Ca in the oligohaline (salinities of 0–5) portions of coastal streams and rivers in Texas have been analyzed by Walther & Nims (2015) and were used here to develop a threshold for expected scale Sr/Ca values for tarpon inhabiting oligohaline waters. Water Sr/Ca values reported by Walther & Nims (2015) were averaged, excluding reported values from water samples with salinities >5. This mean oligohaline endmember value was multiplied by the $D_{Sr/Ca}$ obtained above to calculate the expected scale Sr/Ca threshold value below which oligohaline residence was inferred, and is hereafter used as the mean threshold. To assess the robustness of this threshold to variations in the oligohaline endmember, a high threshold and a low threshold were calcu-

lated using the mean ± 1 SD of oligohaline Sr/Ca values reported by Walther & Nims (2015).

Statistics

Pair-wise comparisons between all 3 proxies ($\delta^{13}C$, $\delta^{15}N$, and Sr/Ca) were made to determine whether proxies co-varied in scales. Because Sr/Ca transects were continuous while isotope analyses were discrete, portions of each Sr/Ca transect covering the area encompassed by the isotope subsamples were averaged to obtain discrete Sr/Ca values that corresponded to comparable growth regions for each isotope subsample to allow pair-wise comparisons.

While some scales had up to 10 subsamples covering large ranges in elemental and isotope values, others had limited subsamples due to small-scale diameters and restricted proxy value ranges. Therefore, the effect of pooling multiple scales together was investigated. Pair-wise comparisons among proxies ($\delta^{13}C$ vs. $\delta^{15}N$, Sr/Ca vs. $\delta^{13}C$, and Sr/Ca vs. $\delta^{15}N$) were calculated, and 5 different scales with multiple subsamples and large proxy value ranges were selected to be used as individuals while the remaining 24 scales were pooled into a sixth 'mega-individual'. Analyses of covariance (ANCOVAs) were calculated for these 6 groups (5 individuals and 1 'mega-individual') and there were no significant differences in the interactions or slopes for Sr/Ca or $\delta^{13}C$ using either $\delta^{13}C$ or $\delta^{15}N$ ($p > 0.05$ for all) as a covariate. This comparison indicated that the relationships among proxies for the pooled 'mega-individual' were similar to individuals with robust subsample replication, thus justifying pooling subsamples among all scales for regression analyses. After pooling all subsamples together across all scales ($n = 29$), least squares linear regressions were then performed between $\delta^{15}N$ and $\delta^{13}C$, $\delta^{13}C$ and Sr/Ca, and $\delta^{15}N$ and Sr/Ca to determine relationships between the chemical tracers.

The proportion of continuous scale Sr/Ca transects spent below the thresholds, indicating oligohaline residence, were calculated for all fish in aggregate as well as separately for immature and mature tarpon. Significant shifts in scale Sr/Ca values across scale transects were identified by a regime-shift detection algorithm (Rodionov 2004). The algorithm was set with a 0.05 significance level, a minimum regime length of 1000 cells or approximately 5000 µm, and a Huber's weight parameter of 1. When adjacent points differed significantly based on the minimum specified regime length and predetermined significance level, a shift was identified and a new moving average was applied until the next shift occurred. Once the algorithm identified all shifts in a transect, mean values between shifts (regimes) were calculated. Each regime value was then compared with the calculated oligohaline thresholds to determine whether the regime was within oligohaline waters (at or below the threshold) or in meso-polyhaline waters (above the threshold). For the purposes of this study, meso-polyhaline water encompasses any salinity ranging from 5 to 30 regardless of being near shore, coastal, or offshore. The proportion of each transect spent below the threshold was then calculated for each scale. These calculations were made separately for each transect using the mean threshold as well as the high and low thresholds. Distributions of the individual shifts and transect proportions spent in oligohaline waters obtained based on the 3 different thresholds were compared to determine sensitivity of results to threshold selection.

Two metrics of shifts in $\delta^{13}C$ and $\delta^{15}N$ values for each scale transect were calculated. First, the total range in isotope ratios across each scale was obtained by subtracting the minimum from the maximum isotope value observed in each scale. This range reflected the maximal difference between observed isotope values among all subsamples from an individual scale. Second, the edge-minus-focus values were calculated to determine overall lifetime shifts in values from squamation to capture. These 2 metrics were compared to determine whether edge-minus-focus values adequately captured the overall lifetime shifts in isotope values. If total ranges and edge-minus-focus values were identical, then the difference between focus and edge values fully captured the range of isotope values observed across the life of the fish. However, if total ranges exceeded focus-minus-edge differences, this implied that an isotopic shift, perhaps reflective of mid-life migrations or diet shifts, occurred in the middle of the scale transect that exceeded lifetime ontogenetic shifts.

RESULTS

Proxies, partition coefficients, and thresholds

Least squares linear regressions yielded significant positive linear relationships ($p < 0.001$) for $\delta^{15}N$ vs. $\delta^{13}C$, $\delta^{13}C$ vs. Sr/Ca, and $\delta^{15}N$ vs. Sr/Ca (Fig. 2). The calculated Sr/Ca partition coefficient for all wild scales was $D_{Sr} = 0.27$. This value was then applied to the mean oligohaline water Sr/Ca concentrations of (mean ± SD) 5.23 ± 1.23 mmol mol^{-1} measured by

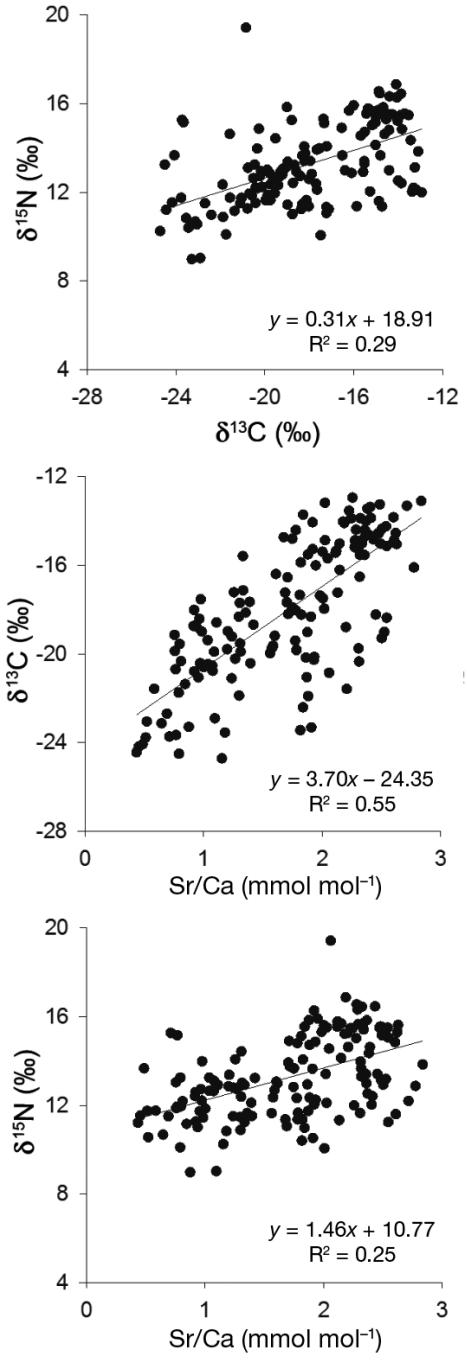

Fig. 2. Linear regressions showing the relationships between 3 chemical proxies in tarpon scales for salinity conditions (Sr/Ca, $\delta^{13}C$) and trophic dynamics ($\delta^{15}N$). Scale subsamples from all wild fish were pooled for these regressions

Walther & Nims (2015) to obtain scale Sr/Ca values corresponding to high, mean and low oligohaline thresholds in scales. Estimated Sr/Ca thresholds in scales were 1.7 mmol mol^{-1} (high threshold), 1.43 mmol mol^{-1} (mean threshold), and 1.10 mmol mol^{-1} (low threshold).

Table 1. Mean ± 1 SD proportions (%) of individual tarpon scale transects below low, mean, and high scale Sr/Ca oligohaline threshold levels for all fish, mature fish only, and immature fish only. These values indicate proportions of transects that are considered time spent in oligohaline waters

Category	N	Threshold		
		Low	Mean	High
All fish	29	27 ± 34	42 ± 34	54 ± 32
Mature	18	15 ± 21	30 ± 26	42 ± 26
Immature	11	46 ± 43	63 ± 38	73 ± 32

Elemental shifts

When considering all fish together, (mean ± SD) 42 ± 34% (n = 29) of scale transects were below the mean Sr/Ca oligohaline threshold. This indicated that many fish spent large portions of their lives in oligohaline waters, although there was considerable inter-individual variability in oligohaline use. When grouped by maturity and using the same mean oligohaline threshold, 30 ± 26% of scale transects from mature fish and 63 ± 38% of scale transects from immature fish were below the mean threshold, indicating that immature fish spent larger proportions of their lives in oligohaline waters. Oligohaline proportions based on high and low thresholds showed similar trends (Table 1), with immature fish spending higher proportions of their lives in oligohaline waters (73 ± 32% or 46 ± 43% using the high or low threshold, respectively) than mature fish (42 ± 26% or 15 ± 21% using the high or low threshold, respectively). Thus, although the absolute values differ, the trends in patterns of oligohaline habitat use are robust to the choice of thresholds examined here.

Examination of regime shifts within individual transects allowed classification of wild fish into 4 contingents based on the presence and sequence of movement into oligohaline waters as determined with the mean threshold. Fish were classified as non-migrant marine (n = 8), non-migrant oligohaline (n = 4), migrant oligohaline–marine (n = 12), or migrant marine–oligohaline–marine (n = 5) depending on whether fish moved into oligohaline waters and the sequence of movements (Fig. 3). Therefore, of the fish examined and excluding the non-migrant marine fish that never entered oligohaline waters, a remainder of 72% (n = 21) made use of oligohaline habitats to some degree during their lifetimes (Fig. 4). These classifications were made regardless of the timing of movements, so movements into oligohaline waters were subsequently examined to deter-

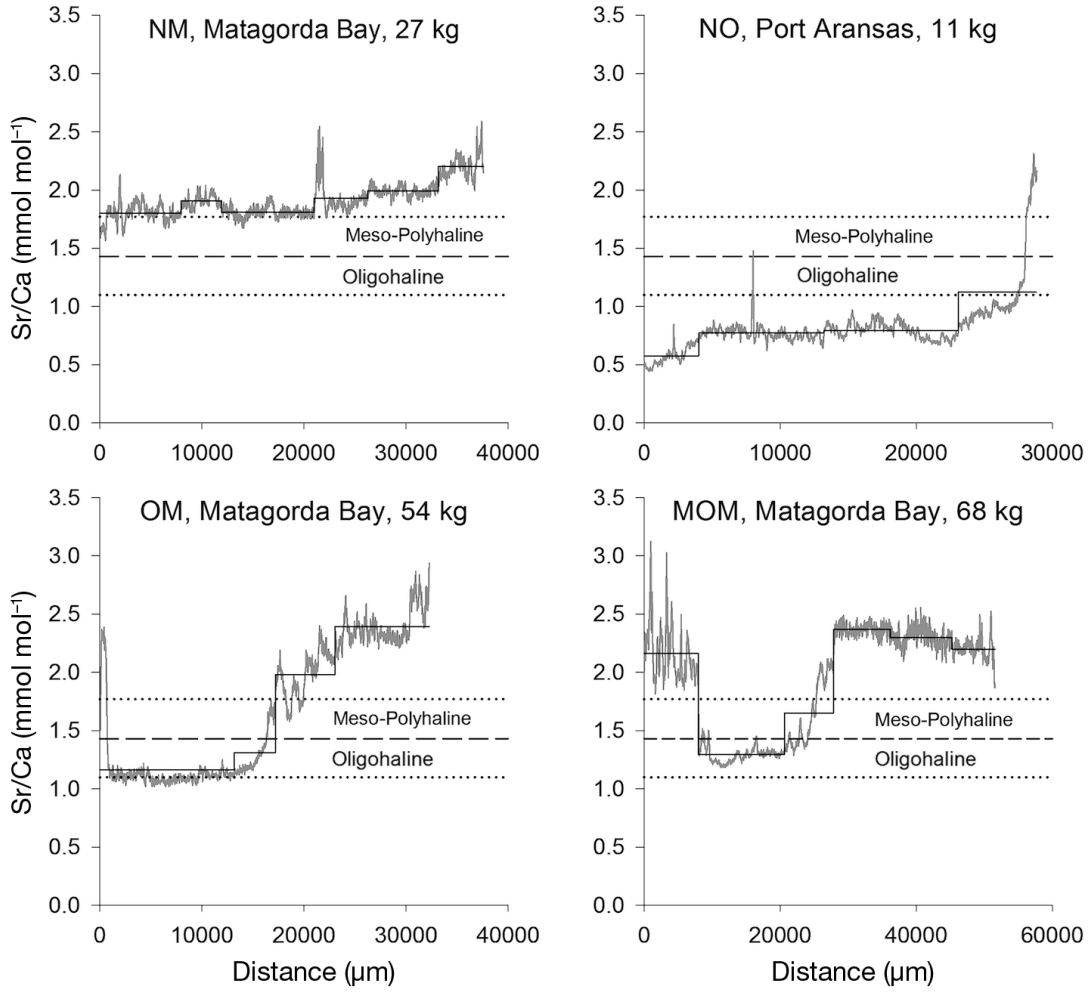

Fig. 3. Representative Sr/Ca scale transects of 4 wild fish (gray line) and major regime shifts (black line). The dashed line represents the mean oligohaline scale Sr/Ca threshold and the dotted lines represent the high and low thresholds. Values below the threshold are considered residence in oligohaline waters, while values above the threshold are considered residence in meso-polyhaline waters. Fish were classified as non-migrant marine (NM), non-migrant oligohaline (NO), migrant oligohaline–marine (OM), or migrant marine–oligohaline–marine (MOM). Capture locations and estimated fish mass are indicated over each transect

mine whether migratory shifts occurred early or late in the transect. Of the 17 fish whose Sr/Ca scale transects crossed the mean oligohaline threshold at some point, 16 of them crossed the threshold in the first 75% of their scale transects, while only 1 fish had a significant shift in the last 25% of their scale transects (Fig. 5).

Isotope shifts

Total ranges and edge-minus-focus values for $\delta^{13}C$ and $\delta^{15}N$ in wild fish were individually variable, although mean ranges and edge-minus-focus values were comparable for all fish and immature and mature fish considered separately (Table 2). Discrepancies between the 2 metrics were more pronounced

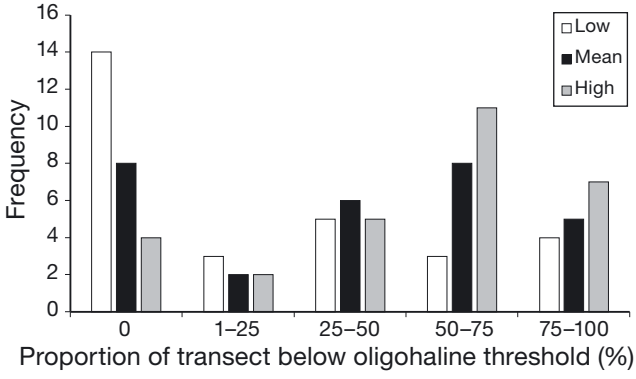

Fig. 4. Frequency of wild tarpon binned according to the proportion of their Sr/Ca scale transect that fell below an oligohaline threshold. Fish whose transect never fell below a threshold are indicated separately (0%). Histograms are shown for transects using low, mean, or high thresholds

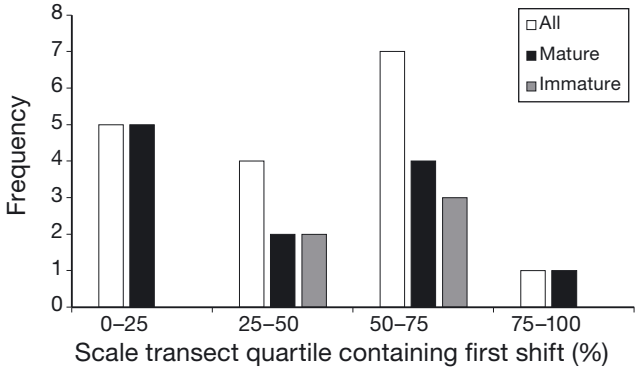

Fig. 5. Frequency of tarpon grouped according to whether their first significant shift in Sr/Ca across the mean oligohaline threshold occurred during the first, second, third, or fourth quartile of each transect. Fish whose transects never crossed the threshold are omitted. Histograms are shown for all fish pooled, and for mature and immature fish separately

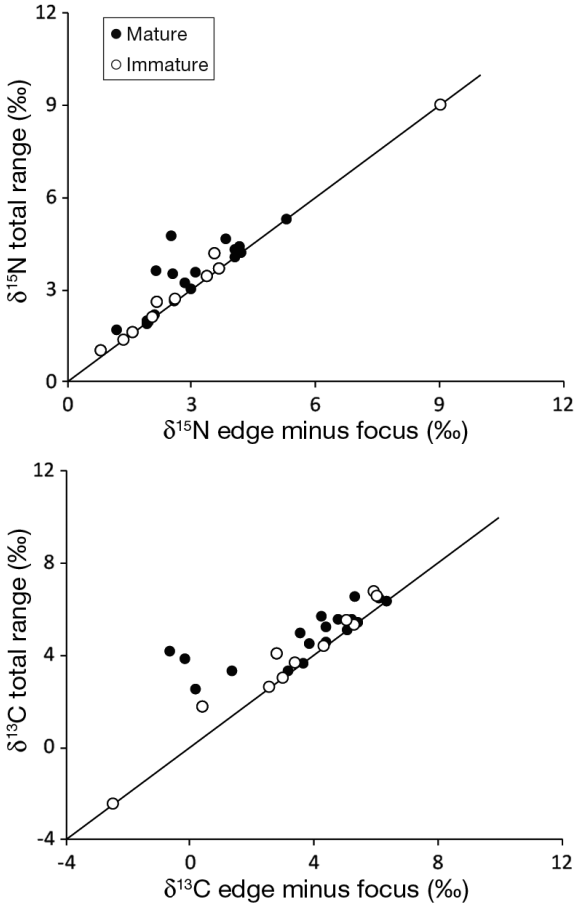

Fig. 6. Comparison between edge-minus-focus values and total range values of tarpon scale $\delta^{15}N$ and $\delta^{13}C$ stable isotope values for immature (open symbols) and mature (closed symbols) fish. The 1:1 relationship is indicated by the solid line

for mature fish, where total ranges occasionally exceeded focus-minus-edge differences (Fig. 6). This situation occurred when an older fish had more opportunity to move between oligohaline and meso-polyhaline waters and therefore likely exceed the expected ontogenetic changes in isotope values due to a mid-life migratory movement or diet shift.

DISCUSSION

This study used paired isotopic and elemental proxies in scales to reveal a wide range of variability in movements across salinity gradients in a highly mobile predatory fish. Although tarpon are known to be tolerant of low-salinity waters, the prevalence and extent of oligohaline habitat use has rarely been assessed. We found a high degree of individual variability in movements into low-salinity waters, including fish that never cross the threshold into oligohaline habitats and others that make extensive use of those same habitats. While oligohaline residence was more likely to occur early in life, it was not exclusively restricted to the early portions of the scale transects, and could occur at any point along a transect. Currently, scale increments in tarpon have not been validated for aging purposes, so absolute ages could not be assigned to these transitions. However, scale growth proceeds with age throughout the life of the fish, and thus the position of oligohaline shifts across transects is at least broadly informative of variable timings of these movements. Finally, movements into oligohaline waters were accompanied by shifts in $\delta^{15}N$ ratios, indicating coincident shifts in food web interactions that suggested fish relied on freshwater and terrestrial energy sources during transitory movements. This study highlights the utility of non-lethal sampling and chemical assays of scales in a highly mobile and vulnerable species.

Table 2. Differences in $\delta^{15}N$ and $\delta^{13}C$ values across tarpon scale transects. Mean ± SD values are shown for differences between focus and edge subsamples (edge values minus focus values) and total range (maximum minus minimum values) for all fish, mature fish, and immature fish

	N	$\delta^{15}N$ (‰)		$\delta^{13}C$ (‰)	
		Edge – focus	Total range	Edge – focus	Total range
All fish	29	3.02 ± 1.58	3.34 ± 1.59	3.54 ± 2.26	4.41 ± 1.88
Mature	18	3.08 ± 1.09	3.52 ± 1.08	3.67 ± 2.13	4.82 ± 1.17
Immature	11	2.93 ± 2.22	3.04 ± 2.22	3.32 ± 2.56	3.73 ± 2.60

Scale chemistry as an otolith analogue

The use of chemical markers in scales has a long history (reviewed by Seeley et al. 2015), although research on mobile fishes has been biased towards otolith analyses. This bias is largely due to architectural properties of otoliths that favor their use over other structures. Otoliths grow concentrically outward, meaning a sectioned plane can allow discrete sampling of specified growth regions with minimal mixing of subsequent increments using either probe-based (e.g. laser ablation; Fowler et al. 1995) or extraction methods (e.g. micromilling; Dufour et al. 2008). Scale architecture is more complex, with a concentrically growing calcified surficial layer and a poorly calcified basal plate. A number of researchers have therefore used top-down ablations of the external layer, either targeting a particular growth region, such as the focus for nursery signatures (Wells et al. 2003, Flem et al. 2005) and the edge for information just prior to capture (Woodcock et al. 2013, Ramsay et al. 2015), or transects across entire scales (Clarke et al. 2007, Borcherding et al. 2008). Because scales in many species are highly rugose and vary significantly in thickness from focus to edge, a top-down probe transect approach can be difficult with the lack of a smooth surface for assays and the depth of focus changes across increments. For this reason, some researchers have employed a sagittal cross-sectional approach that exposes the external layer with a flat surface of uniform thickness preferable for probe-based analyses (Courtemanche et al. 2006, Holá et al. 2011). Cross-sectioning is particularly important for elemental assays of tarpon scales, given their large size, high degree of surficial relief, and significant variation in thickness from focus to edge. We therefore developed a cross-sectional approach that allows continuous ablation from focus to edge and retains high-resolution information about life histories and potential migrations (Seeley et al. 2015).

In contrast to the external layer, growth of organic layers is not concentric, and new basal plates grow underneath previous layers (Trueman & Moore 2007). As a result, subsamples of interior portions of scales assayed for isotope ratio values will contain a mixture of old and new basal plate material, while subsamples from the leading edge of the scale will contain primarily new material (Hutchinson & Trueman 2006). This poses challenges for researchers seeking to reconstruct individual lifetime patterns of diet history because isotope ratio values from interior subsections will be biased towards values accreted later in life. As a result, many studies investigating stable isotope ratios in scales forego sequential subsampling of scales and simply analyze whole or pooled scales (Perga & Gerdeaux 2003, Johnson & Schindler 2012, Ramsay et al. 2012) or excise the most recent exterior region of scale growth to minimize underplating bias (MacKenzie et al. 2011, Cambiè et al. 2016). Although underplating occurs in all scales, the magnitude of resulting isotope bias depends on the relative thickness of recent underlying layers relative to older layers (Hutchinson & Trueman 2006). In addition, fish that cross major salinity gradients (reflected in $\delta^{13}C$) or switch between sufficiently different food webs or trophic positions (reflected in $\delta^{15}N$) may still result in detectable variation across increments that reflect movement and dietary histories despite underplating bias. Although the absolute magnitude of changes in isotope ratio values across increments may be averaged downwards due to underplating, patterns and timing of movements across isoscapes could still be resolved, and relative changes in isotope ratios can be considered a minimum estimate of endmember divergence.

The ability to assay elemental proxies for salinity, such as Sr/Ca in the external layer, which should not be subject to underplating bias, and isotope proxies for salinity, such as $\delta^{13}C$ in the basal plate in very large scales from tarpon, offers a unique opportunity to assess whether underplating bias precludes the use of interior increments for isotope ratio histories. Previous work on tarpon scales using discrete paired subsamples from interior and exterior increments of tarpon showed strong positive correlations between Sr/Ca and $\delta^{13}C$ values, reflecting simultaneous shifts in both proxies (Woodcock & Walther 2014). These positive correlations were confirmed in the present study, and such patterns were expected given that both dissolved ambient water Sr/Ca values and $\delta^{13}C$ ratios of particulate organic and inorganic matter increase with salinity in most systems (Fry 2002, Kaldy et al. 2005, Walther & Limburg 2012). For instance, in Texas freshwater, Sr/Ca endmembers are approximately 5.0 mmol mol^{-1} (Walther & Nims 2015), which is 3.5 mmol mol^{-1} below the globally homogeneous marine endmember of 8.5 mmol mol^{-1} (de Villiers 1999) and provides sufficient resolution to detect movement across salinity gradients in calcified structures. In addition, $\delta^{13}C$ values of particulate organic matter across San Antonio Bay increases from a freshwater endmember of −29‰ to a marine endmember of −21‰ (Bishop et al. 2017). As a result, the positive relationships between Sr/Ca and $\delta^{13}C$ values in scales suggest that both are valuable indicators of salinity history in tarpon, despite any underplating bias that

might be reducing the absolute magnitude of change that would be seen in scale $\delta^{13}C$ values in the absence of underplating. For this species, assays of interior scale increments appear to provide robust assessments of isotope-based salinity and dietary histories.

Atlantic tarpon migrations

Scale chemical transects in wild tarpon demonstrated substantial individual variability in oligohaline habitat use and confirmed that transhaline movements are not obligate but rather highly facultative for this species. The results presented in this work must be interpreted with caution given the relatively small sample size investigated (29 fish). However, even with this small sample size, this work demonstrated that movement patterns are highly variable among individuals and oligohaline residence is by no means uniform for this species. Although there has been consistent evidence that tarpon are found in fresh waters, direct quantification of the proportion of individuals using such habitats has rarely been estimated. Indeed, due to uncertainty about the facultative nature of freshwater habitat occupancy, this species has received a range of life history designations, including amphidromous, catadromous, and facultatively diadromous (reviewed by Rohtla & Vetemaa 2016). Evidence for euryhaline movements and oligohaline residence has come from a variety of sampling methods. Much of the early work on tarpon distribution and larval development noted that juvenile tarpon are regularly captured with traps, cast nets, and seines in low-salinity environments in locations such as Indian River, Florida (Harrington 1958), Seadrift, Texas (Marwitz 1986), and Lake Nicaragua and the Chagres River in Panama (Breder 1944). More recently, Luo et al. (2008) obtained high-resolution satellite-based geospatial data from pop-up archival transmitting (PAT) tags and derived a method to use the wet–dry sensor to estimate salinity histories to match movement tracks. In a field trial using a 50 kg tagged tarpon, the tag recorded movements into the St. Lucie River on the Atlantic coast of Florida where the tarpon resided at salinities from 2 to 10 for 9 continuous days. These data agree with the findings of the scale chemistry assays that oligohaline residence is not restricted to early juvenile life history stages.

There have been a small number of efforts to characterize migratory histories of tarpon using geochemical markers. To our knowledge, only 2 studies have used otolith chemistry for tarpon. Brown & Severin (2007) analyzed otoliths from tarpon collected in Lake Nicaragua and the Rio San Juan in Nicaragua (4 fish from each location), as well as 4 fish from the southern coastal region of Texas, similar to this study. Using a wavelength-dispersive electron microprobe to obtain 2-dimensional maps and focus-to-edge transects of Sr/Ca, they found 2 distinct patterns. For the Nicaraguan fish, Sr/Ca patterns indicated spawning and early life rearing in marine waters followed by subsequent movement into oligohaline waters later in life. For the Texas fish, the opposite pattern was observed, with oligohaline residence dominant early in life and movement towards marine habitats later in life. Although this preliminary assessment involved only 4 fish per sampling region, it offered an intriguing glimpse into the individually and geographically variable habitat use patterns. More recently, Rohtla & Vetemaa (2016) analyzed 37 otoliths from immature specimens obtained at a fish market in French Guiana and obtained Sr/Ca and Ba/Ca transects across otoliths. They found that movements were highly variable among individuals, with some recruiting to brackish waters and others to marine waters, and variable transhaline movements subsequently. Unlike the results reported here and by Brown & Severin (2007), Rohtla & Vetemaa (2016) report that only 8% of sampled individuals used fresh water during their lives. This may be due to regional differences in propensity for movement into rivers, or perhaps the degree of oligohaline habitat suitability in different parts of the world. Because of this individual variability, Rohtla & Vetemaa (2016) discourage the use of the terms catadromous or amphidromous and instead suggest the term 'euryhaline marine migrant' for tarpon. Our results support this conclusion, and note that caution must be taken when employing absolute life history designations in potentially facultative species (Secor & Kerr 2009).

The work presented here is the culmination of ongoing efforts to determine the ability of scale chemistry to reveal migratory and dietary markers in tarpon. In the first assessment of the potential of this method, Woodcock & Walther (2014) successfully used paired subsamples of increments across scales to retrieve both elemental and isotopic values from individual scales. Salinity histories (as indicated by Sr/Ca and $\delta^{13}C$) from fish captured along the Texas coast and Puerto Rico were not consistent, suggesting individual variability in habitat residence. Dietary histories (as indicated by $\delta^{15}N$) generally indicated ontogenetic increases in trophic position, although edge values of scales from Puerto Rican fish were lower than expected, suggesting that movements into

marine waters may have been accompanied by shifts in the isotopic baseline of $\delta^{15}N$ values. Subsequent to this work, Seeley et al. (2015) developed the cross-sectional approach to obtain high-resolution Sr/Ca histories, thereby opening the door for more robust assessments of transhaline movements in large scales. Further, Seeley et al. (2017) compared elemental and isotope ratio patterns across multiple scales from the same individual tarpon to determine consistency among scales. Patterns of both proxies were correlated and shifts were coincident among all non-regenerated scales in both wild fish and fish reared in captivity and constant salinity environments, indicating that scale choice would not bias interpretation of individual dietary and movement histories. Finally, the results here show the utility of applying scale chemistry proxies to reconstruct histories in wild fish.

A final insight provided by our scale chemistry analyses is variable dietary histories that accompanied migratory movements. Mobile fishes may participate in local food webs and thereby link disparate communities through predation and alter biodiversity, community stability, and energetic subsidies (Polis et al. 1997, Duffy et al. 2007). Alternatively, these immigrants may not rely heavily on local dietary items during transitory movements and therefore not provide significant food web linkages among habitats despite their presence. We found that $\delta^{15}N$ values in fish scales were tightly coupled to both Sr/Ca and $\delta^{13}C$ values, potentially suggesting that their diets shifted significantly when making migratory movements into different salinity regimes. Patterns in lifetime $\delta^{15}N$ values appeared to reflect changes in trophic position either with ontogeny or with movement between oligohaline and estuarine or marine waters. Baseline particulate organic matter $\delta^{15}N$ values in anthropogenically impacted Texas estuaries typically decrease with salinity by as much as 10–14‰ between freshwater and marine endmembers (Bishop et al. 2017). As a result, for tarpon that moved from fresh to marine waters, their scales would be expected to have inverse changes in $\delta^{15}N$ and $\delta^{13}C$ values given their inverse relationship in baseline values of each isotope ratio with salinity. However, $\delta^{15}N$ values were positively related to both Sr/Ca and $\delta^{13}C$ values, implying that movements into oligohaline waters were accompanied by decreases in $\delta^{15}N$ values, opposite of the trend expected if scale $\delta^{15}N$ values were driven by local baseline $\delta^{15}N$ values alone. One potential explanation for this discrepancy is that tarpon feed at different trophic positions in either oligohaline or estuarine and marine waters. This explanation is plausible given that tarpon are highly opportunistic feeders and are known to target low trophic position dietary items when inhabiting oligohaline waters as juveniles, including copepods, aquatic insects, terrestrial insects, and fly larvae (Jud et al. 2011). Importantly, shifts in $\delta^{15}N$ values coincided with shifts in $\delta^{13}C$ values regardless of whether those shifts occurred early or later in life, suggesting that tarpon shift diets to local food items, likely at different trophic levels, after a transhaline movement and therefore participate in local food webs. Tarpon are thus transient yet facultative predators that could have important yet currently unquantified effects on food web dynamics in oligohaline and freshwater environments.

This work demonstrates the broad potential of scales as alternatives to otoliths to provide important migration and dietary history information in migratory fishes. The coupled use of isotopic and elemental proxies yields novel information about individual variability and facultative habitat use in mobile predators. While the use of incremental subsampling is not necessarily transferrable to all taxa due to differences in scale size, we encourage continued exploration of the utility of scale chemistry in other species. Scale chemistry and other non-lethally sampled structures, such as fin rays, will be of particular utility for imperiled species that require detailed information about habitat requirements to develop spatially explicit management strategies that explicitly quantify the suite of habitats and rates of residency across life history stages. However, for imperiled species, mortality typically must be avoided and therefore otolith chemistry may be an impractical approach that necessitates the development of proxies in these alternative structures. The continued development and validation of isotopic and elemental proxies in scales is thus of great importance for conservation and management of vulnerable species.

Acknowledgements. The Saltwater Fisheries Enhancement Association, the Rotary Club of Corpus Christi Harvey Weil Sportsman Conservationist Award, and the Texas State Aquarium Wildlife Care, Conservation and Research Fund provided funding to B.D.W. for this project. Thanks to the Project Tarpon Tournament Series for donating scales and Marcus Poffenberger for providing opportunities to conduct fieldwork. Trace element analysis was conducted at Jackson School of Geosciences at the University of Texas at Austin with the help of N. Miller. Stable isotope analysis was conducted at the University of California Davis Stable Isotope Facility.

LITERATURE CITED

Adams AJ, Horodysky AZ, McBride RS, Guindon K and others (2014) Global conservation status and research needs

for tarpons (Megalopidae), ladyfishes (Elopidae) and bonefishes (Albulidae). Fish Fish 15:280–311

Ault JS, Luo J (2013) A reliable game fish weight estimation model for Atlantic tarpon (*Megalops atlanticus*). Fish Res 139:110–117

Ault JS, Humston R, Larkin MF, Perusquia E and others (2008) Population dynamics and resource ecology of Atlantic tarpon and bonefish. In: Ault JS (ed) Biology and management of the world tarpon and bonefish fisheries. CRC Press, Boca Raton, FL, 217–258

Banner JL (2004) Radiogenic isotopes: systematics and applications to earth surface processes and chemical stratigraphy. Earth Sci Rev 65:141–194

Bégout ML, Bau F, Acou A, Acolas ML (2016) Methodologies for investigating diadromous fish movements: conventional, PIT, acoustic and radio tagging and tracking. In: Morais P, Daverat F (eds) An introduction to fish migration. CRC Press, Boca Raton, FL, 214–250

Bishop KA, McClelland JW, Dunton KH (2017) Freshwater contributions and nitrogen sources in a south Texas estuarine ecosystem: a time-integrated perspective from stable isotopic ratios in the eastern oyster (*Crassostrea virginica*). Estuaries Coasts 40:1314–1324

Bond MH, Miller JA, Quinn TP (2015) Beyond dichotomous life histories in partially migrating populations: cessation of anadromy in a long-lived fish. Ecology 96:1899–1910

Borcherding J, Pickhardt C, Winter HV, Becker JS (2008) Migration history of North Sea houting (*Coregonus oxyrinchus* L.) caught in Lake IJsselmeer (The Netherlands) inferred from scale transects of ^{88}Sr:^{44}Ca ratios. Aquat Sci 70:47–56

Breder CM (1944) Materials for the study of the life history of *Tarpon atlanticus*. Zoologica 29:217–252

Brown RJ, Severin KP (2007) A preliminary otolith microchemical examination of the diadromous migrations of Atlantic tarpon *Megalops atlanticus*. In: Ault JS (ed) Biology and management of the world tarpon and bonefish fisheries. CRC Press, Boca Raton, FL, 259–274

Cambiè G, Kaiser MJ, Marriott AL, Fox J and others (2016) Stable isotope signatures reveal small-scale spatial separation in populations of European sea bass. Mar Ecol Prog Ser 546:213–223

Campana SE, Thorrold SR (2001) Otoliths, increments, and elements: keys to a comprehensive understanding of fish populations? Can J Fish Aquat Sci 58:30–38

Chapman BB, Brönmark C, Nilsson JÅ, Hansson LA (2011) The ecology and evolution of partial migration. Oikos 120:1764–1775

Chapman BB, Skov C, Hulthén K, Brodersen J, Nilsson PA, Hansson LA, Brönmark C (2012) Partial migration in fishes: definitions, methodologies and taxonomic distribution. J Fish Biol 81:479–499

Clarke AD, Telmer KH, Shrimpton JM (2007) Elemental analysis of otoliths, fin rays and scales: a comparison of bony structures to provide population and life-history information for the Arctic grayling (*Thymallus arcticus*). Ecol Freshwat Fish 16:354–361

Courtemanche DA, Whoriskey FG, Bujold V, Curry RA (2006) Assessing anadromy of brook char (*Salvelinus fontinalis*) using scale microchemistry. Can J Fish Aquat Sci 63:995–1006

Crabtree RE, Cyr EC, Dean JM (1995) Age and growth of tarpon, *Megalops atlanticus*, from south Florida waters. Fish Bull 93:619–628

Crabtree RE, Cyr EC, Chaverri DC, McLarney WO, Dean JM (1997) Reproduction of tarpon, *Megalops atlanticus*, from Florida and Costa Rican waters and notes on their age and growth. Bull Mar Sci 61:271–285

de Villiers S (1999) Seawater strontium and Sr/Ca variability in the Atlantic and Pacific oceans. Earth Planet Sci Lett 171:623–634

Dingle H, Drake VA (2007) What is migration? Bioscience 57:113–121

Duffy JE, Cardinale BJ, France KE, McIntyre PB, Thebault E, Loreau M (2007) The functional role of biodiversity in ecosystems: incorporating trophic complexity. Ecol Lett 10:522–538

Dufour E, Höök TO, Patterson WP, Rutherford ES (2008) High-resolution isotope analysis of young alewife *Alosa pseudoharengus* otoliths: assessment of temporal resolution and reconstruction of habitat occupancy and thermal history. J Fish Biol 73:2434–2451

Elsdon TS, Wells BK, Campana SE, Gillanders BM and others (2008) Otolith chemistry to describe movements and life-history parameters of fishes: hypotheses, assumptions, limitations and inferences. Oceanogr Mar Biol Annu Rev 46:297–330

Flem B, Moen V, Grimstvedt A (2005) Trace element analysis of scales from four populations of Norwegian Atlantic salmon (*Salmo salar* L.) for stock identification using laser ablation inductively coupled plasma mass spectrometry. Appl Spectrosc 59:245–251

Fowler AJ, Campana SE, Jones CM, Thorrold SR (1995) Experimental assessment of the effect of temperature and salinity on elemental composition of otoliths using laser ablation ICPMS. Can J Fish Aquat Sci 52:1431–1441

Fry B (2002) Conservative mixing of stable isotopes across estuarine salinity gradients: a conceptual framework for monitoring watershed influences on downstream fisheries production. Estuaries 25:264–271

Harrington RW (1958) Morphometry and ecology of small tarpon, *Megalops atlantica* Valenciennes from transitional stage through onset of scale formation. Copeia 1958:1–10

Hobson KA (1999) Tracing origins and migration of wildlife using stable isotopes: a review. Oecologia 120:314–326

Holá M, Kalvoda J, Nováková H, Škoda R, Kanický V (2011) Possibilities of LA-ICP-MS technique for the spatial elemental analysis of the recent fish scales: line scan vs. depth profiling. Appl Surf Sci 257:1932–1940

Hutchinson JJ, Trueman CN (2006) Stable isotope analyses of collagen in fish scales: limitations set by scale architecture. J Fish Biol 69:1874–1880

Johnson SP, Schindler DE (2012) Four decades of foraging history: stock-specific variation in the carbon and nitrogen stable isotope signatures of Alaskan sockeye salmon. Mar Ecol Prog Ser 460:155–167

Jud Z, Layman C, Shenker J (2011) Diet of age-0 tarpon (*Megalops atlanticus*) in anthropogenically-modified and natural nursery habitats along the Indian River Lagoon, Florida. Environ Biol Fishes 90:223–233

Kaldy JE, Cifuentes LA, Brock D (2005) Using stable isotope analyses to assess carbon dynamics in a shallow subtropical estuary. Estuaries 28:86–95

Kerr LA, Cadrin SX, Secor DH (2010) The role of spatial dynamics in the stability, resilience, and productivity of an estuarine fish population. Ecol Appl 20:497–507

Luo JG, Ault JS, Larkin MF, Barbieri LR (2008) Salinity measurements from pop-up archival transmitting (PAT) tags and their application to geolocation estimation for

Atlantic tarpon. Mar Ecol Prog Ser 357:101–109

MacKenzie KM, Palmer MR, Moore A, Ibbotson AT, Beaumont WRC, Poulter DJS, Trueman CN (2011) Locations of marine animals revealed by carbon isotopes. Sci Rep 1:21

Marwitz SR (1986) Young tarpon in a roadside ditch near Matagorda Bay in Calhoun County, Texas. Management Data Series Number 100. Texas Parks and Wildlife Department Coastal Fisheries Branch, Austin, TX

Morse JW, Bender ML (1990) Partition coefficients in calcite: examination of factors influencing the validity of experimental results and their application to natural systems. Chem Geol 82:265–277

Perga ME, Gerdeaux D (2003) Using the $\delta^{13}C$ and $\delta^{15}N$ of whitefish scales for retrospective ecological studies: changes in isotope signatures during the restoration of Lake Geneva, 1980–2001. J Fish Biol 63:1197–1207

Polis GA, Anderson WB, Holt RD (1997) Toward an integration of landscape and food web ecology: the dynamics of spatially subsidized food webs. Annu Rev Ecol Syst 28: 289–316

Ramsay A, Milner N, Hughes R, McCarthy I (2012) Fish scale $\delta^{15}N$ and $\delta^{13}C$ values provide biogeochemical tags of fish comparable in performance to element concentrations in scales and otoliths. Hydrobiologia 694:183–196

Ramsay AL, Hughes RN, Chenery SR, McCarthy ID (2015) Biogeochemical tags in fish: predicting spatial variations in strontium and manganese in *Salmo trutta* scales using stream water geochemistry. Can J Fish Aquat Sci 72: 422–433

Rodionov SN (2004) A sequential algorithm for testing climate regime shifts. Geophys Res Lett 31:L09204

Rohtla M, Vetemaa M (2016) Otolith chemistry chimes in: migratory environmental histories of Atlantic tarpon (*Megalops atlanticus*) caught from offshore waters of French Guiana. Environ Biol Fishes 99:593–602

Schaefer K, Fuller D (2016) Methodologies for investigating oceanodromous fish movements: archival and pop-up satellite archival tags. In: Morais P, Daverat F (eds) An introduction to fish migration. CRC Press, Boca Raton, FL, p 251–289

Secor DH (1999) Specifying divergent migrations in the concept of stock: the contingent hypothesis. Fish Res 43:13–34

Secor DH, Kerr LA (2009) Lexicon of life cycle diversity in diadromous and other fishes. Am Fish Soc Symp 69: 537–556

Seeley M, Miller N, Walther B (2015) High resolution profiles of elements in Atlantic tarpon (*Megalops atlanticus*) scales obtained via cross-sectioning and laser ablation ICP-MS: a literature survey and novel approach for scale analyses. Environ Biol Fishes 98:2223–2238

Seeley M, Logan WK, Walther B (2017) Consistency of elemental and isotope-ratio patterns across multiple scales from individual fish. J Fish Biol 91:928–946

Terrill SB, Able KP (1988) Bird migration terminology. Auk 105:205–206

Trueman CN, Moore A (2007) Use of the stable isotope composition of fish scales for monitoring aquatic ecosystems. In: Dawson TE, Siegwolf RTW (eds) Stable isotopes as indicators of ecological change. Academic Press, Burlington, VT

Tzadik OE, Curtis JS, Granneman JE, Kurth BN and others (2017) Chemical archives in fishes beyond otoliths: a review on the use of other body parts as chronological recorders of microchemical constituents for expanding interpretations of environmental, ecological, and life-history changes. Limnol Oceanogr Methods 15:238–263

Walther BD, Limburg KE (2012) The use of otolith chemistry to characterize diadromous migrations. J Fish Biol 81: 796–825

Walther B, Nims M (2015) Spatiotemporal variation of trace elements and stable isotopes in subtropical estuaries: I. Freshwater endmembers and mixing curves. Estuaries Coasts 38:754–768

Wells BK, Bath GE, Thorrold SR, Jones CM (2000) Incorporation of strontium, cadmium, and barium in juvenile spot (*Leiostomus xanthurus*) scales reflects water chemistry. Can J Fish Aquat Sci 57:2122–2129

Wells BK, Thorrold SR, Jones CM (2003) Stability of elemental signatures in the scales of spawning weakfish, *Cynoscion regalis*. Can J Fish Aquat Sci 60:361–369

Woodcock SH, Walther BD (2014) Trace elements and stable isotopes in Atlantic tarpon scales reveal movements across estuarine gradients. Fish Res 153:9–17

Woodcock SH, Grieshaber CA, Walther BD (2013) Dietary transfer of enriched stable isotopes to mark otoliths, fin rays, and scales. Can J Fish Aquat Sci 70:1–4

Editorial responsibility: Stephen Wing, Dunedin, New Zealand

Submitted: March 15, 2017; Accepted: June 7, 2017
Proofs received from author(s): August 7, 2017

Vol. 598: 247–259, 2018
https://doi.org/10.3354/meps12218

MARINE ECOLOGY PROGRESS SERIES
Mar Ecol Prog Ser

Published June 28[§]

Contribution to the Theme Section 'Innovative use of sclerochronology in marine resource management'

Comparative study of age estimation in wild and cultured *Octopus vulgaris* paralarvae: effect of temperature and diet

C. Perales-Raya[1,*], M. Nande[2], A. Roura[3], A. Bartolomé[1], C. Gestal[3], J. J. Otero[2], P. García-Fernández[3], E. Almansa[1]

[1]Instituto Español de Oceanografía, Centro Oceanográfico de Canarias, Santa Cruz de Tenerife 38180, Spain
[2]Instituto Español de Oceanografía, Centro Oceanográfico de Vigo, Vigo 362390, Spain
[3]Instituto de Investigaciones Marinas Consejo Superior de Investigaciones Científicas, Vigo 36208, Spain

ABSTRACT: The common octopus *Octopus vulgaris* is a highly valuable species worldwide, but to understand its population dynamics and requirements under culture conditions, it is crucial to improve our knowledge about its planktonic stages. Previous studies validating daily beak growth increments in these stages allowed age estimation and comparison of wild and cultured paralarvae. We aimed to improve age estimations in captivity, addressing the effect of temperature and diet, to obtain an accurate estimation of age in wild specimens collected from the coast to the open ocean off NW Spain and Morocco. We analysed the beak growth increments of reared paralarvae at 14 and 21°C with 2 different crustacean prey taxa (*Artemia* and spider crab *Maja brachydactyla* zoeae) over 30 d. Daily increment deposition at 21°C was confirmed, whereas <1 increment d^{-1} was recorded at 14°C. The width of the reading area grew accordingly with age; therefore, this beak region may be suitable for age estimation. A general linear model (GLM) analysis showed that temperature and the interaction of age × temperature significantly influenced increment deposition, whereas diet did not. The number of growth rings recorded in wild paralarvae beaks ranged from 0–8 on the coast, 7–11 on the continental shelf and 2–28 in the open ocean. Corrected age estimates of wild paralarvae were obtained with the GLM using the mean temperatures recorded in the wild, supporting the hypothesis that *O. vulgaris* leave the coastal area and develop in the open ocean transported by upwelling filaments.

KEY WORDS: *Octopus vulgaris* · Cephalopod · Paralarvae · Early life · Ageing · Beaks · Microstructure · Prey · Growth

INTRODUCTION

The common octopus *Octopus vulgaris* Cuvier, 1797 (Cephalopoda, Octopodidae) is a globally important fisheries species with a high economic value (Xavier et al. 2015). Octopuses being exported globally under the name *O. vulgaris* (multiple *O. vulgaris*-like species, Amor et al. 2017) are of extremely high market value in Mediterranean, South American and Asian countries, but especially in north-western Africa, the largest single-species octopus fishery in the world (Norman et al. 2016). Following the decline of traditional fisheries (Balguerías et al. 2000), cephalopods have gained attention in aquaculture practice.

O. vulgaris has great potential for aquaculture diversification since it meets some of the requirements for commercial aquaculture, such as fast growth (Mangold & Boletzky 1973, Semmens et al. 2004), a short life cycle (Boyle & Rodhouse 2005), high food conversion rates (Mangold 1983), easy adaptation to captivity (Iglesias & Fuentes 2014), as well as high demand and market value (Vaz-Pires et al. 2004, Vidal et al. 2014). In addition, it is a valuable experimental animal for biomedical and behavioural

*Corresponding author: catalina.perales@ca.ieo.es

[§]Advance View was available online September 5, 2017; subsequently updated September 12, 2017

Publisher: Inter-Research · www.int-res.com

research (Hochner 2008), and is affected by the requirement of the new European Directive 2010/63/EU which regulates the welfare and use of animals for scientific purposes, minimizing the use of wild animals to be used in experimentation. The species has a planktonic paralarval stage in its early life (Villanueva & Norman 2008), which is critical for the success of both cultured and wild populations.

In captivity, massive mortality during the paralarval stage of the common octopus is the main bottleneck for its commercial exploitation (Iglesias & Fuentes 2014). Based on feeding trials with enriched live food and natural zooplankton, several authors have suggested that this mortality could be caused, to some extent, by nutritional deficiencies in the paralarvae (Navarro et al. 2014). In addition, expression analysis of selected genes suggests an effect of environmental stress on the immune competence of the paralarvae, which could negatively affect their health and welfare (Castellanos-Martínez & Gestal 2013). Therefore, better knowledge about nutritional requirements, physiology and health status of wild specimens could help to identify the causes of the high mortalities under culture conditions.

Difficulties in studying the planktonic early stages in their natural environment are mostly related to their scarcity, due to the high dispersion of wild paralarvae together with the seasonality of the spawning period (Otero 2006). In the first days post-hatching, paralarvae inhabit the coastal area, but they move away towards the oceanic platform and open ocean in the later ages prior to benthic settlement (Roura et al. 2016). These difficulties of sampling, together with the complexity of age estimation in wild paralarvae has prevented the accurate study of paralarval development and the comparative analysis of wild and cultured paralarvae of similar ages (Garrido et al. 2016a). This comparative approach is of great interest to understand the ecology and feeding of planktonic stages in their natural environment (Villanueva & Norman 2008), which could serve as a guide to establish requirements for these early developmental stages under culture conditions.

Regarding age estimation, Hernández-López et al. (2001) studied daily formation of growth increments on the lateral walls of the beaks of cultured *O. vulgaris* paralarvae up to 26 d old. Recently, Perales-Raya et al. (2014b) validated daily deposition using the anterior coloured region of the upper jaw, where parallel and thin increments were observed, broadening the range of paralarvae and transition-to-settlement individuals up to 98 d old. These findings allow us to refine the study of wild paralarvae throughout their development as well as to compare wild and cultured individuals of similar age. Age estimation in the anterior coloured region of the upper jaw has been successfully used in wild paralarvae together with a characterization of fatty acid composition (Garrido et al. 2016a) and identification of potential rearing stress in octopus paralarvae (Franco-Santos et al. 2016). Age validation experiments in these studies were carried out at 19–23°C, within the range of optimal temperature (21°C) under culture conditions (Hamasaki & Morioka 2002, Iglesias et al. 2014). However, no studies have been carried out at thermal conditions of the natural environment of the paralarvae, where the temperature is usually lower (12–14°C; Roura et al. 2016). Development in cephalopods is greatly affected by the environmental temperature, as has been shown in *O. vulgaris* paralarvae, in which growth rate increases proportionally to the water temperature (Hamasaki & Morioka 2002).

The aim of the present study was to estimate, for the first time, the ages of wild coastal and oceanic paralarvae by counting the parallel thin increments (rings) observed in the anterior region of the upper jaw. Wild samples collected in coastal and oceanic waters off NW Spain and Morocco were analysed and compared with reared individuals. As a first step, captive paralarvae were maintained under different conditions to assess the potential effect of temperature and diet on the increment deposition. Individuals were cultured at the conventional rearing temperature (21°C, Iglesias & Fuentes 2014) and at the lowest range of the thermal conditions in coastal environments (around 14°C). As diet is among the most important factors affecting paralarval growth, the effect of 2 different prey was compared: *Artemia* and spider crab *Maja brachydactila* zoeae, which are closer to their natural prey (Roura et al. 2012) and support better growth relative to *Artemia* (Reis et al. 2015, Garrido et al. 2016b). Our aim was to improve age estimations of *O. vulgaris* at early stages, addressing the effect of temperature and diet under culture conditions. This information was then used to interpret the age estimated in wild *O. vulgaris* paralarvae collected in 3 different locations throughout their planktonic stage (coast, continental shelf and open ocean) in 2 upwelling ecosystems.

MATERIALS AND METHODS

Culture of paralarvae

Two rearing experiments with *Octopus vulgaris* paralarvae were carried out at similar conditions

using 2 different temperatures and diets: the first at 21°C (optimal temperature under culture conditions, Iglesias & Fuentes 2014), and the second at 14°C (similar to environmental temperature in coastal waters of Ría of Vigo, NW Spain). For each temperature, 2 different diets were tested, i.e. *Artemia* and zoeae of the spider crab *Maja brachydactyla*.

Octopus broodstock

Thirteen female and 5 male *O. vulgaris* were captured in January 2015 for the first experiment, whereas 5 females and 2 males were captured in January 2016 for the second experiment. In both cases, artisanal fishing gear was used. Octopus broodstock was maintained in a concrete tank (4.60 × 2.10 m) with 1.0 m of water depth. Broodstock was fed 3 times a week with frozen mussels *Mytilus galloprovincialis*, frozen fish (*Merluccius merluccius* and *Sardina pilchardus*) and frozen crustaceans (*Polybius* sp.). Several plastic pipes (0.2 m diameter, 0.5 m length) were placed into the tank as dens for females to spawn. During spring, females began to lay their eggs into the dens independently. Egg batches were placed into the plastic pipes so the clusters remained suspended and the female could clean and constantly oxygenate them with gentle water jets from the funnel. Spawning females were transferred from the broodstock tank and placed in smaller tanks (1 m^3) individually with low light intensity (<100 lux). The embryonic development of *O. vulgaris* lasts from 45 to 65 d, depending on incubation temperature (14 and 18°C respectively; Nande et al. 2017). Broodstock and isolated females were maintained in a flow-through system at the natural environment temperature of the Ría of Vigo (14–18°C), salinity at 35 psu (Refractometer ATC, ATAGO©) (Iglesias et al. 2016), dissolved oxygen at around 8 mg l^{-1} (Oxy-Guard-10XHM053, Polaris©) and ammonia, nitrites and nitrates close to 0 (kit Nutrafin©). Temperature and oxygen were measured daily, whereas salinity and nitrogen were monitored once a week.

Spider crab broodstock

From January to April in 2015 and 2016, 81 spider crabs were maintained in 1 × 1 m tanks with seawater depth of 0.8 m, in an open flow-through system and at ambient temperature of the Ría of Vigo (14–18°C). Light intensity was low (<100 lux). Crabs were fed 3 times per week with frozen mussels *M. galloprovincialis*. The maturation stage was evaluated each week, and the females were reorganised into tanks with similar developmental stages (Iglesias et al. 2014). Spontaneous hatchlings were collected using a 500 µm sieve and transferred to 100 l tanks at 14°C and closed-circuit water circulation.

Octopus paralarvae rearing

O. vulgaris hatchlings were removed from the incubation tank 12 h before the beginning of the rearing experiments to ensure that only newly hatched paralarvae were used. In both experiments (21 and 14°C), 6 paralarvae l^{-1} were transferred into 2 fibreglass cylindrical tanks of 500 l with black bottoms, soft central aeration, temperature at 21 ± 1°C and 14:10 h light:dark photoperiod with an intensity of 250–300 lux at the surface. During the first 5 d post hatching (dph), they were kept in a closed-circuit system, daily controlling the levels of nitrites, nitrates and ammonia (close to 0), after which paralarvae remained in an open circuit for 5 h with a flow of 3.5 l min^{-1}, achieving 2 total renovations. Two types of microalgae, *Isochrysis galbana* (Ig) and *Nannochloropsis gaditana* (Nn) were added daily at a final concentration of 150 000 and 500 000 cells ml^{-1}, respectively. The paralarvae were fed with spider crab zoeae at a concentration of 0.02 ml^{-1} and *Artemia* metanauplii (enriched at 25°C during 24 h with Ig and Nn; >2 mm total length) at a final concentration of 0.2 *Artemia* ml^{-1}. Equivalent methodology was carried out in rearing tanks at low temperature (14 ± 1°C). For beak analysis, a total of 33 paralarvae (at 21°C) and 50 paralarvae (at 14°C) were collected. Different ages were sampled in each treatment (2–5 paralarvae in each sample). The 21°C-*Artemia* group was sampled at 7, 10 and 20 dph, and the 21°C-zoeae group was sampled at 7, 10, 20 and 30 dph. Paralarvae reared at 14°C and fed *Artemia* were sampled at 5, 7 10, 13, 15, 20 and 22 dph, and the 14°C-zoeae group was sampled at 12, 15 and 20 dph. Paralarvae were anaesthetized with a solution of 1.5% magnesium chloride in seawater ($MgCl_2$) for 10 min and then killed by increasing the solution to 3.5% for 30 min (following Fiorito et al. 2015).

Paralarvae dry weight and growth rate

In order to obtain the dry weight, 10 paralarvae were randomly sampled from the rearing tanks at 0 (hatch-

lings), 5, 10, 15, 20 and 30 dph. Paralarvae were killed as described above. Subsequently, dry weight was obtained for each treatment, using small handmade aluminium baskets, after 24 h in a dry oven at 80°C using an ultra-precision (0.000001 g) UM3 Mettler scale. Paralarval dry weight was used to calculate the standard growth rate (SGR) for each type of diet throughout the rearing period:

$$SGR = \frac{\ln (PDW_f) - \ln (PDW_0)}{t_f - t_0} \quad (1)$$

where initial paralarvae dry weight (PDW_0) and final paralarvae dry weight (PDW_f) are the dry weight of the paralarvae at the beginning and end of the rearing experiments; and t_0 and t_f are the times at the beginning/end of the rearing experiments, respectively.

Wild paralarvae captures

Coastal paralarvae

Paralarvae were collected around the Cíes Islands in the Ría of Vigo (NW Spain) (Fig. 1a,b). *O. vulgaris* paralarvae were classified according to Sweeney et al. (1992). Surveys were carried out in 2015 (n = 6) and 2016 (n = 5) between May and September onboard the RV 'José María Navaz' (Instituto Español de Oceanografía). During each survey, 5 trawls were performed along 2 transects (T1 and T2, Fig. 1b) with a planktonic net of 2 m diameter and 500 µm mesh, to an average depth of 10 m over 10 min at a speed of 2 knots. Wild paralarvae were sorted on board from zooplankton samples using 30 l receptacles. Paralarvae were killed in liquid nitrogen and kept at –80°C until analysis.

Oceanic paralarvae

Zooplankton samples were collected during the multidisciplinary project 'Canaries–Iberian Marine Ecosystem Exchanges (CAIBEX)', which took place in the seasonal upwelling system off Cape Silleiro (41–43° N, CAIBEX-I) and the permanent upwelling system off Cape Guir (30–32° N, CAIBEX-III). Data acquisition for this study was carried out on board the RV 'Sarmiento de Gamboa' during CAIBEX-I from 7 to 24 July, and CAIBEX-III from 16 August to 5 September (Fig. 1). High-resolution mapping of the study area determined the oceanographic conditions (temperature, salinity and chlorophyll fluorescence) *in situ* using a towed vehicle (SeaSoar) that undulated between the surface and 400 m depth. The information collected with the SeaSoar, together with real-time satellite images of sea surface temperature and chlorophyll provided by the Plymouth Marine Laboratory (NERC Earth Observation Data Acquisition and Analysis Service), helped to determine the location of upwelled water masses. Once detected, we followed these upwelled water masses by means of 3 Lagrangian experiments with an instrumented

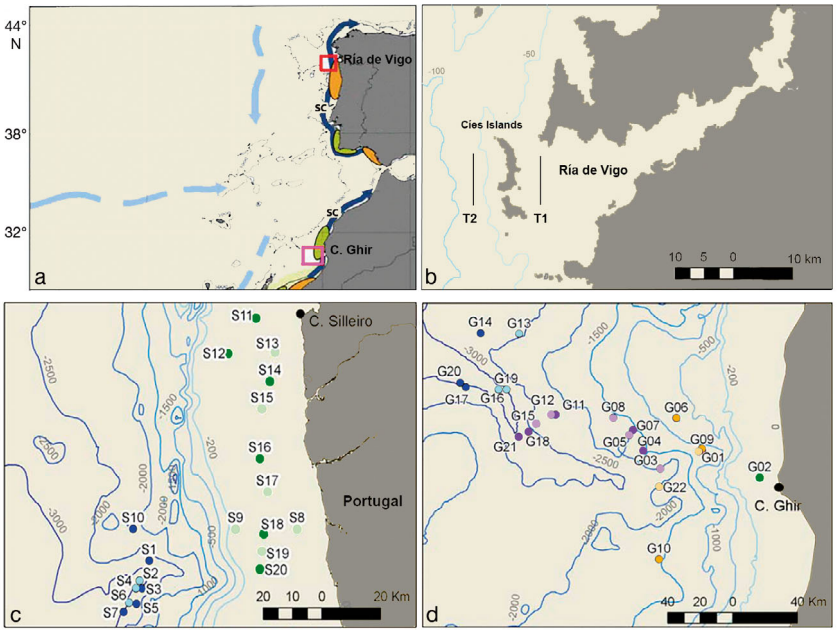

Fig. 1. (a) Iberian–Canary current eastern boundary upwelling system modified from Arístegui et al. (2009), showing the areas sampled (red box: CAIBEX-I cruise, pink box: CAIBEX-III) and the main currents (light blue: surface; dark blue: slope; SC: slope current), retention (orange) and dispersion (green) zones on the shelf. (b) Ría of Vigo (NW Spain) showing the 2 transects (T1 and T2) where 'coastal' *Octopus vulgaris* paralarvae were sampled. (c) Zooplankton samples collected during CAIBEX-I off the NW coast of the Iberian Peninsula, around Cape Silleiro (42° N). Blue (green): samples S1–S7 (S13–S20) corresponding to the first (second) Lagrangian experiment carried out in the open ocean (over the continental shelf). (d) Zooplankton samples collected during CAIBEX-III off the NW Africa coast, around Cape Ghir (30° N). Samples were collected over the continental shelf at night (green, <200 m depth), in an area affected by the upwelling in the open ocean (orange, >200 m depth), following a coastal upwelling filament during the third Lagrangian experiment (violet) and in the open ocean (blue). Light/dark colours represent day/night samplings

drifting buoy (IDB) that was deployed in the core of the upwelled water.

Meteorological conditions resulted in only weak development of upwelling during CAIBEX-I. Two Lagrangian experiments were carried out during this survey: (1) oceanic waters over the continental slope were sampled around 41° 25′ N during the relaxation period after a brief upwelling event (L1: 10–14 July, samples S1–S7, Fig. 1c); and (2) an incipient coastal upwelling with alongshore transport over the continental shelf was sampled from 42 to 41° 23′ N (L2: 16–21 July, samples S13–S20, Fig. 1c). Between these 2 Lagrangian experiments, we collected samples following a coastal–oceanic gradient off the Portuguese coast (S8–S10), to see the changes between these 2 environments, as well as 2 samples in the continental shelf of Galicia (S11 and S12). In contrast, strong winds during CAIBEX-III allowed the development of a strong upwelling filament (Sangrà et al. 2015). The IDB was deployed in the core of the upwelling filament, which was advected from the coast into the ocean during the third Lagrangian experiment (L3: 23–31 August, Fig. 1d). Samples were also collected over the shelf (Fig. 1d), in an area affected by the upwelling over the continental slope (Fig. 1d) and in the open ocean (Fig. 1d) to investigate the zooplankton communities surrounding the upwelling filament.

A CTD was deployed to 500 m depth in the open ocean and to 10 m above the sea-bottom over the continental shelf (<200 m depth) before each zooplankton sampling. Sampling took place close to the IDB both at midnight and midday. Mesozooplankton samples were collected with 2 bongo nets (750 mm diameter) equipped with 375 µm mesh and a mechanical flow-meter. At a ship speed of 2.5 knots, 3 double-oblique tows were carried out at each station over the continental slope (>200 m depth): at 500 m, 100 m and at the surface (0–5 m). Over the continental shelf (<200 m depth), samples were collected at 100 m (or 10 m above bottom when shallower) and at the surface (0–5 m). The bongo net was first lowered to the desired depth, towed for 30 min and subsequently hauled up at 0.5 m s^{-1}. It was then cleaned on board and deployed back to the sea for the next towing. In the laboratory, *O. vulgaris* paralarvae were sorted from the zooplankton samples and stored in 70% ethanol at −20°C (Roura 2013).

Beak analysis

Cultured and wild paralarvae were analysed for age estimation by counting the parallel thin increments (rings) observed in the anterior region of the upper jaw (beak). The beak of each paralarva (Fig. 2) was extracted under a binocular microscope and pre-

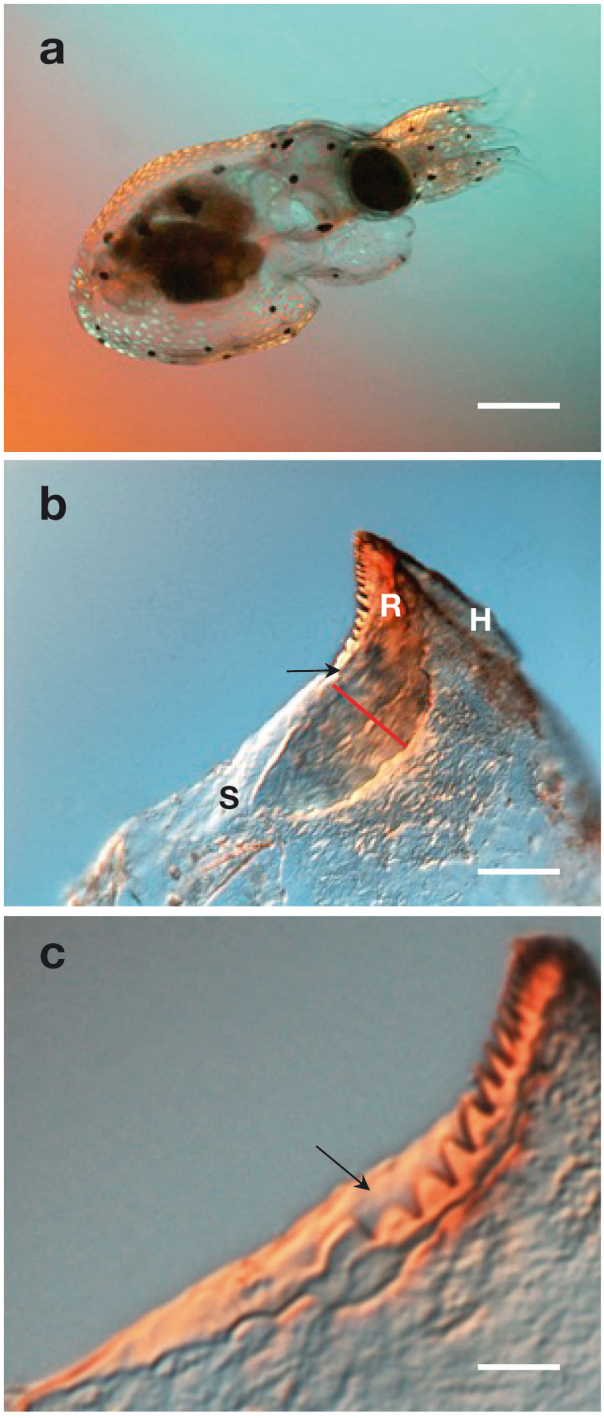

Fig. 2. (a) Lateral view of an *Octopus vulgaris* paralarva at hatching; scale bar = 500 µm. (b) Anterior region of the upper jaw beak in a 20 d old paralarva; location of the main regions (R: rostrum, H: hood, S: shoulder). Arrow: first increment. Red segment: width of the reading area (WRA); scale bar = 50 µm. (c) Location of the thin line of tissue outside the dentition (arrow) in the upper jaw of a hatchling; scale bar = 50 µm

served in distilled water at 4–5°C (Perales-Raya et al. 2010). After longitudinal sectioning of the upper jaw under the binocular microscope, the 2 halves obtained were placed in a slide with a drop of distilled water for observation. Increments in the anterior coloured (pigmented) region of the upper jaw (Franco-Santos et al. 2016) were counted in the half with more clear rings under transmitted light with a Nikon Microscope Multizoom AZ100 (400× magnification). The system has a differential interference contrast attachment (DIC-Nomarski) that creates a 3-dimensional image of the beak surface, where the sequence of micro-increments is revealed (Fig. 2b). Two counts were carried out for each paralarva by 2 trained readers. We discarded individuals with more than ±1 increments of difference between readings (for paralarvae with 0–7 increments) and individuals with more than ±2 increments for other cases (paralarvae with >7 increments). The final number of increments assigned to each paralarva was the mean value of both counts. Reading precision (sensu Campana 2001) was assessed with the coefficient of variation (CV, standard deviation divided by the mean number of increments in each sample; Chang 1982, Campana 2001):

$$\mathrm{CV}(\%) = \frac{100 \times \sqrt{(R1-R2)^2 + (R2-R)^2}}{R} \qquad (2)$$

where $R1$ and $R2$ are the number of increments from the first and second reading, respectively, and R is the mean number of increments from both readings. The mean CV was calculated for reared and wild paralarvae in order to assess the reading precision of both groups. For all samples, the width of the reading area (WRA) was measured (µm) in the widest region of the reading area, where the increments were counted. After calibration, measurement of WRA (Fig. 2b) was conducted using the Image Analysis System, with the package Image Pro Plus 6.3. (Media Cybernetics 2008). All beaks were preserved in distilled water at least 48 h before measurements were taken, in order to re-hydrate the microstructure and avoid any differences in the WRA values due to the ethanol (oceanic wild paralarvae). Nonetheless, several samples preserved in 70% ethanol were measured before and after 48 h of water immersion, and no difference (±1 µm) was found in the WRA value. The number of arm suckers has been used as an approximation of the age and development of paralarvae in previous studies (Villanueva 1995), and these data were also collected in the 165 wild paralarvae analysed.

Statistical analysis

Results are presented as means ± SD, and $p < 0.05$ was considered significant. Statistical analyses of linear regressions were performed using the SPSS package version 17.0 (SPSS Inc. 2008). A general linear model (GLM) was applied to test the effect of temperature and diet on increment deposition in captivity. We used temperature and age as linear predictors for the number of increments (NI), with the interaction of age with temperature. Obtained coefficients (intercept, age, temperature and age × temperature interaction) were used to obtain the equation for age adjustment from NI and a mean temperature value. GLM analysis was performed with R ver. 3.3.2. (R Core Team 2016) as designed by Hastie & Pregibon (1992). ANOVA of the GLM fits (analysis of deviance table, Type II test) was performed using the package 'car' (Fox & Weisberg 2011).

RESULTS

Improvements in age estimation and beak morphology

Morphometric analysis of octopus paralarvae beaks provided insight into this structure (Fig. 2). The reading area (named 'lateral hood surface' by Perales-Raya et al. 2014b) is located in the wider part of the anterior coloured (pigmented) region of the beak (Franco-Santos et al. 2016; Fig. 2b). This area corresponds to the rostrum. Adult beaks have the same morphology in this region, but their dense pigmentation makes it more feasible to count increments in the rostrum sagittal section (RSS, after Perales-Raya et al. 2010). The first increment is located at the base of the oral denticles (teeth) (Fig. 2b). The last increment (indicating the day of death) is the posterior border of the reading area, where the rostrum ends and the hood begins. The hood exhibits a delicate and transparent microstructure where no increment sequence was found (see Fig. 2b). We observed a thin line of transparent tissue outside the dentition, extending along the anterior border of the beak. It was identified as part of the developing shoulder (Fig. 2c), which gradually widens through the ventral region with age. To our knowledge, this is the first time that this structure has been identified in paralarvae. Mean reading precision (CV) from the beak readings was 2.97 ± 2.05% for individuals cultured at 21°C (n = 33) and 3.53 ± 4.32% for individuals cultured at 14°C (n = 50).

Readings of wild coastal paralarvae showed a mean CV of 2.94 ± 5.66% (n = 100), and the mean CV obtained from continental-shelf and oceanic paralarvae was 3.83 ± 4.64% (n = 65). Although the CV showed high variability, mean values were lower than the usual adopted value of 7.6% for annual and daily structures (Campana 2001) and therefore no additional paralarvae were discarded based on the CV.

Cultured paralarvae

The relationship between the number of increments and true age (Fig. 3) in reared paralarvae at both temperatures showed a linear regression for all 4 groups (14°C-*Artemia*, 14°C-zoeae, 21°-*Artemia* and 21°C-zoeae). Results of regression analysis are shown in Table 1a. Daily deposition of increments was confirmed at 21°C, supporting previous validation studies in octopus paralarvae (Perales-Raya et al. 2014b); however, at 14°C there was less than 1 increment d^{-1}. These results indicate that in culture conditions, temperature influences the increment deposition in the beak. GLM and ANOVA of the GLM fit with diet included showed that temperature and the factor age × temperature were highly significant ($p < 0.001$), but diet was not significant ($p = 0.051$) in the increment deposition and consequently, the final GLM was performed without the diet factor. Coefficients obtained from the GLM analysis (Table 1b) resulted in this equation:

$$AGE = \frac{NI - 4.604 + T * 0.176}{T * 0.074 - 0.612} \quad (3)$$

wherewhere NI is the number of increments, T is the temperature, and AGE is the age estimation in days. The highest variability found during the increment readings was for 0 d paralarvae (hatchlings), showing a mean value of 2.1 ± 1.52 increments at 21°C and 1.6 ± 0.55 increments at 14°C. Since hatching does not take place at the same time for all eggs within a tank, and some hours have usually elapsed from hatching when the paralarvae are removed from the tank, we assigned 0.5 d to hatchlings born in culture conditions. Growth of dry body weight (mg) and WRA of the beak (µm) in reared paralarvae by temperature and diet are presented in Fig. 4. Paralarvae reared at 21°C showed higher weight in the zoeae-fed group than in the *Artemia* group (Fig. 4a); however, these differences were not observed in the WRA of the beak (Fig. 4b). These results indicated that the WRA, and by extension the beak, might grow independently of the rest of the body and feeding

Table 1. (a) Results of regression analysis for relationships between the number of growth increments (NI), age (days in cultured individuals, NI in wild individuals) and width of the reading area (WRA; see Fig. 2) by groups of *Octopus vulgaris* paralarvae. Groups are coded by food source (zoeae: spider crab *Maja brachydactyla* zoeae; Art: *Artemia*) and rearing temperature (21 or 14°C). (b) General linear model (GLM) coefficients; *p < 0.05, **p < 0.01, ***p < 0.001

(a) Regressions	Intercept	Slope	n	r^2	p
NI–AGE zoeae 21°	−0.722	1.046	22	0.989	<0.001
NI–AGE Art 21°	−1.468	1.095	16	0.976	<0.001
NI–AGE zoeae 14°	−1.050	1.968	18	0.797	<0.001
NI–AGE Art 14°	−2.349	1.911	37	0.860	<0.001
AGE–WRA zoeae 21°	10.185	2.598	22	0.977	<0.001
AGE–WRA Art 21°	10.056	2.383	16	0.94	<0.001
AGE–WRA zoeae 14°	10.569	0.796	18	0.825	<0.001
AGE–WRA Art 14°	11.513	1.113	37	0.72	<0.001
AGE–WRA all 21°	8.941	2.608	33	0.966	<0.001
AGE–WRA all 14°	11.533	0.986	50	0.619	<0.001
NI–WRA wild	4.465	2.095	165	0.902	<0.001

(b) GLM coefficients	Estimate	SE	*t*	p (>|*t*|)
Intercept	4.604.920	1.416.342	3.251	0.00169 **
Age	−0.612065	0.096551	−6.339	1.33×10^{-8} ***
Temperature	−0.176282	0.079230	−2.225	0.02894 *
Age × temperature	0.073954	0.005239	14.116	$< 2 \times 10^{-16}$ ***

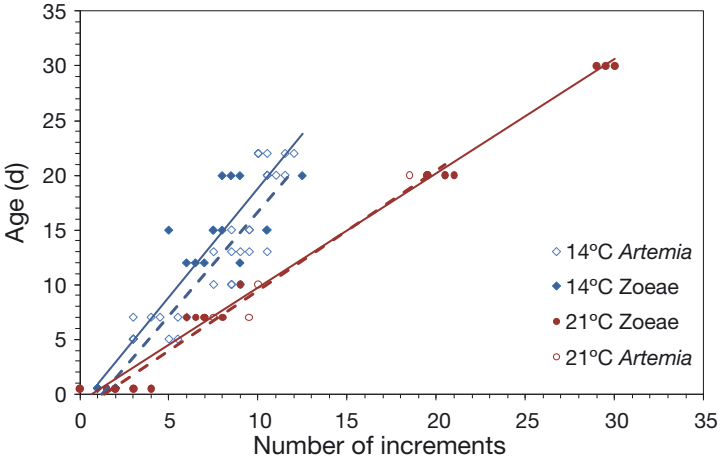

Fig. 3. Relationship between the number of increments in the beak and age of the cultured *Octopus vulgaris* paralarvae. Data grouped by temperature (14°C, 21°C) and diet treatments (dashed lines: *Artemia*; solid lines: spider crab *Maja brachydactyla* zoeae)

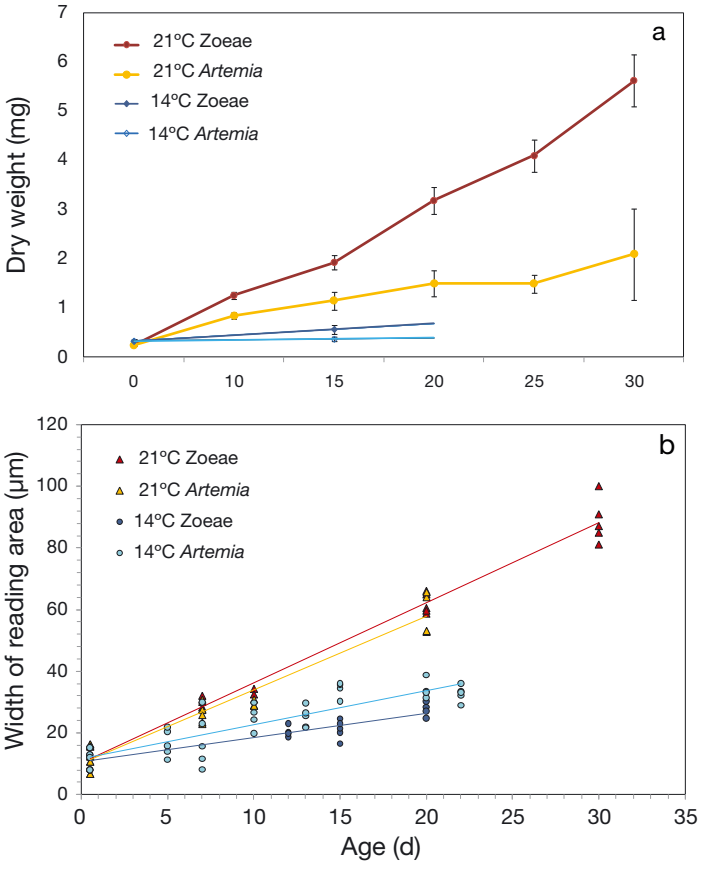

Fig. 4. Growth of cultured *Octopus vulgaris* paralarvae, with data grouped by temperature and diet treatments (see Fig. 3). (a) Mean growth in dry weight by age group. Data of groups at 14°C are extrapolated due to high mortality. (b) Beak growth (width of the reading area; see Fig. 2)

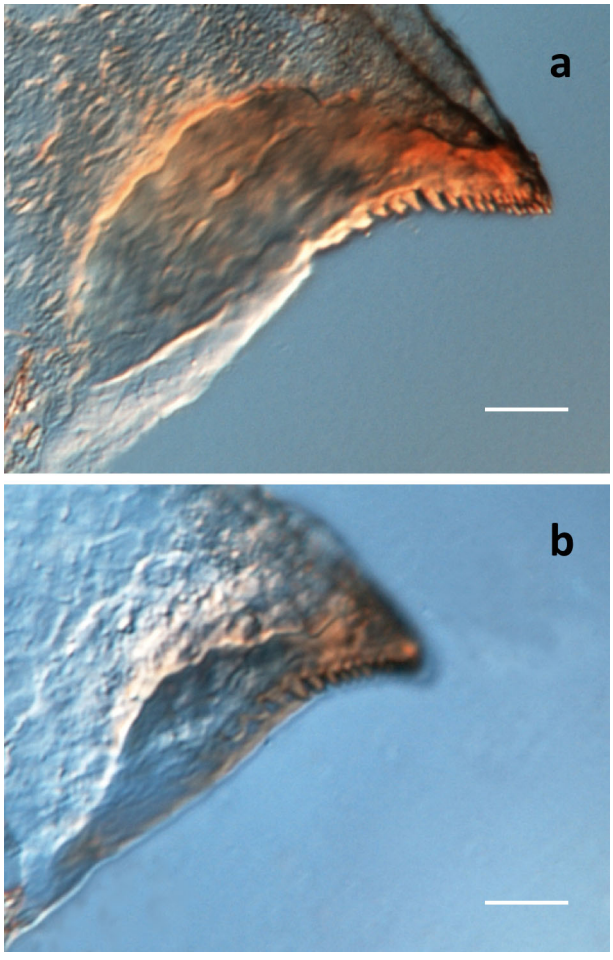

Fig. 5. Beaks of 20 d old *Octopus vulgaris* paralarvae, reared at (a) 21°C and (b) 14°C; scale bar = 50 µm

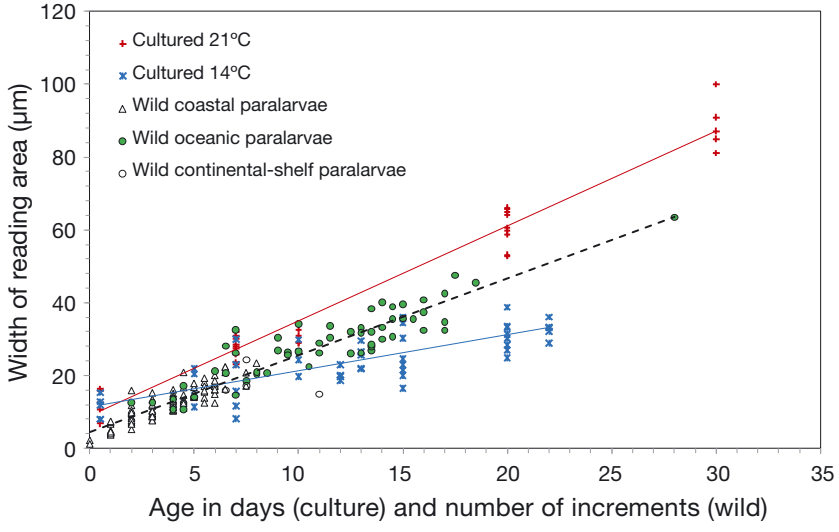

Fig. 6. Growth of the beak (width of the reading area, see Fig. 2) in wild and cultured *Octopus vulgaris* paralarvae. Cultured samples are grouped by temperature. Age estimation in wild samples = number of increments in the beak assuming daily deposition

type in culture conditions at 21°C. In contrast, paralarvae reared at 14°C showed a lower growth with similar trends for both dry body weight and beak WRA. Fig. 4b shows that, at similar ages, beaks of paralarvae reared at 14°C were smaller than those reared at 21°C. Two 20 d old beaks cultured at 21 and 14°C are shown in Fig. 5 to illustrate these differences.

Wild paralarvae

When cultured groups and wild paralarvae are represented using the number of increments as the age estimation (Fig. 6), the highest WRA size resulted for paralarvae cultured at 21°C and the smallest for those cultured at 14°C, with wild specimens showing intermediate WRA values and similar growth trends to paralarvae cultured at 21°C. Both groups (wild and cultured at 21°C) had also a good linear fit ($r^2 > 0.9$; see Table 1a), evidencing that WRA growth is correlated with age. Results of increment counts in beaks of wild individuals are shown in Fig. 7. The mean NI was 4 increments (range: 0–8) for coastal paralarvae from the Ría of Vigo (all with 3 suckers), 8 increments (range: 7–11) for continental-shelf paralarvae off NW-Spain (3–4 suckers), 12 increments (range: 5–18) in oceanic paralarvae off NW Spain (3–5 suckers) and 11 increments (range: 2–28) in oceanic paralarvae off Morocco (3–15 suckers). Fig. 7 also includes information about the NI range for a given number of suckers. All coastal paralarvae had 3 suckers, as did 3 paralarvae (75%) from continental shelf NW Spain, 8 paralarvae (22%) from oceanic waters off NW Spain and 9 paralarvae (38%) from oceanic waters off Morocco. The latter included the youngest group of oceanic paralarvae (2–7 increments), which were transported from the Moroccan coast by the strong filament followed during CAIBEX-III. Considering the possible influence of temperature (Fig. 3) in the periodicity of increment deposition in the natural environment, Fig. 8 provides the GLM simulation for the mean temperatures where coastal, continental-shelf and oceanic paralarvae were respectively caught: 14.5°C for the coastal area (range: 13.00–16.20), 17°C for oceanic waters off Morocco (range: 11.70–21.50) and 16°C for the oceanic and continental waters off NW Spain (range: 12.03–19.16). Table 2 shows mean ages obtained for each NI and each temperature group.

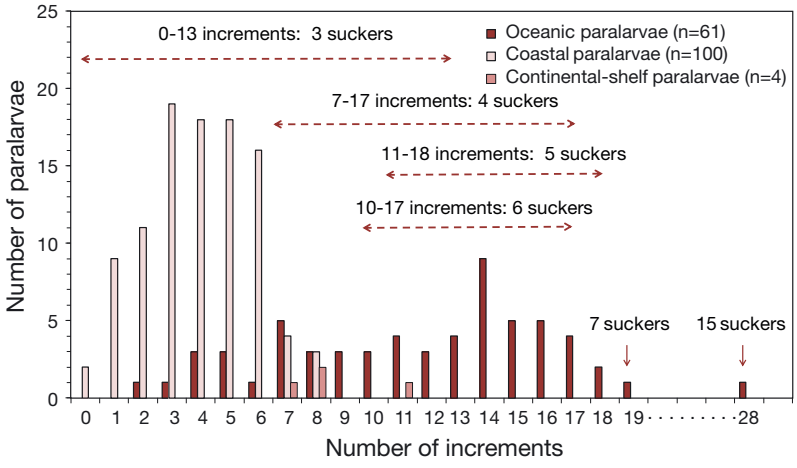

Fig. 7. Number of coastal and oceanic *Octopus vulgaris* paralarvae by number of growth increments in their beaks. Arrows indicate the number of suckers per range of increments. 3 suckers, n = 117; 4 suckers, n = 26; 5 suckers, n = 9; 6 suckers, n = 7; >6 suckers, n = 2

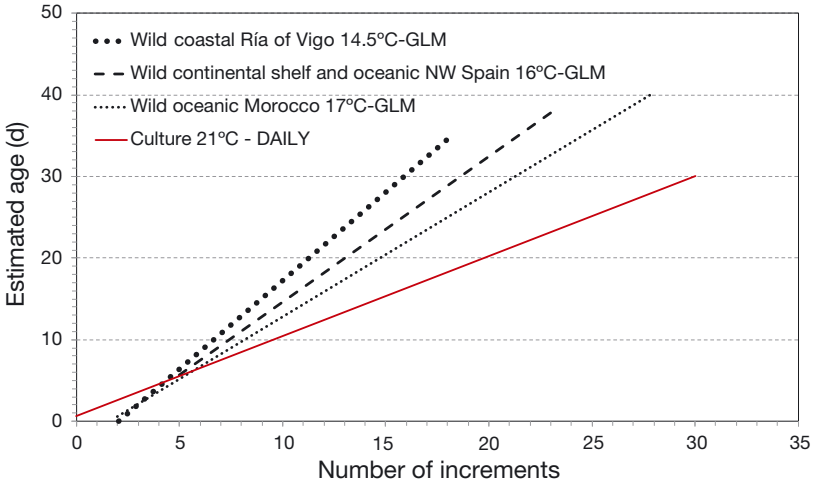

Fig. 8. General linear models (GLMs) for age adjustment of wild *Octopus vulgaris* paralarvae based on the number of growth increments in the beak, considering the effect of temperature in the increment deposition. Thick dotted line: model with 14.5°C as the mean temperature for coastal paralarvae (Ría of Vigo). Dashed line: model with 16°C as the mean temperature for paralarvae from oceanic and continental waters off NW Spain. Thin dotted line: model with 17°C as the mean temperature for oceanic paralarvae off Morocco. Red line: adjustment of cultured data at 21°C (daily deposition, optimal culture conditions)

Table 2. Mean ages (in days) obtained for each number of growth increments (NI) in the beaks of wild *Octopus vulgaris* paralarvae using a general linear model (GLM) simulation for mean temperatures where paralarvae were caught. Larvae originated from coastal waters at the Ría of Vigo, continental shelf and oceanic waters off NW Spain, and from oceanic waters off Morocco

NI	Age GLM 14.5°C Coastal (Ría of Vigo)	Age GLM 16°C Shelf-oceanic (NW Spain)	Age GLM 17°C Oceanic (Morocco)
1	−2.3	–	–
2	−0.1	–	0.6
3	2.1	–	2.2
4	4.2	–	3.7
5	5.8	5.7	4.4
6	8.1	–	6.7
7	9.6	8.9	7.5
8	12.2	10.5	–
9	–	12.5	–
10	–	14	12.8
11	–	16.2	–
12	–	17.3	–
13	–	19.7	16.7
14	–	21.1	18.7
15	–	23.5	19.7
16	–	25.3	21.6
17	–	27.1	23.5
18	–	28.4	–
19	–	–	25.8
28	–	–	40.3

DISCUSSION

The anterior pigmented region in paralarvae beaks has been previously used for age estimation in early stages of *Octopus vulgaris* (Perales-Raya et al. 2014b, Franco-Santos et al. 2016, Garrido et al. 2016a), and Franco-Santos & Vidal (2014) provided a morphological description of the beaks of paralarvae of several squid species, but the relationship between beak parts (rostrum, hood, lateral walls, shoulder) has not been addressed before. In contrast with adult beaks, transparency of this region in early developmental stages allowed us to observe the increments in the lateral surface of the rostrum, and preparation of RSS (following Perales-Raya et al. 2010) is not necessary in paralarvae. Increments used in adult RSS of octopuses (Perales-Raya et al. 2014a,b) and squids (Liu et al. 2015, Fang et al. 2016, Hu et al. 2016) are in fact the same increments as those in the rostrum surface of the paralarvae. The DIC-Nomarski technology also facilitated observation of different planes of the beak. Variability obtained in the reading precision (CV) of paralarval beaks is related to the high values obtained in some young individuals (5–8 increments), where a difference of 1 increment increases the CV. Precision is highly influenced by the species and the nature of the structure to be quantified (Campana 2001), and therefore any target level of CV for ageing studies also depends on the reading complexity of the structure.

Influence of temperature in increment deposition was evident at 14°C (Fig. 3), where paralarvae required more than 1 d for the deposition of each increment. The presence of an endogenous circadian rhythm was shown at 21°C by Meisel et al. (2003). Endogenous rhythms are common in marine organisms, but other factors may mask or reinforce the endogenous rhythm, which is synchronized at an early age with photo-periodicity or other external daily factors (Morales-Nin 1992). In fish otoliths, no evidence was found that increment numbers vary between temperature levels, except where low temperature has resulted in cessation of fish growth (Campana & Neilson 1985). Oyadomari & Auer (2007) reported that fish larvae with lower growth rates in the laboratory could not be aged as accurately by otolith analysis. Environmental conditions, transmitted through the physiology of the fish, affect the otolith growth rate, but increment periodicity may be disrupted only in extreme cases of physiological stress Morales-Nin (2000). Body weight and beak WRA of octopus paralarvae at 14°C (at any diet) showed a very low growth and higher variability when compared with cultured paralarvae at 21°C and wild paralarvae of the same ages (NI in wild individuals), both groups showing similar trends in WRA growth, although wild paralarvae showed smaller WRA sizes than paralarvae reared at 21°C (Fig. 6). Wild specimens inhabit areas with mean temperatures <21°C, and therefore their growth could be affected by temperature, as reported for fish planktonic larvae (*Pomacentrus coelestis*), for which water temperature explained approximately 30% of the growth variation, contrary to diet (zooplankton abundance), which explained only 3.5% (Meekan et al. 2003). Temperature controls H^+ ion availability in bicarbonate-buffered systems; therefore, this is an important control of otolith growth (Morales-Nin 2000), and beak growth might also be affected.

The adverse low temperature in the laboratory can lead to stressful conditions and slower growth, thus inducing slower increment deposition. We should not disregard the possibility that slow growth promotes very thin increments, even overlapping ones, which may also result in age underestimation. In contrast, paralarvae grown in optimal rearing conditions (21°C,

after Hamasaki & Morioka 2002) or in wild environments may be less affected by this physiological stress, and increment deposition may not be disrupted. In natural environment, temperature fluctuations, even if they are experienced through vertical migrations (Fortier & Leggett 1983), would be expected, reinforcing the endogenous daily cycle and thus producing more clear and regularly-spaced increments in wild-caught larvae than in laboratory-reared specimens (Campana & Neilson 1985). Vertical migrations reported in wild paralarvae of *O. vulgaris* (Roura 2013, Roura et al. 2016) may emphasise their daily cycle deposition in the natural environment, as clear increments were observed in most of the individuals analysed. Moreover, 14°C in the wild may not be as adverse as under culture conditions, since this temperature and even lower are common in coastal upwelling areas where the paralarvae hatch and live during their first days of life (Roura et al. 2016). In addition, these cold waters harbour rich zooplankton communities that provide diverse and nutritious prey for the early hatchlings (Roura et al. 2012, Roura 2013, Olmos-Pérez et al. 2017). Assuming daily increments in wild octopus paralarvae, the mean increments and the number of suckers recorded in this study for coastal, continental-shelf and oceanic waters (Fig. 7, Table 3) support the hypothesis of the oceanic strategy displayed by *O. vulgaris* paralarvae that are dispersed far from the shelf (Roura et al. 2016). The youngest oceanic paralarvae with 2–4 increments (i.e. 2–4 d old) caught in Morocco were dispersed far from the coast by the strong upwelling filament recorded off the NW African coast during the CAIBEX-III survey (Sangrà et al. 2015). This upwelling filament was 120 km wide, 150 m deep and stretched more than 200 km offshore, thus transporting recently hatched paralarvae from the coast that were growing within the filament, as evidenced from Fig. 7.

Paralarvae caught in the oceanic waters of NW Spain and Morocco shared the same haplotypes of the cytochrome c oxidase subunit I (Roura 2013), despite the fact that both populations grow in upwelling systems separated by more than 2000 km and adults exhibit evident morphological differences (Amor et al. 2017). The zooplankton availability in these nutrient-rich upwelled waters (Hernández-León et al. 2007, Roura 2013) probably provides good food conditions for paralarval growth, and we consider that the increments counted in both upwelling regions can be compared directly. Indeed, the differences observed between the paralarvae captured off NW Spain (up to 5 suckers and 18 increments or days) and Morocco (up to 15 suckers and 28 increments or days), were attributed to the different oceanographic conditions in both surveys and had little to do with the temperatures recorded (Table 3). During the survey off NW Spain (CAIBEX-I), there was no well-developed filament as in Morocco (CAIBEX-III), and the only samples collected in the open ocean were at the end of a short upwelling pulse (Roura 2013). This short upwelling pulse, however, was strong enough to transport paralarvae as young as 5 d old (with only 3 suckers per arm, Table 3) from the coast to the continental slope ~60 km offshore (samples S1–S7, Fig. 1).

Previous studies have evaluated the influence of temperature on the embryonic development and planktonic duration of *O. vulgaris* in temperate regions (e.g. Nande et al. 2017), and used it to predict hatching and settlement patterns (Katsanevakis & Verriopoulos 2006). In a similar fashion, and considering that temperature influences the initial growth phase of *O. vulgaris* (Semmens et al. 2004), we evaluated the possible influence of temperature on the increment deposition of wild paralarvae (Fig. 8, Table 2), by means of a GLM built with the data obtained in captivity. By doing so and using the mean temperatures at capture of the wild paralarvae from different ecosystems (coast, shelf and oceanic from NW Spain and oceanic from Morocco), we estimated the age of the paralarvae assuming that NI was temperature dependent (Table 1b). This model is an approximation to adjust NI of wild paralarvae assum-

Table 3. Details of the *Octopus vulgaris* paralarvae collected off the coasts of NW Spain (2015–2016) and continental shelf and ocean off NW Spain and Morocco in 2009. NI: number of growth increments

Atlantic area	Water	n	No. of suckers	NI	Temperature (°C)	Depth (m)	Distance to coast (km)
NW Spain	Coastal	100	3	0–8	13.00–16.20	18–20	3–5
NW Spain	Continental shelf	4	3–4	7–11	13.24–18.45	136–147	15–25
NW Spain	Oceanic	37	3–5	5–18	12.03–19.16	1940–3105	62–75
Morocco	Oceanic	24	3–15	2–28	11.70–21.50	787–3110	50–171

ing the influence of cold temperatures in the increment deposition. Consequently, caution should be taken, as the influence of temperature in the wild is not demonstrated and the high dispersion of planktonic paralarvae and their movements along upwelling water masses of different temperatures may result in deviation of the considered thermal mean values.

Extrapolation of results from rearing conditions to the natural environment is a complicated issue, since there are many biotic/abiotic natural conditions that are not easily emulated in captivity (e.g. pressure, temperature and light gradients, zooplankton communities). Nevertheless, further analyses of temperatures between the optimal (21°C) and cold temperature (14°C) with zooplankton-based diets are desirable to provide conclusions about the effect of temperature on the increment deposition of common octopus paralarvae.

Acknowledgements. This study was funded by Spanish Government under Projects OCTOWELF (Ref. AGL2013-49101-C2) and CAIBEX (CTM2007-66408-C02). Most of the authors of this paper participate to the COST network, Action FA1301 (CephsInAction) focussing on cephalopod welfare. We are indebted to the captain, crew and technicians of RV 'Sarmiento de Gamboa' for their assistance in collecting the zooplankton samples and hydrographical data during the project, as well as the staff of the Oceanographic Center of Vigo (IEO) for their assistance in the culture experiments and wild paralarvae captures. We thank the Parque Nacional das Illas Atlanticas (Galicia, Spain) for collaborating with us. Thanks also to Dr. Francisco J. Abascal (Oceanografic Center of Canaries-IEO) for his valuable assistance in performing the GLM.

LITERATURE CITED

Amor MD, Norman MD, Roura A, Leite TS and others (2017) Morphological assessment of the *Octopus vulgaris* species complex evaluated in light of molecular-based phylogenetic inferences. Zool Scr 46:275–288

Arístegui J, Barton ED, Álvarez-Salgado XA, Santos AMP and others (2009) Sub-regional ecosystem variability in the Canary Current upwelling. Prog Oceanogr 83:33–48

Balguerías E, Quintero ME, Hernández-González CL (2000) The origin of the Saharan Bank cephalopod fishery. ICES J Mar Sci 57:15–23

Boyle PR, Rodhouse PG (2005) Cephalopods. Ecology and fisheries. Blackwell Publishing, Oxford

Campana SE (2001) Accuracy, precision and quality control in age determination, including a review of the use and abuse of age validation methods. J Fish Biol 59:197–242

Campana SE, Neilson JD (1985) Microstructure of fish otoliths. Can J Fish Aquat Sci 42:1014–1032

Castellanos-Martínez S, Gestal C (2013) Pathogens and immune response of cephalopods. J Exp Mar Biol Ecol 447:14–22

Chang WYB (1982) A statistical method for evaluating the reproducibility of age determination. Can J Fish Aquat Sci 39:1208–1210

Fang Z, Li J, Thompson K, Hu F, Chen X, Liu B, Chen Y (2016) Age, growth, and population structure of the red flying squid (*Ommastrephes bartramii*) in the North Pacific Ocean, determined from beak microstructure. Fish Bull 114:34–45

Fiorito G, Affuso A, Basil J, Cole A and others (2015) Guidelines for the care and welfare of cephalopods in research—a consensus based on an initiative by CephRes, FELASA and the Boyd Group. Lab Anim 49: 1–90

Fortier L, Leggett WC (1983) Vertical migrations and transport of larval fish in a partially mixed estuary. Can J Fish Aquat Sci 40:1543–1555

Fox J, Weisberg S (2011) Multivariate linear models in R. An R companion to applied regression, 2nd edn. SAGE Publications, Thousand Oaks, CA

Franco-Santos RM, Vidal EAG (2014) Beak development of early squid paralarvae (Cephalopoda: Teuthoidea) may reflect an adaptation to a specialized feeding mode. Hydrobiologia 725:85–103

Franco-Santos RM, Perales-Raya C, Almansa E, Detroch M, Garrido D (2016) Beak microstructure analysis as a tool for identifying stress sources during culture of *Octopus vulgaris* paralarvae. Aquacult Res 47:3001–3015

Garrido D, Navarro JC, Perales-Raya C, Nande M and others (2016a) Fatty acid composition and age estimation of wild *Octopus vulgaris* paralarvae. Aquaculture 464: 564–569

Garrido D, Martín VM, Rodríguez C, Iglesias J and others (2016b) Meta-analysis approach to the effects of live prey on the growth of *Octopus vulgaris* paralarvae under culture conditions. Rev Aquacult (in press), doi:10.4111/raq.12142

Hamasaki K, Morioka T (2002) Effects of temperature on egg incubation period, and paralarval survival and growth of common octopus, *Octopus vulgaris* reared in the laboratory. Suisan Zoshoku 50:407–413

Hastie TJ, Pregibon D (1992) Generalized linear models. In: Chambers SJM, Hastie TJ (eds) Statistical models. Wadsworth & Brooks/Cole, Pacific Grove, CA, p 195–248

Hernández-León S, Gomez M, Arístegui J (2007) Mesozooplankton in the Canary Current System: the coastal–ocean transition zone. Prog Oceanogr 74:397–421

Hernández-López JL, Castro-Hernández JJ, Hernández-García V (2001) Age determined from the daily deposition of concentric rings on common octopus (*Octopus vulgaris*) beaks. Fish Bull 99:679–684

Hochner B (2008) Octopuses. Curr Biol 18:R897–R898

Hu G, Fang Z, Liu B, Yang D, Chen X, Chen Y (2016) Age, growth and population structure of jumbo flying squid *Dosidicus gigas* off the Peruvian Exclusive Economic Zone based on beak microstructure. Fish Sci 82:597–604

Iglesias J, Fuentes L (2014) *Octopus vulgaris*. Paralarval culture. In: Iglesias J, Fuentes L, Villanueva R (eds) Cephalopod culture. Springer, New York, NY, p 427–450

Iglesias J, Pazos G, Fernández J, Sánchez FJ and others (2014) The effects of using crab zoeae (*Maja brachydactyla*) on growth and biochemical composition of *Octopus vulgaris* (Cuvier 1797) paralarvae. Aquacult Int 22: 1041–1051

Iglesias P, Picón P, Nande M, Lago MJ, Otero JJ, Trujillo V, Iglesias J (2016) Effect of low salinity on survival and

ingested food of the common octopus, *Octopus vulgaris* Cuvier, 1797. J Appl Aquacult 28:267–271

Katsanevakis S, Verriopoulos G (2006) Seasonal population dynamics of *Octopus vulgaris* in the eastern Mediterranean. ICES J Mar Sci 63:151–160

Liu BL, Chen XJ, Chen Y, Hu GY (2015) Determination of squid age using upper beak rostrum sections: technique improvement and comparison with the statolith. Mar Biol 162:1685–1693

Mangold K (1983) *Octopus vulgaris*. In: Boyle PR (ed) Cephalopod life cycles, Vol 1. Species accounts. Academic Press, London, p 335–364

Mangold K, Boletzky SV (1973) New data on reproductive biology and growth of *Octopus vulgaris.* Mar Biol 19: 7–12

Media Cybernetics (2008) Package Image Pro Plus 6.3. www.mediacy.com

Meekan MG, Carleton JH, McKinnon AD, Flynn K, Furnas M (2003) What determines the growth of tropical reef fish larvae in the plankton: food or temperature? Mar Ecol Prog Ser 256:193–204

Meisel DV, Byrne RA, Kuba M, Griebel U, Mather JA (2003) Circadian rhythms in *Octopus vulgaris*. Coleoid cephalopods through time. Berl Paläobiol Abh 3:171–177

Morales-Nin B (1992) Determination of growth in bony fishes from otolith microstructure. Fish Tech Pap 322. FAO, Rome

Morales-Nin B (2000) Review of the growth regulation processes of otolith daily increment formation. Fish Res 46: 53–67

Nande M, Iglesias J, Domingues P, Pérez M (2017) Effect of temperature on energetic demands during the last stages of embryonic development and early life of *Octopus vulgaris* (Cuvier, 1797) paralarvae. Aquacult Res 48: 1951–1961

Navarro JC, Monroig Ó, Sykes AV (2014) Nutrition as a key factor for cephalopod aquaculture. In: Iglesias J, Fuentes L, Villanueva R (eds) Cephalopod culture. Springer, Dordrecht, p 77–95

Norman MD, Finn JK, Hochberg FG (2016) Family Octopodidae. In: Jereb P, Roper CFE, Norman MD, Finn JK (eds) Cephalopods of the world. An annotated and illustrated catalogue of cephalopod species known to date. Vol 3. Octopods and vampire squids. FAO Species Catalogue for Fishery Purposes. FAO, Rome, p 36–215

Olmos-Pérez L, Roura Á, Pierce GJ, Boyer S, González ÁF (2017) Diet composition and variability of wild *Octopus vulgaris* and *Alloteuthis media* (Cephalopoda) paralarvae: a metagenomic approach. Front Physiol, doi: 10.3389/fphys.2017.00321

Otero J (2006) Ecología del pulpo común (*Octopus vulgaris* Cuvier, 1797) en un área de afloramiento costero (Galicia, NE Atlántico). PhD thesis, University of Vigo

Oyadomari JK, Auer NN (2007) Influence of rearing temperature and feeding regime on otolith increment deposition in larval ciscoes. Trans Am Fish Soc 136:766–777

Perales-Raya C, Bartolomé A, García-Santamaría MT, Pascual-Alayón P, Almansa E (2010) Age estimation obtained from analysis of octopus (*Octopus vulgaris* Cuvier, 1797) beaks: improvements and comparisons. Fish Res 106:171–176

Perales-Raya C, Jurado A, Bartolomé A, Duque V, Carrasco N, Fraile-Nuez E (2014a) Age of spent *Octopus vulgaris* and stress mark analysis using beaks of wild individuals. Hydrobiologia 725:105–114

Perales-Raya C, Almansa E, Bartolomé A, Felipe BC and others (2014b) Age validation in *Octopus vulgaris* beaks across the full ontogenetic range: beaks as recorders of life events in octopuses. J Shellfish Res 33:481–493

R Core Team (2016) R: a language and environment for statistical computing. R Foundation for Statistical Computing, Vienna. www.r-project.org/

Reis DB, García-Herrero I, Riera R, Felipe BC and others (2015) An insight on *Octopus vulgaris* paralarvae lipid requirements under rearing conditions. Aquacult Nutr 21:797–806

Roura A (2013) Ecology of planktonic cephalopod paralarvae in coastal upwelling systems. PhD thesis, University of Vigo

Roura Á, González ÁF, Redd K, Guerra Á (2012) Molecular prey identification in wild *Octopus vulgaris* paralarvae. Mar Biol 159:1335–1345

Roura A, Álvarez-Salgado XA, González AF, Gregori M, Rosón G, Otero J, Guerra A (2016) Life strategies of cephalopod paralarvae in a coastal upwelling system (NW Iberian Peninsula): insights from zooplankton community and spatio-temporal analyses. Fish Oceanogr 25: 241–258

Sangrà P, Troupin C, Barreiro-González B, Desmond Barton E, Orbi A Arístegui J (2015) The Cape Ghir filament system in August 2009 (NW Africa). J Geophys Res Oceans 120:4516–4533

Semmens JM, Pecl GT, Villanueva R, Jouffre D, Sobrino I, Wood JB, Rigby PR (2004) Understanding octopus growth: patterns, variability and physiology. Mar Freshw Res 55:367–377

SPSS Inc (2008) SPSS statistics for Windows, Version 17.0 released 2008. Chicago, IL

Sweeney MJ, Roper CFE, Mangold K, Clarke MR, Boletzky SV (1992) 'Larval' and juvenile cephalopods: a manual for their identification. Smithsonian Contributions to Zoology No. 513. Smithsonian Institution Press, Washington, DC

Vaz-Pires P, Seixas P, Barbosa A (2004) Aquaculture potential of the common octopus (*Octopus vulgaris* Cuvier, 1797) a review. Aquaculture 238:221–238

Vidal EAG, Andrade JP, Villanueva R, Gleadall IG and others (2014) Cephalopod culture: current status of main biological models and research priorities. Adv Mar Biol 67:1–98

Villanueva R (1995) Experimental rearing and growth of planktonic *Octopus vulgaris* from hatching to settlement. Can J Fish Aquat Sci 52:2639–2650

Villanueva R, Norman MD (2008) Biology of the planktonic stages of benthic octopuses. Oceanogr Mar Biol Annu Rev 46:105–202

Xavier JC, Allcock AL, Cherel Y, Lipinski MR and others (2015) Future challenges in cephalopod research. J Mar Biol Assoc UK 95:999–1015

Editorial responsibility: Stephen Wing, Dunedin, New Zealand

Submitted: March 13, 2017; Accepted: May 30, 2017
Proofs received from author(s): August 11, 2017

Vol. 598: 261–272, 2018
https://doi.org/10.3354/meps12119

MARINE ECOLOGY PROGRESS SERIES
Mar Ecol Prog Ser

Published June 28[§]

Contribution to the Theme Section 'Innovative use of sclerochronology in marine resource management'

Statoliths of the whelk *Buccinum undatum*: a novel age determination tool

P. R. Hollyman[1,*], M. J. Leng[2], S. R. N. Chenery[3], V. V. Laptikhovsky[4], C. A. Richardson[1]

[1]School of Ocean Sciences, College of Natural Sciences, Bangor University, Menai Bridge, Anglesey LL59 5AB, UK
[2]NERC Isotope Geosciences Facilities, British Geological Survey, Nottingham NG12 5GG, UK
[3]Centre for Environmental Geochemistry, British Geological Survey, Nottingham NG12 5GG, UK
[4]Centre for Environment, Fisheries and Aquaculture Science (CEFAS), Pakefield Road, Lowestoft, Suffolk NR33 0HT, UK

ABSTRACT: Sustainability within the fisheries of the commercially important European whelk *Buccinum undatum* has become a major concern because of over-exploitation and increased landings in many European coastal shelf seas due to the expansion of export markets to East Asian countries. Current management of *B. undatum* populations is difficult to achieve as several life history traits are problematic to accurately monitor. The current method of age determination for stock assessment has a low success rate and focuses on the use of putative annual rings on the surface of the organic operculum. Here, we validate an annual periodicity of growth ring formation in *B. undatum* statoliths that provides an alternative, reliable and accurate method for determining a whelk's age. Laboratory-reared juvenile *B. undatum* of known provenance and age deposited a hatching ring at the time of emergence from their egg capsule and a clearly defined growth ring during February of their first and second years. Stable oxygen isotope profiles from the shells of 2 adult whelks confirmed annual growth ring deposition by demonstrating seasonal cycles of $\delta^{18}O$ in the shell that matched the relative position and number of visible growth rings in the statolith. Validation of annually resolved statolith growth rings will, for the first time, provide fisheries scientists with a tool to determine the age structure of *B. undatum* populations and allow analytical stock assessments that will enable informed decisions for future management practices of whelk fisheries.

KEY WORDS: *Buccinum undatum* · Statoliths · Age determination · Fisheries monitoring · Oxygen isotope · Raman spectroscopy · Sclerochronology

INTRODUCTION

The common whelk *Buccinum undatum* is a commercially important species of marine gastropod fished in the coastal waters of the UK and across Northern Europe. In 2015, the UK landings of *B. undatum* by UK vessels totalled 20 900 tonnes with a value at first sale of £18.7 million (MMO 2016). A large proportion of the whelk landings in the UK and Ireland supply an export market to East Asia that has grown steadily since the mid-1990s (Fahy et al. 2000) in response to recent increases in consumer demand which has driven the expansion of the fishery. However, declines in the number of whelks caught have been noted across European waters (Jersey, Shrives et al. 2015; Ireland, Fahy et al. 2005; North Sea/Netherlands, Ten Hallers-Tjabbes et al. 1996) and has caused several local Inshore Fishery and Conservation Authorities (IFCA) to implement restrictions recently on pot and/or catch limits and the number of permits issued (Devon & Severn IFCA 2016, Eastern IFCA 2016, Kent & Essex IFCA 2016).

A reliable assessment of age and longevity in *B. undatum* is problematic for fisheries scientists, because

*Corresponding author: p.hollyman@bangor.ac.uk
[§]Advance View was available online April 24, 2017

Publisher: Inter-Research · www.int-res.com

several of the species' life history traits are difficult to monitor at a population level. The lack of a planktonic larval stage and a relatively inactive adult lifestyle with no apparent migration (Pálsson et al. 2014) has led to the formation of discrete stocks which are vulnerable to overexploitation (Fahy et al. 2000). In many studies, these stocklets have been observed to show clear genetic and morphometric differences (e.g. Weetman et al. 2006, Shelmerdine et al. 2007, Magnúsdóttir 2010) including size at maturity, which can also differ markedly between sites (Haig et al. 2015, McIntyre et al. 2015, Shrives et al. 2015).

To resolve this conundrum, a reliable ageing method needs to be established for *B. undatum* so that accurate population age assessments and analytical stock assessments can be undertaken. The currently accepted method used by fisheries scientists, and validated by Santarelli & Gros (1985), determines the age of whelks by reading growth rings on the operculum, an organic 'shield' that is used to protect the shell aperture when the animal withdraws into its shell. This is achieved by matching cycles in oxygen isotope composition from the shell to the numbers of growth rings observed on the opercula. However, this method traditionally has had a low success rate owing to the poor clarity of the rings, a problem highlighted by Kideys (1996) who reported that only 16% of 10 975 opercula examined in whelks from the Isle of Man, UK, had 'clear and readable' rings, with a further 32% having 'readable' rings, leading to 48% of the samples being discarded. More recently, similar low levels of readability were found in several sites around the UK (Lawler 2013). The exclusion of large portions of samples due to poor clarity of the rings is likely to have biased the data; the constructed population growth curves were highly variable, presumably due to the ambiguity of the operculum readings.

Since whelks are becoming increasingly exploited, there is an urgent scientific need to underpin the fisheries stock assessment of their populations with accurate data concerning the age of individuals and their growth rates. For many mollusc species, the age of an individual can be determined by counting the annual growth lines present in longitudinal shell sections (See Richardson 2001 for review). This is particularly applicable to bivalve molluscs, but in gastropods it is not possible because there are often no obvious annual growth rings on or contained within their shells. Gastropod shells are also often problematic to analyse via sectioning as their coiled morphology makes it difficult to obtain a single clear growth axis using this technique.

Mollusc shells are repositories of information about the past environmental history of shell growth, and contain within the carbonate of their shells biogenic trace elements and oxygen isotopes at ratios ($^{18}O/^{16}O$, described as $\delta^{18}O$) which are incorporated into the shell matrix at equilibrium during mineralisation (Wilbur & Saleuddin 1983, Wheeler 1992). Seawater temperature at the time of shell formation can be reconstructed from the gastropod shell throughout ontogeny by determining $\delta^{18}O$ along the growing axis of the shell (e.g. *Rapana venosa*, Kosyan & Antipushina 2011 and *Conus ermineus*, Gentry et al. 2008). The empirical fractionation of oxygen isotopes in mollusc carbonates with changes in temperature are well known (e.g. Epstein et al. 1953). Oxygen isotopes are sourced from H_2O and CO_2 during shell formation (Leng & Lewis 2016); more negative values of $\delta^{18}O$ reflect warmer seawater temperatures whilst more positive values are indicative of cooler seawater temperatures (Grossman & Ku 1986) at a constant $\delta^{18}O$ of seawater. Sampling the shell carbonate at known intervals along the whorled axis of the shell and determining seasonal changes in $\delta^{18}O$ allows the age (seasonality) of the shell to be determined. This approach, however, is not suitable for large-scale ageing of whelk due to the cost of analysing the potentially huge numbers of samples needed to accurately reconstruct seasonality across a significant number of shells.

In lieu of being able to directly use the shells or opercula to estimate age, an alternative age registering structure was sought; whelks contain an accretory hard structure called a statolith which is the focus of this paper. Statoparticles (such as statoliths) are structures that are integral to the nervous system of a diverse range of animal groups including the Polychaeta (Beesley et al. 2000), Holothuroidea (Ehlers 1997), Crustacea (Espeel 1985) and several classes of the Mollusca e.g. the Bivalvia (Morton 1985), Gastropoda (Barroso et al. 2005, Chatzinikolaou & Richardson 2007, Galante-Oliveira et al. 2013) and Cephalopoda (Arkhipkin 2005). These structures are used in gravity perception and are contained within a statocyst, which detects movement of the statoparticle indicating a change in orientation (Chase 2002). Commonly composed of calcium carbonate, they have a wide-ranging morphology across the phylum in which they are found. The statoparticles of gastropods (called statoliths) are often singular, roughly spherical granules (Richardson 2001, Galante-Oliveira et al. 2013). Gastropod statoliths can contain rings that are deposited annually (e.g. *Nassarius reticulatus*, Barroso et al. 2005; *Neptunea*

antiqua, Richardson et al. 2005b; *Polinices pulchellus*, Richardson et al. 2005a) and are an archive of biota life history, containing information about age and seasonal temperature cycles (Richardson et al. 2005a, Galante-Oliveira et al. 2015) and their transition from a planktonic pelagic larval lifestyle to a benthic existence (Barroso et al. 2005, Richardson et al. 2005a, Chatzinikolaou & Richardson 2007). Once the rings in the statolith have been deciphered, information about a gastropod's life history can be extracted to understand its ontogenic growth. Thus, these structures are potentially an invaluable resource for fisheries scientists, who could use this information to assess population age structure of commercially important gastropod species such as *B. undatum*.

Here we demonstrate, for the first time, that growth rings in the statoliths of *B. undatum* are annually deposited like those within the opercula, and can be used for the reliable age estimation of the species. The timing of statolith growth ring formation was determined in whelks of known age and life history that had been reared in the laboratory under ambient seawater temperatures for 2 yr following their emergence from egg capsules. The structure of the statoliths was also investigated to determine general morphology and mineralogical composition. We then used shell $\delta^{18}O$ profiles drilled from around the whorl and compared these data with the matching whelk statolith growth lines.

MATERIALS AND METHODS

Field collection

Approximately 200 whelks (>25 mm shell length) were trapped and collected in February 2015 from a site in the Menai Strait (North Wales, UK; 53.235556°, –4.141835°, depth 10 to 11.5 m) using a string of 3 baited scientific inkwell pots laid for 24 h. The drainage holes in the pots were covered with 3 mm mesh and the whelk catch was not riddled (a process used by fishermen to remove undersized whelks) to ensure all size classes were retained for analysis. Dispensation for the landing of undersized whelks (<45 mm) was granted by the Welsh Government (disp#004). Once collected, whelks were frozen until required, whereupon they were thawed and the body removed from the shell using forceps to gently pull the foot and detach the collumellar muscle. Shell height (aperture to spire length) was measured to the nearest 1 mm using Vernier callipers, total body weight was recorded to the nearest 0.1 g and reproductive maturity was assessed using the scale of Haig et al. (2015). The body of each whelk was re-frozen for later statolith extraction.

Laboratory experiment

This experiment was designed to study the formation of the whelk statolith during ontogeny and to determine the timing of growth ring formation. Seven whelk egg masses that had been laid naturally in an intertidal location at Tal-y-Foel (53.158512°, –4.279493°) in the Menai Strait were collected in November 2013 and 2014. Egg masses were transported to the laboratory and held in aquaria supplied with flowing ambient seawater from the Menai Strait. Approximately 2 mo later, juvenile whelks hatched directly from the egg capsules and were reared for 1 yr (2014 hatching) and 2 yr (2013 hatching) under an approximate 10 h light:14 h dark cycle, being fed regularly thrice weekly with small pieces of frozen and thawed mackerel *Scomber scombrus*. Each month for 24 mo, 10 whelks were removed and frozen for later statolith extraction.

Statolith extraction and ageing

Selected individuals of the frozen field-caught adult and laboratory-reared juvenile whelks were thawed (3 h) and their bodies bisected (see Fig. 1a). Each half of the whelk body was examined under a low-power binocular microscope to locate, dissect and remove, using fine forceps (0.10 × 0.06 mm tip), a pair of statocyst sacs (left and right side), each containing a statolith (see Fig. 1b). Incident illumination as well as transmitted light were used during the dissections and highlighted the statoliths as small shadows beneath the cerebral ganglion (see Fig. 1c). The <0.75 mm statocysts were transferred to a watch glass with a drop of Milli-Q® ultrapure water (Merck Millipore), then torn open and the statoliths removed using a hypodermic needle (0.5 mm diameter). Where necessary, each statolith was cleaned of any adhering tissue by immersion in 20% sodium hydroxide (NaOH) for 30 min and rinsed in Milli-Q® quality water. Once the statoliths had air-dried they were mounted on a microscope slide using Crystalbond™ 509 thermoplastic resin and imaged under a Meiji Techno MT8100 microscope with a Lumenera Infinity 3 microscope camera at 40× magnification. This allowed visualisation of the statolith growth rings,

which could then be counted and the statolith diameters measured using ImageJ v.1.48 (Ferreira & Rasband 2012) (see Fig. 2).

Scanning electron microscopy

Several statoliths from the right and left side of small and large whelks were selected for structural analysis. Each statolith was mounted in Crystalbond™ 509 on an aluminium scanning electron microscopy (SEM) stub and imaged as above. The statolith was ground by hand to the central plane using progressively finer 400, 1200, 2500 and 4000 silicon carbide grinding papers lubricated with Milli-Q® quality water. Each statolith was finally polished with a 1 µm diamond suspension gel and thoroughly cleaned with detergent and water and dried before submersion in 0.1 M hydrochloric acid for 2 min to etch the exposed statolith surface. The exposed and etched statolith surfaces were then imaged using a FEI QUANTA 600 environmental SEM operated in low vacuum mode, with an electron beam accelerating voltage of 12.5 to 15 kV, a beam probe current of 0.14 to 0.26 nA, and a working distance of 10.6 to 10.9 mm.

Micro-Raman spectroscopy

Micro-Raman spectroscopy (MRS) allows differentiation between the polymorphs of $CaCO_3$ (amorphous $CaCO_3$, calcite, aragonite and vaterite) by focussing a laser light onto the statolith surface. Inelastic scattering of the incident light occurs after contact with the sample structure due to interaction with the vibrational levels of the composite molecules causing a shift in the wavelength of the measured scattered photons (Raman shift) (Higson 2006). The wavelength shifts of the spectra are predictable in position and intensity for different substances. For $CaCO_3$, 2 main wavelength regions of the spectra are of interest: peaks in the 100 to 350 cm^{-1} range pertain to interaction with features of the external lattice structure, whereas peaks in the 600 to 1800 cm^{-1} range relate to interactions with the internal molecular planes (Parker et al. 2010). To determine the statolith composition, individual statoliths were fractured using fine-tipped forceps (0.10 × 0.06 mm tip) to reveal the inner growth axis and analysed with MRS (Reinshaw InVia Raman-Microscope) at the Diamond Light Source, Harwell, UK. The MRS consisted of a 473 nm laser at a power of 15 mW and was focussed using a lens with a magnification of 20×; a grating with 2400 lines mm^{-1} and a pinhole size of 100 µm were used for spectra acquisition. The spectra were acquired between 100 and 3200 cm^{-1}. Three sample spots were taken approximately equidistant along the interior growth axis of 3 statoliths from the central nucleus to the outer edge, although the results from only 1 statolith are presented. Synthetic calcite and speleothem aragonite standards (Brinza et al. 2014) were analysed prior to and after statolith analyses and the resulting Raman spectra were adjusted using a polynomial background correction. Following MRS, the fractured statolith surface was imaged using SEM to obtain a detailed image of the sampled surface.

Isotope ratio mass spectrometry

The outer periostracum and any adhering material were cleaned from the shells of an adult male and female whelk collected from the Menai Strait using a stiff-bristled brush and tap water, and then air-dried. The shell surface was abraded using a 1 mm diamond burr attached to a Dremel® 4000 rotary tool to remove any contamination from the shell surface. A sampling axis around the entire whorled growth was marked out close to the shoulder of the shell whorl with 1 mm notations along its length. Tracks (1 × 10 mm) were drilled at a resolution of 2 mm at the apex and most recently formed whorl, the oldest and youngest parts of the shell, and at 4 mm for the central portion where growth is fastest, in line with the visible growth striations. Care was taken to only sample the outer prismatic layer of the shell and not drill into the inner nacreous layers, which are deposited at a later time. The drilled $CaCO_3$ samples were collected on small square (2 × 2 cm) sheets of greaseproof paper transferred to a labelled 0.5 ml Eppendorf tube. This sampling strategy was extended as close to the tip of the shell as possible; however, in all cases the earliest shell growth (top 1 to 1.5 cm) could not be sampled owing to shell damage and resolution of drilling.

Approximately 50 to 100 µg of powdered carbonate sample were used for isotope analysis using an IsoPrime dual inlet mass spectrometer plus multiprep device (at the British Geological Survey). Weighed samples were added to glass vials which were then evacuated, and anhydrous phosphoric acid (H_3PO_4) was added to each sample at 90°C. The samples were left to digest for 15 min and the expressed gas was collected, cryogenically cleaned to remove any mois-

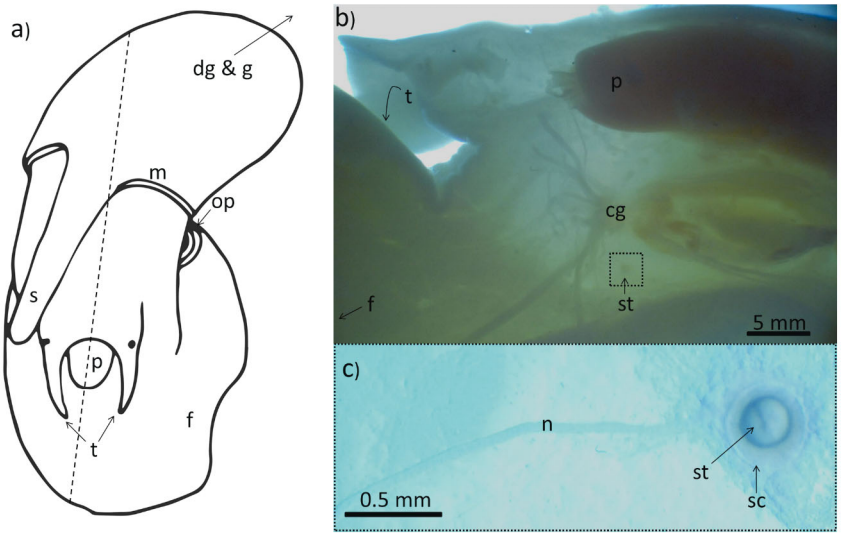

Fig. 1. (a) Ventral view of a female *Buccinum undatum* removed from its shell, showing the siphon (s), mantle (m) proboscis (p), operculum (op), foot (f), and tentacles (t) (the digestive gland [dg] and gonad [g] are out of frame). Dashed line: bisection of the whelk. (b) Half a bisected *B. undatum* illuminated using transmitted light and viewed in a dissection microscope, showing the cerebral ganglion (cg) and statolith (st). Dotted line: area of interest shown in (c). (c) A statolith following removal, showing nerve (n), statolith (st) and statocyst (sc)

ture and passed into the mass spectrometer. Isotope values ($\delta^{13}C$, $\delta^{18}O$) are reported as per mille (‰) deviations of the isotopic ratios ($^{13}C/^{12}C$, $^{18}O/^{16}O$) calculated to the VPDB scale using a within-run laboratory standard (KCM) calibrated against NBS-19. The aragonite-acid fractionation factor applied to the gas values was 1.00855 (Sharma & Clayton 1965). A drift correction was applied across the run, calculated using the standards that bracket the samples. The Craig correction was also applied to account for the influence of $\delta^{17}O$ within the sample (Craig 1957). The average analytical reproducibility of the standard calcite (KCM) is 0.05‰ for $\delta^{13}C$ and $\delta^{18}O$. The resulting ($^{18}O/^{16}O$ ratio) data were treated with a 5-point Savitsky-Golay smoothing filter (Steinier et al. 1972). The $\delta^{13}C$ data are not presented here.

RESULTS

Statolith location and morphology

Each whelk has 2 statocysts in the tissues of its foot, and each statocyst contains a single roughly spherical statolith (<0.75 mm in diameter) (Fig. 1b). Orientation of the statolith in resin in a dorsal-ventral position shows a circular outline shape and is the optimum position to view and measure the visible growth rings (Fig. 2a). Laterally, the statolith has an oval shape (Fig. 2b) and has a dorso-ventrally compressed spherical shape where the rings are less clear. Thus, to maintain consistency and to maximise the visibility of the rings, all analyses/images were undertaken from statoliths orientated in a dorsal-ventral view.

The relationship between statolith diameter and shell length was shown to display a power relationship (Fig. 3a). This was investigated further using the 'smatr' package (Wharton et al. 2015) in R to analyse the $\log_{10}$ transformations of each variable (Fig. 3a inset). A significant correlation was found between the 2 variables ($p < 0.001$) with a slope of 0.438 (lower and upper 95% CI: 0.432 and 0.443 respectively). This shows the relationship has negative allometry, indicating that statoliths and shells do not grow proportionally. Instead, the growth of the statoliths decreases in comparison to the shell length over time. This results in smaller whelks having proportionally larger statoliths in comparison to shell length. The data in Fig. 3a closely fit the line for whelks <60 mm, allowing estimates of shell length to be determined from the diameter of the rings. However, above this size there is wide variation in statolith diameter. By measuring the

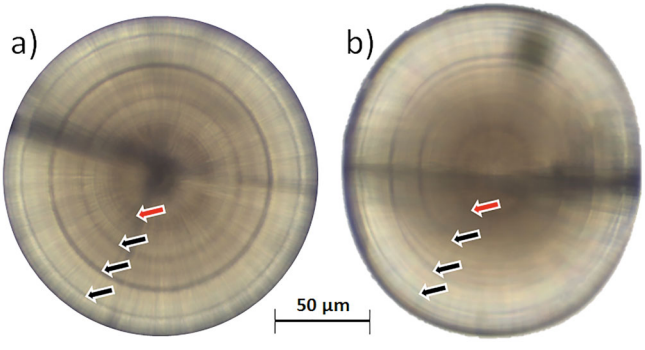

Fig. 2. Photomicrographs of 2 statoliths removed from an individual *Buccinum undatum* collected from the Menai Strait. (a) Dorso-ventral view; (b) lateral view. Annual growth rings are marked with arrows and hatching rings with red arrows in each statolith orientation

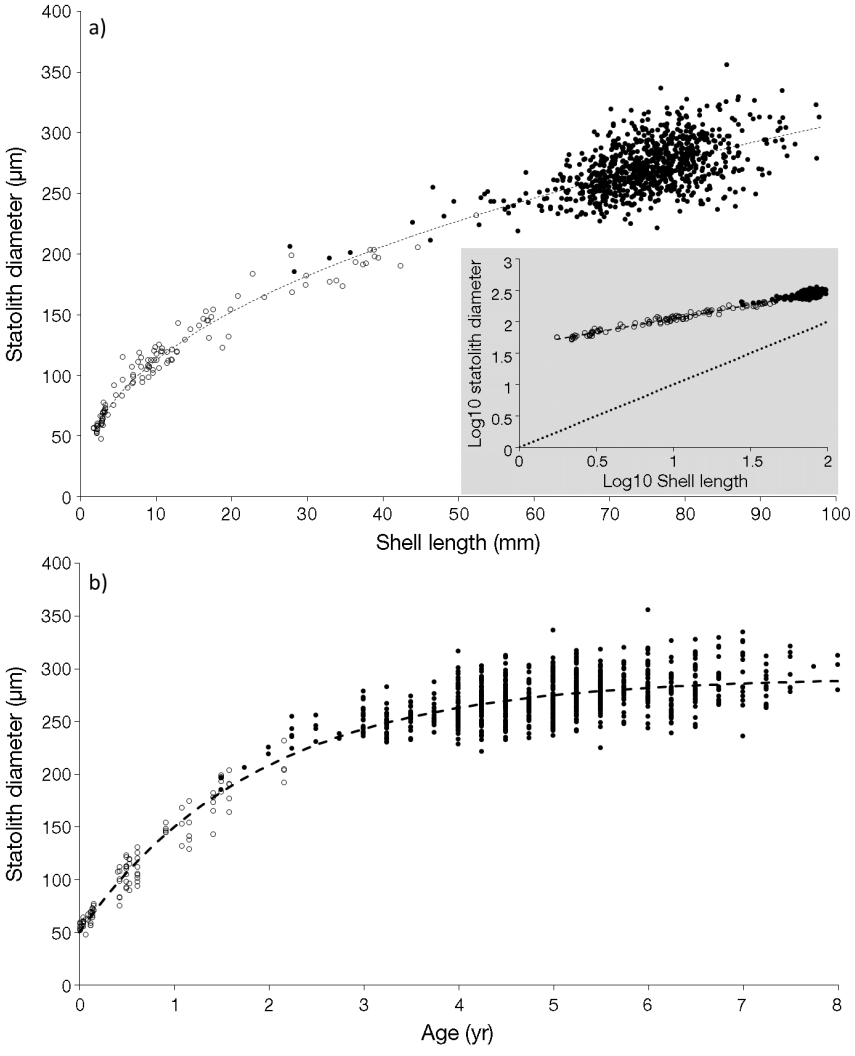

Fig. 3. (a) Relationship between *Buccinum undatum* shell length and statolith diameter, showing field-collected whelks (filled circles), and laboratory-reared juveniles (empty circles), fitted with a power function line (dotted line; $y = 41.38 \times x^{0.4354}$; $R^2 = 0.96$). Inset: scatterplot showing the relationship between $\log_{10}$ statolith diameter and $\log_{10}$ shell length of field-collected individuals (filled circles), and laboratory-reared juveniles (empty circles). The slope of the linear relationship (dashed line) is 0.43 ($R^2 = 0.96$). Dotted line represents an isometric relationship. (b) Scatterplot showing the relationship between statolith diameter and age, constructed from statolith rings from field-collected (filled circles) and laboratory-reared animals of known age (empty circles), fitted with a von Bertalanffy growth curve ($R^2 = 0.90$). n = 931 for all plots

statolith diameter at successive rings for whelks <60 mm it is feasible to reconstruct shell length at each ring. Fig. 3b shows the relationship between statolith diameter and age (ascertained from statolith rings in field-caught whelks), fitted with a von Bertalanffy growth curve ($R^2 = 0.90$). Although it is a strong relationship, there are large amounts of overlap between ages. The clarity of the statoliths was also very high, with the vast majority of samples included in the analysis (n = 800). In total, 48.6% of the samples were classed as 'clear and readable' and a further 43% as 'readable (using the same criteria as Kideys 1996), thus only 8.4% of samples were excluded.

Statolith structure

The broken statolith shown in Fig. 4a is composed of aragonite. All 3 of the analysed statoliths displayed the characteristic peaks for aragonite. The Raman spectra extracted between 100 and 750 cm^{-1} demonstrate a coincidence of peaks at 151, 183 and 206 cm^{-1} and a wide peak at 702 to 706 cm^{-1}, for the 3 sample spots from the statolith as well as the aragonite standard (Fig. 4b). A shoulder is also visible on the 151 cm^{-1} peak at 143 cm^{-1}. By contrast, the calcite standard peaks at 155, 281 and 712 cm^{-1} indicate that this statolith contains no trace of calcite. Fig. 4c shows an additional peak between 2850 and 3000 cm^{-1} for the 3 sample spots. Peaks in this range are thought to be indicative of C–H functional groups found within organic matter (Smith & Dent 2005), and thus are likely indicative of the presence of an organic component within the crystal matrix. Fig. 5 shows the agreement between the visible rings in the optical microscope (OM) image of a whole statolith (Fig. 5a) and the exposed acid-etched SEM image of the central plane of the paired statolith (Fig. 5b). The clarity of the rings in Fig. 5b suggests that a clear structural change has occurred during the formation of a growth ring.

Hatching ring and growth ring formation

The inner opaque area seen in Fig. 5a signifies the period of development in the egg culminating in the formation of a hatching ring. The hatching ring can also be seen and appears in January when these animals hatched (Fig. 6a–d). For the 2013 juvenile cohort, the hatching ring was deposited at a statolith

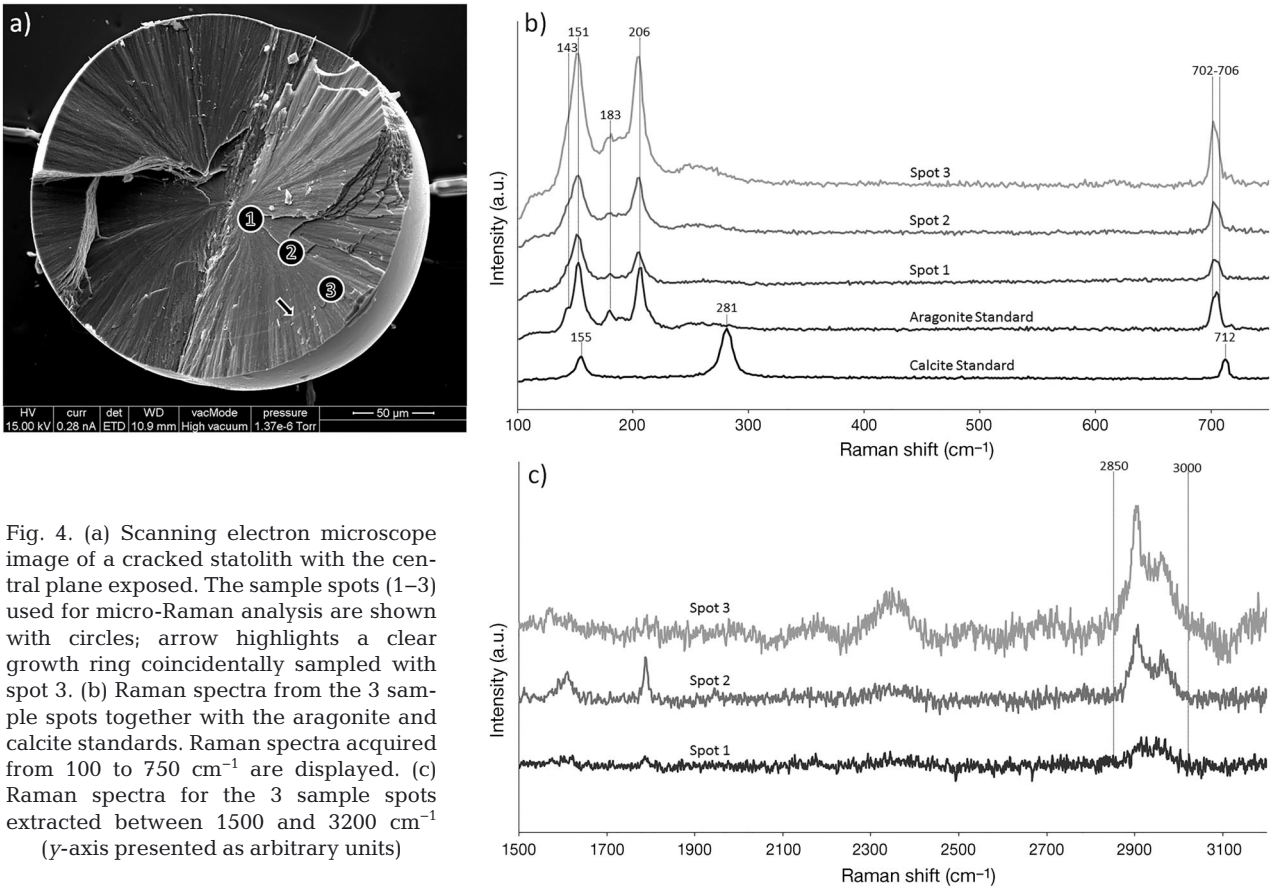

Fig. 4. (a) Scanning electron microscope image of a cracked statolith with the central plane exposed. The sample spots (1–3) used for micro-Raman analysis are shown with circles; arrow highlights a clear growth ring coincidentally sampled with spot 3. (b) Raman spectra from the 3 sample spots together with the aragonite and calcite standards. Raman spectra acquired from 100 to 750 cm^{-1} are displayed. (c) Raman spectra for the 3 sample spots extracted between 1500 and 3200 cm^{-1} (*y*-axis presented as arbitrary units)

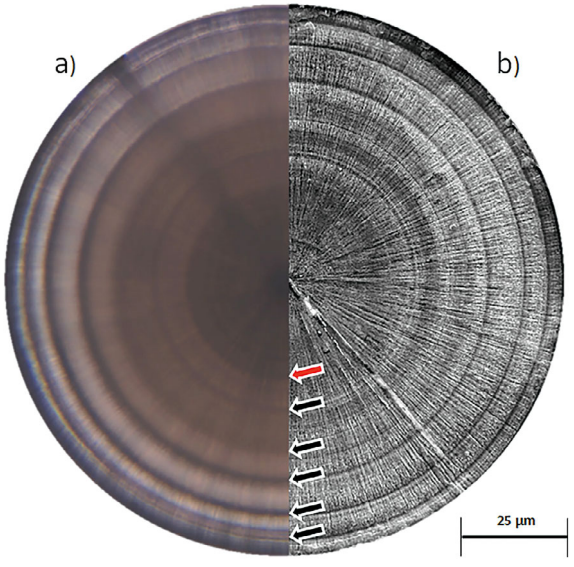

Fig. 5. Composite image of 2 statoliths from the same *Buccinum undatum* specimen. (a) Photomicrograph of an extracted and mounted left hand statolith imaged using optical microscopy; (b) scanning electron microscope image of the matching right hand statolith that has been resin-mounted, ground to the central plane, polished and etched. Annual growth rings highlighted with black arrows, hatching ring highlighted with red arrow

diameter of 53.6 ± 4 µm (mean ±1 SD, n = 30) and for the 2014 cohort, at 55.1± 6 µm (n = 30). The data from the 2 cohorts were not significantly different (independent *t*-test, p = 0.1). The central opaque area (larval growth) seen in Fig. 5a is surrounded by a less opaque region containing weak and diffuse rings. This pattern is also mirrored in Fig. 6, which shows the ontogenetic development of statoliths removed from laboratory-reared animals of different ages between 2 wk and 2 yr. Clear disturbance rings can be seen in the increment following hatching ring deposition and are a common feature of adult statoliths. The clear Year 1 ring in the statolith in Fig. 6d marks a colour change from brown to light brown and was deposited in February during the coldest part of the annual temperature cycle. A similarly positioned ring can be seen in Fig. 5a, signifying the first annual ring formation. The colour change is regularly seen in statoliths taken from field-caught adult whelks and is a good indicator of the position of the first annual growth ring. Following deposition of the slightly unclear first annual ring, subsequent annual rings are clearly delineated in both OM and SEM images (Fig. 5a,b). Disturbance rings (a common fea-

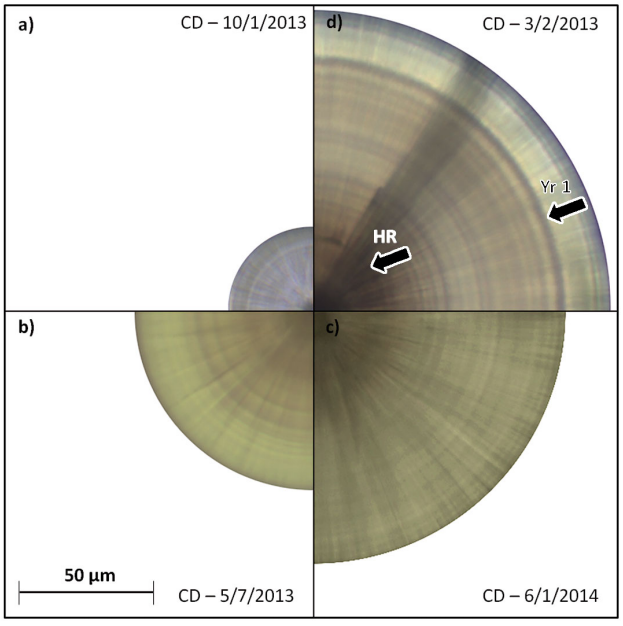

Fig. 6. Composite image showing seasonal juvenile statolith development at (a) 2 wk after hatch, (b) 6 mo after hatch, (c) 1 yr after hatch and (d) 2 yr after hatch. In all cases the hatching ring (HR) is visible, as are multiple faint disturbance lines. The 1 yr ring (Yr 1) is also visible in the image from the 2 yr old individual. CD: collection date (d/mo/yr)

ture of the statoliths in younger whelks) are typically much weaker in definition than the clear annually-resolved rings.

Annual growth ring validation

Fig. 7 shows the coincidence between statolith ring position (Fig. 7c,f) and maximum values in the shell $\delta^{18}O$ cycles (Fig. 7a,d). Maximum $\delta^{18}O$ represents minimum seawater temperatures. The 3 $\delta^{18}O$ minima in the female shell (Fig. 7a) match the position of the 3 statolith rings (Fig. 7c) and the 4 maxima seen in the male shell (Fig. 7d) match the 4 statolith rings (Fig. 7f). In both shells, the tip of the apex was not sampled, represented by the grey hatched area in Fig. 7a,d; the point at which sampling ceased is indicated by a black arrow (Fig. 7b,e).

DISCUSSION

This study validates, for the first time, the annual periodicity of growth rings found within the statoliths of the common whelk, *Buccinum undatum*, as well as investigating their structure and composition. This was achieved using a combination of laboratory rearing of juvenile specimens and geochemical analysis of both statoliths and shells from wild-collected adults. The validation of the annual growth lines as a reliable ageing tool will provide an alternative to the currently used and often unreliable operculum.

Visualization, interpretation and timing of statolith ring formation

In a previous study following extraction and statolith cleaning, Richardson et al. (2005a) hand-ground and polished the statoliths of the neogastropd *Neptunea antiqua* to observe the growth rings. However in the current study, when *B. undatum* statoliths were hand-ground (using the above-described methods for SEM preparation) and observed in the optical transmitted light microscope, weaker disturbance rings became more apparent and often obscured the earliest annual growth rings due to the removal of the overlying statolith structure, which often masked them. However, when a whole statolith was observed the weaker lines were less apparent; this approach was adopted throughout the study.

A single, clear growth ring was deposited annually within the statoliths of the laboratory-reared juveniles during February and March when seawater temperatures were minimal in the Menai Strait. Female *B. undatum* lay egg capsules in which larvae develop, and juveniles hatch directly, leaving their egg capsules without a planktonic larval stage. The first identifiable diffuse statolith ring deposited can be termed a 'hatching ring', which is formed as the juveniles emerge from their capsules. The hatching ring has a similar position in the statolith to the settlement ring in statoliths from *Polinices pulchellus* (Richardson et al. 2005b) and *Nassarius reticulatus* (Barroso et al. 2005, Chatzinikolaou & Richardson 2007), which hatch from egg capsules and undergo a planktonic larval existence prior to settlement. Thus, importantly, these 2 kinds of juvenile rings in gastropods with different early life strategies represent the same life history event i.e. the transition from larvae to juvenile. Whilst hatching ring diameters in reared *B. undatum* juveniles are fairly constant (53.6 to 55.1 µm), it has been shown that maternal size directly influences egg capsule size and subsequent juvenile hatching size, which in turn can also be mediated by intra-capsular cannibalism (Nasution 2003, Nasution et al. 2010, Smith & Thatje 2013). Therefore, in a population with larger than average sized whelks, the hatching ring will be larger than the average observed here. A strong relationship

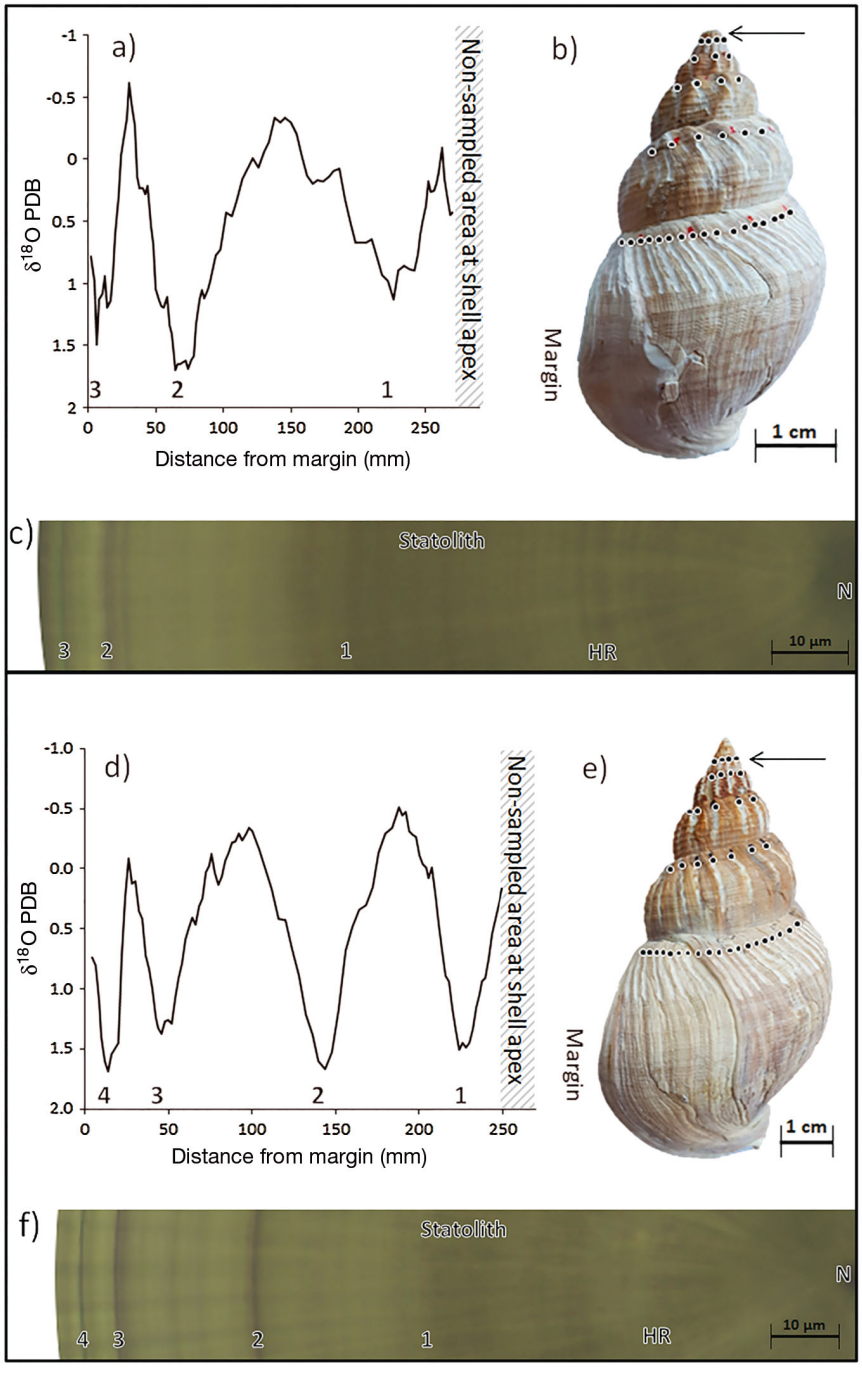

Fig. 7. Comparison of the shell $\delta^{18}O$ profiles with the associated statolith for 2 *Buccinum undatum*. (a) $\delta^{18}O$ profile from the shell of a female *B. undatum*; note that the *y*-axis is inverted to show the position along the shell of the positive peaks in the $\delta^{18}O$ cycles (coldest seawater temperatures, highlighted with numbers). The data were smoothed using 5-point Savitsky-Golay filter. (b) The shell drill-sampled for the data in (a); visible drill tracks are highlighted with red marks; black arrow denotes where sampling at the apex ceased. This non-sampled area corresponds to the hatched area in (a). The shell tip of this specimen was lost due to damage. (c) Photomicrograph of the matching statolith from the individual in (a) and (b), showing the nucleus (N), hatching ring (HR) and annual bands (numbers). (d–f) shows the same as (a–c) respectively for an older male specimen

exists between statolith diameter and shell length; however, the wide variation in statolith diameters that exists in large (>60 mm) and older whelks means that it is not possible to estimate an older whelk's age solely from statolith size. The age of each whelk must be determined by counting the number of annually resolved statolith rings. The annual periodicity of the growth rings was further validated with the reconstruction of $\delta^{18}O$ profiles from shells (Fig. 7). This is the same method used by Santarelli & Gros (1985) to validate the observable growth rings in the opercula. However, in this study a higher sampling resolution was used, producing more clearly defined $\delta^{18}O$ cycles that are directly overlaid on the visible growth rings of the statolith. Santarelli & Gros (1985) did not demonstrate the ages of the animals from the opercula.

Statolith composition

The statoliths of *B. undatum* are composed of aragonite, as shown by Raman spectra indicating no visible trace of calcite. There was close agreement between the aragonite standard and the sample spots taken from the statolith, although several of the reported Raman spectra peaks differed by 1 to 3 cm^{-1} compared with those reported in the literature (see Parker et al. 2010). It is probable that this difference between the observed statolith spectra peaks and the published spectra was caused by the presence of trace elements such as Mg^{2+} substituting for Ca^{2+} within the lattice and distorting it (Parker et al. 2010). This would explain why the synthetic calcite standard exhibited all of the expected peaks whereas the sample spots and the speleothem aragonite standard (which can contain trace elements; Finch et al. 2001) did not. The Raman spectra of the sample spots also exhibited a diffuse band between 2850 and 3000 cm^{-1}, which likely indi-

cates the presence of structural organic matter within the $CaCO_3$ matrix. All 3 of the spot samples showed a peak in the spectra, likely indicating the presence of organic matter throughout the statolith matrix, although the most intense peak was observed when the structure of a growth ring was coincidentally analysed (spot 3 on the statolith). A similar conclusion was reached by Galante-Oliveira et al. (2014) who observed similar spectra in the statoliths of *Nassarius reticulatus*. If the Raman peaks represent differences in the concentration of organic matter present in different parts of the statolith, then this will aid in interpreting the distribution of elements such as Sr and Mg in the statolith. In *N. reticulatus*, annual cycles of Sr:Ca ratios were found to correspond with the visible growth rings (Galante-Oliveira et al. 2015) with minimum ratios associated with the rings and maximum concentrations present in the increments between adjacent rings. Schöne et al. (2010) demonstrated the role of organic material in bivalve shells in regulating the control of biogenic element incorporation into the shell structure, highlighting that insoluble organic matter present in the aragonitic shell of *Arctica islandica* is significantly enriched in Mg and depleted in Sr.

Implications for fisheries

With the development of this ageing technique for such a commercially important species, the construction and comparison of population growth curves can be easily implemented on a potentially large scale. Vast improvements over the operculum age determination method have been shown, with a decrease in discarded samples from 48 to 8.4% and an increase in useable samples from 52 to 91.6%. Whilst the methodology for statolith extraction and analysis is potentially more time consuming than the use of opercula, the huge increase in reliability and decrease in potential sample bias (from large discards) is clear.

CONCLUSIONS

Here, an annually resolved periodicity of growth ring formation in whole resin-mounted statoliths from *Buccinum undatum* was validated by comparison with seasonally collected and laboratory-reared juvenile whelks of known age, and from similarities between growth rings and the $\delta^{18}O$ cycles in their shells. This validated, novel age determination tool (using statoliths) can be used to accurately reconstruct the population structure and population growth rates of *B. undatum*, and the technique will now be available for fisheries scientists to undertake stock assessments of whelk populations European-wide to determine both size-at-age and age at reproduction. These are both metrics that will aid in future management decisions. The statoliths present a viable alternative to the 'difficult to use' opercula. *B. undatum* statoliths are composed of aragonitic calcium carbonate and their structure, determined by Raman-Microscopy, has revealed variations in organic matter throughout the statolith that might have implications for the way in which biogenic elements are incorporated into the organic lattice of the statolith. Overall, we conclude that understanding differences in the age, growth rate and distributions of whelks in coastal waters will add immeasurably to our understanding of how to manage and conserve these important scavengers in coastal zones.

Acknowledgements. This work was supported through a Bangor University/CEFAS partnership PhD scholarship to P.R.H. We are grateful to Gwynne Parry-Jones for collecting *Buccinum undatum* from the Menai Strait. The IRMS analyses were supported by a NERC Isotope Geosciences Facilities Steering Committee (IP-1527-0515) award, and thanks to Hilary Sloane for technical support. Access to the Reinshaw Raman-Microscope was made possible through a rapid access request to the Diamond Light Source (SP13616-1). Production of the SEM micrographs would not have been possible without the help of Dr. Lorraine Field (BGS) and Dr. Andy Marriott (BGS). A number of colleagues and students, Richard Patton, Charlotte Colvin, Helèna Bonici, Anton Antonov and Devaney Werrin are acknowledged for their invaluable help with animal husbandry. We also thank Dr. Ewan Hunter and Dr. Andy Marriott, and 3 anonymous reviewers whose comments greatly improved the manuscript. M.J.L. and S.R.N.C. publish with the permission of the Director British Geological Survey (BGS); P.R.H. is registered as a BUFI student within BGS.

LITERATURE CITED

Arkhipkin AI (2005) Statoliths as 'black boxes' (life recorders) in squid. Mar Freshw Res 56:573–583

Barroso CM, Nunes M, Richardson CA, Moreira MH (2005) The gastropod statolith: a tool for determining the age of *Nassarius reticulatus*. Mar Biol 146:1139–1144

Beesley PL, Ross GJB, Glasby CJ (eds) (2000) Polychaetes and allies: the southern synthesis. Fauna of Australia, Vol 4A: Polychaeta, Myzostomida, Pognophora, Echiura, Sipuncula. CSIRO publishing, Melbourne

Brinza L, Schofield PF, Mosselmans JFW, Donner E, Lombi E, Paterson D, Hodson ME (2014) Can earthworm-secreted calcium carbonate immobilise Zn in contaminated soils? Soil Biol Biochem 74:1–10

Chase R (2002) Behaviour and its neural control in gastropod molluscs. Oxford University Press, New York, NY

Chatzinikolaou E, Richardson CA (2007) Evaluating the growth and age of the netted whelk *Nassarius reticulatus* (Gastropoda: Nassaridae) from statolith growth rings. Mar Ecol Prog Ser 342:163–176

Craig H (1957) Isotopic standards for carbon and oxygen and correction factors for mass spectrometric analysis. Geochim Cosmochim Acta 12:133–149

Devon & Severn IFCA (Inshore Fisheries and Conservation Authority) (2016) www.devonandsevernifca.gov.uk/devon-severn-ifca-whelk-research-2016 (accessed 1 Jul 2016)

Eastern IFCA (2016) www.eastern-ifca.gov.uk/emergency-whelk-byelaw/ (accessed 1 Jul 2016)

Ehlers U (1997) Ultrastructure of the statocysts in the apodous sea cucumber *Leptosynapta inhaerens* (Holothuroidea, Echinodermata). Acta Zool 78:61–68

Epstein S, Buchsbaum JR, Lowenstam HA, Ukey HC (1953) Revised carbonate-water isotopic temperature scale. Geol Soc Am Bull 64:1315–1326

Espeel M (1985) Fine structure of the statocyst sensilla of the mysid shrimp *Neomysis integer* (Leach, 1814) (Crustacea, Mysidacea). J Morphol 186:149–165

Fahy E, Masterson E, Swords D, Forrest N (2000) A second assessment of the whelk fishery *Buccinum undatum* in the southwest Irish Sea with particular reference to its history of management by size limit. Irish Fisheries Investigations 6, Marine Institute, Dublin

Fahy E, Carroll J, O'Toole M, Barry C, Hother-Parkes L (2005) Fishery associated changes in the whelk *Buccinum undatum* stock in the southwest Irish Sea, 1995–2003. Irish Fisheries Investigations 15, Marine Institute, Dublin

Ferreira T, Rasband W (2012) ImageJ user guide–IJ 146r. National Institutes of Health, Bethesda, MD. https://imagej.nih.gov/ij/docs/guide/

Finch AA, Shaw PA, Weedon GP, Holmgren K (2001) Trace element variation in speleothem aragonite: potential for palaeoenvironmental reconstruction. Earth Planet Sci Lett 186:255–267

Galante-Oliveira S, Marçal R, Ribas F, Machado J, Barroso C (2013) Studies on the morphology and growth of statoliths in Caenogastropoda. J Molluscan Stud 79:340–345

Galante-Oliveira S, Marçal R, Guimarães F, Soares J, Lopes JC, Machado J, Barroso C (2014) Crystallinity and microchemistry of *Nassarius reticulatus* (Caenogastropoda) statoliths: towards their structure stability and homogeneity. J Struct Biol 186:292–301

Galante-Oliveira S, Marçal R, Espadilha F, Sá M, Abell R, Machado J, Barroso C (2015) Detection of periodic Sr Ca^{-1} cycles along gastropod statoliths allows the accurate estimation of age. Mar Biol 162:1473–1483

Gentry DK, Sosdian S, Grossman EL, Rrosenthal Y, Hicks D, Lear CH (2008) Stable isotope and Sr/Ca profiles from the marine gastropod *Conus ermineus*: testing a multiproxy approach for inferring paleotemperature and paleosalinity. Palaios 23:195–209

Grossman EL, Ku T (1986) Oxygen and carbon isotope fractionation in biogenic aragonite: temperature effects. Chem Geol 59:59–74

Haig JA, Pantin JR, Murray LG, Kaiser MJ (2015) Temporal and spatial variation in size at maturity of the common whelk (*Buccinum undatum*). ICES J Mar Sci 72:2707–2719

Higson SPJ (2006) Analytical chemistry. Oxford University Press, New York, NY

Kent & Essex IFCA (2016) www.kentandessex-ifca.gov.uk/i-want-to-find-out-about/regulations/keifca-byelaws/keifca-district-byelaws/ (accessed 1 Jul 2016)

Kideys AE (1996) Determination of age and growth of *Buccinum undatum* L. (Gastropoda) off Douglas, Isle of Man. Helgol Meeresunters 50:353–368

Kosyan AR, Antipushina ZA (2011) Determination of *Rapana venosa* individuals' ages based on the $\delta^{18}O$ dynamics of the shell carbonates. Oceanology (Mosc) 51:1021–1028

Lawler A (2013) Determination of the size of maturity of the whelk *Buccinum undatum* in English waters – DEFRA Project MF0231. http://randd.defra.gov.uk/Default.aspx?Module=More&Location=None&ProjectID=17916

Leng MJ, Lewis JP (2016) Oxygen isotopes in molluscan shell: applications in environmental archaeology. Environ Archaeol 21:295–306

Magnúsdóttir H (2010) The common whelk (*Buccinum undatum* L.): life history traits and population structure. MSc thesis, University of Iceland, Reykjavik

MMO (Marine Management Organisation) (2016) UK sea fisheries statistics 2015. Office for National Statistics, London

McIntyre R, Lawler A, Masefield R (2015) Size of maturity of the common whelk, *Buccinum undatum*: Is the minimum landing size in England too low? Fish Res 162:53–57

Morton B (1985) Statocyst structure in the Anomalodesmata (Bivalvia). J Zool 206:23–34

Nasution S (2003) Intra-capsular development in marine gastropod *Buccinum undatum* (Linnaeous 1758). J Natur Indones 5:124–128

Nasution S, Roberts D, Farnsworth K, Parker GA, Elwood RW (2010) Maternal effects on offspring size and packaging constraints in the whelk. J Zool (Lond) 281:112–117

Pálsson S, Magnúsdóttir H, Reynisdóttir S, Jónsson ZO, Örnólfsdóttir EB (2014) Divergence and molecular variation in common whelk *Buccinum undatum* (Gastropoda: Buccinidae) in Iceland: a trans-Atlantic comparison. Biol J Linn Soc 111:145–159

Parker JE, Thompson SP, Lennie AR, Potter J, Tang CC (2010) A study of the aragonite–calcite transformation using Raman spectroscopy, synchrotron powder diffraction and scanning electron microscopy. CrystEngComm 12:1590–1599

Richardson CA (2001) Molluscs as archives of environmental change. Oceanogr Mar Biol Annu Rev 39:103–164

Richardson CA, Saurel C, Barroso CM, Thain J (2005a) Evaluation of the age of the red whelk *Neptunea antiqua* using statoliths, opercula and element ratios in the shell. J Exp Mar Biol Ecol 325:55–64

Richardson CA, Kingsley-Smith PR, Seed R, Chatzinikolaou E (2005b) Age and growth of the naticid gastropod *Polinices pulchellus* (Gastropoda: Naticidae) based on length frequency analysis and statolith growth rings. Mar Biol 148:319–326

Santarelli L, Gros P (1985) Age and growth of the whelk *Buccinum undatum* L. (Gastropoda: Prosobranchia) using stable isotopes of the shell and operculum striae. Oceanol Acta 8:221–229

Schöne BR, Zhang Z, Jacob D, Gillikin DP and others (2010) Effect of organic matrices on the determination of the trace element chemistry (Mg, Sr, Mg/Ca, Sr/Ca) of aragonitic bivalve shells (*Arctica islandica*) – comparison of ICP-OES and LA-ICP-MS data. Geochem J 44:23–37

Sharma T, Clayton RN (1965) Measurement of $^{18}O/^{16}O$ ratios of total oxygen of carbonates. Geochim Cosmochim Acta 56:419–430

Shelmerdine RL, Adamson J, Laurenson CH, Leslie B (2007) Size variation of the common whelk, *Buccinum undatum*, over large and small spatial scales: potential implications for micro-management within the fishery. Fish Res 86:201–206

Shrives JP, Pickup SE, Morel GM (2015) Whelk (*Buccinum undatum* L.) stocks around the Island of Jersey, Channel Islands: reassessment and implications for sustainable management. Fish Res 167:236–242

Smith E, Dent G (2005) Modern Raman spectroscopy: a practical approach. John Wiley & Sons, Chichester

Smith KE, Thatje S (2013) Nurse egg consumption and intracapsular development in the common whelk *Buccinum undatum* (Linnaeus, 1758). Helgol Mar Res 67: 109–120

Steinier J, Termonia Y, Deltour J (1972) Comments on smoothing and differentiation of data by simplified least square procedure. Anal Chem 44:1906–1909

Ten Hallers-Tjabbes CC, Evaraarts JM, Mensink BP, Boon JP (1996) The decline of the North Sea whelk (*Buccinum undatum* L.) between1970–1990: A natural or a human-induced event? Mar Ecol 17:333–343

Warton DI, Duursma RA, Falster DS, Taskinen S (2015) R package 'smatr': (standardised) major axis estimation and testing routines. https://cran.r-project.org/web/packages/smatr/index.html

Weetman D, Hauser L, Bayes MK, Ellis JR, Shaw PW (2006) Genetic population structure across a range of geographic scales in the commercially exploited marine gastropod *Buccinum undatum*. Mar Ecol Prog Ser 317: 157–169

Wheeler AP (1992) Mechanisms of molluscan shell formation. In: Bonucci E (ed) Calcification in biological systems. CRC Press, Boca Raton, FL, p 179–216

Wilbur KM, Saleuddin AS (1983) Shell formation. In: Wilbur KM (ed) The Mollusca, Vol 4: physiology. Academic Press, New York, NY, p 235–237

Editorial responsibility: Yves Cherel, Villiers-en-Bois, France

Submitted: February 1, 2017; Accepted: March 13, 2017
Proofs received from author(s): April 10, 2017

Vol. 598: 273–291, 2018
https://doi.org/10.3354/meps12260

MARINE ECOLOGY PROGRESS SERIES
Mar Ecol Prog Ser

Published June 28[§]

Contribution to the Theme Section 'Innovative use of sclerochronology in marine resource management'

REVIEW

From coral reefs to whale teeth: estimating mortality from natural accumulations of skeletal materials

Vladimir V. Laptikhovsky[1,*], Christopher J. Barrett[1], Philip R. Hollyman[2]

[1]Centre for Environment, Fisheries and Aquaculture Science (CEFAS), Pakefield Road, Lowestoft, Suffolk NR33 0HT, UK
[2]School of Ocean Sciences, College of Natural Sciences, Bangor University, Menai Bridge, Anglesey LL59 5AB, UK

ABSTRACT: Estimation of natural and anthropogenic (fishing, hunting) mortality is the key problem in studies of population dynamics. Numerous theoretical approaches were developed in environmental sciences to find a solution based on information that could be obtained from live representatives of populations of interest. We review the alternative methods used by marine biologists, palaeontologists and zoo-archaeologists to estimate natural and anthropogenic mortality from age-registering structures of the different taxa (corals, molluscs, fishes and mammals) collected in thanatocoenoses and containing information about the exact individual age-at-death. Not all approaches and techniques are transferrable from one field to another because they were elaborated for organisms with different morphologies and ecologies, but cross-fertilisation of ideas presented in this review might provide a new insight into studies related to population dynamics.

KEY WORDS: Age-registering structures · Mortality · Mollusc · Coral reef · Fish · Marine mammals

INTRODUCTION

The estimation of mortality and its ontogenetic changes in a given population is a crucial metric for understanding the population's dynamics. Mortality is an external force that shapes life histories and other traits through natural selection depending on the impact of different biotic and abiotic factors and is also an outcome of these life histories (Jørgensen & Holt 2013). For human-targeted species like commercial invertebrates and vertebrates, the total mortality (Z) arises from 2 sources: natural mortality (M) which can be attributed to several factors such as senescence, predation, density and size (Barbeau et al. 1994, Brocken & Kenchington 1999, Andresen et al. 2014) and anthropogenic mortality, which often arises as a direct or indirect result of fisheries activities ('fishing mortality' in marine ecosystems: F; Gosling 2004).

Anthropogenic mortality and particularly fishing mortality can be very important and even exceed twice the natural mortality in some fish populations without causing a stock to collapse (Jennings et al. 2001). Even a small variation in F and M will cause a stock to increase or decrease, bloom or disappear. Knowledge of mortality rates and their historical changes might have a wide application in studies of evolution (comparing species-specific life strategies), fisheries management (as required by every population model), population demography (variability due to historical environmental changes and human activities) and human demography (social and cultural impact).

Natural mortality is one of the most difficult and critical elements of a stock assessment (Hewitt et al.

*Corresponding author: vladimir.laptikhovsky@cefas.co.uk
[§]Advance View was available online October 23, 2017

Publisher: Inter-Research · www.int-res.com

2007), and the problem of its estimation persists among different commercial marine taxa. Significant scientific effort has been invested into quantifying this variable and elusive parameter using innumerable statistical approaches, based on assumptions about its relation to some features of life histories such as age structure of catches, maximum observed age and growth rates (e.g. Gunderson & Dygert 1988, Quinn & Deriso 1999, Hewitt & Hoenig 2005, Hewitt et al. 2007, Gislason et al. 2008). Another approach consists of observation of effects of actual mortality *in situ* and includes numerous methods to assess rates of the gradual decrease in numbers of known individual invertebrates, fish, seabirds and marine mammals that were either tagged or visually identifiable (e.g. Cormack 1964, Krebs 1999, Best & Kishino 1998, Lettink & Armstrong 2003).

This article summarises methodologies of a third approach for studying mortality in natural habitats: the use of directly observed or estimated data on individual age-at-death (*AD*) using naturally accumulated skeletal materials in thanatocoenoses or 'death assemblages'. A thanatocoenosis is an assemblage of fossils that occurred together in a given area at a given moment of historical/geological time which in some instances may not have been associated during life but were brought together after death by some process (e.g. water currents or predator activity) (Hallam 1967, Aller 1995). This final event (i.e. death) in the life of every creature can be recorded in annual (in some taxa, daily) growth rings embossed in statoliths, otoliths, shells, beaks, scales, vertebrae, eye crystals, spines, bones, whale earplugs and other age-registering structures (AReS) among members of the animal kingdom as well as on tombstones and in books of records from ancient human civilisations to the present day.

This approach requires neither best choice of the theoretical model nor long-term observation of the actual process in the wild. Considering that age–reading methods are highly specific for different taxa of the animal kingdom, we group existing methodologies respectively.

CORALS

Collection data on age-at-death

Mortality in all living things (no living thing is immortal) can be distinguished between natural, such as predation and old age, and anthropogenic (e.g. fishing, hunting or murder). Corals, however, are also subjected to a third category: partial mortality, in which a part of a colony may die but the remaining polyps may still be functional. A single coral colony appears to have a quality similar to the Schrödinger's cat paradox: it can be subjected to individual deaths but the colony still remains alive. Total (natural and anthropogenic) and partial mortalities play different ecological roles and can be assessed differently using *AD*, for which, the coral skeleton itself can be used to estimate age via a range of methods.

Scleractinian stony corals grow isometrically (Chadwick-Furman et al. 2000), presenting annual growth rings, forming in the direction of growth as skeletal density bands (Knutson et al. 1972). However, partial mortality makes determining life-history parameters of such corals (particularly scleractinians) difficult, especially when combined with other factors such as fragmentation and fusion, which often means that corals of a similar size can be of different ages (Caroselli et al. 2012). Because corals are sessile, colonising where they settle as larvae, it is therefore relatively easy to sample their population-specific age structure, particularly when the time of initial colony settling is exactly known, as in the case of shipwrecks (Wendt et al. 1989). Applying ageing techniques can help increase the certainty of the extents of coral species' natural mortalities in response to various disturbances, and as such, coral reef status (Glassom et al. 2004).

The following methods can be considered the most commonly used in dead coral ageing. It should be noted that whilst many case-studies exist which describe how observed *AD* data are collected and interpreted, their applications may suit some coral colonies, but not others; amalgamating their methods could be used to reconstruct natural mortality for population demographic use.

Growth-band analysis

As previously described (Knutson et al. 1972, Chadwick-Furman et al. 2000), corals such as scleractinians and gorgonians present annual growth rings, which can be used to age specimens relatively easily (Logan & Anderson 1991, Goffredo & Lasker 2006). The reliability of growth-band analysis, however, relies on individuals which rarely fuse and/or fragment and where growth-pattern anomalies can detect partial mortality (Babcock 1991, Chadwick-Furman et al. 2000, Caroselli et al. 2012). Where this analysis is appropriate, subsequent age-based population dynamic models make it possible to further determine demographic characteristics; Goffredo &

Lasker (2008) successfully produced an age-based Beverton-Holt model from data on the Caribbean gorgonian coral *Pseudopterogorgia elisabethae*.

Whilst age structure and growth of many coral species may be comprehensively described, some smaller, more cryptic species are less studied, and whether their growth rates differ in different environmental conditions may not be certain (Chadwick-Furman et al. 2000). Per studies by Hughes & Jackson (1985) and Bak & Meesters (1998), most corals grow indeterminately and thus can have no true $L\infty$ (average length of an infinitely ageing specimen). This assumption does not apply to all species, however; Chadwick-Furman et al. (2000) noted isometric growth in stony corals such as *Fungia granulosa*, though colonial virtual growth cessation occurred between 30 and 40 yr old, with $L\infty$ assumed at 118 mm. Chadwick-Furman et al. (2000) suggested that specimens may cease growth at this size to avoid sinking into soft sediment, though it may be possible that the species grow to larger sizes in areas of more stable ground types. In their study, skeletons of dead polyps were dried at 400°C for 24 h. Then, the circular rings externally visible on the skeleton's aboral surface were counted and it was found (by the negative correlation between the frequency of individuals in age classes against coral age) that mortality rates were high when the corals were young. However they noted that if corals were still ageing despite reaching $L\infty$, this ageing would not be identifiable via density ring analysis. Further related to size, Goodbody-Gringley et al. (2015) report that it is possible to correlate coral colony surface area to age, provided partial mortality is low. This has proven a particularly appropriate method for giant, non-branching species such as *Montastraea cavernosa,* the great star coral. Once an age/size structure is assessed, it is then possible to estimate mortality as either partial or complete (such as from bleaching), which can further be used in comparative population studies (Meesters et al. 1996, Caroselli et al. 2012).

Uranium-thorium (U-Th) method

U-Th dating was used by Roff et al. (2015) to calculate the age of 'young' (<100 yr) boulder star coral *Orbicella annularis* to a 1 to 2 yr accuracy using lateral sectioning. Combining U-Th analysis with computed tomography analysis made it possible to identify the coral's rate of growth and *AD*, following parrotfish foraging, the dominant cause of bioerosion in Glovers Reef, Belize.

X-radiography method

Zhao et al. (2014) describe the monitoring of the massive coral *Porites lutea* in response to severe anthropogenic stresses. The collected cores were sectioned into slabs which, once dried and X-rayed, displayed their growth bands. The coral's age was then calculated from the sum of the colony's maximum length, weight and height, divided by 3 times the mean linear growth rate determined by the X-ray analysis. These results were used to reconstruct the age structure of parts of a reef that in theory also provides the possibility to estimate the natural mortality. However, mortality estimations were difficult because the reef had initially declined by >80% since the 1980s and was gradually recovering after the introduction of a marine reserve in the 1990s; therefore, age structure, mortality and recruitment were not stable (Zhao et al. 2014).

Ultra-violet light method

Supriharyono (2004) examined the same coral species as Zhao et al. (2014) but also examined the effectiveness of UV light as an ageing technique. Once coral slabs were cut, fluorescent bands were revealed under black, 350 nm UV light, believed to be due to fulvic and humic acid concentrations which were elevated during Indonesia's wet season. However, not all density bands fluoresced under the light, and the author suggested that radiography was the more reliable ageing method for reconstruction of the age structure of the population.

MOLLUSCS

Collection data on age-at-death

Due to the diverse nature of the Mollusca, there are certain species groups for which *AD* and *M* are easier to determine. Estimates calculated for bivalves and gastropods are based on calcium carbonate shells which can endure in the environment after death. Dead shells can be utilized in a variety of ways to evaluate natural mortality for a given population. Much like living animals, they can be assessed using both length frequency analysis and direct ageing (e.g. Harzhauser et al. 2016).

The most common method for the estimation of *AD* in bivalve populations utilizes shells from recently deceased animals. The collection of dead bivalve

shells from thanatocoenoses can in some cases add a timeframe to the mortality itself. The use of articulated dead valves known as 'cluckers' or 'boxes' can allow the estimation of a time window in which the mortality occurred. With these valves, knowledge of the timing of hinge ligament decomposition (e.g. for oysters — Christmas et al. 1981; scallops — Dickie 1955, Orensanz et al. 1991; and mussels — Ciocco 1996) can allow scientists to assume that the shells are from recently deceased animals. An accurate estimation of hinge ligament decomposition is essential for this analysis because an underestimation will increase the value of *M* (Orensanz et al. 1991, Gosling 2004).

During sampling, both the live and dead (still articulated) shells of a bivalve population can be collected, and estimates of *M* can then be made by comparing the size-frequency distributions of both the live and dead animals. Possible errors in this method, and size frequency estimations in general, arise from the incorrect classification of animals to year cohorts (discussed by Mann et al. 2009). For some animals with easily discernible exterior age bands, such as scallops, shells can be directly aged for an estimate of the month of mortality (Merrill & Posgay 1964, Caddy 1989) to give an estimate of the total deaths since the formation of the last growth ring. Articulated shells have been successfully utilized for several commercially important bivalve groups, including scallops (Ciocco 1996), mussels (e.g. Morsan & Zaidman 2008) and oysters (Volstad et al. 2008, Mann et al. 2009). This method has also been used to estimate incidental fishery mortality by McLoughlin et al. (1991) who tracked the abundances of live, dead and damaged scallops *Pecten fumatus* throughout a season.

There are several potential problems with the use of articulated shells. For example, Cadée (2002) showed that through the process of death and decomposition, still articulated shells of *Spisula subtruncata* had floated up to 20 km away from their original population; however, this is unlikely to affect larger animals with heavier shells or reef-building bivalves. Discordance between shell composition in live and death assemblages was higher on narrow steep shelves than on broad flat shelves, suggesting that down-slope post-mortem transport might be a contributing factor in between-habitat transport of shells (Kidwell 2013). There is also a possibility that in fished areas, articulated shells are broken up by bottom fishing practices (Gosling 2004). Naidu (1988) reported that the abundance of articulated dead shells was higher on fished ground than unfished, concluding that the increase seen on harvested grounds was due to incidental fishing damage which could potentially skew estimates of *M*. Hermit crabs also could carry empty gastropod shells to some distance from their actual habitat and so can potentially alter the molluscan shell death assemblages (Walker 1988), a problem that might be particularly important in palaeontology where studied surfaces are measured by dozens and hundreds of square metres.

Among extinct cephalopods, belemnites are a taxonomic group found in large numbers within fossil deposits and providing abundant material for studies. Direct ageing of belemnite rostra is possible following a study by Wierzbowski & Joachimski (2009), who validated the daily periodicity of visible growth striations using a range of geochemical analyses (such as stable isotope and electron microprobe analysis; Fig. 1). These growth striations have been further used to determine life span and growth rates of fossilized belemnites (Wierzbowski 2013) and could potentially be utilized for the analysis of population structure and thus, natural mortality as in modern coleoids in which growth marks on statoliths and gladii also are deposited on the daily basis. Belemnite statoliths also bore supposedly daily growth

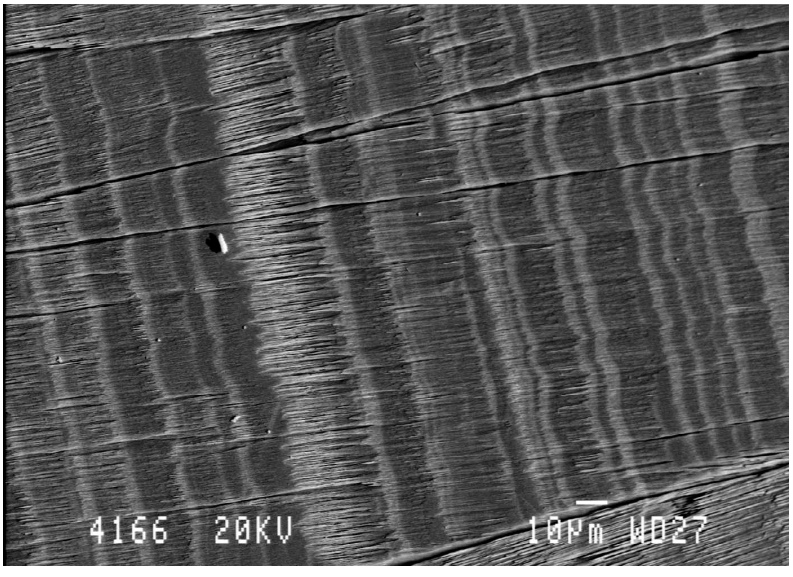

Fig. 1. Scanning electron photomicrograph of an etched (6 h, 25% glutaraldehyde) rostral cross section of a fossilized *Hibolithes hastatus* belemnite with clearly visible daily growth lines (Wierzbowski & Joachimski 2009). Reproduced with permission from H. Wierzbowski and GeoScienceWorld

rings (Hart et al. 2015), but their actual periodicity was never validated.

Gastropods comprise a single shell with no ligament with which to track decomposition; instead, the potential burial time was used as a timeframe (Parsons-Hubbard et al. 1999) for the ratio between dead and live shells in random samples by a towed gear (Laptikhovsky et al. 2016). Because the shells of *Buccinum undatum* contain no discernible annual growth rings, the age structure of the living whelk population from the same area was used as a proxy for estimation of *AD* using age-length keys, determined through the analysis of annual striae on the operculum (Santarelli & Gros 1985). The combination of population age structures of living *B. undatum* and dead shells then allowed the estimation of mortality (Fig. 2). Through the application of this technique which is normally reserved for bivalve populations, the key problem of natural mortality estimation may be answered for this commercially important gastropod species.

Analysis of natural death assemblages (natural mortality)

Shell death assemblages are often found within sea bed sediments which contain a grouping of species that may not represent living communities (Poirier et al. 2010). They are often the precursors to fossil assemblages (Boucot 1953, Kidwell 2013) and contain shells, the age of which could be identified by counting growth marks on the shell (Fig. 3).

Among molluscs, these assemblages have been used to estimate mortality of bivalve species. By collecting and analysing shells, it is possible to calculate the natural mortality of a molluscan population using size frequency analysis (Hallam 1967, Aller 1995). The population structure of the dead bivalve shells can also be compared to the living populations in the same locality to test the reliability of the estimates calculated (Aller 1995, Kidwell & Rothfus 2010). Yanes et al. (2012) used a combination of predator drilling marks (indicating mortality through gastropod predation) and stable oxygen isotope analysis of the shell margin (the most recently formed shell material) to calculate the predation-related mortality and also a seasonal estimation of the mortality which supported increased predation rates seen in the field during summer months (Rilov et al. 2001, Quijón et al. 2007). Specific types of predation-related mortality can often be investigated using this method when the characteristic bore holes of predatory gastropods can be identified on the dead shells (e.g. Aller 1995, Weissberger & Grassle 2003) and combined with known size-at-age.

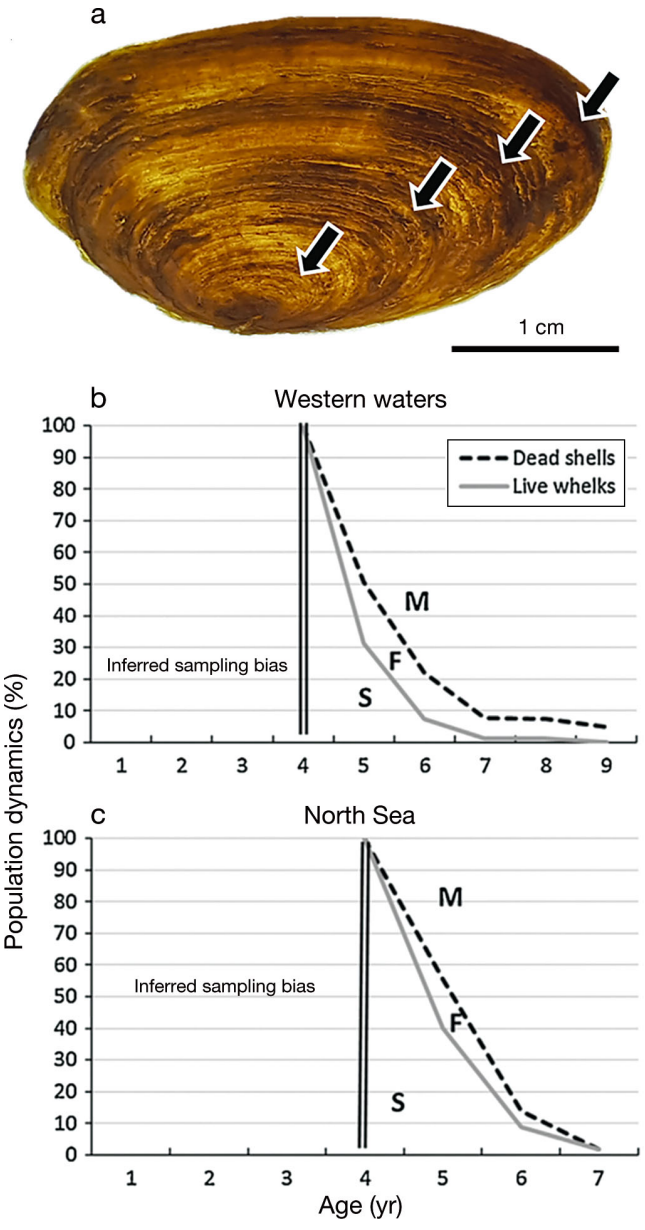

Fig. 2. (a) Tentative annual growth rings present on the surface of a *Buccinum undatum* operculum, validated by Santarelli & Gros (1985, black arrows). (b,c) changes in whelk numbers with ageing as shown by size-frequencies of dead shells and live whelks. M: natural mortality; F: fisheries mortality; S: survival. Double line shows age of 4 yr after which, whelks of ca. 70 mm shell height are supposed to be unselectively collected by fishing gears of 40 mm mesh size (Laptikhovsky et al. 2016). b & c are reproduced with permission from the Elsevier Publishing Group

Population structures (and therefore mortality estimates) are often difficult to discern from fossil shell assemblages because these are usually repre-

Fig. 3. Annual growth rings (black arrows) on the shell of *Chesapecten* (*?*)*madisonius*. Pliocene. Gloucester point, Yorktown, Virginia (photo: D. Roberts)

sentative of a large time period which is averaged into a single deposit (Kidwell 1986, 1991). However, this issue can be avoided if it is proven that the fossil deposit represents a single time point in a population, such as an oyster reef (e.g. Chinzei 2013). Harzhauser et al. (2016) presented population data from such a preserved reef of the giant oyster *Crassostrea gryphoides*. The authors utilised laser scanning and photographic analysis to count and measure the shells within the deposit (Fig. 4) and then employed length frequency analysis of the shell sizes to calculate several population dynamic parameters such as natural mortality. A size-at-age key had already been described for this species through the stable oxygen isotope analysis of shells from the same fossil deposit (Harzhauser et al. 2011).

When the age structure of dead shells from recent thanatocoenoses is available simultaneously with that of live molluscs, both *F* and *M* can be estimated together. It is possible that if the age structure of live molluscs reflects total mortality, and distribution of *AD*—natural mortality, the difference can be accounted for by fishing mortality (Laptikhovsky et al. 2016). This approach requires a species that does not immigrate and emigrate to and from the studied area, which should be large enough to ignore hermit crab impact, and the commercial harvest being processed onshore so that no empty shells are returned to the environment to be potentially confused with those that died from natural causes. Dead shells also should be destroyed or buried in sediments within a few years to minimise the impact of time-averaging, the effect of which could be very important in ecosystems subjected to commercial fisheries.

Analysis of shell middens (fishing mortality)

Shell middens are archaeological collections formed from anthropogenic discards (Andrus 2011). Like naturally occurring fossil shell deposits, the contents of a shell midden are almost always time-averaged (Koppel et al. 2016), making population structure analysis difficult. Unlike fossil shell deposits, however, middens potentially represent unique repositories of information regarding ancient fishery related mortality. There are several techniques used for age analysis of shell middens (see below) that may lend themselves to mortality estimation of the shell populations contained within.

Providing the age of the deposits is known with some confidence (see 'Time-averaging and thanatocoenoses dating'), the composition of the middens can be investigated. As well as standard cohort and length frequency analyses of population structures (Caddy 1989, Mannino & Thomas 2002), analysis of stable oxygen isotopes from the most recently formed shell section can be applied to determine the season of collection and to give a timeframe to mortality (Mannino et al. 2003, Burchell et al. 2013). As with the shells of live collected bivalves, sclerochronological techniques such as direct ageing of shells can also be employed on midden samples to extract a wealth of information regarding historical ecological and environmental conditions (see Andrus 2011 for review). A combination of these techniques could make middens a powerful tool in calculating historical fishery related mortality, which can also give important insight into the changes in foraging habits over the timeframe of human evolution (Klein & Bird 2016).

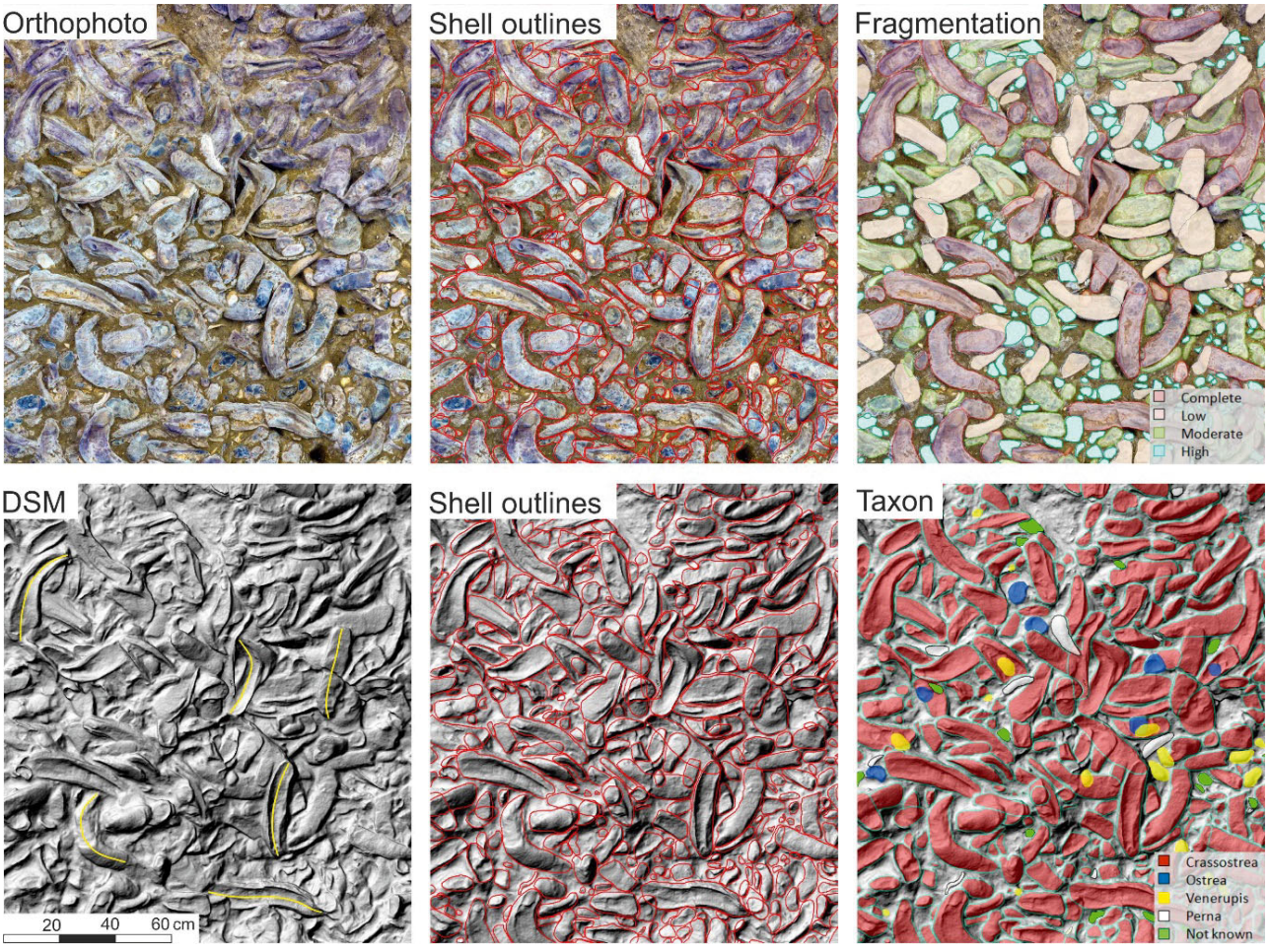

Fig. 4. Examples of population data acquisition on a fossilised oyster bed *Crassostrea gryphoides*: orthophoto and digital surface model (DSM) are used to define shell outlines manually. Together with the degree of fragmentation and species (taxon) identification, these data are georeferenced in an ArcGIS database. Yellow lines in the DSM are examples of centre lines (Harzhauser et al. 2016). Reproduced with permission of M. Harzhauser and Copernicus Publications

FISH

Otoliths are the traditional and most used AReS to estimate age in fishes. They can be preserved in large numbers in fossil assemblages, providing a tool for investigations of evolution of biodiversity when sampled in thousands (e.g. Schwarzhans 2003). Therefore, using otolith microstructure provides broad opportunities for studying the growth, age composition, and early life history of fossil fish (Woydack & Morales-Nin 2001) and therefore, in theory, the natural mortality. One author's experience (V. Laptikovsky) in studying the diet of 22 different commercial and non-commercial fish and squid species of the Southwest Atlantic (Arkhipkin et al. 2012) demonstrated that otoliths and isolated vertebrae can remain intact within the guts before evacuation and therefore could potentially be deposited back into the natural environment. However, otoliths of fish brought by seabirds to nesting sites during the chick rearing period would end up somewhere onshore, invoking important bias for estimation of mortality in surface-living species. Also, by the end of digestion in seabirds, the otoliths usually have their outer layers corroded, making them often difficult even to identify to the species level and excluding any possibility of correct aging.

Otoliths represent a significant biogenic carbonate component and are common in bottom sediments (Lin et al. 2015, 2016 & 2017a). Taxonomic composition and relative abundance of each taxon of otolith death-assemblages at various water depths conformed well to the distribution of the Mediterranean modern fish communities, though due to taphonomic particularities, otolith preservation (and potential readability) deteriorated in waters deeper than 500 m (Lin et al.

2017b). In this respect, it is important to note that among 13 000 fossil Oligocene fish remnants collected in Poland, only 250 represented separate otoliths (presumably from predator stomachs), and ~1500 were isolated heads (Kotlarczyk et al. 2006). Contrast this with ~7000 incomplete and 3314 complete skeletons possibly reflecting other sources of natural mortality (e.g. senility, periodically appearing anaerobic conditions). So, such materials exist and in theory could be used because the isolated heads and complete skeletons likely still contain otoliths. However, it is not always possible to destroy valuable fossils for an ecological study, a particular problem often occurring in paleozoology (Steele 2003).

However, there is at least one case where this approach could be applied to an important commercial species. Weddell seals prey intensively on large Antarctic toothfish under the ice sheet and characteristically remove the heads before consuming the rest. These heads (obviously still containing otoliths) accumulate around the seals' breathing holes and might be found there in dozens (Swithinbank et al. 1961, Kim et al. 2011). Because there is no fishery under the ice shelf and these waters are inaccessible to cetaceans, the seals could be the only important predator defining the species population dynamics in the area.

Other tools used to estimate age-related mortality of fish populations are vertebrae and scales. When taken from whole skeletons, even if the sample is relatively small, they can provide a useful insight about growth rates and general longevity to compare extinct and extant species (Newbrey & Bozek 2003, Newbrey et al. 2007, 2008, 2015, Wilson et al. 2013). Analysis of fossilised scales of the Paleocene fish *Joffrichthys triangulpterus* revealed that fish age could be read from them (Fig. 5), with success being slightly more than half (54.6%) though it required 6 yr of biannual collection at the same paleontological site to obtain a necessary sample size (Newbrey & Bozek 2003). Analysis of *AD* of this laterally compressed, deep-bodied osteoglossid allowed estimation of the mortality rates for fish aged 3+ yr (Fig. 6) as $M = 0.457$. This estimation seems to be reasonable for a medium-sized tropical fish of some 20 to 30 cm total length.

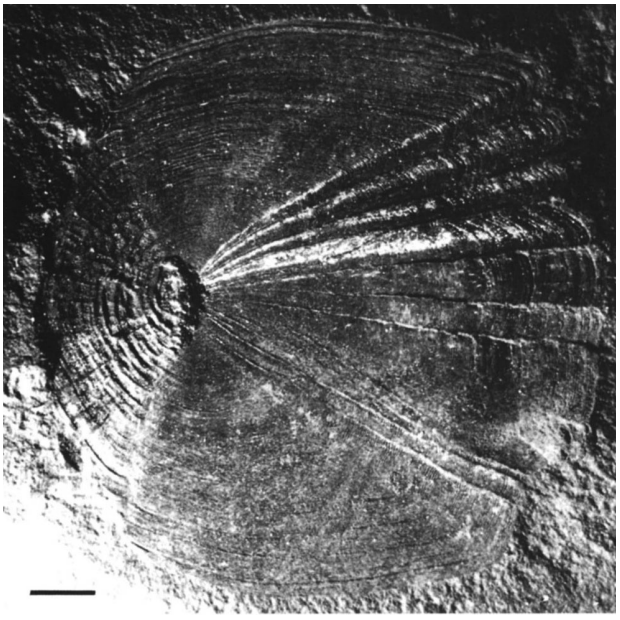

Fig. 5. A *Joffrichthys triangulpterus* fossil fish scale. The scale exhibits 6 annuli with each annulus representing a year of growth. Scale bar = 1 mm (Newbrey & Bozek 2003). Reproduced with permission of Taylor & Francis Group

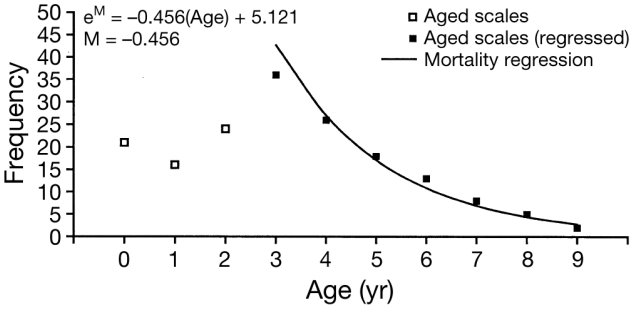

Fig. 6. Age frequency of *Joffrichthys triangulpterus* with age frequency superimposed over the data of age 3 and older fish (Newburg & Bozek 2003). Reproduced with permission of Taylor & Francis Group

MAMMALS

Collection data on age-at-death

A common task in zooarchaeology is to estimate patterns of natural mortality caused by non-human carnivores usually harvesting vulnerable individuals vs. hunting mortality caused by humans that consistently take healthy adults, a unique feature among predators (Stiner 1990, Steele 2003). To some extent, the situation is like fishery science, where natural mortality of harvested marine mammals, fish and commercial invertebrates is estimated independently of fishing mortality. The sustainable fishing activity, at least in theory, is also aimed at avoiding the harvesting of juveniles, specimens of low commercial value (under-fed, senile, sick or damaged) and specimens of high reproductive value (avoidance of breeding aggregations, seasons and/or animals); so, in this respect, hunting is not very different from fishing.

The type of the mortality profile on archaeological sites ('attritional', typical of natural mortality, vs. 'catastrophic', typical of hunting) allows to some extent a judgement of whether the species was mostly hunted or mostly scavenged by our distant hominid ancestors. When estimating human-caused mortality, the possibility that different-aged prey may be handled differently should be considered because it will affect resulting mortality profiles. With respect to natural mortality in the wild, juveniles are more likely to be fully consumed by predators or subsequent scavengers because of their small size and more cartilaginous bones, thus leaving no skulls for zooarchaeologists (Steele 2003). Generally, because archaeologists do not randomly sample target faunal remains, which means that sampling error is not randomly generated, it is recommended to limit analysis to descriptive statistics rather than involve inferential statistics (Wolverton et al. 2016).

Calculation of population-specific natural mortality rates is easy after sampling enough naturally dead animals, which is often not a problem for extant mammals (Fox et al. 2008) including marine mammals, though in the latter case there is often a question surrounding the cause of death: for example, what caused a whale to be stranded, or a seal to be washed onshore? This limitation obscures how representative the material is in respect to the animals that died at sea and drowned (see Evans & Hindell 2004). A scientific sampling of teeth and/or earplugs in hunted marine mammals also provides materials to estimate total and hunting mortality (e.g. Chittleborough 1965, Aguilar & Lockyer 1987, Barlow 1991, Bloch et al. 1993, Luque & Ferguson 2010, Nielsen 2011).

There are 2 main approaches to estimate natural and hunting mortality based on dynamics of *AD* in mammal populations: the growth ring method and the dental eruption and attrition method (for a review, see O'Connor 2000).

Growth ring method

The exact age of a wild mammal with obvious seasonal cycles of activity potentially could be estimated by counting the increments in cementum — an avascular bone-like tissue that serves to hold teeth in their sockets by providing a surface for attachment of the periodontal ligament (Fig. 7; Murphy et al. 2012). Growth rings form as the rate of cement accretion is not constant over the entire year and depends primarily on seasonal variations in diet; it is more intense during the growing period when there is plenty of food (Lieberman 1993, 1994). Growth layers can be present also in dentine, sometimes being formed seasonally, twice per annum (Fig. 8; Brodie et al. 2013). In mammals with no obvious seasonality of life events, such as humans, there is still a correlation between the age of the individual and the thickness of the cementum, which has been used for many years to estimate the age of individuals in forensic studies

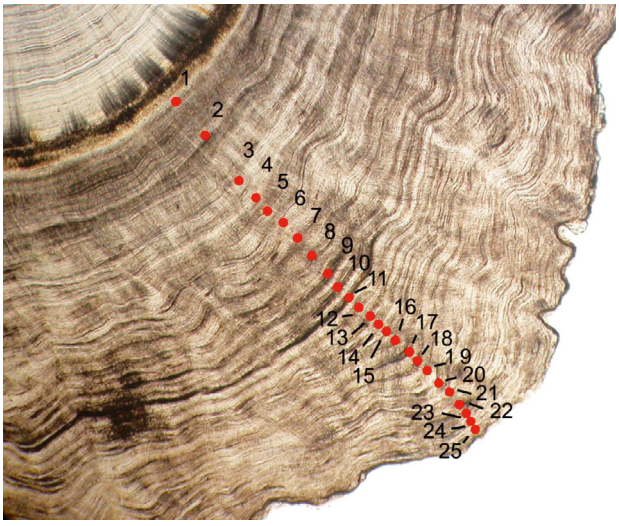

Fig. 7. Seal *Monachus monachus* growth layer groups observed in the unprocessed transverse section T1 under polarized light (×25 magnification) obtained from a 25.5 yr old unsexed individual (Murphy et al. 2012)

Fig. 8. Growth rings in dentine of an adult male beluga *Delphinapterus leucas* that are laid twice per year (photo: Dr. P. Brodie)

(O'Connor 2000). Because growth rings are deposited seasonally in the wild, there is also a possibility to estimate in what season the animal died — an approach applied to such animals as goats, gazelles, mammoths, cave bears and lions (Lieberman & Meadow 1992, Lieberman 1993, Fisher et al. 2003, Fišáková 2014, El Adli et al. 2015). In marine mammals, the annual growth rings can additionally be counted on earplugs, which also carry indispensable information on other life history events such as attaining sexual maturity, exposure to contaminants, reconstruction of life-time profiles of hormonal activities (e.g. Ruud & Jonsgård 1950, Ottestad 1950, Trumble et al. 2013).

The annual regularity of dentine increments still needs validation, though there is a consensus that this method can be applied to some species, taking into account that *AD* might be underestimated above a particular age (Adams & Watkins 1967, Keay 1996, O'Connor 2000). Also, the estimated age might depend on what tooth has been chosen (Roberts 1978, Lanteri et al. 2013). Annual formation of growth rings in cetacean earplugs is confirmed (e.g. Roe 1968, Gabriele et al. 2010) though reading them might also present difficulties in some species or age groups (e.g. Sukhovskaya et al. 1985, Aguilar & Lockyer 1987).

However, the cementum annuli method to calculate natural morality is of a limited use in zooarchaeology and palaeontology because (1) it is time-consuming and requires expertise, (2) it requires large samples to reconstruct accurate mortality profiles, and (3) most archaeologists are reluctant to destroy irreplaceable fossils (Steele 2003). The same issues also apply to extinct marine mammals whose teeth could be aged (e.g. Lambert et al. 2008, Murakami et al. 2015), but the collected data were never sufficient to draw any conclusions about natural mortality rates.

Sample sizes available even for extant marine mammals could be insufficient to calculate mortality and its confidence intervals. Because of this, authors often apply inferential statistics or just a description (Murphy et al. 2012). Analysis of data on *AD* and cause of death of a threatened Mediterranean monk seal *Monachus monachus* revealed that sub-adults are particularly prone to accidental fishery-related death, as they may be less cautious and less experienced. Upon attaining the age of 3 yr, the anthropogenic mortality persists mostly as deliberate killing, which occurs throughout the life cycle; after 10 yr, non-human induced death (natural mortality) becomes important (Fig. 9).

Dental eruption and attrition method

This method is the most used in mammal studies (Steele 2003) though it has an important drawback: it is generally applicable to living species only (or to their closest relatives) because it is not known at what age teeth erupted in extinct animals. To use data on tooth eruption, there should be a reference range of observations on animals of all ages kept in captivity since birthdate. Another issue is that genetically driven physiological processes as well as environmental circumstances may affect eruption in one or all individuals of the population (O'Connor 2000). Rates of teeth wearing may vary between individuals

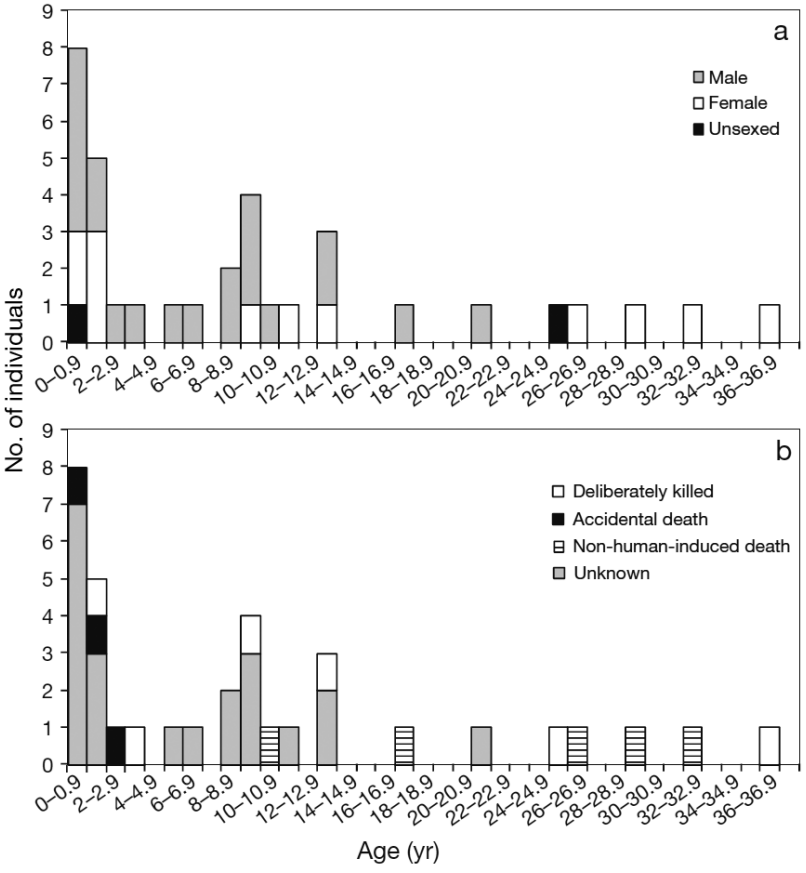

Fig. 9. Age frequency distribution of the seal *Monachus monachus* by sex and death categories (Murphy et al. 2012)

and populations, possibly because of differences in diet or degree of enamel mineralization (for a review, see Steele 2003). After allocation of every dead animal to an age range, scientists create the mortality profile as histograms or line graphs that show the proportion (either frequency or percentage) of individuals that died in each age class. Relative age is often expressed in a percentage of life span assuming constant tooth attrition rates.

Histological and chemical set of methods

The third group of methods relies on the examination of histology and chemistry of bones and other structures for comparison to a known-age series. The common technique of those used for marine mammals is called aspartic acid racemization (AAR) which measures the ratio of the 2 enantiomers of the amino acid, aspartic acid (D and L) in the eye lens as applied to bowhead, Minke and fin whales and harbour porpoises (e.g. George et al. 1999, Olsen & Sunde 2002, Nielsen 2011, Rosa et al. 2013). This implies that death was very recent, with the date known to researchers. For application of these techniques for aging time-averaged archaeological samples, see below.

Methods applicable to humans only

Analysis of methods applicable for description of human mortality rates is generally outside of the scope of this article, so we restrict ourselves to some general notions. In studies of pre-historical population dynamics, the human age might be estimated the same way as in other mammals. However, demographical records through the last 2 to 3 thousand years of human history provide abundant data on individual *AD* as recorded on such reliable AReS as tombstones coming from ancient civilisations, for example the 43000 inscriptions that have survived from the Western Roman Empire alone (Holleran & Pudsey 2011, Woods 2007). In many cases (like Christian funerary commemorations of 4 to 5th centuries), an epitaph contains the exact date of death, which permits the description of seasonal dynamics of mortality, which in the case of the city of Rome, peaked in late summer to early autumn (Scheidel 2015). However, epitaphs are selective in recording age of death, as gender and class are shown to determine the likelihood of epigraphic commemoration (Hopkins 1987, Scheidel 2001), so epitaphs are not entirely dissimilar to AReS of animal kingdom, being subjected to similar sources of bias. Data on *AD* can be also found in written sources such as records of births and deaths in recent centuries. Some of these records can be really outstanding, such as the genealogy of the Qing (1644–1911) imperial lineage containing data on births and deaths of 33000 lineage members born in Beijing between 1700 and 1840 (Lee et al. 1994).

TIME-AVERAGING AND THANATOCOENOSIS DATING

One of the problems in interpreting data from thanatocoenoses is the time-averaging of samples through the build-up of fossilised deposits when multiple generations of organisms are mixed into a single stratigraphic horizon. Such a time-averaged sample might increase variability above that found in living populations with just a few generations available for sampling. Also, it might alter correlations between morphological variables and obscure allometric relationships in evolving populations (Bush et al. 2002). However, natural mortality is a process and could be estimated only over (and in reference to) a period of time. It is different from an instantaneous morphological feature (like a shell length) that can be directly measured as a part of sample and to be related to a particular static situation. Therefore, the time-averaging effect should not prevent comparison of species-specific mortalities between different epochs that could be problematic for morphological studies. For example, analysis of *AD* read in vertebrae of extinct pikes (Newbrey et al. 2008) allowed a comparative analysis of population growth rates from the Campanian (Cretaceous) to the present day. At the studied scale of some 80 MY duration, the time-averaging of samples collected in sediments of particular short-term geological formations (such as the Hell Creek formation 66.8 to 66 MYA or the Oldman formation 77.5 to 76.5 MYA) does not bring any important bias. It demonstrates an ample possibility of studying large collections of isolated vertebrae and fossilised scales of extinct fish, that might permit estimation not only of growth rates and longevities (Newbrey et al. 2008), but also of natural mortality.

Analysis of molluscan shells from recent, non-fossilised death assemblages raises 2 important issues. First, when collecting shells buried in sediment (e.g. from a depth of 5 to 20 cm using a grab), some could be a thousand or even tens of thousands of years old, thus making the 'assemblage time window' very wide. Second, the age of shells within this 'window'

would be skewed to the left, with recently dead molluscs predominating over those that died thousands of years ago (for a review, see Kidwell 2013). These problems should be considered and addressed when planning a study and interpreting results.

Another issue is an increase in species richness (often ~25% higher than living communities) found within the assemblages (Bush et al. 2002, Kidwell 2002, 2013, Kidwell & Rothfus 2010). This is possibly a result of short-term (i.e. seasonal in fish or decadal in molluscs) changes in species ranges that potentially might combine time-averaging with some kind of spatial-averaging.

The general age of the deposits is often determined using radiocarbon dating (Koppel et al. 2016, Thomas 2015); however, advances in an alternative technique, amino acid racemization (AAR), mentioned earlier in regard to corals, may have enhanced the ability of researchers to disentangle the time-averaging within shell middens (Koppel et al. 2016, 2017). There are good and bad aspects to both techniques with regards to mollusc shell material.

Radiocarbon dating relies on the predictable decay of ^{14}C, a radioactive isotope of carbon, over time, which can be measured using accelerator mass spectrometry, resulting in a date range within which the sample lived. Radiocarbon dating of marine shells is often subject to the marine reservoir effect. This occurs when the water used as a source of carbon (and importantly ^{14}C) during shell formation comes from the deep ocean, representing water which is much older than the upper layers of seawater that are in equilibrium with the atmosphere (Bowman 1995, Jull et al. 2013). This causes the radiocarbon dates to be potentially hundreds of years older than the actual date of formation. There are now well known calibration methods to account for the marine reservoir effect (Ascough et al. 2005). However, these calibrations may also differ significantly when estuarine samples are analysed because terrestrial sources of carbonate (from rock and soil) can alter the ^{14}C signal (Reimer 2014). When radiocarbon dating archaeological samples, there is also the possibility that diagenesis has altered the ^{14}C signal within the shell. This occurs when metastable aragonite, present in many marine mollusc shells, transitions to the more stable polymorph of calcite over time. This process can draw carbon from the surrounding environment into the outer layers of the shell, resulting in a radiocarbon age different (younger or older) than that of the original shell (Thomas 2015). Where possible, it is advised to avoid diagenetic shell material. This was achieved by Mannino & Thomas (2001) by removing the outer layers of the shell of *Monodonta lineata* altogether and only sampling the inner shell layers.

AAR measures the proportion of an amino acid that has transitioned from the L-form, which is used by living organisms, to the stereoisomer D-form following death, this process is also known as racemization (Thomas 2015). Glycine does not have a stereoisomer and is therefore unsuitable; it should also be noted that different amino acids have different rates of racemization (Grimley & Oches 2015, Thomas 2015). This change happens naturally over time at a predictable rate, and so the ratio of L isomers to D isomers within a sample can be used to estimate the age. AAR presents a different set of challenges to those observed for radiocarbon dating. Unlike the decay of ^{14}C, the rate of racemization can vary with a variety of environmental conditions such as pH and temperature (Canoira et al. 2003). This means that good knowledge of the surrounding environmental history is often required. For mollusc shells, improvements in the analytical methods and recent work investigating intra-crystalline amino acids, which possibly act as closed systems with minimal external influence (Demarchi et al. 2011, 2013a,b), has improved the future potential of this technique. Although improvements are still required because disparities between analytical results from different labs are still common (Powell et al. 2013, Wehmiller 2013, Thomas 2015), recent work has also highlighted the possibility of calibrating AAR analyses with radiocarbon dating to ensure confidence in the resulting data (Kosnik et al. 2013, Simonson et al. 2013).

Coral samples can be dated using both the radiocarbon and AAR methods (Goffer 2007). In Hawaiian waters, Roark et al. (2006) applied radiocarbon (^{14}C and 'bomb ^{14}C') dating to determine ages and growth rates of pink coral *Corallium secundum*, gold coral *Gerardia* sp. and 2 black corals (*Leiopathes glaberrima* and *Antipathes dichotoma*). This research followed differences in coral ageing using radiocarbon and AAR; on an Atlantic *Gerardia* specimen, Druffel et al. (1995) recorded a basal age of 1800 ± 300 yr when using ^{14}C. However, AAR dating carried out on the same specimen revealed an age of no more than 250 yr (Goodfriend 1997). Roark et al. (2009) considers that high heat experiments were responsible for determining the amino acid date; as the coral grew in low temperatures, the heat experiments may not linearly extrapolate to the lower temperatures associated with the coral. Furthermore, it is considered that AAR is also influenced by the amino acid composition of the protein, amino acid concentration in the water, pH and ionic strength of the environment,

which could be unknown factors when assessing coral age. Until uncertainty surrounding these is decreased, Roark et al. (2009) consider ^{14}C radiocarbon dating to be the more accurate tool for coral ageing. In contrast, Robbins et al. (2001) think the 2 methods go hand-in-hand; where amino acid uncertainties are apparent, the methods can be calibrated using ^{14}C dating to generate a 'constant' used to assess an age based on the calibrated sample.

DISCUSSION AND CONCLUSIONS

Our study reviews methods applied in marine biology and fisheries management, palaeobiology, archaeology and demography. These very different disciplines use the same approach: collection of information from AReS about *AD* and summarising it into mortality profiles. These profiles allow the reconstruction of mortality rates through ontogeny, often distinguishing between natural and anthropogenic mortalities. The AReS might contain more information than just age, but also the season of death (mammals and bivalve molluscs in which it might be judged from the distance between the last growth ring and AReS edge) or even the date of death (humans) that provide a possibility of even a deeper insight into the species' ecology. Most of these body elements register the age due to the seasonal changes of metabolism leading to formation of annual growth rings. However, when the size of a dead animal is known and the species is characterised by indeterminate growth (e.g. molluscs; Sebens 1987, Ridgway et al. 2011), the age structure of thanatocoenoses could be estimated via age-length keys available from live animals (if dead and live animals are contemporary), thus providing indirect age structure assessment for calculation of mortality.

A particular case of mortality is represented by corals in which mortality can be partial. After part of a colony dies, and the rest survives, making inferential statistics becomes next to impossible. In theory, any of the described methods could be viable in ascertaining coral *AD*. However, it is evident that no one technique will be applicable to all coral specimens. Indeed, radiocarbon dating may be the most accurate, but is also likely to be the costliest technique to carry out. Baseline information on targeted species' life-history is therefore invaluable to determine which technique is needed for accurate estimates. Growth-ring analysis may be sufficient for shorter-living and continuously growing species, whereas radiocarbon dating might be more appropriate for long-living species which have an excessive number of growth rings, particularly, ones in which the rings may be very difficult to identify.

In most cases except coral reef colonies, the approach follows the principle 'one animal — one sample', like sectioning a particular half of a bivalve shell or one particular type or tooth (e.g. incisor). Therefore, often authors, mostly palaeontologists, do not need the entire organism to be collected, but sample instead the available isolated parts: shells (or even parts of shells as in the rostra of belemnites), animal teeth, fish scales, otoliths and vertebrae bearing information on age at death, and assert that one item represents one animal. To some extent, this assumption might be reasonable as different specimens will have similar (vertebrae, teeth and scales) or the same (otoliths or shell valves) numbers of AReS. In this case, a researcher often faces the problem of species identification, which can be challenging even in archaeological mammals (Steele 2003) let alone fossilised paleontological materials.

A reconstruction of the mortality profile and its interpretation requires application of inferential statistics, assuming that the collected sample is unbiased so population parameters might be inferred from its statistical properties. Because of this, the collection of data from thanatocoenoses requires a range of issues to be addressed before the study is carried out. Otherwise only descriptive statistics are possible.

(a) Within the studied range of ages, the probability of the individual AReS to be fossilised and thus being available for sampling should be the same for any age class. Mortality factors (like predators and environmental events) should not alter or destroy AReS after death;

(b) AReS of the studied range of ages should be randomly distributed within the sampled area. If mortality of animals at the different ontogenetic stages (e.g. immature vs. adult) occurs mostly in the different areas, it might provide an important source of bias;

(c) The AReS should be abundant enough not to restrict the available sample size, which might be assigned based on goals of the study and randomness of sample collection ensured;

(d) Ageing methods applied to archaeological and palaeontological data are verified and consistent; age reading done by the same persons using the same methodology; and

(e) The time-averaging factor should be negligible for the studied time scale and accounted for when interpreting the results.

In respect to practical application, all approaches to estimate mortality (natural and anthropogenic) that

were applied in the past and could be applied in future studies might be summarised as follows:

(1) No anthropogenic mortality exists or it is negligible (palaeontology, non-commercially exploited taxa of invertebrates, zooarchaeology and human demography):

(1.1) Collection of data on individual *AD* assuming as much randomness as possible (molluscan shell beds, coral reefs, growth ring method in mammals, cemeteries), and then reconstructing the mortality profile and estimating natural mortality rates between adjacent age groups using inferential statistics (e.g. Fox et al. 2008, Harzhauser et al. 2016).

(1.2) Collection of data on individual *AD* in documented multi-annual death events like sperm whale strandings (Evans & Hindell 2004), harbour porpoises bycaught and stranded (Lockyer & Kinze 2003) and monk seals washed onshore (Murphy et al. 2012). Because randomness of sampling cannot be guaranteed, descriptive statistics are applied rather than inferential statistics.

(1.3) Collection of data on some feature indicating the most probable *AD* in the natural habitat (e.g. degree of teeth attrition in mammals, shell size in non-commercial gastropods) and then reconstructing the mortality profile and respective estimation of mortality rates. Inferential statistics is possible based on some additional assumptions.

(2) Both natural and anthropogenic mortality exist (extant commercial or commercial-in-the past species of invertebrates, fishes and mammals including zooarchaeology):

(2.1) Collection of data on age structure of recently dead shells and live shells from the same habitat in molluscan species where such direct aging is possible (scallops, oysters, etc.), then reconstructing natural mortality and survival, respectively. Collection of data on age structure of landed molluscs combined with landing weight will provide harvest at age. This in combination with known difference between natural mortality and survival will provide an estimation of fishing mortality, stock size and harvest rate. This method could be applicable only to molluscs where dead shells do not accumulate over time on fishing grounds and that are not processed at sea so dead shells are disposed somewhere else (Laptikhovsky et al. 2016).

(2.2) Collection of data on some feature indicating the most probable *AD* from the natural habitat and from human middens. The method is applied mostly in zooarchaeology (e.g. Steele 2003), and because the proportion between animal death from natural causes and hunting by humans is unknown, descriptive statistics should be applied.

All these methods might generally be applied to relatively stable populations without sudden fluctuations in mortality during the studied size/age range. In species with highly changeable survival rates, such a methodology will have ecological sense only if catastrophic events are a regular part of population history, repeating over several generations such as strong El Niño events in the contemporary East Pacific. However, it would be senseless to calculate the mean mortality of a population that passed through a single large catastrophe, as for some ammonites that survived the end-Cretaceous extinction into early Paleocene (Landman et al. 2014); the calculated value would be misleading. We do not consider time-averaging to be detrimental to methods reviewed here even if populations are not entirely stable. However, other population parameters like growth rates or size-at-maturity that might be estimated from the same materials could be heavily impacted. A typical example of such a potential problem are the most important commercial squids *Loligo* spp., *Todarodes* spp. and *Illex* spp. that normally live for just 1 yr (so have the same annual mortality rates) but for which growth and maturation rates vary significantly between years due temperature variations. For such species, time-averaging does not pose a problem when mortality is estimated but should be taken into consideration when other life cycle parameters are of interest. However, to take into account the scale at which the time-averaging occurs, the researcher in most cases needs the exact age range when the studied thanatocoenosis was deposited. Therefore, all pros and cons of radiocarbon dating versus AAR discussed above should be carefully considered.

Numerous possible sources of bias should be considered when reconstructing mortality profiles and calculating natural mortality and/or natural + anthropogenic mortalities. Not all aforementioned approaches and techniques are transferrable from one field to another because they were elaborated for organisms with different morphologies and ecologies, but cross-fertilisation of ideas might provide a new insight into studies related to population dynamics.

Analysis of age structure of thanatocoenoses could help with solving large problems like studying population response to climate change in the geological and/or archaeological past and evolution of life cycle parameters in changing environments (e.g. Newbrey & Ashworth 2004, Newbrey et al. 2008, Rick et al. 2016). Achievement of these tasks might require analysis of numerous collections scattered in the different museums and co-ordination of efforts of

several scientific bodies. Such an approach could be simplified by development of exhaustive archaeological/paleontological databases containing information on specimens available for comparative palaeo-ecological studies. However, data collected with different tasks in mind could be difficult to compare. As was exemplified with materials on oysters *Crassostrea virginica*, differences in spatial and temporal resolution and extent of prehistoric, historic and modern ecological data could be an obstacle for their integration. It is because these data generally are not collected to study particular ecological topics like changes in oyster size, growth and colony accretion rates (Rick & Lockwood 2013). However, at the larger scale when the problem of time-averaging is of less importance, it is possible to, for example, track changes in oyster size from the Pleistocene to modern times (Rick et al. 2016). Often, time-averaging is a necessary procedure to obtain evolutionary sensible estimations because amalgamating data from a geological formation of hundreds of thousands of years duration would help avoid such sources of bias as seasonal migrations and inter-annual variability of climate. Application of every methodology and interpretation of results always should be considered with actual circumstances of sample collection because those strongly impact the accuracy of estimations.

Acknowledgements. The authors sincerely thank Drs. Mary Ann Muller (Taylor & Francis Group), Charlotte Winsnes (North Atlantic Marine Mammal Commission), Paul Brodie (Balaena Dynamics, Halifax), Mathias Harzhauser (Natural History Museum Vienna), Hubert Wierzbowski (Polish Geological Institute), George Rose (Elsevier Publishing Group), Kathleen Huber (PALAIOS Managing Editor) and Anna Wenzel (Copernicus GMBH) who granted permissions to use their images to illustrate this review; Prof. Chris Richardson (Bangor University) for the specimen of Chesapecten sp.; and Dr. David Righton (Cefas), Dr. M. G. Newbrey (Royal Tyrrell Museum of Palaeontology) and 3 anonymous reviewers for valuable comments.

LITERATURE CITED

Adams L, Watkins SG (1967) Annuli in tooth cementum indicate age in California ground squirrels. J Wildl Manag 31:836–839

Aguilar A, Lockyer CH (1987) Growth, physical maturity, and mortality of fin whales (*Balaenoptera physalus*) inhabiting the temperate waters of the northeast Atlantic. Can J Zool 65:253–264

Aller JY (1995) Molluscan death assemblages on the Amazon Shelf: implication for physical and biological controls on benthic populations. Palaeogeogr Palaeoclimatol Palaeoecol 118:181–212

Andresen H, Strasser M, van der Meer J (2014) Estimation of density-dependent mortality of juvenile bivalves in the Wadden Sea. PLOS ONE 9:e102491

Andrus CFT (2011) Shell midden sclerochronology. Quat Sci Rev 30:2892–2905

Arkhipkin A, Brickle P, Laptikhovsky V, Winter A (2012) Dining hall at sea: feeding migrations of nektonic predators to the eastern Patagonian Shelf. J Fish Biol 81: 882–902

Ascough P, Cook GT, Dugmore AJ (2005) Methodological approaches to determining the marine radiocarbon reservoir effect. Prog Phys Geogr 29:532–547

Babcock RC (1991) Comparative demography of three species of scleractinian corals using age- and size-dependent classifications. Ecol Monogr 61:225–244

Bak RPM, Meesters EH (1998) Coral population structure: the hidden information of colony size-frequency distributions. Mar Ecol Prog Ser 162:301–306

Barbeau MA, Scheibling RE, Hatcher BG, Taylor LH, Hennigar AW (1994) Survival analysis of tethered juvenile sea scallops (*Placopecten magellanicus*) in field experiments: effects of predators, scallop size and density, site and season. Mar Ecol Prog Ser 115:243–256

Barlow J (1991) Modelling age-specific mortality for marine mammal populations. Mar Mamm Sci 7:50–65

Best PB, Kishino H (1998) Estimating natural mortality rate in reproductively active female southern right whales, *Eubalaena australis*. Mar Mamm Sci 14:738–749

Bloch D, Lockyer C, Zachariassen M (1993) Age and growth parameters of the long-finned pilot whale off the Faroe Islands. Rep Int Whaling Comm 14:163–208

Boucot AJ (1953) Life and death assemblages among fossils. Am J Sci 251:25–40

Bowman S (1995) Radiocarbon dating. British Museum Press, London

Brocken F, Kenchington E (1999) A comparison of scallop (*Placopecten magellanicus*) population and community characteristics between fished and unfished areas in Lunenburg county, NS, Canada. Can Tech Rep Fish Aquat Sci 2258

Brodie P, Ramirez K, Haulena M (2013) Growth and maturity of belugas (*Delphinapterus leucas*) in Cumberland Sound, Canada, and in captivity: evidence for two growth layer groups (GLGs) per year in teeth. J Cetacean Res Manag 13:1–18

Burchell M, Cannon A, Hallmann N, Schwarcz HP, Schöne BR (2013) Refining estimates for the season of shellfish collection on the Pacific Northeast Coast: applying high resolution stable oxygen isotope analysis and sclerochronology. Archaeometry 55:258–276

Bush AM, Powell MG, Arnold WS, Bert TM, Daley GW (2002) Time-averaging, evolution and morphologic variation. Paleobiology 28:9–25

Caddy JF (1989) A perspective on population dynamics and assessment of scallop fisheries, with special reference to the sea scallop, *Placopecten magellanicus* Gmelin. In: Caddy JF (ed) Marine invertebrate fisheries: their assessment and management. Wiley & Sons, New York, NY, p 559–589

Cadée GC (2002) Floating articulated bivalves, Texel, North Sea. Palaeogeogr Palaeoclimatol Palaeoecol 183:355–359

Canoira L, García-Martínez MJ, Llamas JF, Ortíz JE, Torres TD (2003) Kinetics of amino acid racemization (epimerization) in the dentine of fossil and modern bear teeth. Int J Chem Kinet 35:576–591

Caroselli E, Zaccanti F, Mattiolo G, Falini G, Levy O, Dubinsky Z, Goffredo S (2012) Growth and demography of the

solitary scleractinian coral *Leptopsammia pruvoti* along a sea surface temperature gradient in the Mediterranean Sea. PLOS ONE 7:e37848

Chadwick-Furman NE, Goffredo S, Loya H (2000) Growth and population dynamic model of the reef coral *Fungia granulosa* Klunzinger, 1879 at Eilat, northern Red Sea. J Exp Mar Biol Ecol 249:199–218

Chinzei K (2013) Adaptation of oysters to life on soft substrates. Hist Biol 25:223–231

Chittleborough RG (1965) Dynamics of two populations of the humpback whale, *Megaptera novaeangliae* (Borowski). Aust J Mar Freshw Res 16:33–128

Christmas JF, McGinty MR, Randle DA, Smith GF, Jordan SJ (1981) Oyster shell disarticulation is three Chesapeake Bay tributaries. J Shellfish Res 16:115–123

Ciocco NF (1996) 'In situ' natural mortality of the Tehuelche scallop, *Aequipecten tehuelchus* (d'Orb, 1846), from San José Gulf (Argentina). Sci Mar 60:461–468

Cormack RM (1964) Estimates of survival from sighting of marked animals. Biometrika 51:429–438

Demarchi B, Williams MG, Milner N, Russell N, Bailey G, Penkman K (2011) Amino acid racemization dating of marine shells: a mound of possibilities. J Archaeol Sci 239:114–124

Demarchi B, Rogers K, Fa DA, Finlayson CJ, Milner N, Penkman KEH (2013a) Intra-crystalline protein diagenesis (IcPD) in *Patella vulgata*, part I: isolation and testing of the closed system. Quat Geochron 16:144–157

Demarchi B, Collins MJ, Tomiak PJ, Davies BJ, Penkman KEH (2013b) Intra-crystalline protein diagenesis (IcPD) in *Patella vulgata*, part II: breakdown and temperature sensitivity. Quat Geochron 16:158–172

Dickie LM (1955) Fluctuations in abundance of the giant scallop, *Placopecten magellanicus* (Gmelin), in the Digby area of the Bay of Fundy. J Fish Res Board Can 12:797–857

Druffel ERM, Griffin S, Witter A, Nelson E, Southon J, Kashgarian M, Vogel J (1995) *Gerardia*: bristlecone pine of the deep-sea? Geochim Cosmochim Acta 59:5031–5036

El Adli JJ, Cherney MD, Fisher DC, Harris JM, Farrell AB, Cox SM (2015) Last years of life and season of death of a Columbian mammoth from Rancho La Brea. Nat Hist Mus Los Angel Cty Sci Ser 42

Evans K, Hindell MA (2004) The age structure and growth of female sperm whales (*Physeter macrocephalus*) in southern Australian waters. J Zool (Lond) 263:237–250

Fišáková MN (2014) Seasonality of use of za Hájovnou cave by bears and lions. Acta Mus Nat Prague Ser B Hist Nat 70:103–106

Fisher DC, Fox DL, Agenbroad LD (2003) Tusk growth rate and season of death of *Mammuthus columbi* from Hot Springs, South Dakota, USA. In: Reumer JWF, De Vos J, Mol D (eds) Advances in mammoth research: Proc 2nd Int Mammoth Conf, Rotterdam, 16–20 May 1999. Deinsea 9:117–133

Fox S, Luly J, Mitchell K, Maclean J, Westcott DA (2008) Demographic indications of decline in the spectacled flying fox (*Pteropus conspicillatus*) on the Atherton Tablelands of northern Queensland. Wildl Res 35:417–424

Gabriele CM, Lockyer C, Straley JM, Jurasz CM, Kato H (2010) Sighting history of a naturally marked humpback whale (*Megaptera novaeangliae*) suggests ear plug growth layer groups are deposited annually. Mar Mamm Sci 26:443–450

George GC, Bada J, Zeh J, Scott L, Brown SE and others (1999) Age and growth estimates of bowhead whales (*Balaena mysticetus*) via aspartic acid racemization. Can J Zool 77:571–580

Gislason H, Pope JG, Rice JC, Daan N (2008) Coexistence in North Sea fish communities: implications for growth and natural mortality. ICES J Mar Sci 65:514–530

Glassom D, Zakai D, Chadwick-Furman N (2004) Coral recruitment: a spatio-temporal analysis along the coastline of Eilat, northern Red Sea. Mar Biol 144:641–651

Goffer Z (2007) Archaeological chemistry, 2nd edn. Wiley-Interscience, Hoboken, NJ

Goffredo S, Lasker HR (2006) Modular growth of a gorgonian coral can generate predictable patterns of colony growth. J Exp Mar Biol Ecol 336:221–229

Goffredo S, Lasker HR (2008) An adaptive management approach to an octocoral fishery based on the Beverton – Holt model. Coral Reefs 27:751–761

Goodbody-Gringley G, Marchini C, Chequer AD, Goffredo S (2015) Population structure of *Montastraea cavernosa* on shallow versus mesophotic reefs in Bermuda. PLOS ONE 10:e0142427

Goodfriend GA (1997) Aspartic acid racemization and amino acid composition of the organic endoskeleton of the deep-water colonial anemone *Gerardia*: Determination of longevity from kinetic experiments. Geochim Cosmochim Acta 61:1931–1939

Gosling E (2004) An introduction to bivalves. Bivalve molluscs: biology, ecology and culture. Fishing News Books, Blackwell, Oxford

Grimley DA, Oches EA (2015) Amino acid geochronology of gastropod-bearing Pleistocene untis in Illinois, central USA. Quat Geochronol 25:10–25

Gunderson DR, Dygert PH (1988) Reproductive effort as a predictor of natural mortality rate. J Cons Int Explor Mer 44:200–209

Hallam A (1967) The interpretation of size-frequency distributions in mollusc death assemblages. Palaeontology 10: 25–42

Hart MB, Clarke MR, Jonghe AD, Price GD, Page KN, Smart CW (2015) Statoliths from the Jurassic succession of south-west England, United Kingdom. Swiss J Palaeontol 134:199–205

Harzhauser M, Piller WE, Müllegger S, Grunert P, Micheels A (2011) Changing seasonality patterns in Central Europe from Miocene Climate Optimum to Miocene Climate Transition deduced from the *Crassostrea* isotope archive. Global Planet Change 76:77–84

Harzhauser M, Djuricic A, Mandic O, Neubauer TA, Zuschin M, Pfeifer N (2016) Age structure, carbonate production and shell loss rate in an Early Miocene reef of the giant oyster *Crassostrea gryphoides.* Biogeosciences 13:1223–1235

Hewitt DA, Hoenig JM (2005) Comparison of two approaches for estimating natural mortality based on longevity. Fish Bull 103:433–437

Hewitt DA, Lambert DM, Hoenig JM, Lipcius RN and others (2007) Direct and indirect estimates of natural mortality for Chesapeake Bay blue crab. Trans Am Fish Soc 136: 1030–1040

Holleran C, Pudsey A (2011) Demography and the Graeco-Roman world. Cambridge University Press, Cambridge

Hopkins MK (1987) Graveyards for historians. In: Hinard F (ed) La mort, les morts et l'au-delà dans le monde romain: actes du colloque de Caen, 20-22 novembre 1985. Universite de Caen Centre de Publications, Caen, p 113–126

Hughes TP, Jackson JBC (1985) Population dynamics and life histories of foliaceous corals. Ecol Monogr 55:141–166

Jennings S, Kaiser MJ, Reynolds JD (2001) Marine fisheries ecology. Blackwell Publishing, Malden, MA

Jørgensen C, Holt RE (2013) Natural mortality: its ecology, how it shapes fish life histories, and why it may be increased by fishing. J Sea Res 75:8–18

Jull AJT, Burr GS, Hodgins G (2013) Radiocarbon dating, reservoir effects, and calibration. Quat Int 299:64–71

Keay A (1996) Accuracy of cementum age assignments for black bears. Calif Fish Game 81:113–121

Kidwell SM (1986) Taphonomic feedback in Miocene assemblages: testing the role of dead hardparts in benthic communities. Palaios 1:239–255

Kidwell SM (1991) The stratigraphy of shell concentrations. In: Allison PA, Briggs DEG (eds) Taphonomy: releasing the data locked in the fossil record. Plenum Press, New York, NY, p 212–290

Kidwell SM (2002) Time-averaged molluscan death assemblages: palimpsests of richness, snapshots of abundance. Geology 30:803–806

Kidwell SM (2013) Time-averaging and fidelity of modern death assemblages: building a taphonomic foundation for conservation palaeobiology. Palaeontology 56: 487–522

Kidwell SM, Rothfus STA (2010) The live, the dead, and the expected dead: variation in life span yields little bias of proportional abundances in bivalve death assemblages. Paleobiology 36:615–640

Kim SZ, Ainley DG, Pennycook J, Eastman JT (2011) Antarctic toothfish heads found along tide cracks of the McMurdo Ice Shelf. Antarct Sci 23:469–470

Klein RG, Bird DW (2016) Shellfishing and human evolution. J Anthropol Archaeol 44:198–205

Knutson DW, Buddemeier RW, Smith SV (1972) Coral chronometers: seasonal growth bands in reef corals. Science 177:270–272

Koppel B, Szabó K, Moore MW, Morwood MJ (2016) Untangling time-averaging in shell middens: defining temporal units using amino acid racemisation. J Archaeol Sci 7: 741–750

Koppel B, Szabó K, Moore MW, Morwood MJ (2017) Isolating downward displacement: the solutions and challenges of amino acid racemisation in shell midden archaeology. Quat Int 427:21–30

Kosnik MA, Kaufman DS, Hua Q (2013) Radiocarbon-calibrated multiple amino acid geochronology of Holocene molluscs from Bramble and Rib Reefs (Great Barrier Reef, Australia). Quat Geochronol 16:73–86

Kotlarczyk J, Jerzmańska A, Świdnicka E, Wiszniowska T (2006) A framework of ichthyofaunal ecostratygraphy of the Oligocene — early Miocene strata of the Polish outer Carpathian basin. Ann Soc Geol Pol 76:1–111

Krebs CJ (1999) Ecological methodology. Harper & Row, New York, NY

Lambert O, Schlögl J, Ková M (2008) Middle Miocene toothed whale with *Platanista*-like teeth from the Vienna Basin (Western Carpathians, Slovakia). Neues Jahrb Geol Paläontol Abh 250:157–166

Landman NH, Goolaerts S, Jagt JMW, Jagt-Jazykova EA, Machalski M, Yakobucci MM (2014) Ammonite extinction and nautilid survival at the end of the Cretaceous. Geology 42:707–710

Lanteri L, Schmitt A, Foti B, Naji S (2013) Testing inter-teeth variability in adult individual age-at-death estimate using cementochronology (TCA). Am J Phys Anthropol (Spec Iss) 150(S56):177

Laptikhovsky V, Barrett C, Firmin C, Hollyman P and others (2016) A novel approach for estimation of the natural mortality of the common whelk, *Buccinum undatum* (L.) and role of hermit crabs in its shell turnover. Fish Res 183:146–154

Lee JZ, Tang F, Campbell C (1994) Infant and child mortality among the Qing nobility: implications for two types of positive check. Popul Stud (Camb) 48:395–411

Lettink M, Armstrong DP (2003) An introduction to using mark-recapture analysis for monitoring threatened species. Dept of Conservation (NZ) Tech Ser 28A:5–32

Lieberman DE (1993) Life history variables preserved in dental cementum microstructure. Science 261:1162–1164

Lieberman DE (1994) The biological basis for seasonal increments in dental cementum and their application to archaeological research. J Archaeol Sci 21:525–539

Lieberman DE, Meadow RH (1992) The biology of cementum increments (with an archaeological application). Mammal Rev 22:57–77

Lin CH, Girone A, Nolfe D (2015) Tortonian fish otoliths from turbiditic deposits in Northern Italy: taxonomic and stratigraphic significance. Geobios 48:249–261

Lin CH, Girone A, Nolfe D (2016) Fish otolith assemblages from Recent NE Atlantic sea bottoms: a comparative study of palaeoecology. Palaeogeogr Palaeoclimatol Palaeoecol 446:98–107

Lin CH, Nolfe D, Steurbaut E, Girone A (2017a) Fish otoliths from the Lutetian of the Aquitaine Basin (SW France), a breakthrough in the knowledge of the European Eocene ichthyofaunal. J Syst Palaeontol 15:879–907

Lin CH, Taviani B, Angeletti L, Girone A, Nolfe D (2017b) Fish otoliths in superficial sediments of the Mediterranean Sea. Palaeogeogr Palaeoclimatol Palaeoecol 471:134–143

Lockyer C, Kinze C (2003) Status, ecology and life history of harbour porpoise (*Phocoena phocoena*) in Danish waters. NAMMCO Sci Publ 5:143–176

Logan A, Anderson IH (1991) Skeletal extension growth rate assessment in corals, using CT scan imagery. Bull Mar Sci 49:847–850

Luque SP, Ferguson SH (2010) Age structure, growth, mortality, and density of belugas (*Delphinapterus leucas*) in the Canadian Arctic: responses to environment? Polar Biol 33:163–178

Mann R, Southworth M, Harding JM, Wesson JA (2009) Population studies of the native eastern oyster, *Crassostrea virginica*, (Gmelin, 1791) in the James river, Virginia, USA. J Shellfish Res 28:193–220

Mannino MA, Thomas KD (2001) Intensive Mesolithic exploitation of coastal resources? Evidence from a shell deposit on the Isle of Portland (Southern England) for the impact of human foraging on intertidal rocky shore molluscs. J Archaeol Sci 28:1101–1114

Mannino MA, Thomas KD (2002) Depletion of a resource? The impact of prehistoric human foraging on intertidal mollusc communities and its significance for human settlement, mobility and dispersal. World Archaeol 33: 452–474

Mannino MA, Spiro BF, Thomas KD (2003) Sampling shells for seasonality: oxygen isotope analysis on shell carbonates of the inter-tidal gastropod *Monodonta lineata* (da Costa) from populations across its modern range and from a Mesolithic site in southern Britain. J Archaeol Sci 30:667–679

McLoughlin R, Young PC, Martin RB, Parslow J (1991) The Australian scallop dredge: estimates of catching efficiency and associated indirect fishing mortality. Fish Res 11:1–24

Meesters EH, Wesseling I, Bak RPM (1996) Partial mortality in three species of reef-building corals and relation with colony morphology. Bull Mar Sci 58:838–852

Merrill AS, Posgay JA (1964) Estimating the natural mortality rate of the sea scallop (*Placopecten magellanicus*). ICNAF Res Bull 1:87–106

Morsan E, Zaidman PC (2008) Scale, dynamic and management in the harvesting of mussel in North Patagonia (Argentina). In: McManus NF, Bellinghouse DS (eds) Fisheries: management, economics and perspectives. Nova Science Publishers, New York, NY, p 171–197

Murakami M, Shimada C, Hikida Y, Hirano H (2015) New fossil remains from the Pliocene Koetoi Formation of northern Japan provide insights into growth rates and the vertebral evolution of porpoises. Acta Palaeontol Pol 60:97–111

Murphy S, Spradlin TR, Mackey B, McVee J and others (2012) Age estimation, growth and age-related mortality of Mediterranean monk seals (*Monachus monachus*). Endang Species Res 16:149–163

Naidu KS (1988) Estimating mortality rates in the Iceland scallop, *Chlamys islandica* (Müller). J Shellfish Res 7: 61–71

Newbrey MG, Ashworth AC (2004) A fossil record of colonization and response of lacustrine fish populations to climate change. Can J Fish Aquat Sci 61:1807–1816

Newbrey MG, Bozek M (2003) Age, growth, and mortality of *Joffrichthys triangulpterus* (Teleostei: Osteoglossidae) from the Paleocene Sentinel Butte Formation, North Dakota, USA. J Vertebrat Paleont 23:494–500

Newbrey MG, Wislon MVH, Ashworth AC (2007) Centrum growth patterns provide evidence for two small taxa of Hiodontidae in the Cretaceous Dinosaur Park formation. Can J Earth Sci 44:721–732

Newbrey MG, Wilson MVH, Ashworth AC (2008) Climate change and evolution of growth in Late Cretaceous to recent North American Esociformes. In: Arratia G, Schultze HP, Wilson MVH (eds) Mesozoic fishes 4 – homology and phylogeny. Verlag Dr. Friedrich Pfeil, München, p 311–350

Newbrey MG, Siversson M, Cook TD, Fotheringham AM, Sanchez RL (2015) Vertebral morphology, dentition, age, growth, and ecology of the large lamniform shark *Cardabiodon ricki*. Acta Palaeontol Pol 60:877–897

Nielsen NH (2011) Age determination by aspartic acid racemization and growth layer groups, and survival rates of fin whales (*Balaenoptera physalus*) and harbour porpoises (*Phocoena phocoena*). MSc thesis, University of Copenhagen

O'Connor T (2000) The archaeology of animal bones. Sutton Publishing, Stroud

Olsen E, Sunde J (2002) Age determination of minke whales (*Balaenoptera acutorostrata*) using the aspartic acid racemization technique. Sarsia 87:1–8

Orensanz JM, Parma AM, Iribarne OO (1991) Population dynamics and management of natural stocks. In: Shumway SE (ed) Scallops: biology, ecology and aquaculture. Elsevier, Amsterdam, p 625–713

Ottestad P (1950) On age and growth of blue whales. Hvalråd Skr 33:67–72

Parsons-Hubbard KM, Callender WR, Powell EN, Brett CE, Walker SE, Raymond AL, Staff GM (1999) Rates of burial and disturbance of experimentally-deployed molluscs: implications for preservation potential. Palaios 14: 337–351

Poirier C, Sauriau PG, Chaumillon E, Bertin X (2010) Influence of hydro-sedimentary factors on mollusc death assemblages in a temperate mixed tide-and-wave dominated coastal environment: implications for the fossil record. Cont Shelf Res 30:1876–1890

Powell J, Collins MJ, Cussens J, Macleod N, Penkman KEH (2013) Results from an amino acid racemization inter-laboratory proficiency study; design and performance evaluation. Quat Geochronol 16:183–197

Quijón PA, Grassle JP, Rosario JM (2007) Naticid snail predation on early post-settlement surfclams (*Spisula solidissima*) on the inner continental shelf of New Jersey, USA. Mar Biol 150:873–882

Quinn T, Deriso RB (1999) Quantitative fish dynamics. Oxford University Press, New York, NY

Reimer PJ (2014) Marine or estuarine radiocarbon reservoir corrections for mollusks? A case study from a medieval site in the south of England. J Archaeol Sci 49:142–146

Rick TC, Lockwood R (2013) Integrating paleobiology, archeology, and history to inform biological conservation. Conserv Biol 27:45–54

Rick TC, Reeder-Myers LA, Hofman CA, Breirburg D and others (2016) Millennial-scale sustainability of the Chesapeake Bay native American oyster fishery. Proc Natl Acad Sci USA 113:6568–6573

Ridgway ID, Richardson CA, Austad SN (2011) Maximum shell size, growth rate, and maturation age correlate with longevity in bivalve molluscs. J Gerontol A Biol Sci Med Sci 66A:183–190

Rilov G, Benayahu Y, Gasith A (2001) Low abundance and skewed population structure of the whelk *Stramonita haemastoma* along the Israeli Mediterranean coast. Mar Ecol Prog Ser 218:189–202

Roark EB, Guilderson TP, Dunbar RB, Ingram BL (2006) Radiocarbon-based ages and growth rates of Hawaiian deep-sea corals. Mar Ecol Prog Ser 327:1–14

Roark EB, Guilderson TP, Dunbar RB, Fallon SJ, Mucciarone DA (2009) Extreme longevity in proteinaceous deep-sea corals. Proc Natl Acad Sci USA 106:5204–5208

Robbins J, Jones M, Matisoo-Smith E (2001) Amino acid racemization dating in New Zealand: an overview and bibliography. Auckland University, Auckland

Roberts D (1978) Variation in coyote age determination from annuli in different teeth. J Wildl Manag 42:454–456

Roe HSJ (1968) Seasonal formation of laminae in the ear plug of the fin whale. Discov Rep 35:1–29

Roff G, Zhao JX, Mumby PJ (2015) Decadal-scale rates of reef erosion following El Niño-related mass coral mortality. Glob Change Biol 21:4415–4424

Rosa C, Zeh J, George JC, Botta O, Zauscher M, Bada J, O'Hara TM (2013) Age estimates based on aspartic acid racemization for bowhead whales (*Balaena mysticetus*) harvested in 1998-2000 and the relationship between racemization rate and body temperature. Mar Mamm Sci 29:424–445

Ruud JT, Jonsgård Å (1950) Age studies on blue whales taken in Antarctic seasons 1945–46, 1946–47 and 1947–48. Hvalråd Skr 33:5–66

Santarelli L, Gros P (1985) Age and growth of the whelk *Buccinum undatum* L. (Gastropoda: Prosobranchia) using

stable isotopes of the shell and operculum striae. Oceanol Acta 8:221–229

Scheidel W (2001) Roman age structure: evidence and models. J Roman Stud 91:1–26

Scheidel W (2015) Death and the city: ancient Rome and beyond. Princeton/Stanford Working Papers in Classics, doi:10.13140/RG.2.1.1408.4000

Schwarzhans W (2003) Fish otoliths from the Paleocene of Denmark. Geol Surv Den Greenl Bull 2:94

Sebens KP (1987) The ecology of indeterminate growth in animals. Annu Rev Ecol Evol Syst 18:371–407

Simonson AE, Lockwood R, Wehmiller JF (2013) Three approaches to radiocarbon calibration of amino acid racemization in *Mulinia lateralis* from the Holocene of the Chesapeake Bay, USA. Quat Geochronol 16:62–72

Steele TE (2003) Using mortality profiles to infer behaviour in the fossil records. J Mammal 84:418–430

Stiner M (1990) The use of mortality patterns in archaeological studies of hominid predatory adaptations. J Anthropol Archaeol 9:305–351

Sukhovskaya LI, Klevezal GA, Borisov VI, Lagerev SJ (1985) Use of bone layers to determine age in minke whales. Acta Theriol (Warsz) 30:275–286

Supriharyono S (2004) Growth rates of the massive coral *Porites lutea* Edward and Haime, on the coast of Bontang, East Kalimantan, Indonesia. J Coastal Dev 7:143–155

Swithinbank CWM, Darby DG, Wohlschlag DE (1961) Faunal remains on the Antarctic ice shelf. Science 133:764–766

Thomas KD (2015) Molluscs emergent, Part I: themes and trends in the scientific investigation of mollusc shells as resources for archaeological research. J Archaeol Res 56: 133–140

Trumble SJ, Robinson EM, Berman-Kowalewski M, Potter CW and others (2013) Blue whale earplug reveals lifetime contaminant exposure and hormone profiles. Proc Natl Acad Sci USA 110:16922–16926

Volstad JH, Dew J, Tarnowski M (2008) Estimation of annual mortality rates for eastern oysters (*Crassostrea virginica*) in Chesapeake Bay based on box counts and application of those rates to project population growth of *C. virginica* and *C. ariakensis*. J Shellfish Res 27:525–533

Walker SE (1988) Taphonomic significance of hermit crabs (Anomura: Paguroidea): epifaunal hermit crab-infaunal gastropod example. Palaeogeogr Palaeoclimatol Palaeoecol 63:45–71

Wehmiller JF (2013) Interlaboratory comparison of amino acid enantiomeric ratios in Pleistocene fossils. Quat Geochronol 16:173–182

Weissberger EJ, Grassle JP (2003) Settlement, first-year growth, and mortality of surfclams, *Spisula solidissima*. Estuar Coast Shelf Sci 56:669–684

Wendt PH, Knott DM, Van Dolah RF (1989) Community structure of the sessile biota on five artificial reefs of different ages. Bull Mar Sci 44:1106–1122

Wierzbowski H (2013) Life span and growth rate of Middle Jurassic mesohibolitid belemnites deduced from rostrum microincrements. Volumina Jurassica 11:1–18

Wierzbowski H, Joachimski MM (2009) Stable isotopes, elemental distribution, and growth rings of belemnopsid belemnite rostra: proxies for belemnite life habitat. Palaios 24:377–386

Wilson AE, Newbrey MG, Brinkman DB, Neuman AG (2013) Age and growth in *Myledaphus bipartitus*, a Late Cretaceous freshwater guitarfish from Alberta, Canada. Can J Earth Sci 50:930–944

Wolverton S, Dombrosky J, Lyman RL (2016) Practical significance: ordinal scale data and effect size in zooarchaeology. Int J Osteoarchaeol 26:255–265

Woods R (2007) Ancient and early modern mortality: experience and understanding. Econ Hist Rev 60: 373–399

Woydack A, Morales-Nin B (2001) Growth patterns and biological information in fossil fish otoliths. Paleobiology 27: 369–378

Yanes Y, Kowalewski M, Romanek CS (2012) Seasonal variation in ecological and taphonomic processes recorded in shelly death assemblages. Palaios 27:373–385

Zhao MX, Yu KF, Zhang QM, Shi Q, Roff G (2014) Age structure of massive *Porites lutea* corals at Luhuitou fringing reef (northern South China Sea) indicates recovery following severe anthropogenic disturbance. Coral Reefs 33:39–44

Editorial responsibility: Stylianos Somarakis, Heraklion, Greece

Submitted: January 23, 2017; Accepted: July 14, 2017
Proofs received from author(s): October 1, 2017